



HAL
open science

Modeling and optimization of coextrusion spherification process for new food matrices development

Chanez Bennacef

► **To cite this version:**

Chanez Bennacef. Modeling and optimization of coextrusion spherification process for new food matrices development. Food engineering. Université de Lorraine, 2023. English. NNT : 2023LORR0278 . tel-04688585

HAL Id: tel-04688585

<https://hal.univ-lorraine.fr/tel-04688585v1>

Submitted on 5 Sep 2024

HAL is a multi-disciplinary open access archive for the deposit and dissemination of scientific research documents, whether they are published or not. The documents may come from teaching and research institutions in France or abroad, or from public or private research centers.

L'archive ouverte pluridisciplinaire **HAL**, est destinée au dépôt et à la diffusion de documents scientifiques de niveau recherche, publiés ou non, émanant des établissements d'enseignement et de recherche français ou étrangers, des laboratoires publics ou privés.



**UNIVERSITÉ
DE LORRAINE**

**BIBLIOTHÈQUES
UNIVERSITAIRES**

AVERTISSEMENT

Ce document est le fruit d'un long travail approuvé par le jury de soutenance et mis à disposition de l'ensemble de la communauté universitaire élargie.

Il est soumis à la propriété intellectuelle de l'auteur. Ceci implique une obligation de citation et de référencement lors de l'utilisation de ce document.

D'autre part, toute contrefaçon, plagiat, reproduction illicite encourt une poursuite pénale.

Contact bibliothèque : ddoc-theses-contact@univ-lorraine.fr
(Cette adresse ne permet pas de contacter les auteurs)

LIENS

Code de la Propriété Intellectuelle. articles L 122. 4

Code de la Propriété Intellectuelle. articles L 335.2- L 335.10

http://www.cfcopies.com/V2/leg/leg_droi.php

<http://www.culture.gouv.fr/culture/infos-pratiques/droits/protection.htm>



SIReNa



Thèse

Présentée et soutenue publiquement le 04 décembre 2023, pour l'obtention du titre de

DOCTEUR DE L'UNIVERSITE DE LORRAINE

Mention : Génie Biotechnologique Et Alimentaire

Par Chanez BENNACEF

Sous la direction du Professeur Stéphane DESOBRY

et la co-direction de Sylvie DESOBRY-BANON

Modélisation et optimisation du procédé de sphérification par coextrusion pour le développement de nouvelles matrices alimentaires

Membres du jury :

Président du jury :	Pr Thomas KARBOWIAK	Université Bourgogne Franche Comte, Dijon, France.
Directeur de thèse :	Pr Stéphane DESOBRY	Université de Lorraine, Nancy, France.
Co-Directrice de thèse :	Pre Sylvie DESOBRY-BANON	Université de Lorraine, Nancy, France.
Rapporteurs :	Dr Ali ASSIFAOU	Université Bourgogne Franche Comte, Dijon, France
	Dr Virginie DULONG	Université de Rouen, Mont-Saint-Aignan, France.
Membres invités :	M. Laurent PROBST	Cookal S.A.S, Maxéville, France.

DEDICATION

To the experiences I never expected,
And the paths that were redirected.
To the friends and family I found along the way.

“When it looks impossible, look deeper and then fight like you can win”

-Rost, Horizon Forbidden West.

Acknowledgments

Je tiens à exprimer ma plus profonde gratitude à toutes les personnes qui m'ont soutenue et guidée tout au long de mon parcours pour achever cette thèse.

Tout d'abord, je suis profondément reconnaissant envers mon directeur de thèse, Stéphane Desobry pour son soutien indéfectible, ses précieux conseils et sa patience. Son expertise et son engagement envers ma croissance académique et personnelle ont été essentiels pour façonner cette recherche et combattre ma phobie administrative. Je remercie aussi infiniment ma co-directrice de thèse, Sylvie Desobry-Banon pour son temps et sa patience durant les longues réunions à base de schémas sphériques et d'équations alambiquées.

Je suis également redevable aux membres de mon comité de thèse, qui ont accepté d'évaluer ce travail de thèse. Merci pour votre temps et votre expertise.

De plus, je tiens à remercier le corps professoral et le personnel du laboratoire d'ingénierie des biomolécules (LIBio) qui ont contribué à mon expérience académique, je remercie aussi l'entreprise Cookal en particulier Laurent PROBST pour son accueil et son temps tout au long de cette thèse industrielle.

Je tiens à exprimer ma reconnaissance envers ma famille pour leur amour inconditionnel, leurs encouragements et leur compréhension tout au long de cette aventure académique. Leur foi en moi a été une source constante de motivation.

Je dois aussi exprimer ma gratitude envers mes amis et mes collègues doctorants, Adeline, Corentin, Maureen, Preethi, Régis, Urielle (et j'en oublie sûrement), qui m'ont encouragée, dont, j' ai partagé ls expériences et retours durant les longues, mais essentielles, pauses cafés/gâteaux.

De plus, je souhaite remercier les participants de cette thèse pour leur temps et leur volonté de contribuer à ma recherche. Sans leur participation, cette thèse n'aurait pas été possible.

Cette thèse représente l'effort collectif de toutes ces personnes, et je leur suis profondément reconnaissant pour leurs contributions à ma croissance académique et personnelle.

Table of content

INTRODUCTION	9
CHAPTER 1. LITERATURE REVIEW	18
1.1 ADVANCES ON ALGINATE USE FOR SPHERIFICATION TO ENCAPSULATE BIOMOLECULES (PUBLISHED IN FOOD HYDROCOLLOIDS)	20
1.1.1 Introduction.....	20
1.1.2 Spherification process.....	22
1.1.3 Factors influencing alginate gelation and spherification	26
1.1.4 Composite Alginate gels	32
1.1.5 Other Encapsulation processes using alginate	37
1.1.6 Conclusion	40
1.2 ALGINATE CORE-SHELL CAPSULES PRODUCTION THROUGH COEXTRUSION METHODS: PRINCIPLES AND TECHNOLOGIES (PUBLISHED IN DRUG MARINES)	43
1.2.1 Introduction.....	43
1.2.2 Principle of Coextrusion Process.....	45
1.2.3 Advantages and limitations of coextrusion methods	58
1.2.4 Conclusions.....	60
1.3 ALGINATE BASED CORE-SHELL CAPSULES PRODUCTION THROUGH COEXTRUSION METHODS: RECENT APPLICATIONS (PUBLISHED IN FOODS)	61
1.3.1 Introduction.....	61
1.3.2 Oil and Essential Oil Encapsulation	62
1.3.3 Probiotics Encapsulation.....	68
1.3.4 Encapsulation of Other Ingredients	71
1.3.5 Conclusions.....	73
CHAPTER 2. STUDY OF ENCAPSULATION FACTORS IMPACT ON THE PHYSIO-CHEMICAL PROPERTIES OF CORE-SHELL CAPSULES PRODUCED BY COEXTRUSION.	76
2.1 STUDY AND OPTIMIZATION OF CORE-SHELL CAPSULES PRODUCED BY ANNULAR JET BREAKING COEXTRUSION (PUBLISHED IN COLLOIDS AND SURFACES A : PHYSICO-CHEMICAL AND ENGINEERING ASPECTS)	78
2.1.1 Introduction.....	78
2.1.2 Materials and methods.....	79
2.1.3 Results and discussion	84
2.1.4 Conclusion	95
2.2 OPTIMIZATION OF CORE-SHELL CAPSULES PROPERTIES (OLIVE OIL/ALGINATE) OBTAINED BY DRIPPING COEXTRUSION PROCESS (PUBLISHED IN LWT)	97
2.2.1 Introduction.....	97
2.2.2 Materials and methods.....	98
2.2.3 Results and discussion	102
2.2.4 Conclusion	112

CHAPTER 3. CAPSULES DESIGN THROUGH PARAMETERS AND FORMULATION ADJUSTMENTS. .	114
3.1 INFLUENCE OF ALGINATE PROPERTIES AND CALCIUM CHLORIDE CONCENTRATION ON ALGINATE BEADS RETICULATION AND SIZE.....	116
3.1.1 Introduction.....	116
3.1.2 Materials and Methods.....	117
3.1.3 Results and discussion	121
3.1.4 Conclusion	131
3.2 ENCAPSULATION OF MICROCIN IN ALGINATE CORE-SHELL MICROCAPSULES THROUGH COEXTRUSION TECHNOLOGY	133
3.2.1 Introduction.....	133
3.2.2 Materiel and methods.....	134
3.2.3 Results and discussion	139
3.2.4 Conclusion	143
3.3 STUDY OF FORMULATION AND PROCESS VARIABLES IMPACT ON CAPSULE MECHANICAL AND PHYSICAL PROPERTIES.	144
3.3.1 Impact of gelling bath ionic environment and post-encapsulation treatment on shell resistance.....	144
3.3.2 Impact of core-oil viscosity on the core-shell centricity index of capsules	146
CHAPTER 4. GENERAL DISCUSSION.....	151
CHAPTER 5. CONCLUSION AND PERSPECTIVES.....	156
CHAPTER 6. REFERENCES.....	161

List of abbreviations

Abbreviations	Definitions
$(\text{NH}_4)_2\text{HPO}_4$	Diammonium Phosphate
3D	Three Dimensional
Alg	Alginate
Alg	Alginate Protanal
AlgLF	Alginate Louis-François
AlgSA	Alginate Solution Aging
ANOVA	Analysis Of Variance
AQ	Alginate Flow Rate
BHT	Butylated Hydroxytoluene
C	Coefficient Of Size Variation
Ca-Alg	Calcium-Alginate
CaCl_2	Calcium Chloride
CLAMs	Cross-Linked Alginate Microcapsules Process
D0	Day 0 Of Storage
D_2O	Heavy Water
D4	Day 4 Of Storage
D7	Day 7 Of Storage
Dex	Dextran
DHA	Docosahexaenoic Acid
dn/dc	Specific Refractive Index Increment
DrEAM	Doctor, Explore And Achieve More
<i>e.g.</i>	<i>Exempli Gratia</i> , For Example
EDTA	Ethylenediaminetetraacetic Acid
EE	Encapsulation Efficiency
EE	Encapsulation Efficiency
EHD	Electrohydrodynamic
EPA	Eicosapentaenoic Acid
<i>Etc.</i>	<i>Et Cetera</i>
F	Frequency
FFA	Free Fatty Acid
FOS	Fructo-Oligosaccharides
FS-J25	Free Solution Of J25 Microcin
FTIR	Fourier Transform Infrared
GRAS	Generally Recognized As Safe
HCL	Hydrochloric Acid
HMP	High-Methoxyl Pectin
HPLC	High-Performance Liquid Chromatography
HPMC	Hydroxypropyl Methylcellulose
<i>i.e.</i>	<i>Id Est</i> , In Other Words
IF	Internal Flow
K_2HPO_4	Dipotassium Phosphate

KH ₂ PO ₄	Monopotassium Phosphate
LALS	Left Angle Light Scattering
LB	Luria-Bertani Culture Media
LMC	Lysed Microcapsules
M/G	Mannuronate/Guluronate Ratio
MgSO ₄	Magnesium Sulfate
MIC	Minimal Inhibitory Concentration
Mw	Molecular Weight
Na-Alg	Sodium Alginate
NaCl	Sodium Chloride
NaNO ₃	Sodium Nitrate
NaOH	Sodium Hydroxide
ND	Not Determined
NMR	Nuclear Magnetic Resonance
OF	Outer Flow
OQ	Oil Flow Rate
p-AV	P-Anisidine Value
PB	Phosphate Buffer
PEG	Polyethylene Glycol
PEO	Poly(Ethylene Oxide)
PES	Polyethersulfone
pH	Potential Hydrogen
PS	Polysorbate 20
PV	Peroxide Value
Q	Flow Rate
RALS	Right Angle Light Scattering
Refs	References
RP-HPLC	Reversed-Phase High-Performance Liquid Chromatography
RSM	Response Surface Method
SDS	Sodium Dodecyl Sulfate
SEC	Size-Exclusion Chromatography
SGC	Simulated Gastric Conditions
SGJ	Simulated Gastric Juice
SIJ	Simulated Intestinal Juice
TBARS	Thiobarbituric Acid Reactive Substances
TOCO	Tocopherols
Totox	Total Oxidation Value
UV	Ultra-Violet

List of Publications

- Bennacef, C., Desobry-Banon, S., Probst, L. & Desobry, S. Advances on alginate use for spherification to encapsulate biomolecules. *Food Hydrocoll* **118**, (2021).
- Bennacef, C., Desobry-banon, S. & Probst, L. Alginate Core-Shell Capsules Production through Coextrusion Methods: Principles and Technologies. *Mar Drugs* **21**, 235 (2023).
- Bennacef, C., Desobry, S., Probst, L. & Desobry-banon, S. Alginate Based Core – Shell Capsules Production through Coextrusion Methods: Recent Applications. *Foods* **12**, 1788 (2023).
- Bennacef, C., Desobry-Banon, S., Probst, L. & Desobry, S. Optimization of core-shell capsules properties (Olive oil/alginate) obtained by dripping coextrusion process. *LWT* **167**, 113879 (2022).
- Bennacef, C.; Desobry-Banon, S.; Linder, M.; Khanji, A.N.; Probst, L.; Desobry, S. Study and optimization of core-shell capsules produced by annular jet breaking coextrusion. *Colloids Surf A Physicochem Eng Asp* **629**, (2021).
- Bennacef, C., Desobry, S., Probst, L. & Desobry-Banon, Influence of alginate properties and calcium chloride concentration on alginate beads reticulation and size, *Submitted in Polymers on October 2023*.

List of Communications

- Bennacef, C. Desobry-Banon, L. & Desobry, S. spherification of alginate capsules through jet breaking coextrusion 6th conference on Innovations in Nutrition and Food Science, London, UK, October 06 - 08, 2022. Invited speaker.
- Bennacef, C. Desobry-Banon, L. & Desobry, S. Investigation of jet breaking coextrusion process parameters impacts on produced core-shell capsules. *SIReNa annual seminar*, 2023, Nancy, France.

Introduction

Ces dernières années, la demande de techniques avancées de transformation des aliments s'est accrue. L'objectif principal étant d'améliorer la qualité, la fonctionnalité et la valeur nutritionnelle des produits alimentaires.

L'encapsulation est un procédé fondamental dans lequel des molécules ou des substances actives sont incorporés dans une structure porteuse ou une matrice appelée « capsules » ou « vecteur d'encapsulation ». L'objectif principal étant de les protéger de l'environnement extérieur et de contrôler leur libération. La membrane agit comme une barrière, protégeant l'ingrédient central de la dégradation causée par des facteurs tels que la chaleur, la lumière et le pH. L'encapsulation améliore donc la stabilité et la durée de conservation des molécules actives. De nombreuses substances (vitamines, enzymes, principes actifs), sont susceptibles de se dégrader lors d'une exposition non-protégée à l'environnement extérieur. L'encapsulation offre un moyen conserver leur intégrité et efficacité pendant la période de stockage et d'utilisation. En outre, l'encapsulation permet une libération contrôlée et ciblée des molécules actives, optimisant ainsi leur fonctionnalité et leurs effets. Grâce à la modulation des matrices et des techniques d'encapsulation, les capsules produites peuvent libérer leur contenu en réponse à des déclencheurs, tels que des changements de pH, de température ou de niveau d'humidité. Ce mécanisme est très utile en pharmacie galénique, où il garantit une libération optimale des principes actifs.

Diverses méthodes d'encapsulation sont employées en industrie pour produire des particules ou des granulés, notamment, le séchage par pulvérisation, l'enrobage sur lit fluidisé et l'enrobage par fusion à chaud. De plus, Les techniques de microencapsulation dont l'évaporation de solvant, la coacervation et la séparation de phase, sont utilisées pour la production de petites particules individuelles ou de gouttelettes. Toutefois, les méthodes d'encapsulation présentent des avantages et des limites spécifiques qu'il convient de prendre en compte lors de la sélection des techniques.

Les procédés d'extrusion et de coextrusion offrent des avantages en termes de contrôle de la taille des particules et d'efficacité de l'encapsulation. Ils proposent, entre autres, l'utilisation de l'alginate comme matrice d'encapsulation. L'alginate est un biopolymère naturel extrait de diverses algues brunes. Il a fait l'objet d'une attention particulière dans le domaine de l'encapsulation en raison de ses propriétés uniques et de sa polyvalence. Il présente une excellente biocompatibilité, une biodégradabilité et une faible antigénicité. Il est généralement reconnu comme sûr (GRAS), ce qui permet de l'utiliser dans des applications diverses. Sa structure composée de guluronate et mannonate lui confère la capacité de former un hydrogel

stable lorsqu'il est exposé à des cations divalents tels que les ions calcium. Ce phénomène de gélification peut être contrôlé en ajustant des facteurs tels que le pH, la température, la concentration de l'agent de réticulation, le temps de séjour et la force ionique, ce qui permet une encapsulation précise des molécules actives. En outre, l'efficacité de l'encapsulation, la stabilité mécanique, les propriétés de barrière et la stabilité thermique de l'alginate peuvent être améliorées par l'incorporation de copolymères et la modulation des conditions de gélification.

La coextrusion permet la formation de capsules cœur-couronne avec un contrôle précis de l'épaisseur de la membrane et de sa composition, ce qui la rend très adaptable à une large gamme d'applications industrielles. Cette thèse présente une vue d'ensemble des méthodes de coextrusion, en mettant l'accent sur l'utilisation de l'alginate comme matrice d'encapsulation. Quatre méthodes de coextrusion reposant sur l'utilisation de buses coaxiales ont été présentées, à savoir l'égouttage, la découpe au jet, la centrifugation et le système électro-hydrodynamique, en tenant compte des différents principes de fonctionnement nécessaires pour atteindre des tailles de capsules précises et ciblées.

Les techniques de coextrusion offrent des avantages significatifs de réduction du phénomène d'oxydation et d'évaporation des composés volatils, mais aussi d'amélioration de stabilité des substances encapsulés et de leurs durées de conservation. C'est pourquoi l'intérêt scientifique et industriel envers cette technologie s'est accru.

Cookal S.A.S, société française, dispose d'une large gamme de produits encapsulés qui sont aujourd'hui commercialisées à l'international. Cependant, en tant que société innovante, il est crucial d'améliorer continuellement les produits commercialisés et d'augmenter la performance industrielle.

Cette thèse a donc pour objectif de : (i) comprendre la structuration du réseau d'alginate ; (ii) maîtriser les paramètres de coextrusion influençant l'encapsulation et leurs interactions ; (iii) développer de nouvelles formulations de matrice pour améliorer la résistance mécanique ; (iv) stabiliser les conditions du procédé pour prédire et assurer une parfaite régularité des propriétés des capsules tout au long de leur production ; (v) établir des modèles pour prédire les propriétés des capsules sur la base des conditions du procédé. Cette thèse a également fourni des informations essentielles pour la poursuite de la recherche et du développement dans le domaine de la production de capsules cœur-couronne à base d'alginate.

Le manuscrit est organisé comme suit :

Le premier chapitre présente les caractéristiques de l'alginate, les facteurs qui influencent sa gélification et les progrès récents liés à son utilisation pour l'encapsulation de

biomolécules. Le chapitre se concentre ensuite sur les méthodes de coextrusion, y compris les systèmes de goutte-à-goutte, de rupture de jet, de centrifugation et d'électro-hydrodynamique. Chaque technique possède des paramètres spécifiques permettant de produire différentes tailles de capsules. L'encapsulation par coextrusion trouve des applications dans la conservation des huiles, et huiles essentielles, des probiotiques ainsi que d'autres substances bioactives, grâce aux propriétés barrières de la membrane d'alginate. C'est pourquoi les principes et les technologies de la coextrusion sont étudiés ici. Aussi, les applications récentes des principales méthodes de coextrusion pour la production de capsules à base d'alginate sont mises en évidence dans ce chapitre.

Le deuxième chapitre, marque le début des études expérimentales menés dans le but principal de proposer des modèles pouvant aider à la compréhension du procédé et au développement de nouvelles applications. Les études menés ont été sélectionnées en lien avec la problématique industrielle de la société Cookal en termes de variables de procédé et de matériaux encapsulés. Les effets de divers paramètres sur la forme des capsules et la charge de l'encapsulation sont étudiés à l'aide de la méthode des surfaces de réponse. Une première étude par plan d'expérience réalisée via un montage laboratoire a permis d'examiner, les débits d'alginate et d'huile, la fréquence appliquée, la concentration de calcium et l'âge de la solution d'alginate. Cette étude a été suivie par un deuxième travail réalisé sur le pilote industriel de coextrusion par goutte-à-goutte pour produire des capsules d'huile. Les impacts de la concentration en chlorure de calcium, les débits d'alginate et d'huile et de la hauteur d'égouttage ont été étudiés. Le diamètre, la sphéricité, la résistance à la rupture et la charge d'encapsulation des capsules ont été examinés.

Ces deux études ont permis le développement de modèles de prévision des caractéristiques principales des capsules produites par coextrusion en rupture de jet annulaire ou en goutte-à-goutte, ce qui les rend applicables à diverses industries. Dans l'ensemble, cette recherche contribue à la compréhension et à l'optimisation de la production de capsules d'huile à base d'alginate à l'aide de différentes méthodes de coextrusion et fournit des outils utiles pour les applications industrielles.

Le troisième chapitre présente l'impact des conditions d'encapsulation sur la formation de la membrane et du réseau d'alginate. Divers facteurs peuvent influencer les propriétés des capsules, et il est essentiel de comprendre leurs effets pour optimiser le procédé. Ainsi, l'impact du rapport M/G, du poids moléculaire de l'alginate et de la concentration en chlorure de calcium sur la réticulation de l'alginate et la taille des billes a été étudié. Les données techniques obtenues en laboratoire pourront être utilisées pour répondre à un besoin industriel de

modélisation des propriétés, comme mentionné dans le deuxième chapitre, mais aussi pour répondre à un besoin d'amélioration des produits. Dans ce contexte, des études appliquées ont été menées pour (i) améliorer l'aspect sensoriel des capsules d'huile d'olive, (ii) examiner l'impact de la viscosité de l'huile sur l'indice de centricité du cœur .

Enfin, le 3^{ème} chapitre retrace une mobilité de 6 mois au Canada qui m'a permis d'appliquer l'encapsulation par coextrusion pour améliorer la stabilité et maîtriser la libération de peptides antimicrobiens puissants (microcine J25). La poursuite de l'exploration de cette méthode pourrait être la clé du développement de systèmes d'administration antimicrobiens innovants pour une variété d'applications industrielles.

Ce travail montre que les techniques de sphérification et de coextrusion offrent des voies prometteuses pour l'encapsulation dans diverses industries. L'alginate, avec ses propriétés uniques et sa polyvalence, reste un matériau très prometteur pour les processus de sphérification. Ce travail se concentre sur l'utilisation de la technologie de coextrusion comme méthode d'encapsulation spécifique, en explorant son application dans la production de capsules cœur-couronne. Enfin, cette thèse contribue à la connaissance en examinant les propriétés et les applications de l'alginate dans la sphérification, ainsi qu'en explorant les méthodes de coextrusion pour l'encapsulation et leurs applications spécifiques.

English introduction

In recent years, there has been a growing demand for advanced food processing techniques that can enhance quality, functionality, and nutritional value of food products. Encapsulation is a fundamental process in which active molecules or substances are enclosed within a protective shell or coating to shield them from external influences and regulate their release ¹. The shell acts as a barrier, protecting the core material from degradation caused by external factors such as heat, light, and pH. Therefore, encapsulation enhances stability and shelf life of active molecules ².

Many substances, such as pharmaceutical drugs, vitamins, and enzymes, are susceptible to degradation when exposed to harsh environmental conditions ^{3,4}. Encapsulation provides a means to protect these sensitive compounds, allowing them to retain their potency and efficacy over extended periods of storage and use ⁵. Furthermore, encapsulation enables controlled release and targeted delivery of active molecules, optimizing their functionality and effects ^{6,7}. Through the choice of encapsulating materials and techniques, encapsulated products can be designed to release their contents at specific rates or in response to triggers, such as changes in pH, temperature, or moisture levels ⁸. This controlled release mechanism is valuable in pharmaceuticals, where it ensures optimal drug delivery and minimizes potential side effects ⁹.

In the industry, various encapsulation methods are employed to achieve the desired protective and controlled release effects. Coating techniques, such as spray drying, fluidized bed coating, and hot melt coating, are commonly used to produce particles or granules ^{1,10}. Microencapsulation techniques, including solvent evaporation, coacervation, and phase separation, are used for small individual particles or droplets production ¹¹. These methods are widely applied in pharmaceutical formulations, food additives, and encapsulated fragrances, among others. Encapsulation methods and applications exhibit specific advantages and limitations that should be considered when selecting appropriate techniques for specific purposes¹². Extrusion and coextrusion methods have emerged as powerful techniques for encapsulation, offering advantages in terms of particle size control and encapsulation efficiency¹³. Coextrusion allows formation of core-shell capsules with precise control over shell thickness and material composition, making it highly adaptable for a wide range of applications in industries like cosmetics, pharmaceuticals, and food ¹⁴.

Alginate is a natural biopolymer extracted from various brown seaweeds. It has gained significant attention in the field of encapsulation due to its unique properties and versatile

applications. Alginate exhibits excellent biocompatibility, biodegradability and low antigenicity^{12,15}. It is Generally Recognized As Safe (GRAS) making it suitable for use in foods and biomedical applications.

This thesis serves as a comprehensive overview of coextrusion methods, with a specific focus on the alginate polymer and coaxial nozzles for core-shell capsules production. Four coextrusion methods, i.e. dripping, jet cutting, centrifugal, and electrohydrodynamic system, are presented, considering the various operating principles necessary for attaining precise and targeted capsule sizes.

Coextrusion techniques offer significant advantages by reducing oxidation processes, limiting evaporation of volatile compounds, stabilizing probiotics, and improving the shelf life of encapsulated substances¹⁶. Therefore, this PhD thesis focused on applications for the preservation of oils, essential oils, probiotics, and other bioactives.

Cookal S.A.S, a French company, has a wide panel of encapsulated product that are now marketed internationally. However, it is crucial as an innovative company to continuously improve commercialized product and increase industrial performance and optimization. To support cookal's innovative process, the present work aimed to: (i) understand the coextrusion parameters influencing encapsulation and their interactions; (ii) develop new matrix formulations to adjust mechanical strength resistance; (iii) stabilize the process conditions to predict and ensure perfect consistency of bead properties throughout the production duration; (iv) establish models to predict capsules properties based on process conditions. It also provided a valuable insights and foundation for further research and development in the field of alginate-based core-shell capsules production.

The manuscript is organized as follows:

The first chapter provides a literature review on alginate use to encapsulate biomolecules. A first part deals with the presentation of alginate characteristics, factors that influence its gelation, and recent progress in its use for spherification techniques in biomolecule encapsulation. The basics of producing alginate millimetric particles (beads, capsules) are presented, with the use of co-polymers for particles properties enhancement.

The chapter shifts to a detailed examination of coextrusion methods for encapsulation, including dripping, jet cutting, centrifugal, and electrohydrodynamic systems. Each technique has specific parameters based on the desired capsule size. Beyond preservation, coextrusion encapsulation finds applications in conserving oils, essential oils, probiotics, and other bioactive substances. By shielding these substances from external factors, enhancing their stability, and allowing controlled release, coextrusion offers an environmentally friendly option

for different sectors. Finally, recent applications of coextrusion methods in the production of alginate-based core-shell capsules are highlighted.

From second to fourth chapters, experimental studies are presented. The technical data obtained in the laboratory are used to satisfy an industrial need to model properties, but also to satisfy a need to improve products. The main objective was to improve current applications and propose models to help develop future applications. Therefore, current variables study and process understanding permitted the development of phenomenological models adapted to coextrusion. With this aim, in the second chapter, production of oil/alginate capsules using two different techniques: annular jet breaking coextrusion and dripping coextrusion is investigated. The effects of various parameters on the shape of the capsules and the encapsulation payload are studied using response surface methods. In the annular jet breaking coextrusion method, flow rates of alginate and oil, applied frequency, calcium concentration, and alginate solution age are examined. A phenomenological model is applied to predict the effects of variables, facilitating potential industrial applications. In the dripping coextrusion method, the impacts of calcium chloride concentration, alginate and oil feed rate, and dripping height are investigated. Capsule diameter, sphericity, rupture strength, and encapsulation payload are studied using response surface methods. Mathematical models are developed to predict the diameter, sphericity, rupture strength, and encapsulation payload of the capsules, making them applicable for various industries such as food and cosmetics. Overall, this research contributes to the understanding and optimization of the production of oil-alginate capsules using different coextrusion methods and provides useful tools for industrial applications.

In the third chapter, the impact of encapsulation conditions on shell formation and alginate network construction is presented. Various factors can influence the properties of the capsules during encapsulation process, and understanding their effects is crucial for optimizing the encapsulation process. Therefore, the impact of alginate M/G ratio and molecular weight, and calcium chloride concentration on alginate reticulation and beads size was studied. In this context, studies were carried out to improve the sensory aspect of core-shell olive oil capsules, but also to examine the impact on oil viscosity on core centricity index. In addition, impact of hemp oil encapsulation on its oxidation is studied. Moreover, coextrusion using alginate capsules promises to improve the stability, controlled release, and targeted delivery of potent antimicrobial peptides such as J25 microcin and nisin, this study was carried out in collaboration with the Department of Food Technology of Laval University, as part of DrEAM project. Further exploration of this method may be the key to the development of innovative antimicrobial delivery systems for a variety of industrial and therapeutic applications.

In conclusion, spherification and coextrusion techniques offer promising avenues for encapsulation in various industries. Alginate, with its unique properties and versatility, remains a highly promising material for spherification processes. This work focuses on the utilization of coextrusion technology as a specific encapsulation method, exploring its application in production of core-shell capsules. This thesis aims to contribute to the existing knowledge basics by examining properties and applications of alginate in spherification, as well as exploring the coextrusion methods for encapsulation and specific applications.

Chapter 1. Literature Review

L'encapsulation de composés actifs est un domaine de recherche et d'application essentiel pour diverses industries, permettant de relever les défis liés à la conservation, à la libération contrôlée et à l'amélioration de la stabilité des composés actifs. Ce chapitre présente une synthèse bibliographique sur l'encapsulation de biomolécules par l'utilisation d'alginate. Il regroupe trois publications personnelles correspondant aux différents volets abordés durant la thèse. Une première revue, publiée dans *Food Hydrocolloids*¹, aborde les mécanismes de formation du réseau d'alginate et les paramètres influents, notamment en coextrusion. Dans une deuxième revue, publiée dans *Marine Drugs*², les principes de la coextrusion sont détaillés, notamment pour les procédés goutte-à-goutte, à rupture de jet, par centrifugation et électrohydrodynamiques. Les avantages et les limites de chacun de ces procédés sont présentés. Une troisième étude, publiée dans *Foods*³, porte sur les applications récentes des méthodes de coextrusion pour la production de capsules cœur-couronne à base d'alginate. En lien avec les travaux menés dans le cadre de la thèse, les exemples choisis sont les huiles, les huiles essentielles, les probiotiques et les biomolécules actives.

The encapsulation of active compounds has emerged as a critical field of research and application across various industries, addressing challenges related to preservation, controlled release, and stability enhancement. In this context, this chapter serves as a comprehensive introduction of the current research on the alginate-based encapsulation process and more specifically coextrusion process. In a first review, published in *Food Hydrocolloids*¹, alginate network formation mechanism is presented. In addition, various parameters (process parameters, the matrix nature, process type, etc.) controlling the alginate reticulation and thus the capsules/beads formation are highlighted. In a second review, published in *Marine Drugs*², various coextrusion methods principles were overviewed. Four methods for encapsulation by coextrusion were examined in detail, including dripping, jet cutting, centrifugal, and electrohydrodynamic systems, along with process advantages and limitations. In a third review, published in *Foods*³, recent applications of coextrusion methods producing alginate-based core-shell capsules are presented. The review focuses on coextrusion for the preservation of oils, essential oils, probiotics and bioactives.

¹ Bennacef, C., Desobry-Banon, S., Probst, L. & Desobry, S. Advances on alginate use for spherification to encapsulate biomolecules. *Food Hydrocoll* **118**, (2021)

² Bennacef, C., Desobry-banon, S. & Probst, L. Alginate Core-Shell Capsules Production through Coextrusion Methods: Principles and Technologies. *Mar Drugs* **21**, 235 (2023)

³ Bennacef, C., Desobry, S., Probst, L. & Desobry-banon, S. Alginate Based Core – Shell Capsules Production through Coextrusion Methods: Recent Applications. *Foods* **12**, 1788 (2023)

1.1 Advances on alginate use for spherification to encapsulate biomolecules (published in Food Hydrocolloids)

1.1.1 Introduction

Alginate is the salt of alginic acid, a natural polymer of uronic acids (mannuronic and guluronic acids) extracted especially from brown marine algae¹⁷⁻¹⁹ and also from some bacteria, such as *Pseudomonas aeruginosa*.

The alginate gelation is one common way to produce beads or capsules. The term spherification used in this review covers all the methods employed to design such particles of millimetric size, ideally spherical. In this review, we consider spherification with the aim of encapsulating different ingredients and active principles.

Alginate is Generally Recognized as Safe (GRAS), being nontoxic, nonantigenic, satisfactorily biocompatible, and sufficiently biodegradable²⁰. As a result of its physicochemical properties, alginate is used for a large variety of technical applications, as a coating material in textile industry²¹ or as a disintegrating agent for Tablets²². Alginate is also commonly found in cosmetic²³, pharmaceutical, medical²⁴ and food industries, as thickener and stabilizer^{25,26}.

Table 1-1. Alginates types and their applications.

Code	Alginate types	Applications	References
E400	Alginic acid	Zero calorie ingredients for diet foods (biscuits, low-sugar marmalade, ice-creams).	22
E401	Sodium alginate	Stabilizer and thickener in frostings, puddings and processed	27,28
E402	Potassium alginate	fruits and fruit juices.	
E403	Ammonium alginate	Matrix for encapsulation of volatiles constituents. Coating films to preserve frozen fish.	
E404	Calcium alginate	Pearls from spherification process.	
E405	Propane-1,2 diol alginate	Stabilizer of emulsion in acidic environment (salad dressing). Stabilizer of foam in brewing industry.	27

A major use of alginate today is the encapsulation technology through its biocompatibility and capability to form a hydrogel through ionic cross-links with divalent cations, such as calcium ions²⁹⁻³¹ (see Table 1-1).

1.1.1.1 Alginate molecular structure and its modification by processing methods

Alginate is formed by a chain of β -D-mannuronic acid (M units) and α -L-guluronic acid (G units), linked via (1 \rightarrow 4) glycosidic linkage (see Figure 1-1). The percentage of those units varies among algae species³² and impacts alginate properties³³.

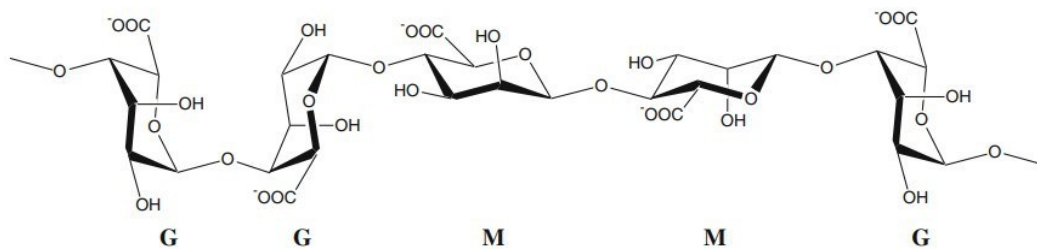


Figure 1-1. Structural characteristics of alginate. M: mannuronate residue; G: guluronate residue.

As polysaccharides properties are tightly related to their structures, the modification of alginate structure has been widely explored. For that, alginate acid hydrolysis showed a uronic acids release through an elimination reaction that led to molecular weight reduction ^{34,35}. Chhatbar *et al.* (2009) studied the effect of microwave-assisted acidic hydrolysis of alginate and reported an acceleration of this reaction with similar oligo-alginate properties than conventional acidic hydrolysis ³⁶.

Alginate can also be enzymatically and thermally treated ³⁷⁻³⁹ to modify its structure and functional properties through the molecular weight reduction or M/G ratio modification. The enrichment with G units results in a rigid structure when an enrichment with M units produces a flexible molecular structure ⁴⁰.

Ultrasounds treatment of alginate at different frequencies induce polymer structure degradation, rearrangements, and modifications of its molecular weight. A decrease of M/G ratio has also been reported with changes of hydrophobic interactions making alginate treated by 135 kHz having a stronger stiffness compared to the untreated polymer ^{41,42}.

In addition to their physicochemical properties, biological activities of oligo-alginate obtained by alginate acidic hydrolysis have been investigated. Plant growth bio-stimulating activity was demonstrated ⁴³. Anti-allergic activity of a 13.3 kDa oligo-alginate was reported after scission of an initial 1 605 kDa alginate polymer by a 3 kGy alpha-irradiation ⁴⁴.

1.1.1.2 Ion-binding for alginate gelation

One of the most studied properties of alginate, is its ability to form hydrogels by cross-linking with divalent or trivalent cations such as Ca^{2+} , Cu^{2+} , Sr^{2+} , Al^{3+} , for example. Those cations present various affinities toward alginate, that result in hydrogels with different structural and mechanical characteristics (Young modulus, gel morphology, etc) ⁴⁵.

For food or cosmetic application, Ca^{2+} is the most commonly used. So, in the literature, calcium alginate gels are the most largely investigated. Gelation occurs in solution when calcium ions replace sodium to cross-link two alginate chains and form a network ⁴⁶. Alginate

gelation is commonly described as an eggbox model formed by two antiparallel chains of polyuronates linked with Ca^{2+} binding blocks as illustrated in ^{30,47}. Stokke et al. (2000) suggested a lateral association of G units in the eggbox structure represented in Figure 1-2 ⁴⁸.

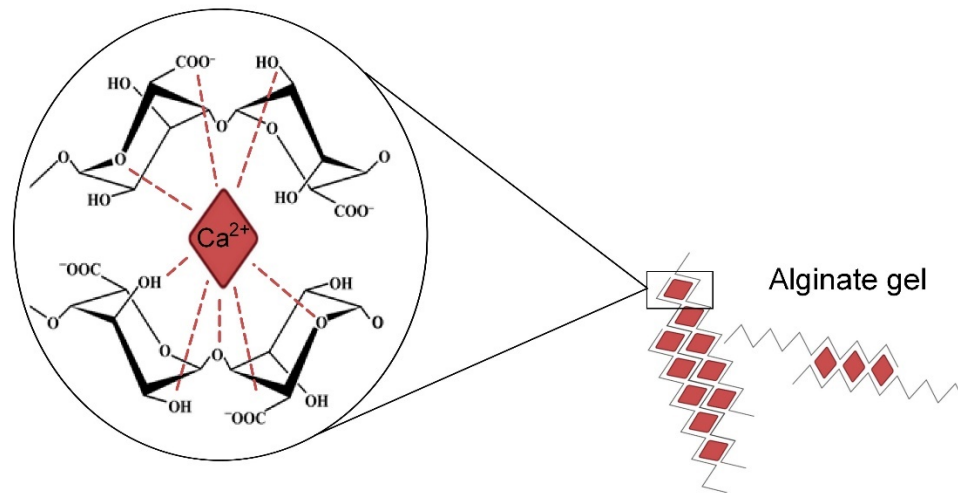


Figure 1-2. Alginate gel structure in presence of calcium ions (egg-box model) (Adapted ³⁰).

1.1.2 Spherification process

1.1.2.1 Gelation methods

Two main gelation methods can be presented: (i) the external gelation, also called diffusion process ^{49,50}; and (ii) the internal gelation also called pH-controlled gelation as pH determines gelation kinetics ^{51,52}. These two methods are described below.

1.1.2.1.1 External gelation

The external gelation method leads to gel formation through diffusion of calcium ions in an alginate solution ⁵³. Alginate solution droplets are usually extruded into a calcium bath; this method is called conventional or classical spherification. A solution containing calcium ions can also be dropped into an alginate bath and this process is known as inverse spherification.

Gel prepared by external gelation presents an inhomogeneous structure with low mechanical properties, this is due to the presence of calcium ions mostly at the surface ⁵⁴⁻⁵⁷. A concentration gradient of polymer/ions exists from beads surface to core ⁵⁸. Several researches focused on this feature to overcome it ^{52,59}, or to study bioactive substances delivery systems in food and medicine applications ^{22,53}.

1.1.2.1.2 Internal gelation

Internal gelation method is based on calcium release simultaneously into the system under controlled conditions. Usually, calcium lactate is dissociated to initiate alginate gelation ⁶⁰. Internal gelation allows a better control of gelation kinetics and produces a homogeneous

gel structure with pores. It is used for controlled delivery of active compounds⁵². As an example, Strobel *et al.* (2020) reported a significant enhance of fish oil stability after its encapsulation with internal gelation method⁶¹.

Javvaji *et al.* (2011) reported a novel light activated gelation method induced by photoacid generation in an insoluble calcium salt dispersion. After 10min of UV-treatment, the released H⁺ ions from the photoacid generator react with the calcium salt and release calcium ions that cross linked with alginate to form a hydrogel⁶².

1.1.2.2 Spherification process using alginate

Encapsulation process permits to coat a substance for its preservation and/or addition of functional properties. Several encapsulation methods involving alginate can give rise to particles or capsules with several structural organizations. Thus, many parameters must be considered to choose the appropriate particle structure associated to an encapsulation method: particle size, composition of encapsulated substance, stability of matrix and delivery features. Besides, those methods must be scaled up for industrial production⁶³.

1.1.2.2.1 Extrusion

1.1.2.2.1.1 Simple dripping

Simple extrusion process is the most commonly spread encapsulation way. The principle consists in extrusion through a nozzle of an alginate solution or an emulsion containing alginate. The formed droplets fall into a gelation bath containing an alginate crosslinker (generally Ca²⁺) under stirring. Following this basic principle, the process can be varied to incorporate interesting components into alginate solution/emulsion in order to encapsulate it and trap it into the matrix⁶³.

Different structural organization can be produced depending on the extruded solution. For instance, an alginate solution loaded with the target compound tends to produce beads with homogenous microstructure Figure 1-3A. An emulsion consisting in a lipidic phase dispersed in an aqueous phase of alginate results in obtention of beads with a dispersed microstructure Figure 1-3B.

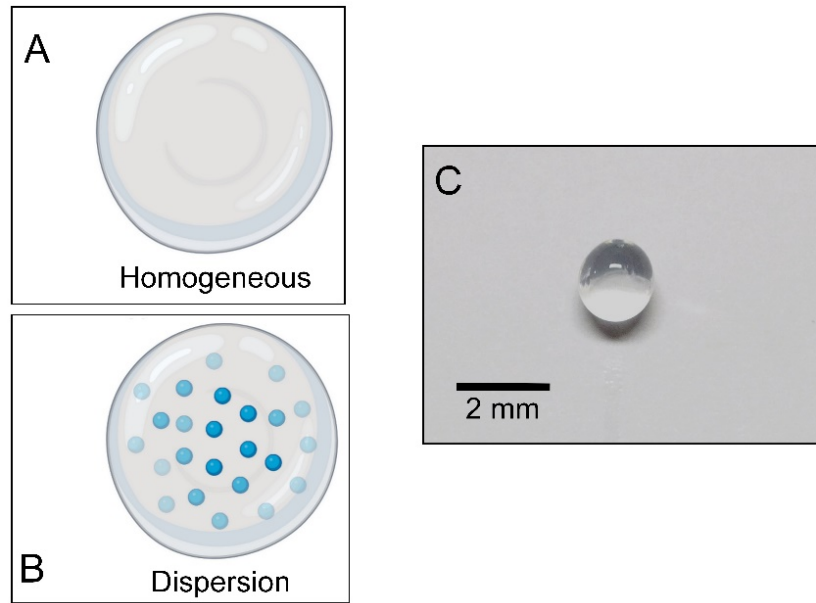


Figure 1-3. Scheme of homogeneous structural organization for capsules (A), scheme of dispersed structural organization for capsules (B) and a photograph of a homogenous capsule.

The beads shape depends on experimental conditions such as pH, calcium concentration and temperature. However, beads sphericity is also determined by alginate solution viscosity and fall distance between nozzle outlet and bath surface. The optimized fall distance to obtain spherical beads has been determined in the range 7 to 10 cm knowing that droplets are formed as a result of solution surface tension. This distance is necessary to the liquid to drag the forces exerted by the gelling bath and overcome the impact to form a spherical bead. Also, sphericity can be improved through surface active compounds addition ^{63,64}.

Simple extrusion process allowed encapsulation of various compounds for delivery systems and to increase their stability, including oils ⁶⁵, essential oils ^{66,67}, drugs ⁶⁸, probiotics ^{69,70}, enzymes ⁷¹ and proteins ⁷².

In order to produce particles of different sizes (from 20 μm to 7 mm), numerous encapsulation processes have been derived from simple dripping process. Those methods differ generally by the ways of formation and separation of alginate droplets. Usually, these methods are divided into three groups: jet dispersion, spinning disk and atomization.

- *Jet dispersion*

The extruded polymer gel is split up following different methods. In this group, vibrating nozzle ⁷³, electrostatic atomization ⁷⁴ and jet cutting ⁷⁵ are commonly used. It is also possible to merge particular processes for increased efficiency, as the vibrating electrostatic method for example ⁷³.

- *Spinning disk*

Under centrifugal force, the alginate solution flow forms droplets due to the rotation of the nozzle (or rotating disc). Spinning disk method is used to encapsulate flavor ingredients ⁷⁶.

- *Atomization*

Another extrusion method is atomization. The process basis is the extrusion of pressurized polymer solution through a nozzle while injecting pressurized air, atomized particles fall then into a gelling bath. Atomization can be applied for lipid encapsulation for example ⁷⁷.

1.1.2.2 Coextrusion

Coextrusion, also called annular jet method, is an encapsulation technique which allows to obtain core-shell capsules as shown in Figure 1-4A. Alginate solution and solutions containing the substances to encapsulate are simultaneously injected through a coaxial nozzle, which permits to obtain an annular jet formed by two concentric jets. The outer material represents the shell material, *i.e.* alginate solution, and the inner contains the solution with the target substance. The jet is then separated into droplets and collected in a gelling bath. As for the simple dripping process, different separative methods are possible: vibration, electrostatic forces, spinning disk or simple dropping into crosslinker solution ⁷⁸.

In addition to the previously mentioned factors that impact beads size, a couple of factors are specific to coextrusion process to reach a given shape of core-shell capsules. For instance, nozzles sizes (internal/external) affect capsules size. Slow flow rate tends to produce larger capsules (drop by drop system) than capsules produced at high flow rate ^{78,79}.

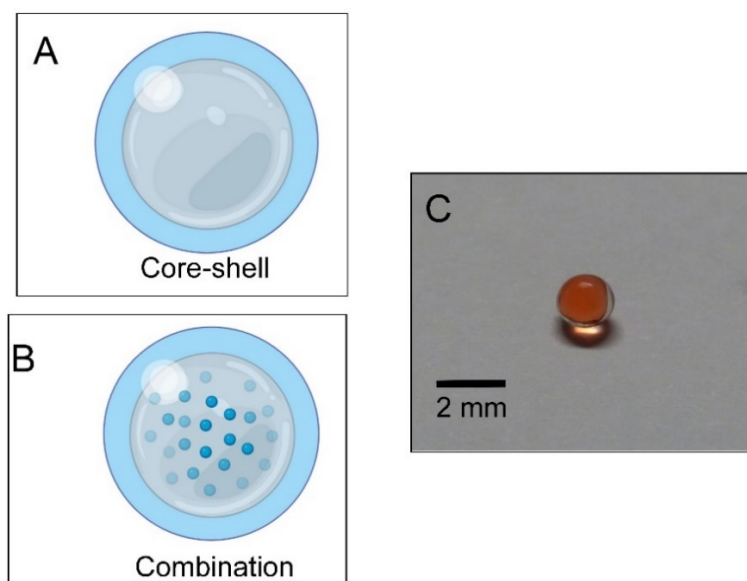


Figure 1-4. Scheme of a core-shell structural organization for capsules (A), scheme of a combination structural organization for capsules (B) and a photograph of a core-shell capsule.

Coextrusion technology allows production of capsules with a huge payload (over 90 %) and a large range of capsules size can be obtained with a diameter from few microns to a several millimeters. The process is easily scaled-up for industrial use ^{78,80}. For example, Lucia et al (2017) worked on the production of almonds essential oil liquid-core capsules obtained by coextrusion process ⁷⁹. Silva et al (2018) studied the encapsulation of *Lactobacillus acidophilus* and compared the simple dripping method to the coextrusion technique. An additional protective function was observed for beads produced by coextrusion and especially for capsules obtained with a composite shell made of an alginate/shellac matrix ⁸¹.

1.1.3 Factors influencing alginate gelation and spherification

1.1.3.1 Molecular weight of alginate

Generally, high molecular weight of alginate due to long polymeric chains results in a larger number of Ca-binding sites then tighter crosslinking in the gel ⁸². These interactions impact gelation process and produce a high viscosity gels, so that low molecular weight alginate (1,43x10⁵ g.mol⁻¹) viscosity is 2.4 times lower than higher molecular weight alginate (3,5x10⁵ g.mol⁻¹) viscosity (0.05 Pa.s versus 0.12 Pa.s) in the same experimental conditions.

Gelation kinetics are also faster with increasing alginate molecular weight ⁸³. Moreover, similar conclusions have been found after acidic treatment of high molecular weight alginate so that low molecular weight alginate obtained produced low viscosity gels ^{34,84}.

Effects of other novel processing methods have been studied. Such as high-pressure homogenization also called dynamic high pressure that caused a reduction of alginate molecular weight and viscosity under 300 MPa and after 5 cycles when a minimal viscosity plateau was observed ⁸⁵.

1.1.3.2 M/G ratio and distribution of G, M and GM units along the alginate chains

Alginate gelation is dependent of the percentage of G and M units, as a consequence of a higher degree of hindered rotation around the glycosidic linking. Because of this configuration, cross linking between alginate Ca²⁺ is mostly due to G units ^{41,84,86}. M units moderate elasticity and lateral association in alginate gelation. Gels formed with high percentage of M units are reported as soft and elastic while those formed with high percentage of G units are described as compact and rigid ⁸⁷ (Figure 1-5). Beads produced with low molecular weight and high G content alginate are the strongest, the biggest and best relevant to protect probiotics by encapsulation ³¹.

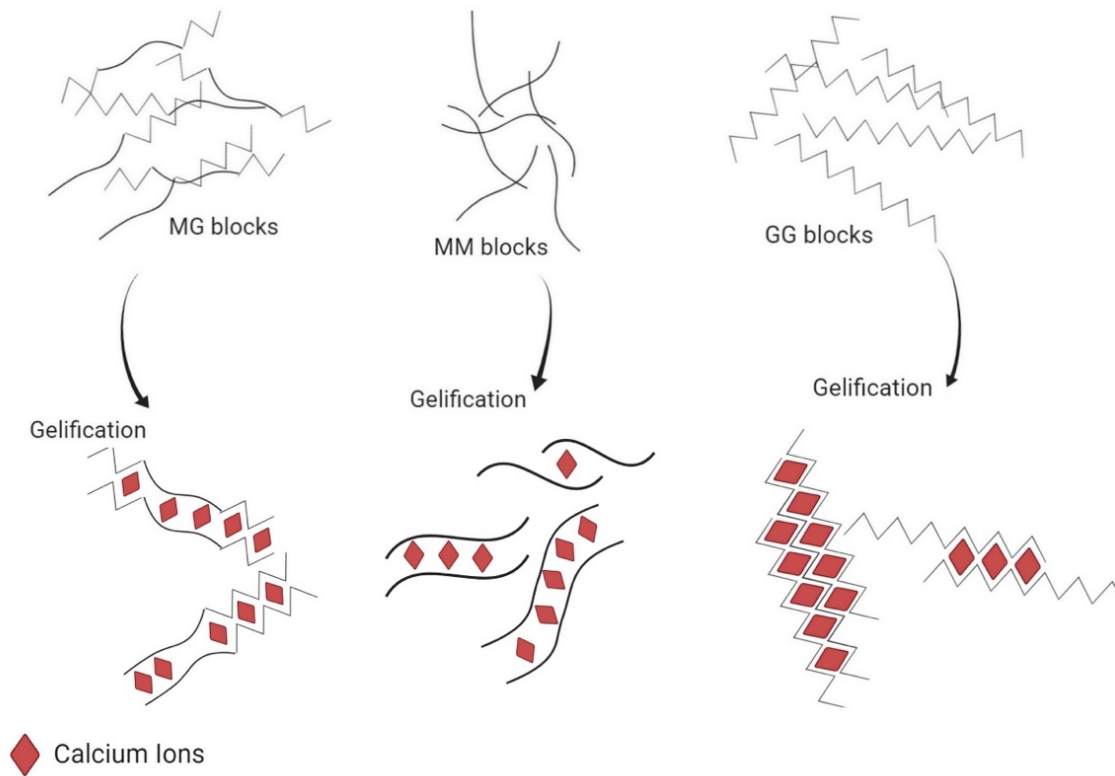


Figure 1-5. Effect of calcium on the MG, MM and GG alginate units.

1.1.3.3 Alginate Concentration

Gelation can be impacted by alginate concentration. Fernández Farrés *et al.* (2013) found that higher concentration of the biopolymer, in the range of 1% to 4% (w/w), induced higher viscosity, elasticity rupture strength and gel hardness. As expected, higher concentration of alginate molecules increased the number of cross-linking interactions with calcium ions and reinforced gel structure⁸³. However, excessive concentration of alginate reduced binding opportunities by decreasing Ca^{2+} diffusion through the matrix⁸⁸. Nevertheless, for moderate changes in alginate concentration from 1.3 to 1.7% [w/w], Hu *et al.* (2020) did not notice significant variations of alginate beads structure⁸².

In the case of beads processing, alginate concentration has also an impact on beads shape in alginate extrusion process, alginate beads tend to be more spherical when viscosity increases. The result of a bead made with the appropriate viscosity can be found in Figure 1-3C. Nevertheless, when viscosity is too high, beads are drop-shaped as shown in Figure 1-6⁸⁹.

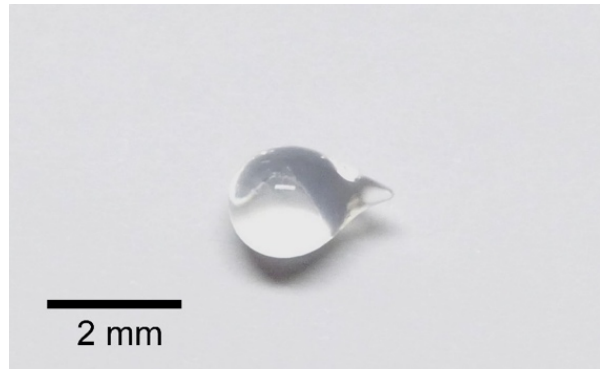


Figure 1-6. Example of a drop-shaped alginate bead.

1.1.3.4 Concentration of calcium ions

An increase of Ca^{2+} concentration results in an increase of cross-linking gelation rate. Faster diffusion of calcium ions in gels lead to higher gel viscosity, elasticity, and stability⁹⁰. The calcium versus carboxyl group concentrations ratio is called the R value and describes effect of Ca^{2+} on alginate gelation and it is defined as follows:

$$R = \frac{[\text{Ca}^{2+}]}{[\text{COO}^-]} \quad (1.1)$$

Alginate crosslinking with calcium ions can be described in three steps: (i) the mono-complexation at $R < 0.25$, (ii) dimerization at $0.25 < R < 0.55$ resulting in formation of the egg-box model; and (iii) third step occurs at $R > 0.55$ and results in the lateral association of the polymer chains forming intra or inter-clusters⁹¹.

Higher viscosity and maximum tensile stress of alginate gel are reached at around 1.4% (w/w) of $[\text{CaCl}_2]$ for alginate concentration equaled to 127 mM. Ca^{++} saturation of alginate chains can explain that maximum tensile stress occurred⁹². At high calcium concentration calcium ions induce excessive positive charges that will segregate alginate chains leading to the gel disintegration. The mechanism between alginate structure and calcium chloride concentration is illustrated in Figure 1-7.

It should be noted that, while producing alginate beads, a high calcium concentration also affects beads sphericity which tends to be less spherical at high calcium concentrations⁹².

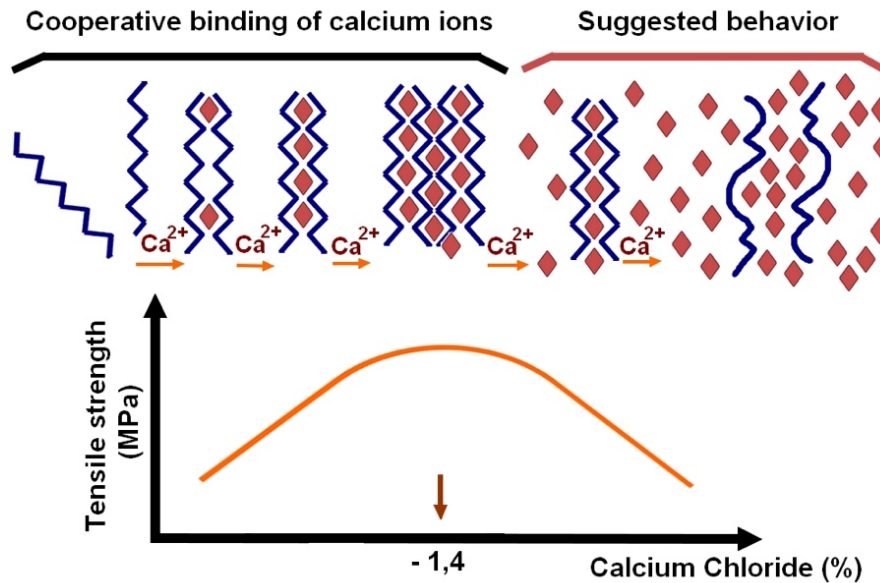


Figure 1-7. Scheme representing the mechanism of strengthening and weakening of the alginate gel as a function of the concentration of calcium chloride (Adapted ⁹²)

1.1.3.5 Residence Time

The time during which alginate is into contact with calcium ions in gelation bath is called residence time. When alginate drops are exposed to calcium, ions migrate from surface to core. Required residence time for reticulation (t_{gel}) can be calculated using Fick's second law which can be expressed as:

$$\frac{C}{\partial t} = D \frac{\partial^2 C}{\partial x^2} \quad (1.2)$$

Where C is alginate concentration (mol/m^3), t is time (s), D is diffusion substance coefficient (m^2/s) and x is the position (m).

Fick's second law can be approximated as:

$$\frac{C}{t_{gel}} \approx D \frac{C}{L^2} \quad (1.3)$$

Where C represents alginate concentration (mol/m^3), L is a characteristic length given by the bead radius (m), and D the diffusion coefficient of calcium chloride in water: $10^{-9}m^2/s$ ^{92,93}. It has been demonstrated that after a residence time of 30 min, samples exposed to different calcium concentrations showed similar behaviors ⁹². Residence time seems to have no effect on beads sphericity ³⁸.

1.1.3.6 pH

pH impacts alginate water solubility and ion-binding as it determines the electrostatic charges of G and M units. M and G units have pKa of 3.38 and 3.65, respectively. Alginate

polymer residues have pKa value usually estimated around 3.4⁹⁴. Alginate composed of a high content of MG-sequences are more soluble at low pH and precipitate at pH around 2.6 and 2.7 while high G units content alginate precipitate at pH around 3.25^{94,95}. At higher pH values (below pH = 10.5) glycosidic bonds of alginate gel start to weaken and break leading to structural degradation⁹⁶.

The microstructure of the alginate gel has been largely studied and it has been established that gel obtained at pH = 3.8 has a denser and interconnected microstructure due to stronger chains interactions. This phenomenon leads to less syneresis and shrinkage of the gel. Gels produced pH ≥ 5 present lower interconnectivity in their microstructure and lower density, then allowing syneresis and shrinkage⁹⁷⁻¹⁰⁰.

During preparation of alginate beads, interfacial tension is impacted by pH, lower pH values result in lower interfacial tension. pH also influences beads shape, beads produced in low pH gelation bath tend to be oblate, particularly in low alginate and ions concentrations, while those produced at pH > 4 tend to be spherical^{95,96,101} (see Figure 1-8).

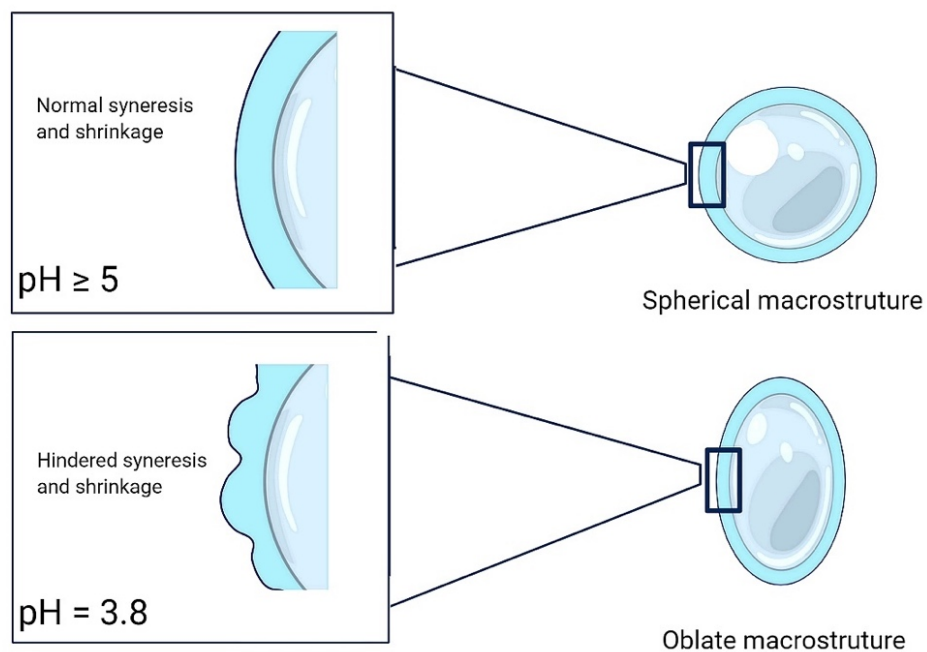


Figure 1-8. Macrostructure of alginate beads synthesized at pH= 3.8 and pH ≥ 5 .

1.1.3.7 Temperature

Gelation temperature has an impact on alginate gel microstructure. High temperature seems to enhance and facilitate calcium ions penetration through alginate network while low temperature slows down diffusion and gelation process. Low temperature led to more ordered and regular network and higher temperature produced a denser network with lower young's

modulus¹⁰². At physiological gelation temperature around 36-40°C, an alginate gel with high young's modulus was produced^{103,104}.

Jeong *et al.* (2020) reported that an increase in gelation temperature led to lower alginate viscosity and reduced beads size¹⁰². Gelation temperature seems also to influence beads sphericity that increased with higher gelation temperature. Besides, a high beads rupture strength was reported at low gelation temperature (5°C)¹⁰⁵⁻¹⁰⁸. If the gels are stable at range 0 to 100°C, more G units content increase alginate gels thermal stability³⁸. Above 100°C the structure began to depolymerize and at 180°C the gel was totally destructured³⁷.

1.1.3.8 Ionic strength

Gelation is impacted by solution ionic strength. Low ionic strength allows gel formation, but high level of monovalent salts competed with calcium ions for carboxyl alginate groups resulting in an instable and weak system. Van Leusden *et al.* (2017) reported a structural alteration of alginate beads exposed to high NaCl concentration¹⁰⁹. This modification might be due to a decrease of electrostatic attractive interactions into the system and/or increase in beads pore size resulting in the release of the encapsulated compounds⁸⁴. Apparently, salts ions dislocated some Ca²⁺ leading to gel disintegration. The extent of network destructuration increased with higher salts concentration⁸⁴.

1.1.3.9 Shear rate

Jiao *et al.* (2019) reported the influence of shear rate on the gelation method described as “*in situ* addition of calcium”, to favor homogenous gelation by avoiding disadvantages of external gelation. Shear rate had an impact on gelation kinetics: when shear was applied at the beginning of gelation process, the onset time of gelation was higher and gel particles were faster formed^{52,59,84}. However, gel viscosity decreased with increasing shear rate applied demonstrating the relation between shear rate and gel rheology²².

In conclusion for factors influencing alginate gelation and spherification, Table 1-2 summarizes the effect of the principal parameters on alginate beads gelation. We choose to present the clearer effect for an efficient production of alginate bead with desired properties. Some parameters have not been enough studied to appear in our summarized Table 1-2 and factors as pH has an effect depending on application.

Table 1-2. Effects of increased factors influencing alginate gelation and spherification

Enhanced Parameters	Effects of gel formation				Effects on beads formation			
	Viscosity	Compactness	Network stability	Ca ²⁺ penetration kinetics	size	strongness	sphericity	rupture strength
Alginate structure								
↗Molecular weight	↗	↗	↗	↘	↘	↗	↗↘	↗
↗M/G ratio	↘	↘	↘	-	-	↘	-	↗
Experimental environment								
↗ [alginate]	↗	↗	↗	↘		↗	↗↘	
↗ [Ca ²⁺]	↗	↗	-	↗	-	-	↘	
↗Temperature	Optimum at 36-40°C	↘	↘	↗	↘	-	↗	↘

1.1.4 Composite Alginate gels

Composite gels with alginate and other polymers have been studied for multiple purposes and in many fields, such as encapsulation, packaging films, or edible films. This interest results from the ambition to modify gel mechanical properties ¹¹⁰, brings new characteristics and extends its use. Polysaccharides and proteins are the main components used for copolymerization. Depending on copolymer nature mixed with alginate, gelation process varies as described below.

1.1.4.1 Polysaccharides as co-polymer

1.1.4.1.1 Pectin

Pectin is a biopolymer extracted from plant cell walls like citrus peel or apple pomace. B. Zhang et al. (2019) reported that pectin gelation is enhanced by addition of guluronic units. Encapsulation in alginate-pectin gel exhibited a significant reduction of anthocyanins degradation ^{111,112}. A lower energy consumption has also been demonstrated in jelly candy manufacturing using alginate-pectin cold gelation instead of traditional heating process ¹¹³.

In the medical field, alginate-pectin hydrogel presented great improvement of mechanical properties, water absorption, thermal stability, and drug release for wound dressing application ^{50,114}. In food industry, pectin-alginate-gelatin composite gels showed promising results for probiotics encapsulation, by increasing stability of encapsulated bacteria ¹¹⁵.

1.1.4.1.2 Gums

1.1.4.1.2.1 Guar gum

Guar gum is extracted from guar beans (*Cyamopsis tetragonoloba*). It is composed of a linear chain of (1-4)- β -D-mannopyranose linked with β -galactopyranosyl groups. Guar gum is water soluble and usually used in coating. Guar gum is used as thickener of alginate-guar gum gel ^{116,117}.

Gel made with alginate/guar gum was stronger at lower calcium level than pure alginate gel and presented a high elasticity and rigidity due to a lower degree of porosity. It reduced syneresis and shrinkage during storage. Guar gum addition to alginate enhanced network stability in acidic conditions and thermal processing ^{116,118}. Alginate-guar gum gel exhibited an improved polyphenols and betacyanins encapsulation ¹¹⁹, and enhanced preservation of antioxidant activity for encapsulated fatty acids ¹²⁰.

1.1.4.1.2.2 Gum arabic

Also known as acacia gum, gum arabic is a natural polymer extracted from acacia trees and it consists of β -D-galactopyranosyl units branched with side chains of L-rhamnose, D-galactose, L-arabinose and D-glucuronic acid. This polymer is largely used in food, cosmetic and pharmaceutical industries as thickening agent and stabilizer ¹²¹. Interaction between alginate and gum arabic has been recently studied by Sabet *et al* (2021). These authors reported interactions between polymers at pH 7 and a stronger synergy at pH 4, due to ionic interactions between respective negative and positive charges of alginate and gum arabic. The ionic binding between alginate and gum arabic results in an increase of gel viscosity and viscoelasticity ¹²².

The alginate/gum arabic composite exhibited great results in drug encapsulation. Moreover, Nayak *et al* (2012) reported an encapsulation efficiency of $86.02 \pm 2.97\%$ ¹²³.

1.1.4.1.2.3 Other gums

Other gums such as galbanum gum or basil seed gum have been investigated recently for different applications, especially in food packaging field. Addition of gum to alginate matrix brings a real advantage in terms of barrier function against gas, water, oil transport ^{118,124}.

1.1.4.1.3 Chitosan

Chitosan is a linear polysaccharide extracted from crustaceans' shells chitin. It is a nontoxic biopolymer formed by D-glucosamine and N-acetyl glucosamine units. Chitosan is used in numerous fields due to its numerous properties, *i.e.* antioxidant, lipid binding, anti-inflammatory and antimicrobial effects ¹²⁵.

Chitosan gel viscosity increases with pH. The strongest alginate-chitosan gels were obtained with increasing pH and chitosan weight percentage, but considerable viscoelasticity and maximum encapsulation capability were obtained at neutral pH¹²⁶. Combining alginate and chitosan improves mechanical and chemical gel properties and favors thermal resistance. Chitosan has been largely investigated in coating alginate capsules, due to its positive charges that lead to an ionic complexation with negative charges of alginate. This complexation allows chitosan solubilization into a non-acetic acid or hydrochloric solutions. Thereby, coating with chitosan enhanced capsules membrane thickness and their protective abilities^{127–129}.

Composites exhibited great results for globulin preservation during thermal treatment^{125,130}. De Prisco et al (2015) reported a better stress tolerance to food processing for probiotics encapsulated with alginate-chitosan composites¹³¹.

Alginate/chitosan composites have been examined for oil co-encapsulation or microencapsulation to protect oil from oxidation, capsules showed good oxidative stability and oxidation products were lower for chitosan/alginate compared to non-encapsulated oil. Results also showed an effective oil vehicle for nutraceuticals^{132,133}. Microwave treatments have also been considered for drugs controlled-release alginate/chitosan microbeads. Depending on experimental conditions, microwave treatments could induce cross-linkage or breakdown. Thus, Wong et al. (2002) reported a retarded drugs release from alginate/chitosan beads treated at 80 W for 10 minutes as a consequence of enhanced alginate/chitosan cross-linking¹³⁴.

1.1.4.1.4 Carrageenan

Carrageenan is a sulphated polygalactan that can be obtain from red seaweeds, it contains 15 to 54% charged sulphate ester groups. This polysaccharide is formed by D-galactose and 3,6-anhydro-galactose linked by α -1,3 and β -1, 4-glycosidic bonds. There are various carrageenan types: λ , κ , ι , ϵ , μ . The classification depends on the sulphate ester groups number and position¹³⁵. Alginate/carrageen composite have been largely investigated in edible films formulation for food and non-food applications; good barrier and protection properties have been reported¹³⁶.

Combination of κ -carrageenan and alginate enhances gel rigidity and mechanical stability. Carrageenan/alginate composite gel appeared more transparent than conventional alginate gel with a compact and smooth surface. Addition of carrageenan tends also to improve thermal properties, elastic modulus, gel water content, and swelling which is induced by

sulphate groups from carrageenan molecules. Beads formed with carrageenan/alginate composite had a larger diameter than alginate beads ^{137,138}.

The pH-dependent properties allowed use of carrageenan/alginate complex in a pH-responsive beads for insulin encapsulation. In this study, protection against acidic condition and controlled release were investigated ¹³⁹. Good protection was observed at pH=1.2 and progressive release with good kinetics was noticed at pH=7.4. This point made composite carrageenan/alginate beads promising encapsulation matrix for oral insulin intake. Gu et al (2021) worked on immunoglobulin encapsulation for controlled release and reported high encapsulation efficiency. Composite exhibited a denser internal microstructure and a good protection in acidic gastric conditions ¹⁴⁰.

1.1.4.1.5 Starch

One of the most abundant and cheap natural polysaccharides is starch. Starch contains amylose and amylopectin with linkage of α -D-glucopyranose molecules. Starch is largely used in hydrogel production, due to its free hydroxyl groups. Starch works in synergy with alginate. Water absorption capacity and encapsulation efficiency are improved. For instance, López Córdoba et al. (2013) reported improvement of encapsulation efficiency from 55 to 65% of liquid extract of yerba mate (a high polyphenols tea-like beverage) ^{141,142}.

The synergy between starch and alginate depends on chemical structures of both polymers, but also on processing conditions, such as pH, ionic strength, and salts concentration ¹⁴². Gelation of alginate/starch composite occurs using different divalent cations (Mn^{2+} , Zn^{2+} , Ca^{2+} for example), and characteristics of the composite gel vary from an ionic crosslinker to another ¹⁴².

Addition of starch to alginate creates composite gels with variable porosity depending on starch type, but starch addition provides a slower release of encapsulated substances ^{143,144}. Starch type impacts gel water retention, stability, and digestibility. Those features must be considered in the formulation of controlled release beads. For instance, Hassan et al (2020) obtained promising results for gradual release of nisin encapsulation ^{144,145}.

Feltre, Sartori, et al (2019) recently reported an efficient encapsulation of oil with starch incorporation in alginate systems, due to greater oil dispersion into oil/starch/alginate emulsion. Beads formed by oil/starch/alginate emulsions containing equal proportions of alginate and starch presented good results in terms of antioxidant activity preservation and storage stability

¹⁴⁶. Similar results concerning encapsulated component stability have been obtained by Jain et al (2020) for lycopene encapsulation with an enhanced bioaccessibility. This could be promising for nutraceuticals and functional foods application ¹⁴⁷. As an example, alginate/starch/gelatin composite has been recently investigated for encapsulation of β -carotene in oil/starch/alginate/gelatin emulsion. The study demonstrated a great stability and oxidation reduction for encapsulated β -carotene compared to β -carotene in free oil. Those results are very important to extend shelf-life of components sensitive to oxidation during processing for food or drugs application ¹⁴⁸.

1.1.4.2 Proteins/ polypeptides as co-polymer

1.1.4.2.1 Whey Proteins

Under specific conditions, proteins can be used as cations source for alginate gel cross-linking. Thus, alginate/proteins composite hydrogels are largely investigated and exhibited great results in protein carriers with controlled release kinetics ¹⁴⁹. Denatured whey protein isolates and alginate composite gels have shown great thermal stability after 1 minute at 63 and 72°C and a good resistance to acidic conditions for encapsulated probiotics by extrusion or spray-drying process ^{70,150,151}. Dehkordi et al (2020) worked on an alginate/whey protein isolate composite for probiotics encapsulation and reported a highest survivability of *lactobacillus acidophilus* for an optimal matrix composed of 4.54% (w/v) of alginate and 10% (w/v) of whey protein isolate ⁶⁹.

Recent studies showcased interest of protein addition in edible alginate films. Chkravartula et al (2019) reported significant beneficial effects of whey protein on the physico-chemical, rheological, mechanical, and optical properties of edible packaging. Addition of whey proteins to alginate decreased film viscosity and enhanced its hydrophobicity and reduced film water absorption ¹⁵².

1.1.4.2.2 Gelatin

Gelatin is largely studied in coacervation process, which is a spontaneous phase separation between an insoluble complex and of another aqueous phase that occurs with pH change ¹⁵³. Consequently, gelatin and alginate are pertinent materials for encapsulation process by coacervation. Promising results have been obtained for essential oils microencapsulation, especially with a 4% gelatin and high essential oils concentration matrix, with a 73.7% encapsulation efficiency, and a good terpenes preservation ^{153,154}. Moreover, Y. Li et al (2019) reported a good effectiveness of alginate/arabic gum /gelatin composite for preservation of

encapsulated antioxidant substances for oral delivery ¹⁵⁵. Lemos et al (2017) also observed high encapsulation efficiency in the production of buriti oil microcapsules through coacervation ¹⁵⁶.

M. Lopes et al (2017) worked on probiotics encapsulation using an alginate/gelatin composite matrix. Spherical and regular beads were obtained, and higher cells viability was reported at 1% w/v alginate and 0.1% w/v gelatin. Therefore, beads contained up to 10⁵ CFU g⁻¹ after 4 months of storage ¹⁵⁷. Table 1-3. (next page) summarizes all copolymers cited and the effects of their addition to alginate solution.

1.1.5 Other Encapsulation processes using alginate

1.1.5.1 Spray-drying

Spray-drying is known since the 1930's as one of the earliest encapsulation techniques due to its simplicity of application and high productivity among many other advantages ¹⁶². The process principle is injection of a solution (emulsion or dispersion with active compounds) through a simple nozzle or centrifugal wheel. The liquid is then atomized into small droplets which fall and meet hot air in a drying chamber. After water evaporation, particles fall to the bottom of the chamber and are collected in a powder form. Spray-drying process is applied in many fields and several wall materials can be used. Alginates exhibit good results for volatiles and emulsions encapsulation ^{163,164}.

The efficiency of spray-drying process depends strongly on inlet air temperature, particularly for thermolabile substance encapsulation, and can affect particles chemical and physical properties in addition to core materials stability ¹⁶⁵. In this perspective, Sun et al (2020) studied the impact of inlet air temperature on spray-drying microencapsulation of lipophilic carvacrol in an oil-in-water emulsion with alginate/pectin composite shell material. They reported an optimum temperature for spray-drying encapsulation between 100 and 130°C for carvacrol. However, even if a higher temperature tends to increase encapsulation efficiency, it leads to reduce moisture content and retention efficiency ¹⁶⁵.

Recently, Stobel et al. (2018) presented a new encapsulation process using spray-drying technology and called the Cross-Linked Alginate Microcapsules process (CLAMs process). It uses a calcium ions source which is insoluble at feed pH, but when solution is atomized the base present in the matrix evaporates which drop its pH and allows calcium ions to solubilize and react with alginate. The advantage of this process is to reduce the multi-step conventional spray-drying process into a one-step operation ^{60,166}.

Table 1-3. Co-polymers for alginate composite gels for encapsulation

Co-polymers	Composition	Positive effect of co-polymer addition to alginate	Application	Refs
Pectin	α -D-galacturonic acid α -L-rhamnose	Encapsulated substance stability. Gel water absorption and thermal stability. Lower gel viscosity.	Probiotics encapsulation. Cold gelation for candy manufacturing.	113–115,158.
Guar gum	β -D-mannopyranose β -galactopyranosyl	Strong gel Low porosity gel Network stability to heat and acidic conditions	Coating for food packaging Fatty acids encapsulation	116,117,120
Gum arabic	β -D-galactopyranosyl L-rhamnose D-galactose	High viscosity and viscoelasticity gel Encapsulation efficiency	Drugs encapsulation Radish juice liquid-core encapsulation	121–123
Chitosan	D-glucosamine N-acetyl-glucosamine	Mechanical, chemical properties and thermal stability. Gel protective abilities and permeability	Protein encapsulation Omega-3 rich oil encapsulation Coating capsules	125,127,130,133
Carrageenan	D-galactose 3,6-anhydro-galactose	Gel rigidity and mechanical stability (elastic modulus). Water content, thermal properties, and swelling.	Immunoglobulins encapsulation Edible films for food application	135,136,140
Starch	Amylose Amylopectin α -D-glucopyranose	Water absorption. Better oxidation stability Capsule digestibility	Spirulina encapsulation Edible films for food packaging Nisin or lycopene encapsulation	146,147,159,160.
Whey protein	α -lactalbumin β -lactoglobulin Albumin Immunoglobulins	Gel antioxidant properties Active protection against visible light, heat, and acidic conditions	Films for food packaging Probiotics encapsulation	70,152,161
Gelatin	Amino acids	Encapsulation efficiency Set up coacervation process	Essential oils encapsulation Probiotics encapsulation Antioxidant encapsulation	154,155,157

Stobel *et al* (2020) worked on fish oil encapsulation using the CLAMs process and reported good results in term of shelf-life of encapsulated fish oil in a shell material made of modified starch and alginate. Some promising enteric release properties were also observed for gastrointestinal delivery of lipophilic bioactives ⁶¹.

1.1.5.2 Spray-cooling

Also known as spray-congealing or prilling, spray-cooling is a process that allows atomization of a liquid into small particles. The process is similar to spray-drying, the solution is injected through a pressure nozzle, vibrating nozzle or a spinning disk into an atomization chamber. Unlike spray-drying, the atomized liquid is cooled and hardened ¹⁶⁷. Encapsulation by spray-cooling allows encapsulation of actives ingredients dispersed into a liquid matrix. Instead of spray-drying, encapsulation by spray-cooling allows encapsulation of thermolabile substances ¹⁶⁷. This process is used in food and nutraceutical industry for preservation of flavour ¹⁶⁷, vitamins ¹⁶⁸, or other bioactive ingredients like probiotics ¹⁶⁹.

1.1.5.3 Coacervation

Coacervation occurs in a colloidal system and leads to liquid/liquid phase separation between a colloid-rich phase also known as coacervate phase and a solvent-rich diluted phase. The coacervate phase can be composed of a single polyelectrolyte. In this case, it is called simple coacervation. Complex coacervation occurs when the coacervate phase is composed of an ionic complex of two opposite charges polyelectrolytes as for alginate complex coacervation for encapsulation purposes. Solution pH strongly impacts coacervate formation, in addition to polyelectrolytes concentrations and their mixing ratio, ionic strength and temperature ^{170,171}.

Combination of proteins and alginate is often studied for delivery systems, and in many fields such as food, cosmetic and pharmaceutical industries. Gorji *et al* (2018) worked on characterization of alginate, beta-lactoglobulin and bovine serum albumin interactions in solution. A protein-alginate ratio of 2:1 was used for this study. Being amphoteric proteins, Beta-lactoglobulin and bovine serum albumin have an isoelectric point of 5.2 and 5, respectively. They present positive charges at lower pH where alginate exhibit negative charges at low pH. Therefore, complex coacervation occurred mainly at pH range between ~1.6 and 4.2 where due to opposite charges of alginate and proteins ¹⁷¹.

Another complex coacervation using gelatin and alginate has also been largely studied for encapsulation. Alginate, negatively charged at low pH, can form a complex coacervate with gelatin for essential oil encapsulation. Heckert Bastos *et al.* (2020) reported an optimum ratio of 6:1 gelatin to sodium alginate and a pH of 4 for black pepper essential oil encapsulation with an efficiency up to 82 % ¹⁵⁴. Similar efficiency result (74 %) has been reported for citronella

essential oil encapsulation using 4% of gelatin and 10 % of alginate. Microcapsules with a 434 μm diameter have been obtained with promising results for controlled release ¹⁵³.

For olive oil encapsulation, microcapsules sizes increase with the increase of oil amount but decreases with the increase of surfactant amount. Besides, FTIR spectra of free olive oil and microencapsulated oil have shown same characteristics so that no interactions between oil and alginate/gelatin composite have been exhibited ¹⁷².

1.1.6 Conclusion

Alginate is a widely used and investigated polymer for a large variety of technical applications as thickener or stabilizer but also in spherification process for its gelation ability to encapsulate sensible materials. It is Generally Recognized as Safe (GRAS), being nontoxic, nonantigenic, satisfactorily biocompatible, and sufficiently biodegradable.

Alginate gelation depends on polymer chemical structure counting its molecular weight and M/G units ratio and distribution along the alginate chain. Experimental environment greatly influences alginate gelation including pH, temperature, polymer concentration, crosslinker concentration, residence time and ionic strength.

Alginate has the advantage to be an encapsulation material adapted for most encapsulation process especially spherification (extrusion and coextrusion) through its biocompatibility and capability to form a hydrogel through ionic cross-links with divalent cations, such as calcium ions. However, alginate has some limitations in certain applications (Table 1.4). Therefore, alginate can work in synergy with many polymers (e.g. polysaccharides and proteins). Thus, composite alginate gels are widely studied recently in order to improve alginate encapsulation and spherification properties, including encapsulation efficiency and payload, storage stability and barrier properties.

Alginate is certainly one of the most promising encapsulation materials. Therefore, in the following section of the manuscript, we focused on alginate-based core-shell capsules produced through coextrusion process, which is the main encapsulation process treated in our work. Thus, main principles and technologies coextrusion process are presented here, prior to a state of the art of recent applications employing coextrusion technology.

Table 1-4 Advantages and limitations of principal encapsulation methods using alginate.

Methods	Advantages	Limitations	Refs
Extrusion	<ul style="list-style-type: none"> - Easy application and industrialization - Hydrophilic matrix - Encapsulation of a large variety of substances - Protection against oxidation - Long shelf-life - various capsules size 	<ul style="list-style-type: none"> - Low payload - Requirement of thermal treatment not compatible with heat-sensitive ingredients encapsulated -High porosity of microcapsules -Pure oil encapsulation in complicated 	63,173
Coextrusion	<ul style="list-style-type: none"> -Large payload -Slow-release kinetics compared to other methods -Large variety of core materials -Scaled up process -Additional protective barrier brought by the shell - Encapsulated material is surrounded by wall material 	<ul style="list-style-type: none"> - Risk of nozzles obstruction due to their small size - Process highly dependent on core and shell fluid rates - Multifluidic technology expensive costs vs other methods -Difficulty to encapsulate extremely viscous matrix 	78,81,173
Spray-drying	<ul style="list-style-type: none"> -Inexpensive technology and availability of the equipment - Possibility to perform double or triple encapsulation - Good encapsulation efficiency - Good stability for storage -Quick process. -Low product volume for reduced transport cost 	<ul style="list-style-type: none"> - Limited shell materials choice - Exposition risk due to volatiles compounds at high temperature - Oxidation and degradation of thermolabile substances - Particles agglomeration - Particules size control 	163–165
Spray-cooling	<ul style="list-style-type: none"> -Inexpensive technology for encapsulation -Large possibility of materials -Fast release (depending on the main objective) -Controlled size and higher specific surface area vs particles spray-dried. 	<ul style="list-style-type: none"> - Weak protection on particles surfaces - High energy and cost required -Longer process time vs spray-drying - Handling and storage specific requirements 	167,173,174
Complex coacervation	<ul style="list-style-type: none"> -High payload -Controlled release possibilities -Flexible regarding shell material -Large particles size range -No specific equipment required 	<ul style="list-style-type: none"> -Expensive process -Technique complexity - Low size range of capsules - Cohesion and adhesion of microcapsules. - Presence of solvents residues in spheres 	173,175–177

Key highlights

- Alginate gelation is related to its molecular structure and experimental conditions.
- Spherification is one of the most studied encapsulation processes.
- Alginate a very versatile material that can be used in most encapsulation processes.
- Polymers addition improves alginate spherification and encapsulation properties.

1.2 Alginate Core-Shell Capsules Production through Coextrusion Methods: Principles and Technologies (*published in Drug marines*)

1.2.1 Introduction

Encapsulation technologies began back in 1872 with Samuel Percy's conception of spray drying. By 1875, Cains suggested a coating technique and described the basic fundamentals of coating and enrobing still used today, in particular with bottom spray fluid-bed coating. Later, in 1957, Green and Schleicher invented a micrometric oil-containing capsule that would later be called coacervation. Liposomes, as self-assembled phospholipids structures were initiated by Bangham mid-1960s^{1,178-181}. Encapsulation as a protective method to stabilize active materials of interest appeared mid-1980s. Active molecules as drugs, flavours and perfumes have attracted industrial and scientific attention for encapsulation, particularly with porous shelled encapsulant^{1,182}.

Nowadays, encapsulation involves coating or entrapment of a core material (liquid, solid or gas) such as food ingredients, enzymes cells, bioactives or others¹⁸³. Encapsulation can help compounds incorporation into others matrices (e.g. flavours)^{184,185}, controlled delivery (e.g. drugs)^{186,187}, or compound stabilization during storage (e.g. Antioxidants)¹⁸⁸. Encapsulation technology is applied in cosmetic, food, pharmaceutical, agriculture and textile industries due to economic interest of the technology^{185,189-192}. Microencapsulation permits to generate small particles with a wide range of size from 1 μm to 1 mm. Spherification process is an encapsulation technique that generates capsules larger than 1 mm (macrocapsules or spheres). Further, capsules with sizes lower than 1 μm are usually called nanocapsules¹².

The process of alginate gelation is commonly used in encapsulation to create small, ideally spherical particles known as capsules¹⁹³. Alginate, which is Generally Recognized As Safe (GRAS), is often used in this process due to its non-toxic, non-antigenic biocompatible, and biodegradable properties. Alginate is a versatile material with numerous applications in industries such as textiles, cosmetics, pharmaceuticals, and food, where it is used as a thickener, stabilizer, coating material, and disintegrating agent¹⁹⁴. Alginate ability to form a hydrogel through ionic cross-links with divalent cations, usually calcium ions, makes it a popular choice for encapsulation technology. Alginate is composed of β -D-mannuronic acid (M blocks) and α -L-guluronic acid (G

blocks), linked through glycosidic linkage, with the percentage of these blocks varying among different algae species ¹⁹⁵.

Alginate gelation is influenced by the size of the polymeric chains, with higher molecular weight leading to tighter cross-linking and higher viscosity gels. Gels with a high percentage of M units are soft and elastic, while those with a high percentage of G units are more compact and rigid ¹⁹⁶. Beads and capsules made from low molecular weight alginate with high G content are compact and rigid ¹⁹⁶. Alginate concentration also affects the gelation process, with higher concentrations resulting in stronger gels, but also high viscosity gels. This aspect should be considered and adapted to nozzle size used to avoid clogging ¹². It also appears that high viscosity gels tend to produce non spherical capsules. Also, excessive concentration can limit binding opportunities ¹².

Numerous studies have explored modifying alginate structure to change its properties, including using acid hydrolysis, microwave-assisted acidic hydrolysis, enzymatic treatment, thermal treatment, and ultrasound treatment ^{197,198}.

Alginate is a highly suitable encapsulation material for a wide range of processes, However, there are certain limitations of alginate for certain applications. To overcome these limitations, researchers are investigating composite alginate gels made with other polymers such as polysaccharides and proteins. These composite gels aim to enhance alginate encapsulation properties, such as encapsulation efficiency, payload, storage stability, and barrier properties ^{199–201}.

Many encapsulation methods can be used to face the wide range of core and shell material and targeted capsules size. Spray-drying technology is probably one of the most used encapsulation techniques due to its high productivity but presents limitations for heat sensitive compounds ²⁰². Extrusion methods and liposomes are also largely used for encapsulation ^{13,203}. Coextrusion can be applied to solve limitations encountered for core-shell capsules production by simple extrusion ²⁰⁴, such as size higher than 1mm, capsules agglomeration, or shells thickness nonuniformity ^{202,205}.

In the present paper, a state of the art of coextrusion technology is established. Regrouping the main coextrusion methods used core-shell capsules production. Here we detailed their principles and functioning to facilitate further applications.

1.2.2 Principle of Coextrusion Process

The target capsules size often determines the coextrusion process and the appropriate parameters as liquid feed rate and nozzle diameter (Figure 1-9). It appears that larger capsule size for large nozzle internal diameter is produced at low and high feed rates by dripping (drop-by-drop) and jetting techniques, respectively. Also, a spray can be obtained by adjusting nozzle size/feed rate for reduced capsule size. Based on that, our review will consider four principal methods for encapsulation by coextrusion: dripping system, jetting system, centrifugal system and electrodynamic system.

Additionally, solutions characteristics should be considered before choosing a coextrusion method, especially viscosities, as seen in Figure 1-9 some methods require the use of very small nozzles, those can be easily clogged at high viscosities. Surface tensions being a key parameter for droplets formation has also to be considered. Also, especially for methods applying electric charges, volatility and safety aspects should be examined.

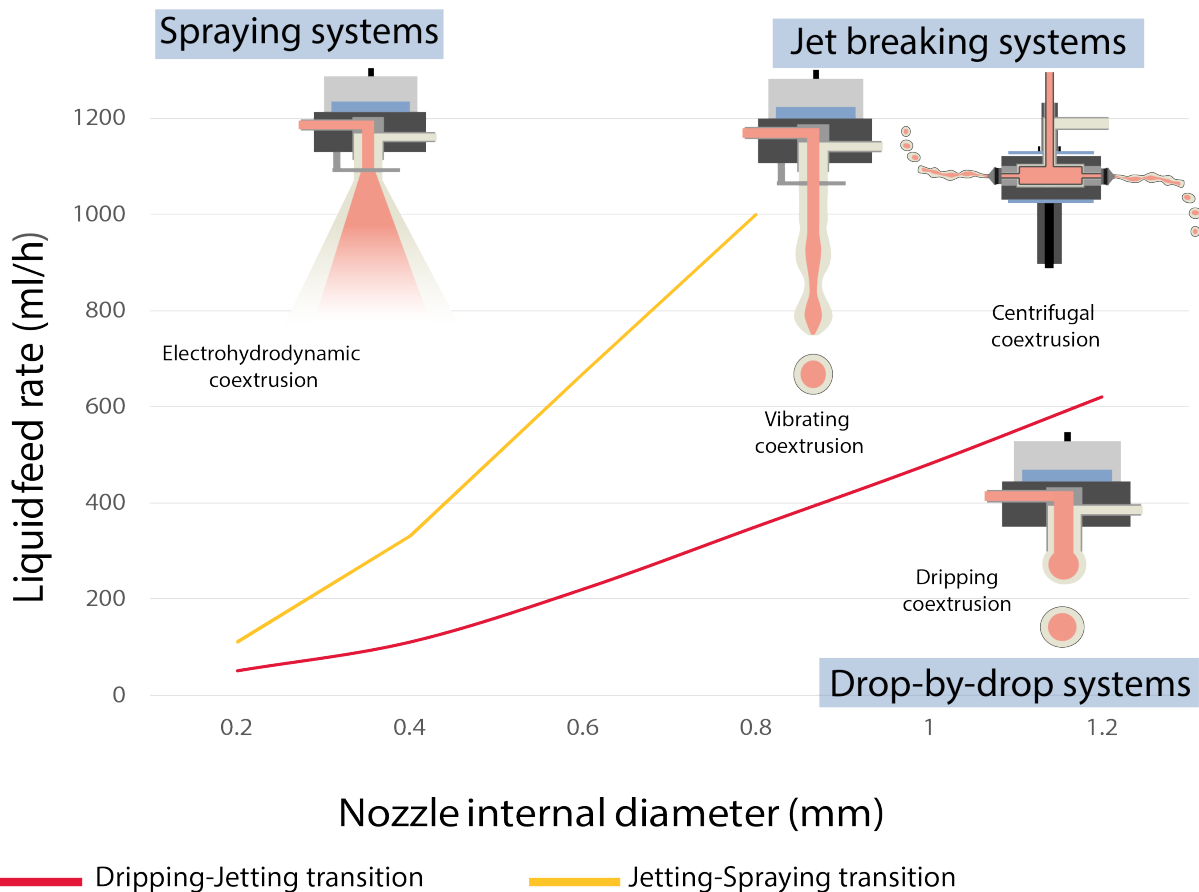


Figure 1-9. Illustration of different injection methods produced with various feed rates and nozzle internal diameter.

For efficient encapsulation, core and shell solutions must have mechanical properties compatible with the coextrusion process: viscosities under 2000 mPa.s, interfacial tensions between 10 and 72 mN/m and fluid densities between 0.7 and 1.3 ⁷⁸. For core-shell structure formation, immiscibility of core and shell solution is an important factor to prevent core and shell solutions mixing before and during shell gelation. Furthermore, thermal properties of core and shell solutions should be considered to avoid heating of core material if the coextrusion process requires heating, *i.e.* waxes, ^{13,206}.

1.2.2.1 Dripping Coextrusion System

Dripping coextrusion, also called drop-by-drop coextrusion, is the simplest coextrusion method and serves as foundation for many other coextrusion methods. It produces core-shell capsules through simultaneous extrusion of shell material (generally polymer solution *i.e.* alginate) into an external nozzle and the core material (aqueous or lipidic formulation containing the substances to encapsulate) in an internal nozzle. Dripping coextrusion system is presented in Figure 1-10 where gelling bath contains calcium ions as crosslinking agent for alginate.

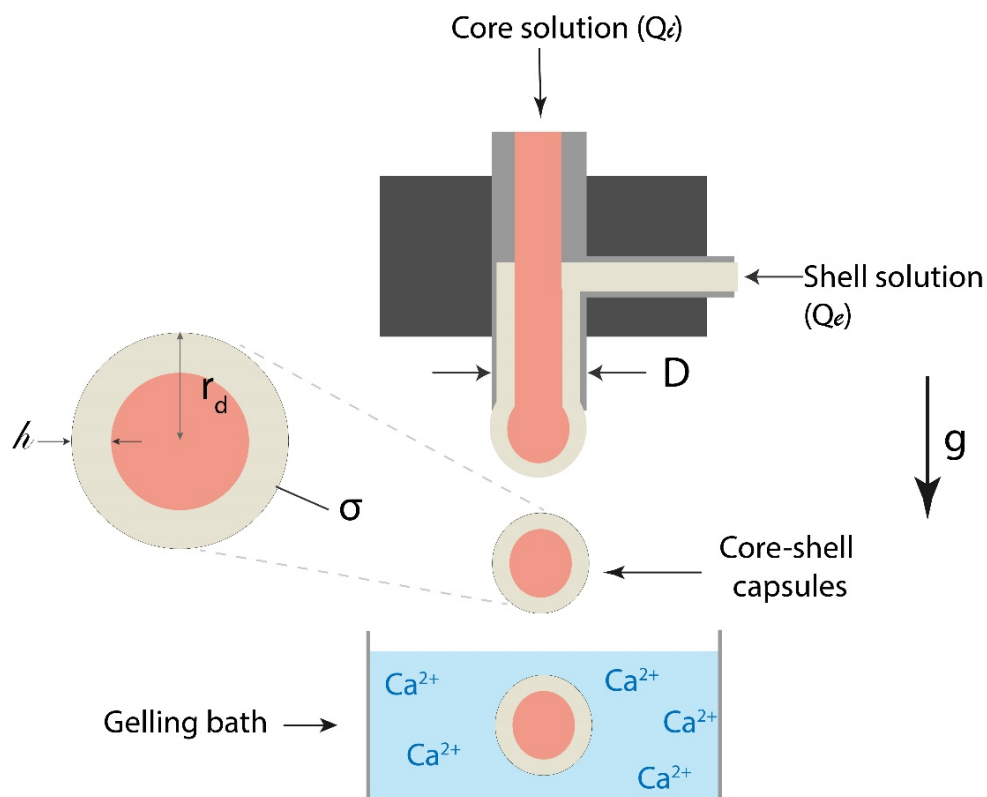


Figure 1-10. Dripping coextrusion system process for “alginate shell-core” capsules formation.

Dripping coextrusion is a great technology to produce alginate-based capsules for oil or aqueous cores. Therefore, the process has been described mathematically ²⁰⁷. Therefore, the low flow rate results in the formation of a core-shell drop which stays attached to the injection system until its weight exceeds the capillary force maintaining it on the nozzle. After drop fall, a part of it, stays attached in the injector, so that, when falling from the nozzle with a diameter D , the radius of a core-shell drop r_d can be given by the following empiric equation:

$$\frac{r_d}{D} \approx 3,5 \left(\frac{C_l}{D} \right)^{2/2.81} \quad (1.4)$$

Where $2/2.81$ as constant and With C_l is the capillary length and is defined by:

$$C_l = \sqrt{\frac{\sigma}{\rho g}} \quad (1.5)$$

Where σ is the surface tension (N m^{-1}), ρ the volumic mass of the liquid (kg m^{-3}) and g is gravitational force equivalent (9.81 N/Kg) ²⁰⁸. The capillary length is of the order of 2 mm for most liquids ²⁰⁹.

The shell thickness, h , of the capsule can be controlled with the ratio between internal and external flow rates ²¹⁰. h can be approximated from equation 1.6:

$$h = r_d \left(1 - \left(\frac{R_q}{1 + R_q} \right)^{\frac{1}{3}} \right) \quad (1.6)$$

With R_q is the flow rates ratio given as:

$$R_q = \frac{Q_i}{Q_e} \quad (1.7)$$

Where Q_i is the internal flow rate (core) and Q_e is the external flow rate (shell).

Experimentally, the shell thickness is not homogenous and usually thicker at the breaking point with the injector (see Figure 1-11B). From equation 1.6, an increase in the ratio R_q induces a decrease in the average shell thickness ²⁰⁸. The core-centricity depends probably on core solution properties, in addition to core flow rate. Experimentally, it was observed that small capsules have a more centered core. Additionally, disparity in core and shell solution densities could generate off-centered core in core-shell capsules ⁷⁸.

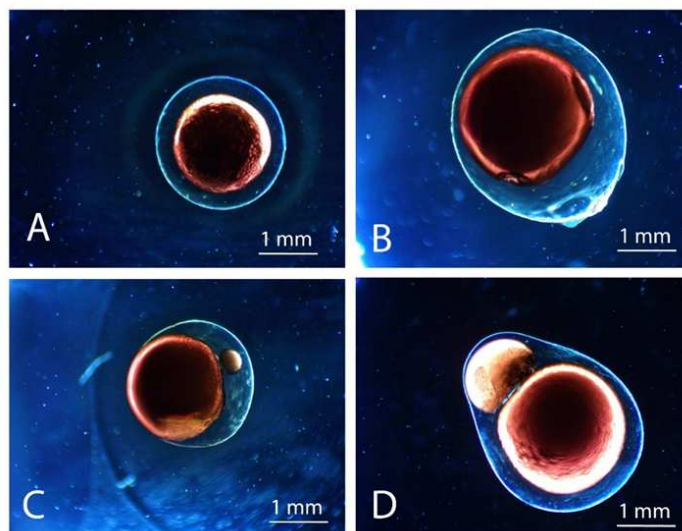


Figure 1-11. Microscopy pictures of different core-shell capsules aspects produced by coextrusion technology, (A) centered core, (B) decentered core, (C) satellite incorporation into the shell, (D) doublet capsule.

During dripping, the core-shell drop is characterized by the surface tension related to the shell solution as well as the core solution. For miscible phases, a mix happens inside the drop before gelation and no core shell capsule can be produced. In addition, when the core-shell drop falls it hits the gelling bath surface leading to the deformation of the capsule. However, surfactant addition to the shell solution as well as in the gelling bath, exhibited great results in terms of capsules formation and facilitated drop penetration into gelling solution. Surfactants allowed the production of capsules with thinner shells than without surfactant ²¹¹.

Capsules properties, such as shape, size and stability, depend on experimental conditions in addition to the alginate composition, i.e. high viscosity alginate solutions tend to produce more spherical capsules ^{12,212}

To overcome diffusion phenomenon and fast release of core content, multi-layer capsules can be considered. Dripping coextrusion has been adapted with the addition of a third coaxial tube to allow multi-layered capsules ^{208,213}. Different shells and core thicknesses can be controlled with core and shells solutions flow rates. An increase of core flow rate induces capsule and core diameter increase, with a decrease of both outer and inner shells thickness. Increasing intermediate layer flow rate leads to an increase of capsules diameter, an increase of inner shell thickness and a decrease of outer shell thickness. An increase in outer layer flow rate results in an increase in capsules diameters and outer shell thickness without significant effect on inner shell thickness and core diameter ^{213,214}.

To reduce and/or avoid diffusion problem a lipophilic phase can be injected as intermediate layer to protect core phase from core diffusing through outer shell. As for simple dripping coextrusion, capsules diameters and layers thickness can be predicted. However, this method stays challenging, especially to overcome coalescence between inner layers, when they are composed of hydrophilic core and a lipophilic intermediate layer ²⁰⁸. The triphasic system is also used to facilitate capsules formation with injection of a carrier stream within the outer tube, i.e. polyvinyl alcohol solution. It has shown great results for size and shell thickness control using vibrating system coextrusion ²¹⁵.

1.2.2.2 Vibrating Coextrusion System

Vibrating system or annular jet breaking method is used to produce capsules diameter smaller than the capillary length (around 1 mm) which was not possible with the dripping method (see Equation 1.4) ^{206,216}. Shell-core capsules are obtained after the injection of the shell material *i.e.* alginate solution, and a core material *i.e.* oil, simultaneously through a coaxial nozzle. A concentric jet is then produced and will be separated into droplets under Rayleigh-Plateau instability using a vibrating system. The system is often reinforced with an electrical field with the addition of electrode ring at the outlet of the injector to create droplets electrorepulsion. This artificial stimulation for droplet formation enables sooner formation., closer to the nozzle for smaller droplets ²¹⁷. The droplets produced are then collected in a gelling bath ²¹⁸. The electro-vibrating system is illustrated in Figure 1-12.

Experimentally, solutions injection at low flow rates induces a drop-by-drop flowing and generates large capsules, while an increase of the system flow rate (Q) generates smaller droplets through a jet formation (Q_{jet}). The annular jet relies on Rayleigh's theory of liquid jet instability in order to break-up into droplets ^{78,217}. Axisymmetric jets lead to droplet formation for conditions described in the following equation 1.8:

$$Q_{axisymmetric} < 81\pi \frac{D^{1.14} \mu^{0.72} \sigma^{0.14}}{\rho^{0.86}} \quad (1.8)$$

Where D is the nozzle diameter, μ is the solution viscosity, σ is the surface tension and ρ is the solution density. However, with the increase of flow rate (Q_{max}), jet length increases until surface instabilities are too high to produce axisymmetric break-up. So, flow rate should be between Q_{jet} and Q_{max} . Beyond Q_{max} , jet instabilities are too great to produce symmetric breakup

and correct capsules. Additional increase of flow rate possibly generates spray (Q_{spray}) as illustrated in Figure 1-13, depending on experimental conditions *i.e.* solution viscosity ^{78,219}.

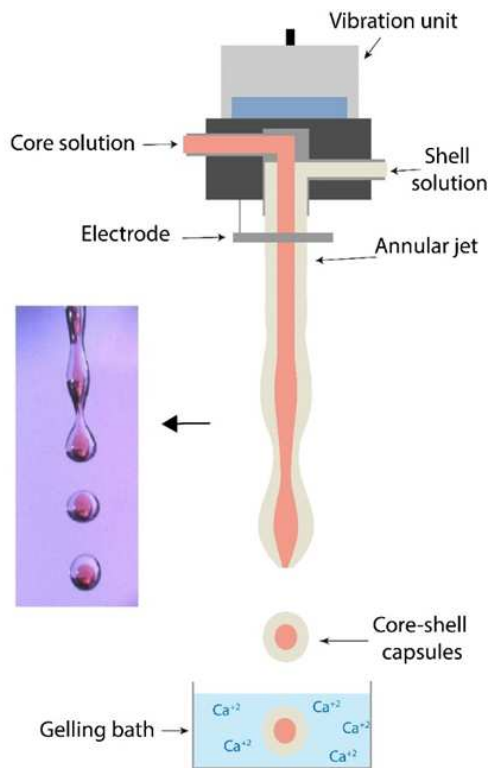


Figure 1-12. Example of electro-vibrating coextrusion device for alginate capsules.

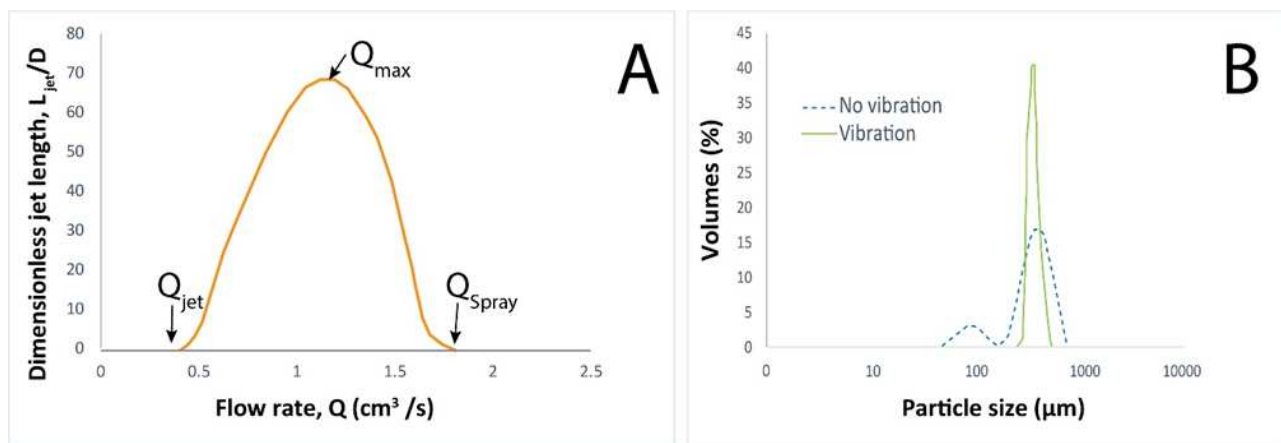


Figure 1-13. Particle size distribution of core-shell microcapsules with and without vibration system (A), Flow rate influence on jet break-up (B) (Adapted ⁷⁸).

The polymer extruded through the injector must have a flow rate (Q) high enough to form a continuous and stable jet, in order to overcome effects of viscosity and surface tension. However, an excessively high flow rate ($Q_{\text{spray}} < Q < Q_{\text{max}}$) would generate a jet high velocity that result in increasing capsules impact forces on the gelling bath surface and capsule deformation. This

deformation can be limited by decreasing jet velocity or reducing distance between the nozzle and the gelling bath surface. Such a high velocity could also increase coalescence between droplets and generates doublets capsules (Figure 1-11D). The phenomenon results from droplets velocity fluctuations related to liquids viscoelastic properties; small velocity fluctuations are amplified by capillary and viscous forces acting along the jet.^{218,220} Surfactant addition i.e. Tween 80, can reduce surface tension and decrease deformation, and also reduce coalescence phenomenon²¹⁸.

The transition from dripping mode to jet formation results from an increase of pressure inside the injection system. This transition is known as dripping-jetting transition (D-J transition) and it is controlled by Weber number (ratio of inertial to surface tension force)^{221,222} given by:

$$W_e = \frac{\rho D v^2}{\sigma} \quad (1.9)$$

Where ρ is the solution volumetric mass, D is the nozzle diameter, v is the jet velocity relative to the nozzle and σ is the surface tension between the solution and the air. From this, at $W_e \ll 1$ dripping system is observed while at $W_e \gg 1$ jetting is observed. For intermediates values, a dripping faucet system can be observed resulting in a non-homogenous dripping system with interruptions and variable capsules sizes²⁰⁶.

However, during the jetting-dripping transition, a phenomenon of hysteresis can be observed probably due to wetting conditions and solution viscosity, but this should be studied further²²². In addition, solutions with high elastic module present a particular system, known as “gobbling phenomenon”. The jet is maintained and the drop at its end continues to grow until the maximum droplet size.

When the force exerted on the jet become too great, the drop falls. With polymers solution, and due to the elasticity of those solution, two Weber numbers can be considered, the first W_e beyond the gobbling phenomenon and the second at the transition to jetting²⁰⁶.

Further, jet breakup can result in polydisperse droplets size due to jet inconsistencies and more, satellite particles can be observed. Vibration frequency should match droplets formation to result in monodisperse particle size distributions with d_{\max}/d_{\min} value down to 1.01. The positive effects of vibrating system for jet breaking on capsule size distribution are shown in Figure 1-13.

In order to monitor and adapt the production, the radius of resulting droplets can be predicted by the equation 1.10:

$$r_d = \left(\frac{3r_j^2 v_j}{4f} \right)^{1/3} \quad (1.10)$$

Where r_d is the droplet radius, r_j is the jet radius, v_j is the jet linear velocity and f is frequency of vibration ^{216,223}.

High frequencies increase coalescence phenomenon, while lower frequencies result in formation of small droplets (satellites). Satellites can collide with larger droplets during jet-breaking and/or during gelation. Thus, satellites could produce independent core adjacent to the main one (Figure 1-11C) or join the core material. Addition of electrostatic voltage system can reduce coalescence phenomenon by inducing string polymer negative charges on droplets surfaces and causes them to repel each other ²¹⁸. Higher velocities, droplets diameters and viscosities require higher electrical potential. Charges up to 2-2.15kV can be applied to the droplets, higher charges could generate their instability ²¹⁸.

As for capsules size, nozzle dimensions also impact jet formation, so that capsules are generally 1.8 times larger than nozzle diameter, i.e. 900 μ m capsules can be expected from a 500 μ m nozzle. This is probably due to the jet swelling at nozzle outlet. The swelling is related to the flow rate, for low flow rates, the swelling occurs immediately at nozzle outlet, while an increase in flow rate delays the phenomenon as observed in Figure 1-14 ^{78,206}. Also, multiple cores phenomenon seemed to occur at very high shell and core flow rates²²⁴.

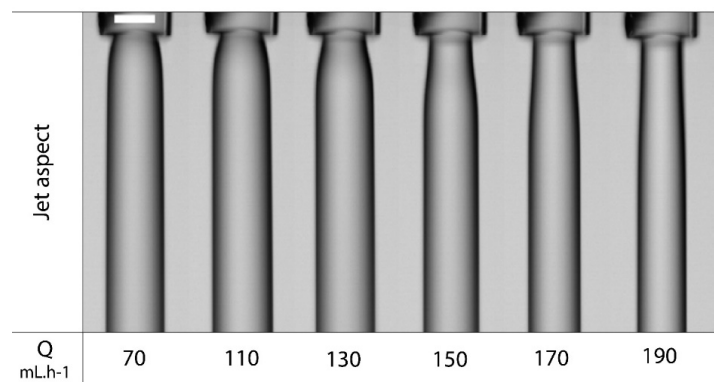


Figure 1-14. Jet diameter increase at nozzle outlet and its variation with injection feed rate (Q) (adapted ²⁰⁶).

Understanding mechanisms of capsules formation and the effects of different factors on it, improves adaptability of annular jet coextrusion. It enlarges applications, especially with such a recent encapsulation process. However, the technology simplicity makes it a perfect candidate for scale-up. Production rates up to 1000 L/hour can be reached ²¹⁶.

Vibrating coextrusion systems are used in many industries. Nevertheless, vibrating systems present some limitations. Capsules with sizes below $150\mu\text{m}$ are complicated to reach and require smaller nozzles. But, decreasing nozzle size enhances probabilities of nozzle plugging, especially with viscous materials. Production of capsules with a size range of $30\text{--}8000\mu\text{m}$ is then possible with frequency and nozzle size modification ^{78,225}.

Various nomenclatures are used in the encapsulation field, therefore, electrovibrating coextrusion as well as dripping coextrusion are sometimes considered as electrospraying methods, when an electrical field is applied for capsule dispersion. Also, depending on nozzle size, applied voltage and vibrating frequency, electrovibrating coextrusion can produce millimetric capsules (spheres) or microcapsules; it is then considered as a spherification or microencapsulation method ^{78,226}.

1.2.2.3 Centrifugal Coextrusion System

Centrifugal or spinning disc coextrusion consists in the injection of core and shell solutions through concentric orifices located on a rotating cylinder's outer circumference. As for dripping and vibrating systems, core solutions are pumped separately and injected through an internal tube and shell solution through an external tube. As the cylinder rotates, solutions are coextruded, and shell fluid sheaths the core solution (Figure 1-15). Cylinder rotations can operate at a speed in the range of 100 to 1000 rpm. Core-shell drops are formed under centrifugal forces and Rayleigh instabilities due to surface tension. Core-shell capsules are then collected in a gelling bath (alginate gelation) or in another collecting system i.e. starch moving bed ²²⁷.

As for dripping and vibrating system coextrusion, capsule size is controlled by nozzle size, so that capsules with a diameter ranging from 150 to $2000\mu\text{m}$ can be produced. Core-shell capsule size is also controlled by the cylinder's rotational speed and capsule size decreases by the increase of rotational speed ^{78,216}. Other parameters should also be considered for size control: solutions' total flow rate, core and shell flow rates ratio, material properties and other experimental conditions surrounding the centrifugal cylinder, such as turbulence or air flow ^{78,227}.

Centrifugal coextrusion generates high production capacities compared to dripping systems, so that a 50 nozzle system has a production rate up to 500kg/h (Figure 1-15B). However, due to nozzle multiplication and rotational system, it has a high space consumption. Nevertheless, this

provides capsules with longer flight paths so that capsules do not collide onto one another in the collection module. Also, direct observation of droplets formation is more difficult during injection, so monitoring droplets formation for feedbacks and adjustments is complicated^{78,228}.

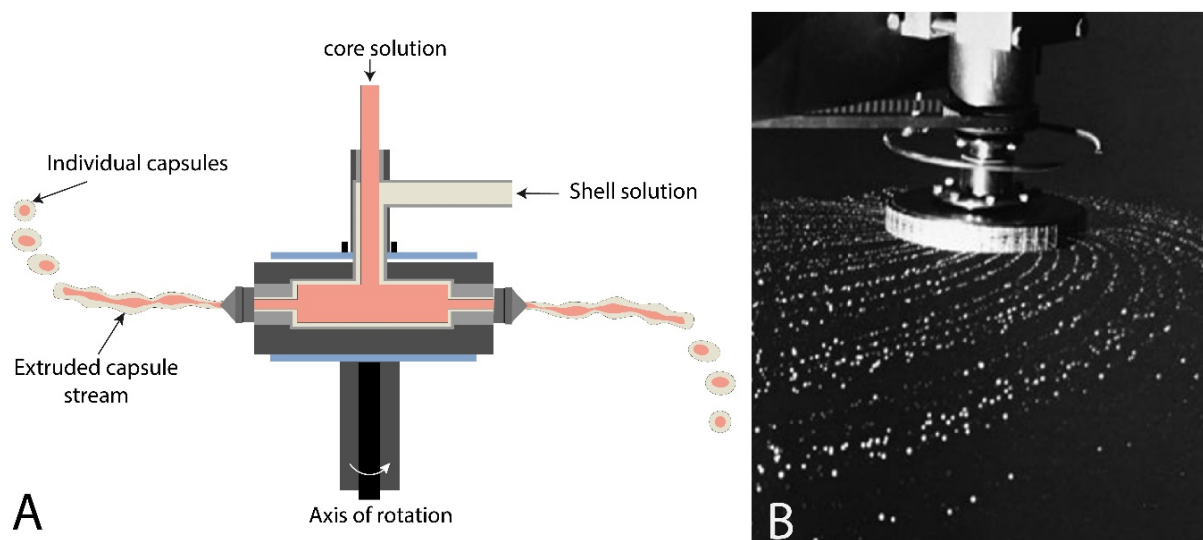


Figure 1-15. (A) Illustration of centrifugal coextrusion and (B) Photograph of centrifugal coextrusion units with fifty nozzles (Adapted⁷⁸)

1.2.2.4 Electrohydrodynamic Coextrusion or Electrospaying

Electrohydrodynamic (EHD) coextrusion system, also called electrospaying, is an encapsulation process that uses electric field to produce droplets. Two materials are simultaneously electrospayed through a coaxial nozzle (needle). Core solution flows through the central capillary, while shell solution flows through the annular nozzle. An electrical charge is applied on material between the injection nozzle and the grounded electrode (2kV-30kV)²²⁹.

The process depends mainly on shell solutions properties (viscosity and conductivity). With a sufficient shell solution conductivity, encapsulation of high resistivity core solution is possible^{216,231}. Thus, in EHD coextrusion, capsules shapes depend on shell solution conductivity. Shell solution is often called the driving liquid, even if EHD coextrusion is also possible using conducting core solution and dielectric shell solution^{231,232}. Materials extruded through coaxial nozzle adopt a meniscus shape under the Coulombic interactions, and depending on experimental conditions, turn into a conical-like shape (Taylor's cone) (see Figure 1-16). Electrical forces overcome surface tension and allow a jet formation that breaks up into a highly charged droplets aerosol^{216,229}.

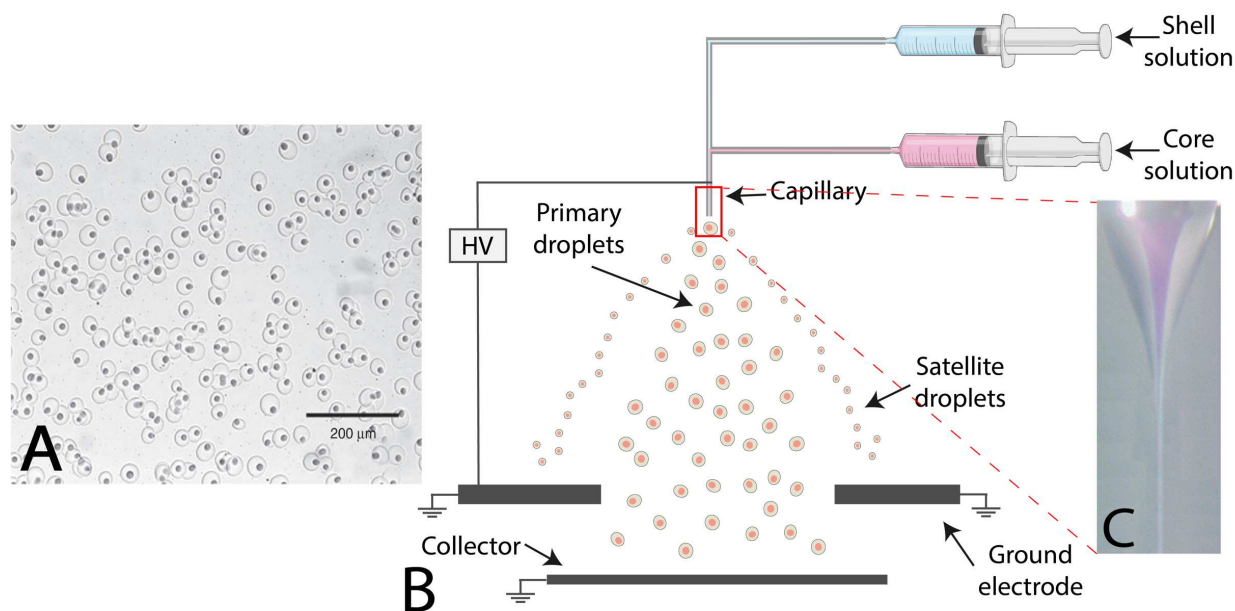


Figure 1-16. (A) Microphotography capsules produced with electrohydrodynamic coextrusion, (B) Schematic of electrohydrodynamic (EHD) system setup, (C) A close-up view of coextruded feed stream through a coaxial nozzle forming a Taylor cone (Adapted ²³⁰).

Depending on process conditions, electrospraying can be classified into: (i) dripping mode or (ii) cone-jet mode (Taylor core mode). Droplets generation and size are controlled by process parameters (i.e. feed flow rates, applied voltage and temperature) and materials characteristics (i.e. solutions viscosity, surface tension, fluid properties) ²³³. Unfortunately, droplets size distribution is generally bimodal or multimodal. Generally, primary droplets are the main ones, satellite droplets are formed from instabilities and offspring droplets formed from Coulomb fission ²³⁴. However, monodispersed capsules can be obtained by exploiting spray spatial expansion, and by adjusting process and materials parameters ²³⁵.

Microcapsules made with EHD coextrusion have a wide range of sizes. However, compared to dripping coextrusion, EHD coextrusion generates smaller capsules in the range of 1 – 100 μm. Microcapsules diameter can be predicted using Fernandez de La Mora and Loscertales law, described by equation 1.11:

$$d = \alpha \left(\frac{Q \epsilon_0 \epsilon_r}{K} \right)^{1/3} \quad (1.11)$$

Where d is the capsule diameter, α is a constant, Q is the material flow rate, ϵ_0 is the permittivity of the free space, ϵ_r is the relative permittivity of the material and K is the material conductivity ^{216,236}. The EHD coextrusion process is promising for microcapsules production with

high encapsulation efficiency and loading capacity in many fields ²³¹. However, droplets free of materials can be observed when shell solutions flow rate is too high. On the contrary, when core solution flow rate is too high compared to shell solutions flow rate, core materials droplets can be observed with shell ²³¹.

Nevertheless, electrohydrodynamic coextrusion process has some challenging limitations, one of them is the low throughput, especially for very small microcapsules production (1 -10 μm). As for previous systems, nozzles multiplication has shown efficiency for production rates enhancement and scale-up. Moreover, arrangement in flow rates ratio with shell solution rate higher than core solution rate showed effective encapsulation. The safety aspect is in another challenging point concerning EHD process, since the application of high voltages presents major safety concerns, especially in the presence of fine particles ^{216,231}.

1.2.2.5 Other Coextrusion Systems

Other coextrusion systems exist with different module used to cut annular jet to droplets. To cite some, jet cutting technique uses a rotating cutting tool equipped with several wires that cut the jet into smaller cylinder that take form of spherical droplets under solution surface tension. For jet cutting method, capsules size is controlled by the cutting tool rotating frequency, number of wires on the cutting tool, wires diameter, solutions flow rate and nozzle design ^{216,237}. However, capsules smaller than 100 μm are difficult to produce, capsules with size in range of 150 μm to several millimeters have been reported. The method presents also cutting losses produced during the jet cutting which reduced production yields. Those losses can be reduced by recycling and adjusting cutting tool angle. Unlike annular jet breaking coextrusion, jet cutting process can be used to produce capsules with high viscosity feed materials. Production yields can be enhanced with multinozzle systems ²¹⁶.

Submerged nozzle coextrusion method is also used for core-shell capsules production. Materials are injected through a coaxial nozzle which is submerged within a third concentric nozzle containing the carrier fluid (as illustrated in Figure 1-17). The nozzle can also be submerged directly into the gelling bath ^{78,238}. Precipitation and carrier fluid must be immiscible and non-reactive with core and shell solutions for capsules correct formation. Submerged nozzle method generates regular capsules with monodispersed size. Also, using carrier fluids prevents capsules

collisions and deformation under surface tension forces ⁷⁸. Several materials can be used *i.e.* oils, water, enzymes, cells ^{238–240}. Submerged nozzle coextrusion generates a wide range of capsules size (500 μm to 8 mm) with smaller capsules by using milli-fluidic technology ^{78,238,240}.

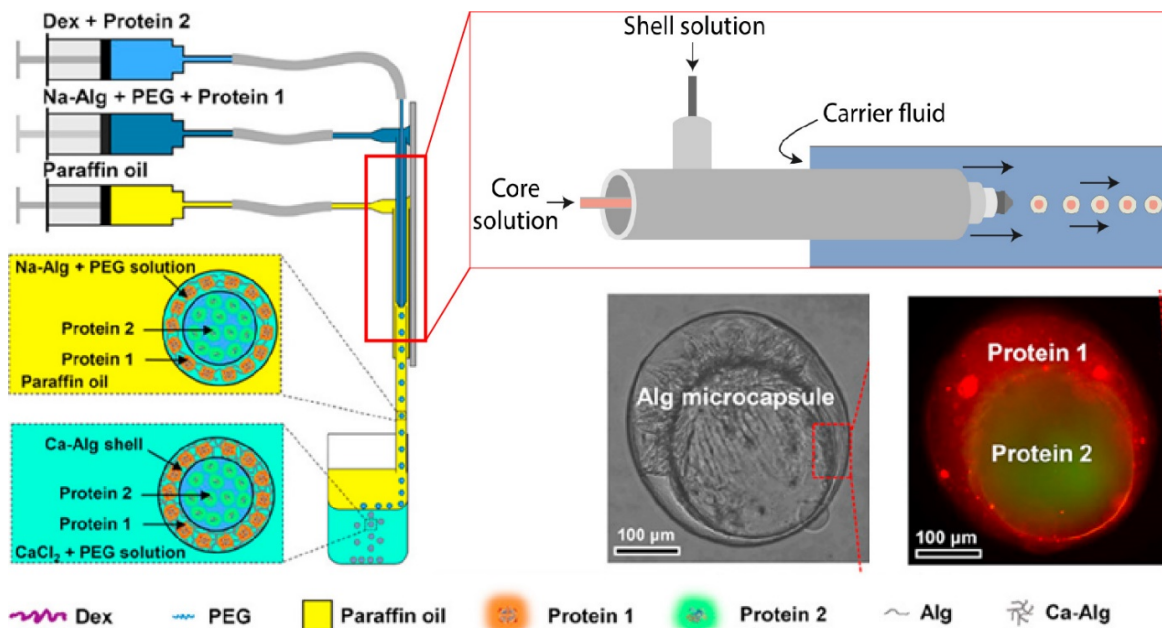


Figure 1-17. Illustration of submerged nozzle coextrusion (Adapted ²⁴¹)

Recently, research focused on multi-core coextrusion encapsulation. Some innovative methods have been developed to produce capsules with more than one core, allowing the encapsulation of different ingredients into separated cores. The number of cores can be controlled by the number of inner tubes ²⁴². Multi-core capsules have been successfully used for α -tocopherol encapsulation. This presented also great results for probiotics encapsulation, where *Lactobacillus* and *Bacillus subtilis* have been encapsulated into separated cores without affecting bacterial proliferation ²⁴³.

Qu et al. (2022) reported a very promising protocol for producing eukaryotic cell-like system, *i.e.* multicompartmental capsules with distinct enzymatic cellular reactions (Figure 1-18) ²⁴⁴. Another approach to produce multicompartmental capsules proposed by He et al. (2016) consists of the combination of two or three coaxial nozzles by placing them near vertically. Thus, the generated droplets could merge before hitting the gelling bath and form compartmental capsules ²⁴⁵. High application potential is promised by the multi-core and the multicompartmental

capsules for coencapsulation applications such as drug codelivery, confined reactions, enzyme immobilizations, and cell cultures ²⁴⁴.

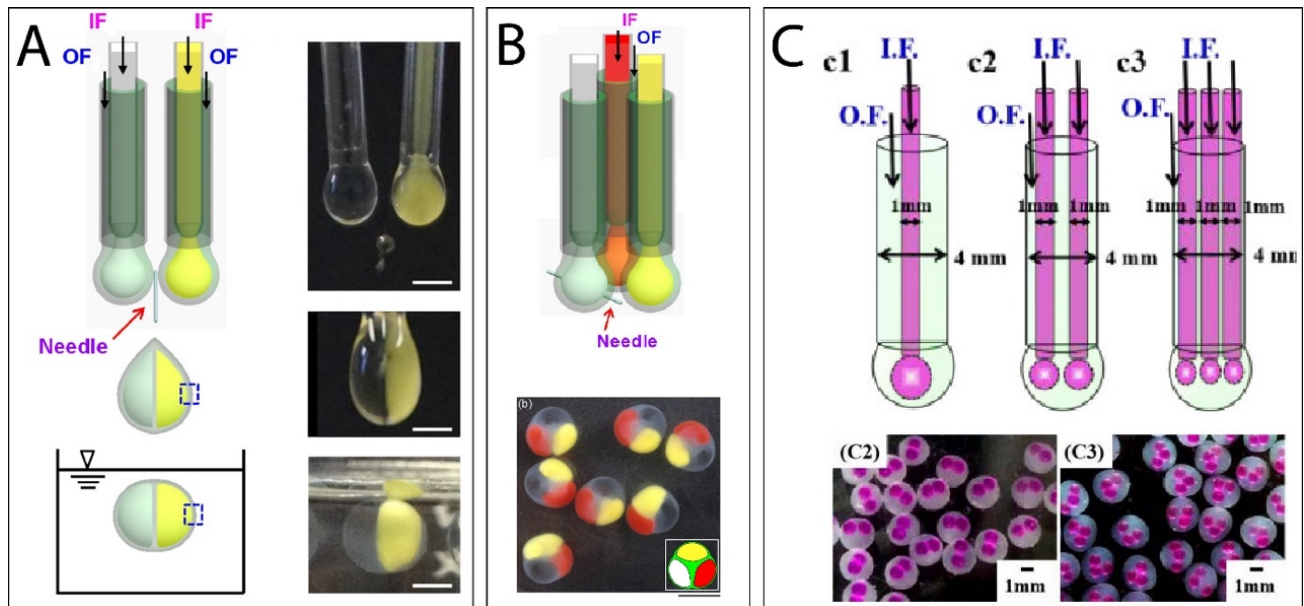


Figure 1-18. (A) coextrusion system for production on dual-compartmental capsules, (B) coextrusion system for production of triple-compartmental capsules, (C) coextrusion systems for production of multi-cores capsules. (Adapted ^{242,244}). IF: Internal flow, OF: Outer flow.

1.2.3 Advantages and limitations of coextrusion methods

All the coextrusion methods offer advantages such as a protective barrier for encapsulated ingredients, slow-release kinetics, and stability against oxidation. However, there are limitations such as process dependency on core and shell fluid rates and the requirement for high precision equipment ^{12,13,246–248}. Nevertheless, this paper described four coextrusion methods each have interests and weaknesses, Dripping produces multilayered and large capsules, but has a non-homogeneous shell thickness ^{78,208,213}. Vibrating produces small capsules with high production rates but requires many trials and has a high probability of nozzle plugging and capsule coalescence. While centrifugal allows for high production capacities but requires a large space and direct monitoring can be difficult ^{78,218,220}. Also, EHD produces a wide size range and smaller capsules but has a lower payload and safety concerns due to high voltage use, more advantages and limitations are displaced in Table 1-5.

The choice of encapsulation method depends on the specific requirements of the application, such as the size of the desired capsule, the fluid properties, and the production capacity.

Table 1-5 Advantages and limitations of coextrusion methods for core-shell capsules production

Methods	Advantages	Limitations	Refs
Dripping system	<ul style="list-style-type: none"> • Scale-up possible through nozzle multiplication • Possibility to produce multilayered capsules. • Production of Large capsules 	<ul style="list-style-type: none"> • Non homogenous shell thickness • High dependency on fluids surface tensions 	78,208,213
Vibrating system	<ul style="list-style-type: none"> • Facilities to control size and shell thickness • Production of small capsules • High production rates • Wide range of capsule size 	<ul style="list-style-type: none"> • Required many trials to find the appropriate vibration frequency. • Process not adapted to high viscosities fluids encapsulation. • Possibility of capsule coalescence. • Multiple core phenomenon when variables are not adapted. • High nozzle plugging probabilities. 	78,218,220
Centrifugal system	<ul style="list-style-type: none"> • Possibility to use various collecting systems. • High production capacities • Reduced coalescence 	<ul style="list-style-type: none"> • High space consumptions • Direct monitoring can be difficult 	78,216,228
EHD system	<ul style="list-style-type: none"> • Wide size range • Possibility to produce smaller capsules. • Scale-up with nozzle multiplication 	<ul style="list-style-type: none"> • Dependence on solutions viscosities and conductivities • Bimodal or multimodal size distribution. • Low throughput • Lower payload • Safety aspect, due to high voltage use. 	78,216,231
Common to all methods	<ul style="list-style-type: none"> • Large payload related to a reservoir-type structure. • The shell acts as a protective barrier for encapsulated ingredient protection compared to simple extrusion process. • Slow-release kinetics brought by the shell. • Stability of the encapsulated ingredient against oxidation. • Limitation of highly volatile actives evaporation (<i>e.g.</i> Essential oils). • Burst-like effect obtained by the highly loaded core-shell capsules breakage. (<i>e.g.</i> high flavor release in chewing gum). • Continuous process. 	<ul style="list-style-type: none"> • Process dependency on core and shell fluids rate • Hydrophilic liquids encapsulation may be complicated. • Many experimental parameters must be defined for their impact on capsules properties. • High precision equipment is required. • Additional step is required to get powder form. 	12,13,246-248

1.2.4 Conclusions

Encapsulation process aims to enclose one or more substances within a semi-permeable coating material to produce particles, solid beads, or capsule. It a protective technology that is nowadays widely used.

Coextrusion technology involves a concentric nozzle, an additional system for capsules separation (vibration unit, spinning disc, etc...). The technology allows production of capsules with a wide size range from few microns to several millimeters ⁷⁸. Coextrusion is used for core-shell capsules production, with a higher payload than other techniques, such as spray drying. As discussed, there are various coextrusion process variations, i.e. dripping system, vibrating system, centrifugal system and EHD system.

The choice of coextrusion technology is therefore, driven by the droplet formation which depends on a combination of multiple parameters: (i) material properties i.e. viscosity, interfacial tension, solubility, density, (ii) nozzle size according to capsules size expected, (iii) scale up possibilities, (iv) production rates, (v) need of sterile environment.

This review showed that coextrusion technology presents several advantages compared to other encapsulation methods, *i.e.* large payload, continuous process etc., but also limitations such as requirement of high precision equipment and difficulty of process optimization.

Key highlights

- Coextrusion techniques are based on the use of coaxial nozzles to create core-shell capsules.
- Four specific coextrusion methods for encapsulation, namely dripping, jet cutting, centrifugal, and electrohydrodynamic systems, were examined, including their respective parameters and suitability for achieving different capsule sizes.
- Coextrusion is a promising technique for controlled production of core-shell capsules.
- Each method has advantages and limitation, and the choice of encapsulation method depends on the specific application requirements.

1.3 Alginate Based Core–Shell Capsules Production through Coextrusion Methods: Recent Applications (*published in Foods*)

1.3.1 Introduction

Alginate is a biopolymer extracted from brown algae and some bacteria and is composed of guluronate and mannuronate units (G and M units, respectively) ¹⁹⁵. The polymer is a versatile and safe material that is widely used in various industries such as cosmetic, textile, pharmaceutical, and food as a coating material, stabilizer, thickener, and disintegrating agent ¹⁹⁴. It is generally recognized as safe (GRAS), due to its non-toxic, non-antigenic, biocompatible, and biodegradable properties ¹⁹³. The ability of alginate to form a hydrogel through ionic cross-links with divalent and trivalent ions (generally, calcium ions) makes it a preferred choice for the encapsulation technology, especially for extrusion and coextrusion methods ¹⁹³.

The composition of alginate varies among different algae species, and its gelation is influenced by factors such as molecular weight, percentage of M and G units, and its concentration, in addition to various experimental conditions. Therefore, high-molecular-weight and high-G-content alginate allows obtaining high-viscosity hydrogels and thus compact and rigid beads and capsules ¹⁹⁶. However, excessive viscosity can cause nozzle clogging and produce non-spherical capsules ¹⁹³. On the other side, a high percentage of M units will lead to an elastic alginate network ⁸⁷. To enhance the functional properties of alginate, researchers are exploring various modifications and composite gels made with the addition of other polysaccharides and proteins ^{41,42}. These modifications aim to improve the encapsulation efficiency, payload, storage stability, and barrier properties of alginate.

Encapsulation is a flexible and adaptable technology that is utilized in various industries, including the pharmaceutical, food, and agriculture industries ^{249–251}. One of the primary reasons for using encapsulation is to protect and control the release of the encapsulated material. This technology involves enclosing small particles or droplets within a protective coating or shell, which can prevent them from being degraded or affected by external factors such as temperature, humidity, and light. This protective coating can also enable the targeted delivery of the encapsulated material, allowing it to be released at a specific time or location ²⁵². Additionally, encapsulation can enhance the stability and shelf life of products, improve their sensory properties, and reduce their volatility

or reactivity ¹. Various structures can be obtained by encapsulation, i.e., particles, powders, capsules, beads, and core–shell capsules.

Core–shell capsule production is possible utilizing a single nozzle for the encapsulation process. This type of encapsulation involves gelation reactions that result in cross-linking only occurring in the area around the interface between the “inside” and the “outside” of the capsule ^{253,254}. This technique is known as reverse spherification and is used in many industries, such as bubble tea production. However, these products are subject to content diffusion from the core through a very fragile and very porous shell ²⁵⁵.

On the other hand, the coextrusion encapsulation method allows the production of core–shell capsules by injecting a core solution and a shell solution through a concentric nozzle. The shell material and core material pass through outer and inner orifices, respectively ⁷⁸. The shell in this system presents a higher mechanical resistance ²⁵⁶ and lower core diffusion than reverse-spherification core–shell systems. Therefore, we chose to focus on coextrusion systems in this review.

Additionally, the core–shell system allows a higher payload ^{254,257}, than other encapsulation technologies, such as spray–drying and simple extrusion that usually produce powders and solid particles. Such formulations are more likely to lose their content payload and stability due to external environment exposure ¹¹.

Numerous reviews treating encapsulation technologies and methods have been published recently focusing on food applications ^{233,258} or cell encapsulation and biomedical applications ^{259,260}. However, to our knowledge, no review has been published on coextrusion encapsulation and its recent applications.

1.3.2 Oil and Essential Oil Encapsulation

Besides the food and nutraceutical industries, oils are commonly used in cosmetics for fragrance or in plant-based extracts ^{261,262}, agricultural pesticides or insecticides ^{263,264}, and pharmaceutical active molecules ^{265,266}.

Numerous papers describe oil and essential oil encapsulation using different coextrusion methods and process parameters. These have been adapted to each experimental environment to successfully produce capsules with a wide size range of 300–2000 μm and various payloads, as

shown in Table 1-6. For these examples, oil is injected through the internal nozzle, and alginate, either with or without copolymers, through the external annular nozzle, as illustrated in Figure 1-19.

Table 1-6 Characteristics of alginate core-shell capsules produced by coextrusion methods

Shell and/or Coating Material	Oil/Essential Oil	Key Parameters of the Coextrusion Method	Average Capsule Size (μm)	Treatment Post Encapsulation	EE (%)	Load (%)	References
Alginate	Olive	Frequency: 1706 Hz Inner/Outer rate: 30/200 mL/h	ND	None	ND	ND	267
Alginate	Canola	Outer nozzle: 200 μm Frequency: 1750 Hz	400	pH treatment, freeze drying	ND	55.2	268
Alginate	Rosemary EO	Inner/Outer nozzle: 200/400 μm Inner/Outer rate: 900/300 mL/h Frequency: 350 Hz	950 (756 dried)	Oven-drying (60°C for 2 h)	ND	ND	269
Alginate	Fish oil	Frequency: 1300 Hz	600	None	ND	ND	270
Alginate	Sunflower	Inner/Outer nozzle: 750/900 μm Inner/Outer rate: 14,55/34 mL/min.	2060	None	ND	37	271
Alginate	Sunflower (emulsion with CaCl_2)	Inner/Outer nozzle: 400/600 μm	800	None	ND	ND	272,273
Alginate	Linseed	Dripping height: 5 cm	ND	None	91	38.4	273
Alginate	Rapeseed	Dripping height: 5 cm	ND	None	91.6	39.9	273
Alginate-Soy protein isolate	Sunflower + β -carotene	Inner/Outer nozzle: 150/300 μm Inner/Outer rate: 120/400 mL/h Frequency: 1000 Hz	567	None	99.2	82.8	274
Alginate-HPMC	Avocado	Frequency: 1706 Hz Inner/Outer nozzle: 300/400 μm	323-416	Freeze-drying	68	ND	275
Alginate-HMP	Roselle seed	Frequency: 300 Hz Air pressure: 600 mbar Inner/Outer nozzle: 150/300 μm	ND	Oven-drying	ND	95	276
Alginate-HMP	Kenaf seed	Inner/Outer rate: 0.2/7 mL/min Air pressure: 600 mbar Inner/Outer nozzle: 200/300 μm	900 (500 dried)	Air-drying-Freeze-drying	33-67	ND	224,277
Alginate-HMP	Kenaf seed	Frequency: 500 Hz Inner/Outer rate: 30/200 mL/h	700-920 (330-500 dried)	Freeze-drying	63	ND	278
Alginate- low or high amylose content starch	Canola	Outer nozzle: 200 μm Frequency: 1750 Hz Inner/Outer nozzle: 200/300 μm	310-380	pH treatment Freeze-drying	ND	58	279
HMP alginate/chitosan	Kenaf seed	Inner/Outer rate: 0.2/7 mL/min Frequency: 500 Hz	475-775	Oven-drying (50°C for 2 h)	33-65	ND	280
Alginate-HMP-chitosan	Kenaf seed	Inner/Outer nozzle: 200/300 μm Frequency: 500 Hz	ND	Freeze-drying	ND	ND	281
Alginate/ κ -carrageenan/chitosan	Ginger oil	Inner/Outer nozzle: 450/900 μm Frequency: 40 Hz Air pressure: 400 mbar	1600 μm	None	85	76	132

ND: not determined. EE: encapsulation efficiency. Load: loading. HPMC: Hydroxypropyl methylcellulose. HMP: High-methoxyl pectin.

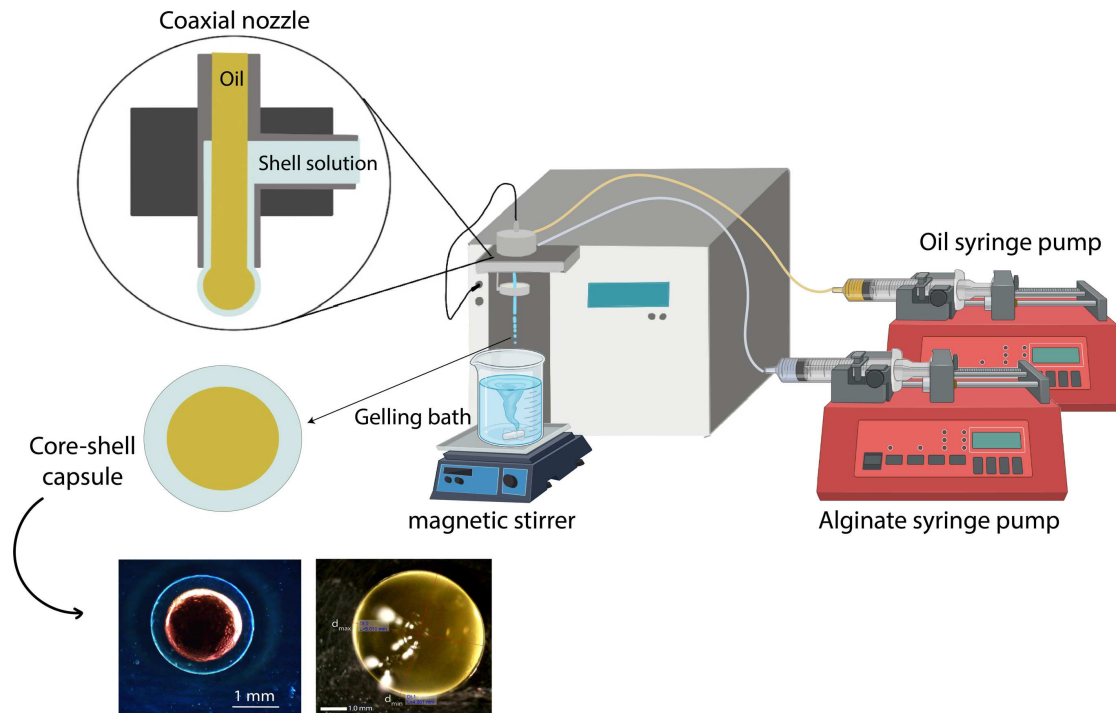


Figure 1-19. Illustration of oil encapsulation in core-shell capsules using the coextrusion method.

1.3.2.1 Reduced Oxidation

In order to avoid lipid oxidation and deterioration, the most common strategy is the exclusion of initiators and promoters of lipid oxidation. Lipids are usually stored under vacuum or inert gas in opaque and non-metallic containers²⁸².

However, oil encapsulation is a great approach to isolate oil from the external environment. Besides the protective function and stability enhancement, oil encapsulation presents many others benefits such as taste, color, and odor masking, many studies described various oil encapsulation as illustrated in Table 1-6. An encapsulated oil can also allow the controlled release of liposoluble molecules²⁵⁹. For some applications such as in the food and cosmetic industries, the encapsulated oil presents a solid form (spray-dried oil). This physical conversion allows its incorporation in various products such as yoghurts, sausages, and various power-based products^{283–285}.

Core-shell oil capsules present a high oil content depending on the oil, shell material, and encapsulation parameters used in their production. As shown in Table 1-6, it appears that a higher core flow rate will result in the entrapment of a greater amount of core material and engender

capsule production with high encapsulation efficiency (up to 99.2 % with an oil load of 82.8 %) ²²⁴.

Alginate as a shell material for oil encapsulation is probably one of the most used polymers in coextrusion technology. Its use as a unique shell material exhibited good results for various oils encapsulation, and some predictive mathematical models for oil capsules properties have been reported ^{256,271}. The addition of other polymers to alginate can improve the oil load as observed for low-/high-amylose-content starch where a high canola oil content has been reported (58 %) ²⁷⁹. The addition of soy protein isolates and HMP resulted also in high load values, i.e., 83 and 95 %, respectively. Other additional shell materials have been explored, including hydroxypropyl methylcellulose (HPMC), agar, fish gelatin, and κ -carrageenan. They exhibited interesting results in combination with alginate for oil capsule production ^{267,286}. The addition of chitosan as an additional coating material for kenaf seed oil and ginger oil alginate capsules permitted to reduce the shell porosity ^{273,275}. This was similarly observed for soy protein isolates added to alginate ²⁷⁴.

Several research works have studied the oxidative stability of different oils, with or without antioxidant addition in the hydrophobic phase and with various shell material composition ^{132,268,277}, Oil oxidation was generally evaluated through the determination of the peroxide value (PV) and the anisidine value (p-AV) that indicate primary oxidation and secondary oxidation, respectively ^{273,283}. According to Table 1-7, most oils encapsulated by coextrusion had reduced values of oxidation indicators, and for most of them, less bioactives loss was reported. Effective reduction of oxidation was observed for linseed and rapeseed oil encapsulated with chitosan or alginate, where alginate/linseed oil capsules and chitosan/linseed oil capsules presented PV < 48.6 meq/kg and PV < 7.49 meq/kg, respectively, after 4 weeks at 40°C compared to PV > 65 meq/kg for free linseed oil. Secondary oxidation indicators were also lower for encapsulated-oil alginate/linseed oil capsules and chitosan/linseed oil capsules, which showed p-AV < 5.06 and p-AV < 3.03 respectively, while free linseed oil had p-AV > 9.33.

Similar results were obtained for encapsulated rapeseed oil, where alginate/rapeseed oil capsules and chitosan/rapeseed oil capsules presented PV < 20.77 meq/kg and PV < 19.92 meq/kg, respectively, after 4 weeks at 40°C compared to PV > 65 meq/kg for free rapeseed oil; indicators for secondary oxidation were also lower for encapsulated rapeseed oil, as shown in Table 1-7 ²⁷³.

Table 1-7. Oxidation indicators comparison of free oil and encapsulated oil produced by coextrusion.

Shell and/or Coating Material	Oil/Essential Oil	Antioxidant	Oxidation Indicators		Storage Conditions	References
			Free Oil/Essential Oil	Encapsulated		
Alginate	Olive	Caffeic acid (300 ppm)	PV > 16 meq/kg p-AV > 3.2 FFA > 0.12%	PV < 14 meq/kg p-AV < 2.5 FFA < 0.14%	30 days at 37°C	267
Alginate	Canola	Quercetin (200 ppm)	PV > 16 meq/kg p-AV > 3.90 FFA > 0.21%	PV < 10.2 meq/kg p-AV < 2.99 FFA < 0.23%	60 days at 38°C	268
Alginate	Fish oil	/	PV > 11.3 meq/kg, p-AV > 11.7 DHA loss 2.72% EPA loss 0.84%	PV < 4.8 meq/kg, p-AV < 6.7 DHA reduction 0.68% EPA reduction 0.74%	17 days at 37°C	270
Alginate	Linseed	/	PV > 65 meq/kg, p-AV > 9.33 FFA > 1.22	PV < 48.26 meq/kg, p-AV < 5.06 FFA < 1.26	4 weeks at 40°C	273
Alginate	Rapeseed	/	PV > 65 meq/kg p-AV > 11.30 FFA > 0.30	PV < 20.77 meq/kg p-AV < 6.99 FFA 0.32	4 weeks at 40°C	273
Alginate	Ginger	/	PV > 23 meq/kg p-AV > 34 TBARS: 5.8 mg MDA/kg	PV > 21 meq/kg p-AV > 40 TBARS: 5.8 mg MDA/kg	15 days at 4°C	132
Alginate-HPMC	Avocado	Phloridzin or BHT (300 ppm)	Totox: 25.4	Totox: 18.0/19.7	90 days at 37°C	275
Alginate-HMP	Roselle seed	/	PHY loss: 35% TOCO loss: 34.6% PV > 11.3 meq/kg,	PHY loss: 13.78% TOCO loss: 87.6 PV < 4.8 meq/kg,	24 days at 65°C	276
Alginate-HMP	Kenaf seed	/	p-AV > 11.7 FFA > 1.6	p-AV < 6.7 FFA < 1.41	24 days at 65°C	224,277
Alginate-HMP	Kenaf seed	/	PHY loss: 59.7% TOCO loss: 51.2%	PHY loss: 32.8% TOCO loss: 12.9%	24 days at 65°C	278
Alginate-low- or high-amylose-content starch	Canola	Quercetin, Vitamin E or BHT (200 ppm)	PV > 16.4 meq/kg p-AV > 3.90 FFA > 0.22%	PV < 10.8 meq/kg, p-AV < 4.19 FFA < 0.19%	60 days at 38°C	279
Alginate-κ-carrageenan	Ginger	/	PV > 23 meq/kg p-AV > 34 TBARS: 5.8 mg MDA/kg	PV > 16 meq/kg p-AV > 25 TBARS: 4.86 mg MDA/kg	15 days at 4°C	132
Alginate-κ-carrageenan-chitosan	Ginger	/	PV > 23 meq/kg p-AV > 34 TBARS: 5.8 mg MDA/kg	PV > 15 meq/kg p-AV > 16 TBARS: 4.44 mg MDA/kg	15 days at 4°C	132
Alginate-HMP-chitosan	Kenaf seed	/	PV > 10.1 meq/kg, p-AV > 20.2 FFA > 2.26%	PV < 3.9 meq/kg, p-AV < 15.94 FFA < 1.72%	24 days at 65°C	281
Alginate-chitosan	Ginger	/	PV > 23 meq/kg p-AV > 34	PV > 19 meq/kg p-AV > 26 TBARS: 5.2 mg MDA/kg	15 days at 4°C	132

PV: peroxide value, p-AV: p-anisidine value, FFA: Free Fatty Acid, BHT: butylated hydroxytoluene, HMP: high-methoxyl pectin, HPMC: hydroxypropyl methylcellulose, DHA: docosahexaenoic acid EPA: eicosapentaenoic acid. TOCO: tocopherols. Totox: total oxidation value. TBARS: thiobarbituric acid reactive substances.

Better results against oxidation were obtained with chitosan coating than with uncoated alginate/polymers capsules^{132,281,287}. Reduced kenaf seed oil oxidation was achieved as well as low phytosterol and tocopherol losses after 24 days of storage at 65°C for alginate–HMP–chitosan shells^{224,277,281}. HMP enhanced shell and oil stability²⁸¹ and exhibited great results combined with alginate for roselle seed oil encapsulation²⁷⁶.

To enhance the oil stability against oxidation, some authors studied the influence of antioxidant addition in the oily phase, i.e., caffeic acid, phloridzin, butylated hydroxytoluene (BHT), quercetin, and vitamin E. Caffeic acid addition (300 ppm) provided a better protection against the oxidation of olive oil, though not against hydrolytic rancidity. In addition, caffeic acid improved monounsaturated and polyunsaturated fatty acids protection²⁶⁷.

Encapsulated canola oil fortified with quercetin presented great results for primary oxidation²⁷⁹, similar to those obtained with BHT, which is no longer used due to its toxicity²⁸⁸. Capsules with quercetin addition in the core material presented a higher phenolic content after storage but a lower oil stability²⁶⁸.

1.3.2.2 Reduced Evaporation and Release

Essential oils represent good candidates for encapsulation also as they contain highly volatile and oxygen-sensitive functional molecules²⁸⁹. The core–shell structure provided by coextrusion methods should then be efficient to protect them from alteration and evaporation²⁶⁹. Rosemary essential oil has been successfully encapsulated by coextrusion with alginate as the shell material and still presented great results in antimicrobial activity (bacteria and fungi reduction) after processing. Further, the prolonged release conferred by the encapsulated form increased the essential oil shelf life and bioactivity²⁶⁹.

Some other beneficial properties are provided by encapsulation. For instance, *in vitro* digestion used to simulate human gastrointestinal digestion demonstrated great results in terms of protection of kenaf seed oil encapsulated in alginate and chitosan capsules²⁸¹. A good absorption of the encapsulated biomolecules in the duodenum was observed after *in vitro* digestion²⁸⁰. Furthermore, soy protein isolate introduction into alginate increased the shrinkage degree of β -carotene capsules and delayed β -carotene release in the stomach²⁷⁴.

1.3.2.3 Reduced Taste

Taste is important in determining the success of oral formulations' commercialization. Several drugs and nutraceuticals have an unpleasant taste, especially in liquid dosage forms. To overcome this issue, they are often formulated with flavors and sweeteners to mask the bitterness associated with the active and inactive ingredients ²⁹⁰. In this way, the bitter taste reduction can enhance the acceptability and adherence to medication and complements. Encapsulation is one of the most effective methods that are used for taste masking, especially of methods using an additional external coating to cover undesirable tastes and flavors ³. Therefore, the core-shell structure is a great candidate for this purpose. Core-shell oil capsules allow the consumption of hydrophobic antioxidants and biomolecules with bitter taste at a high concentration, at which they present the greatest effectiveness and bioactivity ¹³. The fortification of encapsulated oil in core-shell capsules facilitate the oral intake of such compounds ²⁶⁸.

1.3.3 Probiotics Encapsulation

Probiotics are described as viable microorganisms that can provide health benefits, largely described in the literature, such as maintaining the gut microbiota, improving digestion, reducing lactose intolerance, lowering serum cholesterol, inhibiting pathogen growth, and preventing certain cancers ^{291,292}. These effects are observed if microorganisms are alive and in a sufficient amount (10^6 – 10^9 CFU/g) ^{293,294}. Generally, probiotics are categorized as food supplements and can be divided in (i) probiotics for foods, including foods, food ingredients, and dietary supplements, (ii) probiotics for drugs that are used as a cure and for disease treatment or prevention, (iii) designed probiotics (genetically modified probiotics), and (iv) feed probiotics, which are used for animals ^{246,295}.

Probiotics are very sensitive to damaging conditions, and their viability is highly impacted by environmental parameters, i.e., pH, temperature, water activity (a_w), storage conditions, and processing ^{293,296}. Consequently, multiple encapsulation methods have been employed for the protection and controlled release of probiotics ^{297,298}.

Spray-drying ²⁹⁹, emulsions ³⁰⁰, and electrohydrodynamic atomization ¹⁹⁹ have been used to produce probiotics particles for food matrices. Nonetheless, a lot of studies reported a lower viability of spray-dried probiotics due to thermal, osmotic, and oxidative stress induced by the process conditions ⁸¹. The extrusion technology does not require high temperatures and organic solvents; thus, it is of high interest for cells and probiotics encapsulation ⁸¹. The coextrusion process

producing reservoir-type particles can stabilize and isolate the probiotics from the surroundings during storage and delivery into the human body ^{201,291,296}. In addition to its protective role, probiotics encapsulation facilitates their controlled release across the intestinal tract ³⁰¹. Probiotic core-shell capsules are produced using the coaxial nozzle system with adaptation due to sterile environment requirements; the process is illustrated in Figure 1-20.

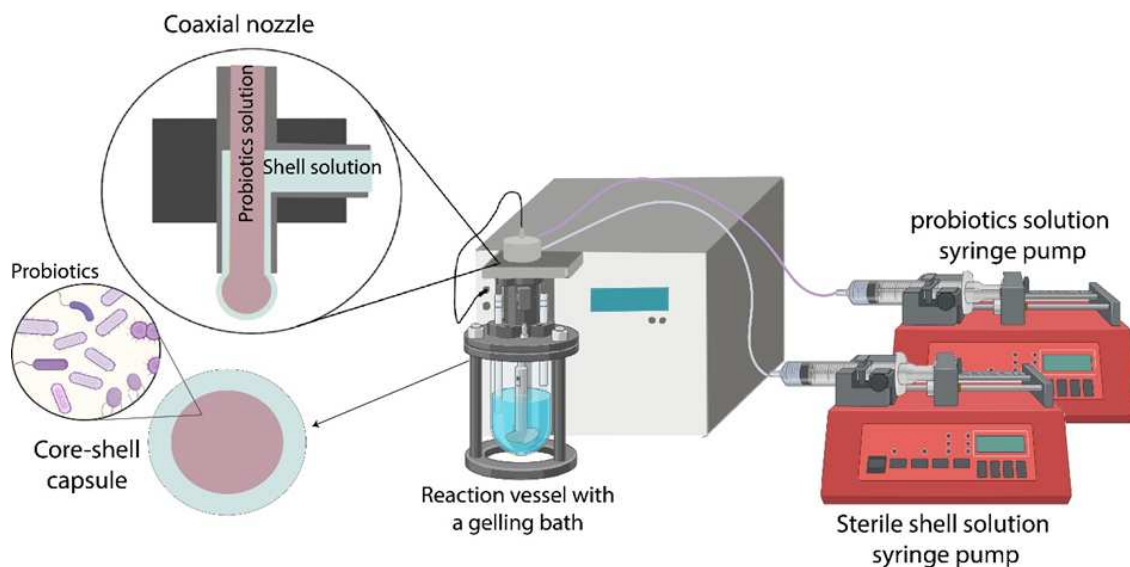


Figure 1-20. Illustration of probiotics encapsulation in core-shell capsules using the coextrusion method.

However, the encapsulation effectiveness in keeping probiotics alive depends on many factors, i.e., material type and concentration used for immobilization, encapsulation method, capsule size, and physicochemical characteristics of the environment ³⁰².

Numerous materials have been evaluated for probiotics encapsulation. The most used is alginate for its biocompatibility and cheapness ²⁰⁰, but its use is limited due to its high porosity and sensitivity to acidic environments ¹⁹⁶. The addition of copolymers to the alginate shell, as the blend alginate-shellac, presented promising results in porosity reduction ²⁹³. Table 1-8 shows alginate-polymers combinations that have been used recently. In addition, chitosan-coated alginate beads showed a denser structure with great protective properties due to their good resistance to the deteriorating and chelating effect of calcium ²⁹⁶. Pectin was also successfully used in combination with alginate. Blends improved probiotics viability and preservation from the environment ³⁰². Additionally, pectin from fruit can also be incorporated as an effective prebiotic, enhancing probiotics growth and activity ^{303,304}. Overall, as shown in Table 1-8, probiotics survivability in simulated gastrointestinal conditions was significantly higher after their encapsulation.

Table 1-8. Encapsulation efficiency and survivability of probiotics encapsulated in various shell materials using coextrusion.

Shell and/or Coating Material	Probiotics	Prebiotics	Parameters	Capsules Size (μm)	EE (%)	SGC (ph, duration)	Survivability (%)		Refs
							Encapsulated Probiotics	Free Probiotics	
Alginate	<i>Lactobacillus acidophilus</i>	Apple skin Polyphenols	Frequency: 2723 Hz	423–486	96.7	SGF (pH 2, 2 h)	73.9	54.1	307
Alginate	<i>Lactiplantibacillus plantarum</i>	Inulin	Inner/outer nozzle: 150/300 μm , Frequency: 300 Hz, Air pressure: 600 mbar	685	95	SGF (pH 2, 2 h) SIF (pH 7.5, 5 h)	92.0 97.5	88.4 94.5	296
Alginate	<i>Bifidobacterium lactis</i> Bi-07	Galacto-oligosaccharides	Inner/outer nozzle: 200/300 μm , Frequency: 300 Hz, Air pressure: 600 mbar	736	94	SGF (pH 2, 2 h) SIF (pH 7.5, 5 h)	91.3 82	80.5 75.0	310
Alginate–low-methoxylated	<i>Bifidobacterium infantis</i>	/	Inner/outer nozzle: 150/300 μm	520–568	ND	ND	ND	ND	302
Alginate/pectin	<i>Lactobacillus rhamnosus</i> GG	Black bean extract	Inner/outer nozzle: 150/300 μm , Frequency: 500 mL, Air pressure: 300 Hz	715	98.3	SGF (pH 2, 2 h) SIF (pH 7.4, 4 h)	94.1 79.9	90.1 62.5	201
Alginate/chitosan	<i>Lactobacillus plantarum</i> 299v	Oligofructose	Inner/outer nozzle: 150/300 μm , Air pressure: 600 mbar, Frequency: 300 Hz	648–790	93.0	SGF (pH 2, 2 h) SIF (pH 7.5, 5 h)	97.0 85.0	80.0 75.0	301
Alginate–chitosan	<i>Bifidobacterium animalis</i> subsp. <i>lactis</i> BB-12	Mannitol	Inner/outer nozzle: 200/300 μm Air pressure: 600 mbar, Frequency: 300 Hz	800	89.2	SGF (pH 2, 2 h) SIF (pH 7.5, 3 h)	97.3 86.7	74 97.5	311
Alginate–chitosan	<i>Lactobacillus plantarum</i> 299v	/	Inner/outer nozzle: 150/300 μm Air pressure: 600 mbar, Frequency: 300 Hz	620	97.7	SGF (pH 2, 2 h) SIF (pH 7.2, 4 h)	97.0 95.5	93.5 0.0	310
Alginate–chitosan	<i>Lactobacillus rhamnosus</i> GG	Flaxseed mucilage	Inner/outer nozzle: 200/300 μm , Inner/outer rate: 1.0/7.8 mL/min	780	98.8	SGF (pH 2, 2 h) SIF (pH 7.0, 4 h)	84.9 93.2	35.4 47.9	309
Alginate–chitosan	<i>Lactobacillus acidophilus</i> 5	Isomalto-oligosaccharide	Inner/outer nozzle: 200/300 μm , Air pressure: 600 mbar, Frequency: 300 Hz	616	92.2	SGF (pH 2, 2 h) SIF (pH 7.2, 2 h)	60.9 0.0	0.0 0.0	312
Alginate–alginate/shellac	<i>Lactobacillus paracasei</i> BGP-1 in sunflower oil/coconut fat	/	Inner/outer nozzle: 450/700 μm , Inner/outer rate: 2/16 mL/min, Frequency: 100 Hz	710–860	ND	SGF (pH 1.8, 2 h) SIF (pH 6.5, 3 h)	95.0 100	50.0 70.0	293
Alginate–Alginate/Shellac	<i>Lactobacillus acidophilus</i> LA3 in sunflower oil	/	Inner/outer nozzle: 450/700 μm , Inner/outer rate: 2/16 mL/min Frequency: 100 Hz	690–760	ND	SGF (pH 1.8, 2 h) SIF (pH 6.5, 3 h)	92.0 93.0	ND ND	81
Alginate–Alginate/Poly-L-lysine	<i>Lactobacillus rhamnosus</i> GG	Isomalto-oligosaccharide	Inner/outer nozzle: 200/300 μm , Air pressure: 600 mbar, Frequency: 300 Hz	491–541	90.4	SGF (pH 2, 2 h) SIF (pH 7.5, 2 h)	75.0 0.0	39.2 0.0	305
Alginate/locust bean gum	<i>Lactobacillus acidophilus</i> NCFM	Mannitol	Inner/outer nozzle: 200/300 μm , Air pressure: 600 mbar, Frequency: 300 Hz	550–700	96.8	SGF (pH 2, 2 h) SIF (pH 7.5, 3 h)	78.4 70.2	64.9 0.0	291

ND: not determined, SGC: simulated gastric conditions, SGJ: simulated gastric juice, SIJ: simulated intestinal juice, EE: encapsulation efficiency, Refs: references

Combining prebiotics, i.e., pectin, mannitol, maltodextrin, inulin, and fructo-oligosaccharides (FOS), enhances probiotics survival in the upper gastrointestinal tract and improves their benefits due to a synergistic health effect^{291,305,306}.

Therefore, due to the increasing health awareness of consumers, the demand for functional foods containing probiotics is constantly growing^{307,308}. So far, most probiotics can be found in dairy products, and their consumption is in constant increase. However, lactose-intolerant, allergic, vegan, and vegetarian populations are in continuous growth, which introduces the need to develop dairy-free probiotic products, i.e., milk-less beverages of plant origin and functional foods²⁹¹. Therefore, encapsulation is a great way to incorporate probiotics into any food matrices. Beverages such as herbal teas and fruit juices enriched with probiotics presented promising results as functional food candidates^{291,307,309}. Core-shell capsules of lactobacillus acidophilus NCFM have been successfully incorporated in mulberry tea. The shell was made of alginate and mannitol as a prebiotic and provided stability for 4 weeks, with a probiotic concentration higher than the minimum required (6 log₁₀ CFU/mL)²⁹¹.

1.3.4 Encapsulation of Other Ingredients

In addition to oil and probiotic encapsulation, extrusion has been used for the encapsulation of various other ingredients. For instance, cells encapsulation using the coextrusion technology is one of the most promising methods for three-dimensional cell culture that mimics in vivo the three-dimensional structure of tissues and organs³¹³.

The core-shell structure appears to be superior to other bead structures for long-term cell culture and for three-dimensional self-assembled cellular structures formation³¹⁴. A semipermeable shell is necessary to provide a favorable microenvironment for the cells, with excellent permeability for mass transfer³¹³⁻³¹⁵. It ensures minimal solute diffusion and peripheral cells escape through the shell. Considering the self-organization capacities of human pluripotent stem cells, Cohen et al. (2023) successfully engineered a bioreactor based on a coextrusion milli-fluidic system³¹⁶. The system provided 3D micro-compartments in core-shell capsules, with controlled size, seeding cell density, and oxygen, as illustrated in Figure 1-21. Additionally, polyethyleneimine incorporation in the hydrogel shell reduced capsule swelling, resulting in improved stability and minimal protein adsorption³¹⁵.

A similar system for producing 3D cellular assays to study tumor progression have been previously described³¹⁷. The method involves encapsulating and growing cells inside

permeable, elastic, hollow microspheres. These spheres can serve as mechanical sensors to measure the pressure exerted by the expanding spheroid. It is then possible to investigate the dynamics of pressure buildup and its effects on cellular density and organization within the spheroid³¹⁷. Research on invasion assays in a collagen matrix has suggested that mechanical cues from the surrounding microenvironment may trigger cell invasion from a growing tumor³¹⁷.

Coextrusion offers a unique avenue to produce *in vitro* cell-based assays useful for developing new anticancer therapies and investigating the interplay between mechanics and growth in tumor evolution.

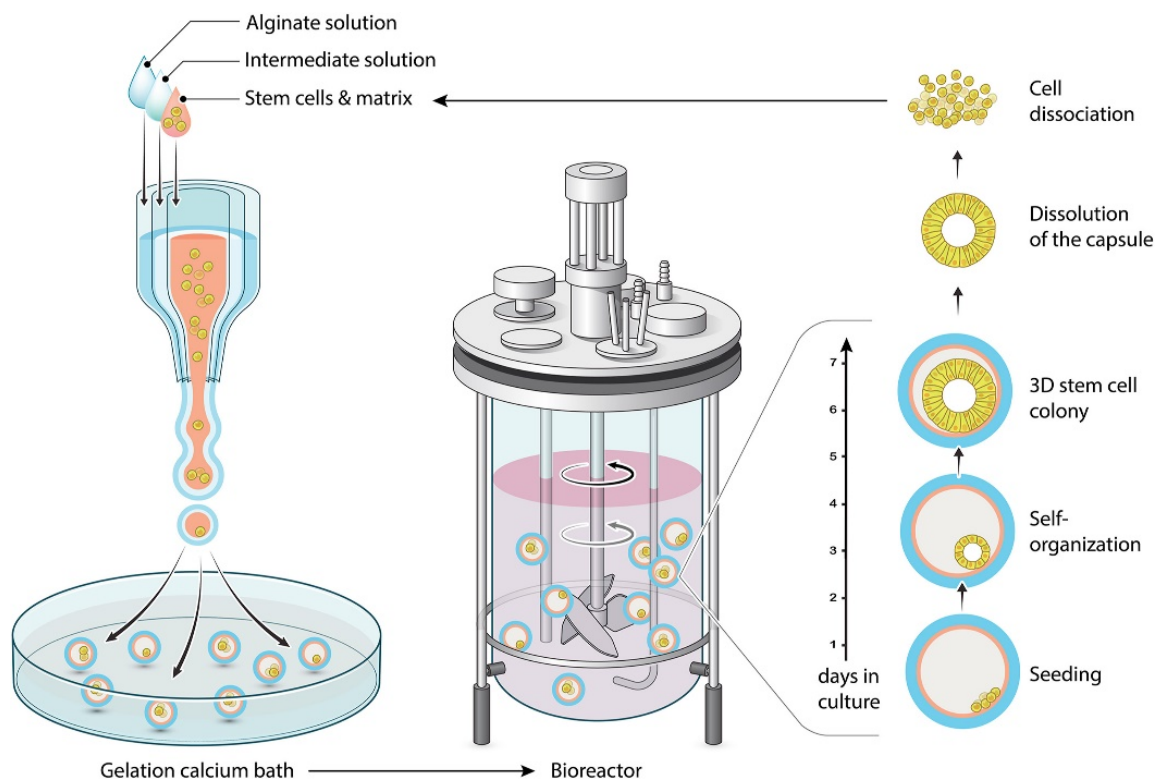


Figure 1-21. Encapsulation and scale-independent culture of encapsulated 3D human pluripotent stem cell colonies in bioreactors³¹⁶.

Furthermore, individual compartments provided by core-shell capsules are a great way to control a coculture behavior, e.g., in host-microbiome studies, through intestinal cells and bacteria encapsulation³¹³. Promising results have been reported for cell encapsulation using the coextrusion technology. Stem cells and multipotent stromal cells have been effectively encapsulated by coextrusion. Great cell viability, metabolic activity, and cell-cell interactions were achieved. Cancer cells (CT26, Caco-2) have also been successfully encapsulated in core-shell capsules with a thin shell; in this case, the addition of sodium dodecyl sulfate surfactant was required for capsule production²²⁰.

An adequate core viscosity ensures the flowability, and low-viscosity high-G alginate improved in vitro culture stability and promoted pluripotency in multipotent stromal cells. Furthermore, the M/G ratio in alginate appeared to impact the encapsulated cells³¹⁴. Core-shell capsules showed a high potential as advanced functional carriers for stem cells and organoids efficient cultivation and transplantation and are a promising tool for tissue engineering and regenerative systems for medical applications^{318,319}.

The coextrusion technology is also promising for core-shell carrier system production for the simultaneous encapsulation of multiple active substances in a single carrier. The system is solvent-free and allows a precise control of particle size and composition. Highly efficient encapsulation and controlled release of two synergistic anticancer drugs were achieved. In this study, 0 % of cancerous human cells viability was reached after 20 h of incubation with the drugs doxorubicin hydrochloride and paclitaxel³²⁰.

Core-shell liquid microcapsules presented great results for pharmaceutical extraction from drinking water. Whelehan et al. (2010) used liquid-core microcapsules loaded with dibutyl sebacate and oleic acid and obtained promising results for the rapid extraction of diclofenac, metoprolol, warfarin, and carbamazepine from water³²¹.

Capsules are suitable, as reactive cells, for fatty acid methyl esters production, which is an alternative to diesel fuel. Modified alginate capsules were used as a micro-reactor for transesterifying triglycerides and esterifying free fatty acids³²².

The core-shell structure system is also a great candidate for phase-change materials encapsulation. Capsules of n-nonadecane have been successfully produced with the electro-coextrusion process for thermo-regulating textiles. These 200–400 μm microcapsules contained up to 84 % of n-nonadecane and had an energy-storing density over 137 J.g^{-1} ³²³.

1.3.5 Conclusions

For many years, encapsulation has been utilized across multiple fields and for diverse applications. Encapsulation can be employed to shield the enclosed substance from its external environment, enhancing the stability of a dispersion, preventing denaturation and chemical reactions with external compounds, as well as slowing down the oxidation and evaporation of the encapsulated substance. Encapsulation also facilitates the controlled release of the enclosed substance, which can be released with the degradation of the encapsulating material at a desired

time. For this purpose, actives are encapsulated in various forms, i.e., powder, liposomes, beads, core-shell capsules. This function is particularly useful as it allows utilizing these objects as carriers and functionalizing them with active substances in cosmetic or pharmaceutical applications.

Nonetheless, core-shell capsules offer several advantages over simple extrusion processes. Firstly, they allow for a large payload due to their reservoir-type structure, enabling a higher quantity of active ingredients to be encapsulated, which is a very important feature for encapsulation efficiency and oil encapsulation payload, as discussed above. Secondly, the shell provides a protective barrier for the encapsulated ingredient, improving its stability against oxidation and limiting the evaporation of highly volatile actives such as essential oils. Thirdly, the shell also enables slow-release kinetics, regulating the release of the encapsulated substance over time or enabling a targeted release to allow actives, e.g., probiotics, to be protected from degradation in the gastrointestinal tract. Additionally, core-shell capsules can produce a burst-like effect when broken, resulting in a high release of flavor, for example, in chewing gum. The continuous production process of core-shell capsules is also an added advantage.

Overall, the use of certain polymer/copolymers matrices for shell solutions enhances the shell properties, both for oil protection against oxidation and for probiotics protection during gastric digestion. The coextrusion technology is a very versatile method, in addition it is applicable for the encapsulation of a large variety of materials (oils, dyes, probiotics, cells, peptides, etc.). It can be conducted in a sterile environment and is scalable for industrial production. The encapsulation of complex ingredients or viable cells and at a large industrial scale is developing to answer the wide requests in the food, medical, pharmacological, and environmental fields.

Key highlights

- Core-shell structure is an interesting and promising encapsulation structure for active molecules protection and controlled release.
- Coextrusion technology held promising results in oils, essential oil by reducing oxidation, evaporation of volatile compound.
- Core-shell capsules showed great results in probiotics stability and shelf-life extension.
- Coextrusion is a versatile encapsulation technique, and a valuable tool with significant application opportunities, ranging from pharmaceuticals to food production.

Conclusion of the literature review

As described in this chapter encapsulation through coextrusion process has a key role as a vectorization tool for bioactive and ingredients. Through the versatility of its applications, it is important and essential to understand the process operating to facilitate and expand its use in various fields. Coextrusion method, as every encapsulation technology is impacted by various variables related to process parameters, and/or to the properties of matrices and ingredients encapsulated (concentration, molecular weight, molecular structure).

Some variables are common to several encapsulation methods and have been widely studied. However, being relatively recent, coextrusion technology requires additional investigations to facilitate applications. Therefore, it is essential to study variables interactions impacts on capsules characteristics as a set of interrelated process parameters.

Several coextrusion technologies have been developed with various functioning principles. As described above, the operating principles are very precise and require very rigorous adjustment. Precise study of experimental conditions is necessary, where response surface methodology seem adapted.

In order to improve current industrial applications and develop encapsulation field, study and process understanding could permit the development of phenomenological models adapted to coextrusion. The objectives are to understand and knock down the biotechnological barriers limiting the effectiveness and feasibility coextrusion process.

Chapter 2. Study of encapsulation factors impact on the physio-chemical properties of core-shell capsules produced by coextrusion.

Ce chapitre étudie les effets de différents facteurs du procédé sur la formation des capsules d'alginate (forme, taille, centrage du noyau), leur aptitude à encapsuler (charge utile encapsulée) ainsi que leur résistance mécanique. La méthode des surfaces des réponses a été choisie pour étudier les facteurs et leurs interactions dans deux procédés de coextrusion couramment utilisés.

Une première étude⁴ traite de la coextrusion par rupture de jet annulaire. Les effets des débits d'alginate et d'huile, de la fréquence appliquée, de la concentration en calcium et du vieillissement de la solution d'alginate sur les capsules cœur-couronne produites ont été détaillés. Une seconde étude, publiée dans *LWT*⁵, a porté sur le procédé industriel de coextrusion goutte-à-goutte. Elle a concerné l'influence de la concentration en chlorure de calcium, du débit d'alginate et d'huile et de la hauteur de chute sur les capsules produites. Enfin, des modèles ont été développés pour les deux procédés afin de faciliter les applications industrielles en tant qu'outils prédictifs. Le modèle concernant le procédé de coextrusion en système goutte-à-goutte a permis d'obtenir un outil prédictif ainsi que des paramètres optimaux de production utilisés dorénavant par l'entreprise partenaire pour la production de capsules d'huile d'olive.

This chapter aims to investigate the effects of different factors on capsule properties (shape, core centricity, encapsulated payload, mechanical resistance). For this purpose, response surface methodology has been used for the investigation of the factors and their interactions. The most commonly used methods, dripping coextrusion and annular jet breaking coextrusion, are the focus of this chapter. The effects of alginate and oil rates, applied frequency, calcium concentration and alginate solution aging on core-shell capsules produced by annular jet breaking were studied in a paper published in *Colloids and Surfaces A: Physicochemical and Engineering Aspects*. A paper published in *LWT* also examined the effects of calcium chloride concentration, alginate and oil flow rate and drop height on an industrial dripping process. Finally, mathematical models were successfully developed for both methods to facilitate industrial applications as predictive tools. Dripping coextrusion optimum parameters are now used by the company for olive oil capsules production.

⁴ Bennacef, C., Desobry-Banon, S., Probst, L. & Desobry, S. Optimization of core-shell capsules properties (Olive oil/alginate) obtained by dripping coextrusion process. *LWT* **167**, 113879 (2022)

⁵ Bennacef, C. *et al.* Study and optimization of core-shell capsules produced by annular jet breaking coextrusion. *Colloids Surf A Physicochem Eng Asp* **629**, (2021)

2.1 Study and optimization of core-shell capsules produced by annular jet breaking coextrusion (*published in Colloids and Surfaces A : Physicochemical and Engineering Aspects*)

2.1.1 Introduction

Encapsulation technology is widely used nowadays, especially for stabilizing active compounds and materials of interest, such as active food ingredients or probiotics ^{289,324}. Encapsulation process ensures also controlled compounds delivery ³²⁵. Depending on encapsulation purpose and core material nature, many encapsulation methods can be used ³²⁶.

Spray-drying process is probably one of the most widespread encapsulation techniques due to its high productivity and inexpensive technology. Unfortunately, spray-drying presents limitations due to heating of sensitive compounds ¹⁶⁵.

Extrusion methods are also largely used for encapsulation in many fields ³²⁷ using various core-material nature (mainly hydrogels or liposomes) or application conditions ¹². In coextrusion technology, the material of interest (*i.e.* oil, sensible biomolecules, high added value ingredient) is entrapped into a core-shell capsule, ranging in diameter from micrometers up to millimeters, depending on injectors diameters ²⁹³. This spherification process is an effective way to produce uniform capsules in size and shape ³²⁸. Spherification process is a relatively recent encapsulation process compared to more largely used encapsulation methods. It results in the formation of a drop-in-drop structure with a liquid core. An attractive visual effect can be achieved with a transparent matrix as alginate ¹². As an example, in food industry a caviar-like structure can be obtained with an interesting visual effect for food gastronomy ²⁵³, while cosmetic industries find an interest in liquid core capsules to protect and deliver cosmetic bioactives ²⁰⁸. Furthermore, due to its porosity that facilitates exchanges and its mimicry of native tissue environment, core-shell capsules present a great interest as a cell culture medium and 3D cellular constructs for micro-organisms survival and growth in medical and biological areas ^{314,317,324}.

Core-shell structure presents a high encapsulation payload with higher core material content than other structures such as spray-dried particles ³²⁹. Also, coextrusion technology allows an easy injection of core-material without any further component addition or treatment. It also gives a promising candidate for oil encapsulation ^{257,267}, that tended to fail with other encapsulation techniques ³³⁰. Several types of polymer materials have been tested with the coextrusion process to produce core-shell capsules and to encapsulate hydrophilic and hydrophobic liquids, *i.e.* alginate, poly(L-lactide), poly(D,L-lactide-co-glycolide),

poly(dimethylsiloxane), also photopolymer (*i.e.* DuPont photopolymer Somos TM), and cocoa butter ³²⁸.

Alginate presents the advantage to be a nontoxic natural polymer that is composed of uronic acids (mannuronic and guluronic acids) linked via (1→4) glycosidic bonds ³². Due to its biodegradability, biocompatibility and non-antigenicity, alginate is Generally Recognized As Safe (GRAS) and is characterized by its large variety of applications ²⁰. Alginate gelling properties allow hydrogel formation that is widely used in coextrusion process ³². The mechanisms to form an alginate reticulated networks begin with divalent cations such as Ca²⁺ that cross-link alginate antiparallel polyuronates chains with lateral associations of guluronic acids ^{30,48}. Understanding spherification mechanisms and effects of processing factors are very important to enlarge alginate application fields.

The present work aims to understand the effects of flow rates (alginate solution and oil), vibration frequency, calcium chloride concentration in the gelling bath and alginate solution age, on shape and oil payload of capsules produced by annular jet breaking coextrusion method. The selected experimental parameters were studied with the statistical technique, Response Surface Method (RSM), to analyze coextrusion process and determine the parameters interactions. Our approach using experimental design facilitates the production of top-quality capsules for further applications.

2.1.2 Materials and methods

2.1.2.1 Materials

High viscosity sodium alginate was purchased from Louis-François (Croissy-Beaubourg, France) with a M/G ratio of 1.5. Purified Calcium chloride ≥ 94% was purchased from VWR (VWR Chemicals ®, France). Organic virgin Sunflower oil (Bio Village, France) was purchased from leading supermarket chain based in France. Sudan III and Ethylenediaminetetraacetic acid disodium salt dihydrate (EDTA) come from Sigma-Aldrich (Saint Quentin Fallavier, France). HPLC grade heptane 99 % was purchased from Carlo Erba (Val-de-Reuil, France).

2.1.2.2 Preparation of shell and core solutions

Shell solution was prepared by dissolving sodium alginate (0.8 % w/w) in distilled water and kept under stirring for 3h until complete dissolution then stored at room temperature from 24 to 72 h before spherification.

Core solution was prepared by dissolving 0.2 g of dye (Sudan III) into 400 g of sunflower oil. This coloration allowed easier and more precise analysis of capsules properties.

2.1.2.3 Preparation of alginate/oil capsules

Shell and core solutions were transferred separately into two 50 mL syringes. Alginate/oil capsules were prepared using a B-395 Pro Encapsulator (Buchi, Switzerland). As illustrated in Figure 2-1, using syringe driver, shell and core solutions were simultaneously injected through a coaxial nozzle composed of a 750 μm diameter internal nozzle (core) and a 900 μm external nozzle (shell) into a calcium chloride gelation bath. A 2000 V electric charge and a vibration frequency were applied during spherification for droplets separation and dispersion. Capsules scattering was due to Rayleigh-Plateau instability and electrostatic charges on capsules surfaces applied through the electrode. Alginate/oil capsules were formed and maintained in the gelation bath for one hour to ensure complete crosslinking. Capsules were then washed with distilled water, weighted and, finally, stored in distilled water at 20°C before analysis.

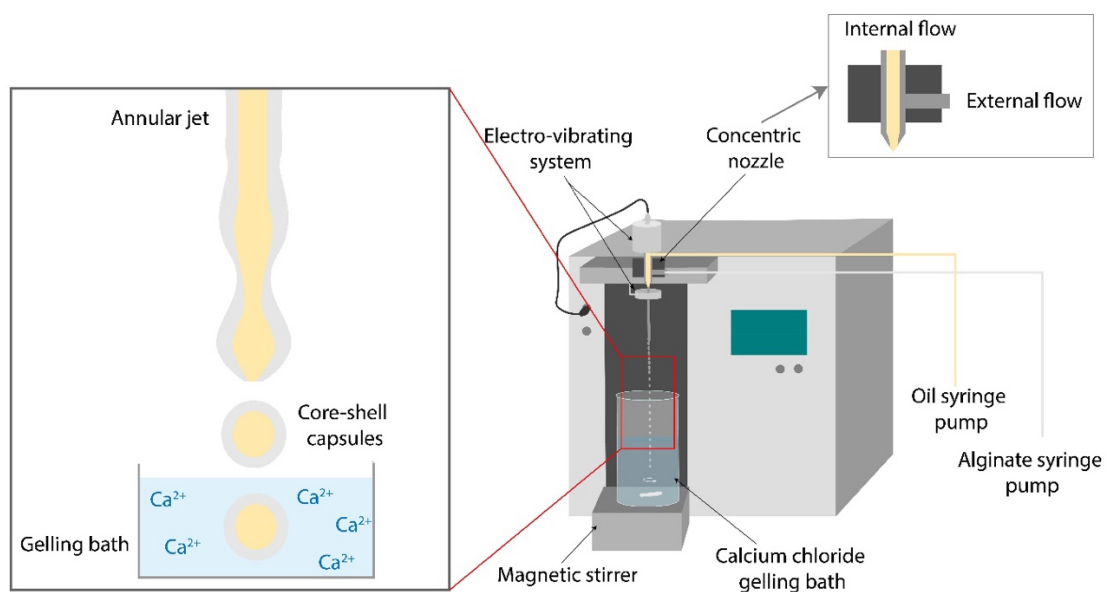


Figure 2-1. Electro-vibrating coextrusion process and core-shell capsules formation using a B-395 Pro Encapsulator (Buchi, Switzerland)

2.1.2.4 Determination of capsules size

To measure alginate/oil capsules size, 10 capsules of each sample were observed using an Olympus light microscope equipped with a CMOS 5 MPixels camera. For this study, capsules area was defined as more representative value for capsules size. Knowing that value such as diameter could be biased if capsules are more or less oval. Average area was calculated from captured images using Toupview software.

2.1.2.5 Determination of sphericity and centricity indices

In order to quantify the capsules shape, the method developed by Partovinia & Vatankhah (2019) was used to calculate two indices from diameters and shell thicknesses from captured images using Toupview software³³¹. Sphericity index was defined as indicated in (Figure 2-2) following equation 2.1:

$$\text{Sphericity index} = \frac{d_{\min}}{d_{\max}} \quad (2.1)$$

Where d_{\min} is minimum diameter and d_{\max} is maximum diameter. A sphericity index equal to 1 correspond to a perfect spherical shape ($d_{\min}=d_{\max}$)

Minimum and maximum shell thickness were used to determine the centricity index of oil core inside the alginate capsule (Figure 2-2). The centricity index was calculated using equation 2.2:

$$\text{Centricity index} = \frac{ST_{\min}}{ST_{\max}} \quad (2.2)$$

Where ST_{\min} and ST_{\max} are respectively minimum and maximum shell thickness. Centricity index equal to 1 correspond to a perfectly centered core. However, being a three-dimensional parameter, centricity was difficult to measure, so that real distance between the core and the shell could not appear in the two-dimensional microscope captures.

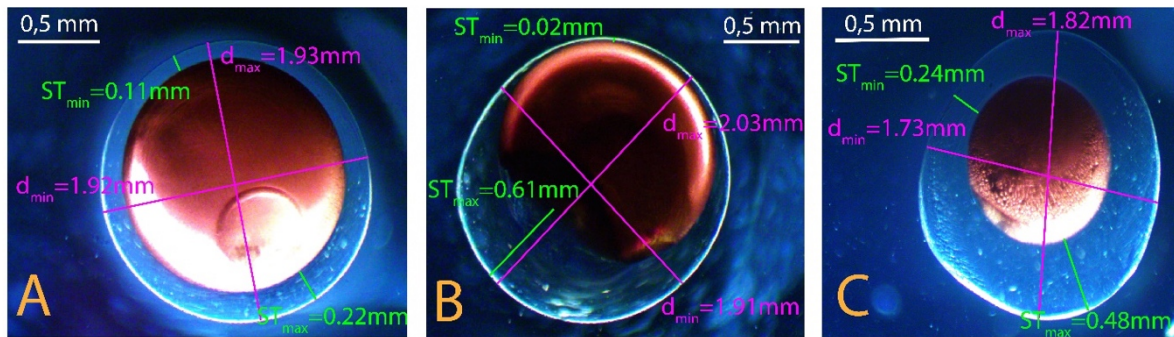


Figure 2-2. Microscopy pictures of core-shell capsules with a relatively spherical capsule and centered core (A), a capsule with low centricity index (B) and an example of centered core with a low payload (C)

2.1.2.6 Determination of encapsulation payload

For determination of oil encapsulation payload, a sample 15 g of alginate/oil capsules were disintegrated in 100 mL of a EDTA solution (0.2 mol.L^{-1}) using a vortex mixer. In the same vessel, 30 mL of heptane was added to extract oil phase. 50 % of the supernatant volume (heptane + oil) were collected in a preweighted flask and evaporated on rotavapor. The residue obtained was considered as half of the total oil quantity encapsulated in 15 g of capsules.

Encapsulation payload was calculated with the following equation:

$$\text{Encapsulation payload} = \frac{\text{Weight of the residue} \times 2}{\text{Weight of the capsules sampled}} \quad (2.3)$$

2.1.2.7 Experimental design

An experiment design was established after preliminary studies that allowed levels definition for the experimental domain. To evaluate the effect of five process parameters on capsule properties. Encapsulation process parameters, as variables, are detailed in Table 2-1.

Table 2-1. Experimental design levels for independent variables used in the spherification process.

Variable	Name	Unit	Low level value	High Level value	Number of levels
X1	External flow rate	mL.min ⁻¹	30	50	5
X2	Internal flow rate	mL.min ⁻¹	4	18	7
X3	Frequency	Hz	80	200	7
X4	Log ₁₀ [CaCl ₂]	g.L ⁻¹	0.176	1.699	7
X5	Shell solution age	Hours	24	72	3

Doehlert experimental design was used to study processing variables influence on capsules shape and payload in spherification process. It has the advantage to represent uniform distribution of the studied experimental points. Doehlert needs fewer experiments and allows to study variables with different levels which gives flexibility to assign more levels for strongest effects so that maximum information could be obtained³³². In this sense, external flow rate (X₁), internal flow rate (X₂), frequency (X₃), Log₁₀ [CaCl₂] (X₄) and shell solution age (X₅) were selected as independent variables (Table 2-2). In this study, Log₁₀[CaCl₂] was used instead of [CaCl₂] in order to test a large domain of concentration and preserve a large part of the experimental design for the lowest concentrations of calcium ions. Table 2-2 presents the corresponding calcium chloride concentrations for each Log₁₀ [CaCl₂] variable.

Table 2-2 Calcium concentrations corresponding to Log₁₀ [CaCl₂] variable.

Log ₁₀ [CaCl ₂]	[CaCl ₂] g.L ⁻¹
0.176	1.50
0.328	2.12
0.785	6.09
0.937	8.66
1.089	12.29
1.546	35.21
1.699	50.00

Sequence and number of experiments were determined using NEMROD software. Doehlert matrix shows a great flexibility and a uniform distribution of experimental points

within the experimental domain. The total number of experiments in Doehlert design was calculated as $N \geq K^2 + K + cp$. Where K is the number of variables studied and cp is the number of replicates at center point. A total of 34 experiments, including three replicates at the center point was employed for the study.

Capsules size (Y_1), sphericity index (Y_2), centricity index (Y_3) and encapsulation payload (Y_4) were taken as output data of the system. In order to predict the response function, an empirical model was built. By using experimental data, a model with linear, interaction and quadratic effects involving five independent variables, was employed and it can be approximated by the model:

$$Y = b_0 + \sum_{i=1}^k b_i x_i + \sum_{i=1}^k b_{ii} x_i^2 + \sum_{i=1}^{k-1} \sum_{j=i+1}^k b_{ij} x_i x_j \quad (2.4)$$

Where Y is the studied dependent response, where the i and j vary from 1 to 5 (number of independent variables studied here). b_0 and b_i are respectively constant term and regression coefficient for linear effects; b_{ii} are regression indices for squared effects and b_{ij} are regression indices for interaction effects. x_i and x_j are coded experimental levels of the independent variables.

2.1.2.8 Statistics

Analysis of variance (ANOVA), regression and graphical study and optimization experiments were examined using NEMRODW software.

2.1.2.9 Optimization and validation of the model

The optimum conditions resulting in maximum beads size, sphericity, centricity and encapsulation payload were determined based on the predictive models using NEMRODW. To validate the model, predicted optimal performances were carried out, and capsules size, sphericity and centricity indices and encapsulation payload experimental values were compared to predicted values.

2.1.3 Results and discussion

Table 2-3. Experimental data obtained by the application of the experimental design.

N°Exp	Independent Variables					Responses			
	AQ	OQ	Frequency	Log10 [CaCl ₂]	AlgSA	Area	Sphericity	Centricity	Payload
	mL/min	mL/min	Hz		Hour	mm ²			
1	50	11.0	140	0.937	48	3.01	0.94	0.06	0.37
2	30	11.0	140	0.937	48	3.04	0.97	0.26	0.34
3	45	18.0	140	0.937	48	4.33	0.70	0.04	0.36
4	35	4.0	140	0.937	48	2.67	0.97	0.13	0.16
5	45	4.0	140	0.937	48	2.49	0.91	0.46	0.17
6	35	18.0	140	0.937	48	3.64	0.92	0.16	0.42
7	45	13.3	200	0.937	48	2.34	0.94	0.35	0.37
8	35	8.7	80	0.937	48	3.65	0.94	0.06	0.33
9	45	8.7	80	0.937	48	3.93	0.88	0.11	0.29
10	40	15.7	80	0.937	48	3.52	0.92	0.06	0.43
11	35	13.3	200	0.937	48	2.33	0.98	0.39	0.39
12	40	6.3	200	0.937	48	1.88	0.95	0.27	0.28
13	45	13.3	155	1.699	48	2.34	0.93	0.20	0.44
14	35	8.7	125	0.176	48	3.95	0.96	0.08	0.25
15	45	8.7	125	0.176	48	7.11	0.92	0.03	0.21
16	40	15.7	125	0.176	48	6.79	0.84	0.07	0.29
17	40	11.0	185	0.176	48	4.98	0.86	0.07	0.23
18	35	13.3	155	1.699	48	2.31	0.97	0.15	0.46
19	40	6.3	155	1.699	48	2.08	0.96	0.18	0.25
20	40	11.0	95	1.699	48	2.68	0.96	0.16	0.39
21	45	13.3	155	1.089	72	2.99	0.91	0.10	0.36
22	35	8.7	125	0.785	24	3.09	0.91	0.03	0.28
23	45	8.7	125	0.785	24	3.66	0.79	0.08	0.27
24	40	15.7	125	0.785	24	3.56	0.90	0.12	0.35
25	40	11.0	185	0.785	24	2.62	0.95	0.23	0.32
26	40	11.0	140	1.546	24	2.42	0.88	0.11	0.47
27	35	13.3	155	1.089	72	2.88	0.91	0.26	0.35
28	40	6.3	155	1.089	72	2.10	0.94	0.08	0.34
29	40	11.0	95	1.089	72	2.88	0.90	0.03	0.38
30	40	11.0	140	0.328	72	5.78	0.88	0.04	0.27
31	40	11.0	140	0.937	48	2.97	0.94	0.04	0.33
32	40	11.0	140	0.937	48	3.29	0.93	0.06	0.32
33	40	11.0	140	0.937	48	3.09	0.90	0.16	0.35
34	40	11.0	140	0.937	48	3.20	0.93	0.09	0.34

AQ: Alginate solution flow rate; **OQ:** Oil flow rate; **AlgSA:** Alginate solution aging

2.1.3.1 Effect of experimental parameters on capsules shape

In order to study the impact of experimental variables on capsules shape, 34 experiments were carried out and the responses are displayed in Table 2-3. Capsules size (Y_1), sphericity (Y_2) and centricity (Y_3) indices gave information about capsule shape and regularity.

Analysis of the results confirmed the validity of the experimental design responses. The model consistency deduced from the Doehlert experimental design and its fitness values were expressed by the coefficient of determination ($R^2 = 0.950$ for Y_1 , $R^2 = 0.883$ for Y_2 and $R^2 = 0.883$ for Y_3) which is greater than 0.800 for the three responses and indicates that the polynomial models fitted well with experimental data. In Table 2-4, analysis of variance (ANOVA) for the capsules shape related responses confirmed the model adequacy and significance, more statistical data is displayed in Table 2-5. The regression showed the high significance of the 3 responses. After this validation, it was possible to develop a model for each response.

Table 2-4. ANOVA analysis for capsules shapes responses from Doehlert experimental design

Response	Source of variation	Sum of squares	degree of freedom	Mean square	F-value	Significance
Size	Regression	47.6650	20	2.3833	124.398	< 0.01 ***
	Residual	2.5013	13	0.1924		
	Lack-of-fit	2.4438	10	0.2444	12.756	2.97 *
	Pure error	0.0575	3	0.0192		
	Total	50.1664	33			
Sphericity index	Regression	0.0860	20	0.0043	4.507	0.511 **
	Residual	0.0115	12	0.0010		
	Lack-of-fit	0.0106	9	0.0012	3.907	14.5
	Pure error	0.0009	3	0.0003		
	Total	0.0975	32			
Centricity index	Regression	0.3423	20	0.0171	4.521	0.504 **
	Residual	0.0454	12	0.0038		
	Lack-of-fit	0.0371	9	0.0041	1.496	40.8
	Pure error	0.0083	3	0.0028		
	Total	0.3877	32			

(***): significant at the level > 99.9% (for $0.0001 < P \text{ value} < 0.001$).

(**): significant at the levels comprised between 99% and 99.9% (for $0.001 < P \text{ value} < 0.01$).

(*): significant at the levels comprised between 95% and 99% (for $0.01 < P \text{ value} < 0.05$).

The capsule size response, Y_1 , is represented with following second-order polynomial equation based on the experimental results:

$$\begin{aligned}
Y_1 = & 3,138 + 0,384x_1 + 0,666x_2 - 0,869x_3 - 2,177x_4 + 0,165x_5 \\
& - 0,113x_1^2 + 0,231x_2^2 - 0,323x_3^2 + 1,469x_4^2 - 0,110x_5^2 + 0,502x_1x_2 \\
& - 0,343x_1x_3 + 0,634x_2x_3 - 2,074x_1x_4 - 0,779x_2x_4 + 0,216x_3x_4 \\
& + 0,030x_1x_5 + 0,604x_2x_5 + 0,223x_3x_5 - 0,900x_4x_5 \quad (2.5)
\end{aligned}$$

It appears from equation 2.5 that the higher value for coefficient $b_4 = -2.117$ indicates that $\text{Log}_{10} [\text{CaCl}_2]$ (factor X_4) negatively impacts the response Y_1 so that an increase in calcium chloride concentration induced a decrease in capsules size as shown in Figure 2-3, probably by tightening the hydrogel network of capsule shell³³³. Moreover, the interaction coefficient b_{1-4} (-2.074) confirms the higher antagonist effect of calcium chloride concentration than positive effect of alginate flow rate solution on sphere size. More statistical data is presented in Table 2-4.

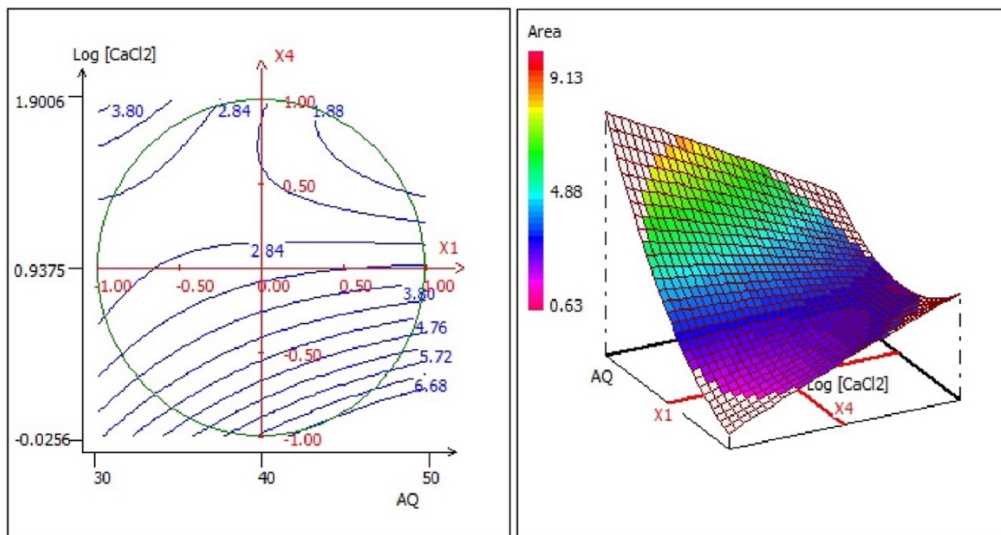


Figure 2-3. Surface and contour plots showing the effects of the mutual interaction between alginate solution flow rate (AQ) and calcium chloride concentration ($\text{Log}_{10}[\text{CaCl}_2]$) on the capsules size, while the other variables are kept at their center point.

An antagonist effect was also observed for the factors X_3 (Frequency) with a coefficient $b_3 = -0.869$. An increase of frequency to break the solution jet decreased the capsules size since the flow of the fluid was more rapidly cut at each vibration break as observed by other authors^{218,224}. X_1 (Alginate solution flow rate), X_2 (Oil flow rate) and X_5 (Alginate solution age) linearly increased capsules sizes. The coefficient $b_2=0.666$, higher than $b_1=0.384$, reflected that oil flow rate had a stronger impact on capsule size than alginates solution flow rate. This is also due to the tightening of shell hydrogel which shows a smaller volume due to high ion crosslinking in alginate network, while oil volume stays stable through the process and is not impacted by calcium concentration.

From experimental data, the capsules sphericity index, Y2, was modeled with the following equation:

$$\begin{aligned}
 Y2 = & 0,925 - 0,036x_1 - 0,014x_2 + 0,023x_3 + 0,035x_4 + 0,014x_5 + 0,030x_1^2 - 0,147x_2^2 \\
 & + 0,044x_3^2 + 0,015x_4^2 - 0,037x_5^2 - 0,214x_1x_2 + 0,088x_1x_3 - 0,062x_2x_3 \\
 & + 0,055x_1x_4 + 0,017x_2x_4 + 0,084x_3x_4 + 0,123x_1x_5 - 0,113x_2x_5 \\
 & - 0,013x_3x_5 + 0,058x_4x_5 \quad (2.6)
 \end{aligned}$$

According to the equation 2.6, the response Y2 (capsules sphericity index) was more impacted by the quadratic effects and parameters interactions than by linear effects. A great antagonist effect was observed on the interaction coefficient b_{1-2} . This indicated that capsule sphericity was related to combined effect of alginate flow rate and oil flow rate (Figure 2-4). The quadratic effects b_{2-2} showed also an antagonist effect of oil flow rate. This effect of inner solution flow rate has been reported, in complement to the impact of calcium concentration, outer flow rate and frequency interaction on capsules shape ²⁷².

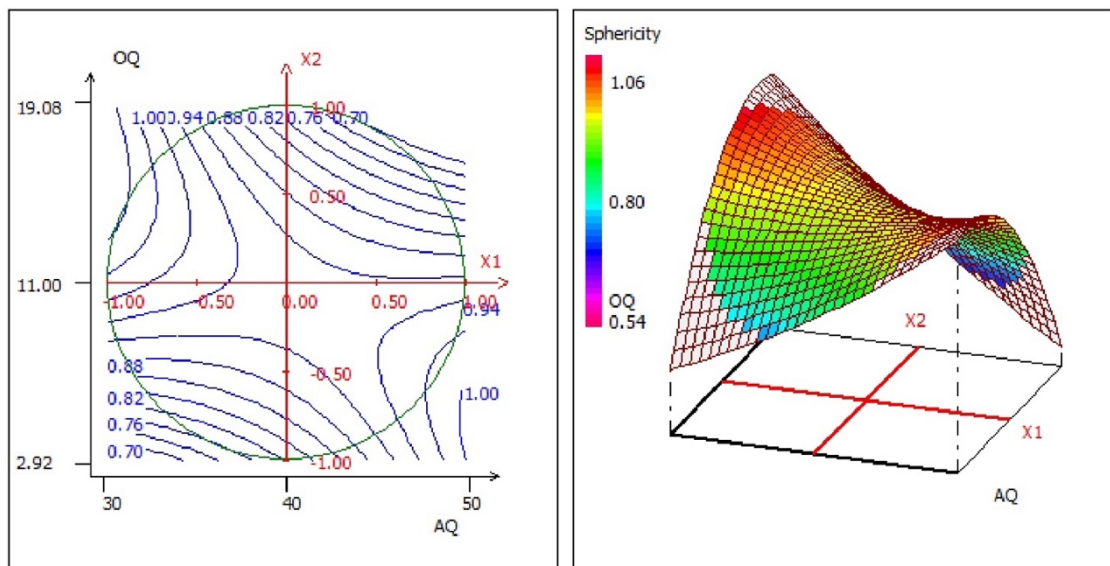


Figure 2-4. Surface and contour plots showing the effects of the mutual interaction between alginate solution flow rate (AQ) and oil flow rate (OQ) on the capsules sphericity, while the other variables are kept at their center point.

Based on experimental data (Table 2-3), the core centricity index, Y3, was described according to the mathematical model in equation 2.7:

$$\begin{aligned}
 Y3 = & 0,088 - 0,058x_1 + 0,026x_2 + 0,136x_3 + 0,066x_4 - 0,008x_5 \\
 & + 0,072x_1^2 + 0,257x_2^2 + 0,096x_3^2 - 0,037x_4^2 - 0,031x_5^2 - 0,492x_1x_2 \\
 & + 0,119x_1x_3 + 0,154x_2x_3 + 0,212x_1x_4 + 0,013x_2x_4 - 0,030x_3x_4 \\
 & - 0,027x_1x_5 + 0,52x_2x_5 - 0,059x_3x_5 - 0,042x_4x_5 \quad (2.7)
 \end{aligned}$$

From equation 2.7, the coefficient b_3 (0.136) showed that the frequency factor (factor X_3) linearly contributes on core centricity index. This observation could be due to the centering of oil core into the capsules under vibration. Another hypothesis could be made so that centricity would be correlated to capsules size, smaller capsules could induce a smaller viscoelastic resistance reducing the flapping phenomenon that leads to a decentered core²²⁰.

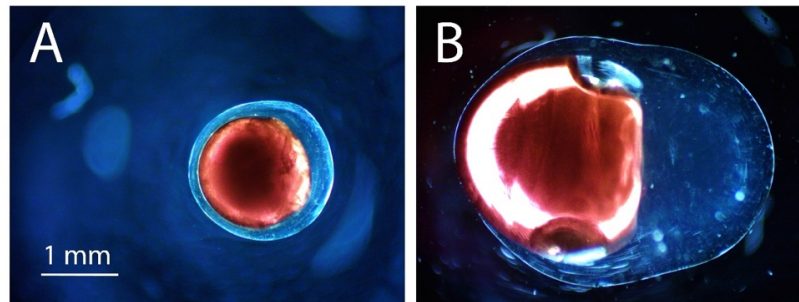


Figure 2-5. Microphotography of two capsules showing different characteristics, a small capsule with a high centricity and sphericity indices (A), and a larger capsule with low sphericity and centricity indices (B).

The coefficient b_{1-2} (-0.492) indicated an antagonist effect for the interaction between factors X_1 and X_2 . In addition, the quadratic effect of b_2 was also significant as presented in Table 2-5, and confirms, as expected, that centricity of oil core was strongly related to alginate and oil flow rates as presented in Figure 2-6²²⁰.

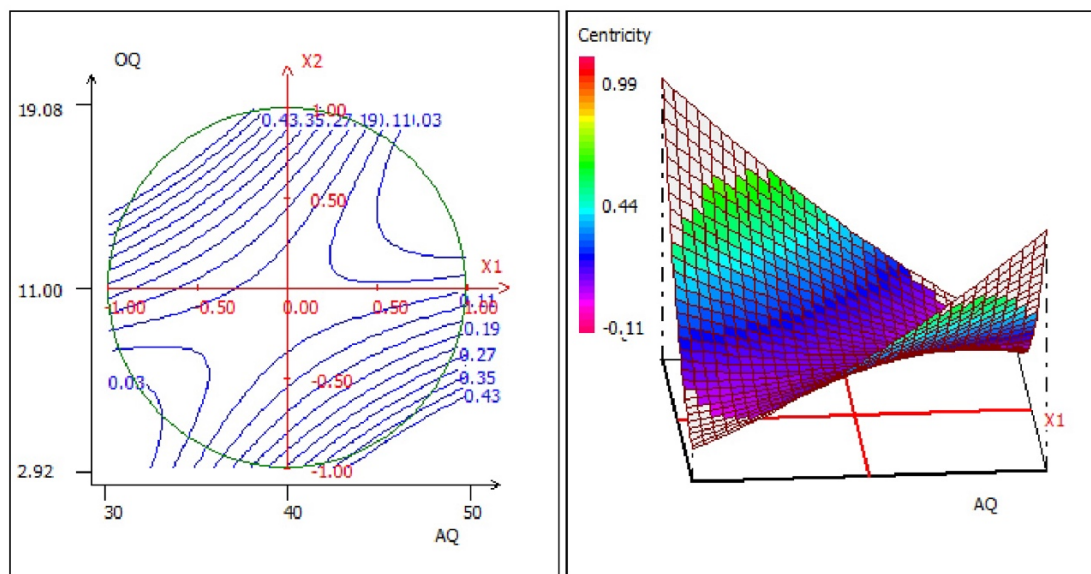


Figure 2-6. Surface and contour plots showing the effects of mutual interaction between alginate solution flow rate (AQ) and oil flow rate (OQ) on capsules centricity, while the other variables are kept at their center point.

Table 2-5. Model coefficients analysis of Doehlert Design for: Capsule size (Y1), Sphericity index (Y2), Centricity Index (Y3) and encapsulation Payload (Y4) responses by coextrusion process.

Coefficient	Value				Standard Error				t-value				Significance			
	Y1	Y2	Y3	Y4	Y1	Y2	Y3	Y4	Y1	Y2	Y3	Y4	Y1	Y2	Y3	Y4
b0	3.138	0.925	0.088	0.335	0.069	0.015	0.031	0.016	45.34	59.89	2.84	21.08	< 0.01 ***	< 0.01 ***	1.48 *	< 0.01 ***
b1	0.384	-0.036	-0.058	-0.009	0.057	0.013	0.027	0.013	6.80	-2.68	-2.17	-0.71	0.651 **	2.01 *	5.1	49.2
b2	0.666	-0.014	0.026	0.120	0.057	0.015	0.029	0.013	11.79	-0.94	0.88	9.23	0.131 **	36.4	39.7	< 0.01 ***
b3	-0.869	0.023	0.136	-0.005	0.057	0.013	0.025	0.013	-15.38	1.81	5.43	-0.39	0.0597 ***	9.6	0.0152 ***	70.1
b4	-2.177	0.035	0.066	0.100	0.057	0.013	0.025	0.013	-38.53	2.74	2.61	7.74	< 0.01 ***	1.80 *	2.27 *	< 0.01 ***
b5	0.165	0.014	-0.008	0.001	0.057	0.013	0.025	0.013	2.92	1.13	-0.31	0.10	6.1	28.2	76.3	92.2
b1-1	-0.113	0.030	0.072	0.020	0.120	0.027	0.053	0.028	-0.94	1.12	1.36	0.73	41.7	28.4	19.9	48.0
b2-2	0.231	-0.147	0.257	-0.083	0.120	0.032	0.064	0.028	1.93	-4.56	4.01	-3.03	15.0	0.0653 ***	0.174 **	0.971 **
b3-3	-0.323	0.044	0.096	0.036	0.113	0.026	0.051	0.026	-2.86	1.72	1.89	1.38	6.5	11.0	8.3	19.1
b4-4	1.469	0.015	-0.037	-0.026	0.107	0.024	0.048	0.025	13.70	0.60	-0.77	-1.08	0.0841 ***	55.8	45.4	30.1
b5-5	-0.110	-0.037	-0.031	0.016	0.103	0.023	0.046	0.024	-1.07	-1.61	-0.67	0.66	36.3	13.3	51.6	51.8
b1-2	0.502	-0.214	-0.492	-0.040	0.160	0.047	0.094	0.037	3.14	-4.53	-5.24	-1.10	5.2	0.0693 ***	0.0209 ***	29.1
b1-3	-0.343	0.088	0.119	0.027	0.179	0.041	0.082	0.041	-1.92	2.12	1.44	0.65	15.1	5.5	17.4	52.9
b2-3	0.634	-0.062	0.154	-0.051	0.179	0.040	0.080	0.041	3.55	-1.55	1.91	-1.24	3.81 *	14.8	8.0	23.9
b1-4	-2.074	0.055	0.212	0.021	0.186	0.042	0.084	0.043	-11.17	1.31	2.52	0.48	0.154 **	21.5	2.69 *	63.8
b2-4	-0.779	0.017	0.013	0.078	0.186	0.042	0.083	0.043	-4.20	0.42	0.16	1.82	2.47 *	68.5	87.8	9.2
b3-4	0.216	0.084	-0.030	0.045	0.186	0.042	0.084	0.043	1.16	2.00	-0.36	1.06	33.0	6.9	72.6	30.9
b1-5	0.030	0.123	-0.027	0.017	0.189	0.043	0.085	0.043	0.16	2.87	-0.31	0.39	88.5	1.41 *	75.9	70.5
b2-5	0.604	-0.113	0.052	-0.086	0.189	0.042	0.084	0.043	3.20	-2.66	0.61	-1.97	4.95 *	2.10 *	55.2	7.0
b3-5	0.223	-0.013	-0.059	-0.013	0.189	0.043	0.085	0.043	1.18	-0.31	-0.69	-0.30	32.3	76.3	50.1	76.7
b4-5	-0.900	0.058	-0.042	-0.074	0.189	0.042	0.085	0.043	-4.76	1.38	-0.50	-1.70	1.76 *	19.4	62.6	11.3

(***): significant at the level > 99.9% (for 0.0001 < P value < 0.001).

(**): significant at the levels comprised between 99% and 99.9% (for 0.001 < P value < 0.01).

(*): significant at the levels comprised between 95% and 99% (for 0.01 < P value < 0.05).

2.1.3.2 Effect of experimental parameters on encapsulation payload

The effects of experimental variables on encapsulation oil payload have also been studied and modeled. The model fit was evaluated by coefficient of determination ($R^2 = 0.931$) that was very close to 1 which expressed that the recorded experimental data adequately adjusted to the quadratic model. Moreover, an ANOVA was performed to determine statistical significance (Table 2-6). ANOVA showed a P-value <0.001 for encapsulation payload response, making the model significant at $>99.99\%$.

Table 2-6. ANOVA analysis for encapsulation payload indices from Doehlert experiments

Response	Source of variation	Sum of squares	Degree of freedom	Mean square	F-value	Significance
Payload	Regression	0,177	20	0,0088	8,758	0,0126***
	Residual	0,0131	13	0,001		
	Lack-of-fit	0,0126	10	0,0013	7,581	6,1
	Pure error	0,0005	3	0,0002		
	Total	0,1901	33			

(***): significant at the level $> 99.9\%$ (for $0.0001 < P \text{ value} < 0.001$).

Encapsulation payload responses (Y4) was modelled with the following mathematical equation:

$$\begin{aligned}
 Y4 = & 0.335 - 0.009x_1 + 0.120x_2 - 0.005x_3 + 0.100x_4 + 0.001x_5 \\
 & + 0.020x_1^2 - 0.083x_2^2 + 0.036x_3^2 - 0.026x_4^2 + 0.016x_5^2 - 0.040x_1x_2 \\
 & + 0.027x_1x_3 - 0.051x_2x_3 + 0.021x_1x_4 + 0.078x_2x_4 + 0.045x_3x_4 \\
 & + 0.017x_1x_5 - 0.086x_2x_5 - 0.013x_3x_5 - 0.074x_4x_5 \quad (2.8)
 \end{aligned}$$

From equation 2.8, modelling the encapsulation payload response, linear contributions of X_2 and X_4 can be observed with a high significance (P-value < 0.001) (Table 2-5). As expected, an increase of oil flow rate induces an increase of encapsulation oil payload²⁰⁸. Oil flow rate impact was confirmed with the quadratic effect coefficient b_{2-2} . However, calcium chloride seems to have a high impact on the payload, so that an increase in calcium chloride concentration resulted in an increase in payload as shown in Figure 2-7. The effect of calcium chloride on oil payload is probably also due to shell hydrogel tightening, so that the majority of the capsule volume and mass would be occupied with the oil core resulting in a high oil proportion and thus high encapsulation payload^{333,334}.

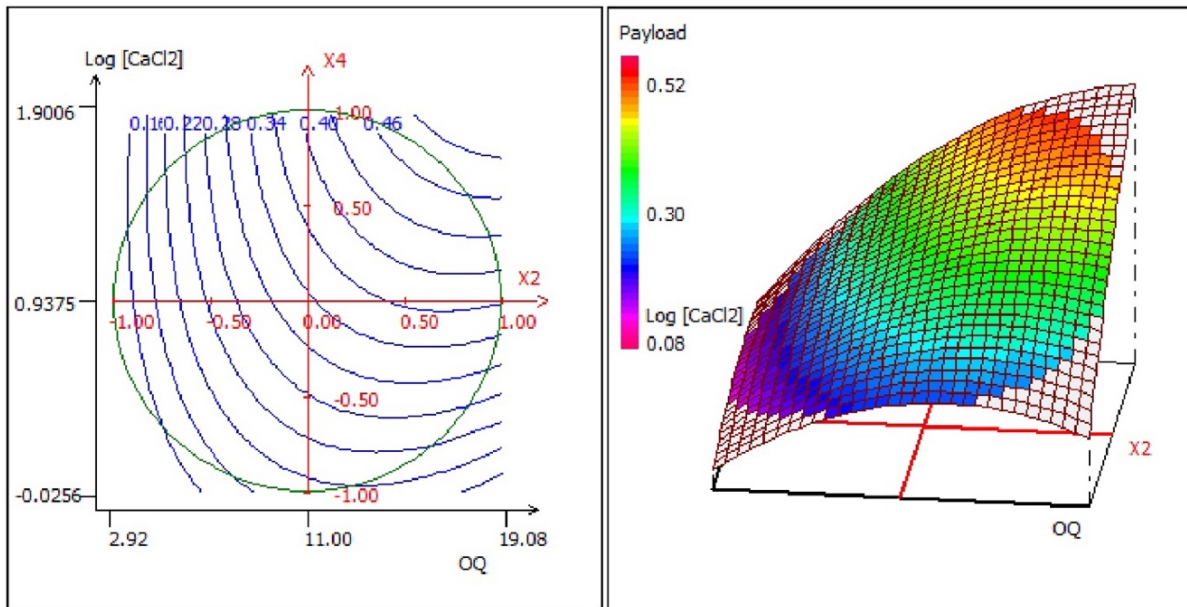


Figure 2-7. Surface and contour plots showing the effects of the mutual interaction between calcium chloride concentration ($\text{Log}_{10}[\text{CaCl}_2]$) and oil flow rate (OQ) on the encapsulation payload, while the other variables are kept at their center point.

2.1.3.3 Optimization of capsules shape and encapsulation payload

In this work, optimal production conditions were determined for capsules with a maximal encapsulation payload, a maximal sphericity and centricity, a capsules size of 3 mm. The challenge was that high capsules size tend to reduce considerably sphericity and centricity. Furthermore, small capsules with high score of sphericity and centricity resulted in low encapsulation payload.

Using multi-response NEMRODW software, optimal conditions for our criteria have been determined as alginate solution flow rate of $34 \text{ mL} \cdot \text{mn}^{-1}$, oil flow rate of $14.55 \text{ mL} \cdot \text{mn}^{-1}$, an applied frequency of 120 Hz, a calcium concentration of $6.71 \text{ g} \cdot \text{L}^{-1}$ and an alginate solution age of 47 h.

2.1.3.4 Model validation

For model validation, the predicted optimum independents variables were carried out, the experimental data obtained was compared to the predicted by multi-response model.

Table 2-7 presents the experimental conditions of optimum, the experimental response data and the predicted values and their intervals, in addition to the error percentage between predicted and experimental values.

Table 2-7. Experimental and predicted data for capsule size, sphericity and centricity index and encapsulation payload for optimum.

	Capsule area (mm ²)	Sphericity index	centricity Index	Encapsulation payload (%)
Predicted data	3.02	1.01	0.35	0.40
Experimental data	3.39 ± 0.31	0.95 ± 0.07	0.12 ± 0.14	0.37± 0.07

Experimental results match with the predicted mathematical model for capsules size which is very near the predicted value, sphericity index and encapsulation payload responses and showed a good correlation between experimental and predicted data.

However, experimental value for the centricity index did not correspond to the predicted value (0.12 ± 0.14 and 0.35 respectively). As mentioned previously, this could be due to the lack of precision for centricity measurements as a result of the two-dimensional measurement instead of a three-dimensional one. The face presented in the photograph (2D) was not fully representative of oil core centering in the capsule (3D).

2.1.3.5 Phenomenological modeling of capsules formation⁶

After calculating the optimum condition for beads processing, a phenomenological modelling can be proposed to describe the effects of alginate flow rate and CaCl₂ concentration on beads size. Two major effects occurred during alginate reticulation in the CaCl₂ solution, as described by Bennacef et al (2021)¹² (Figure 2-8).

The first effect was Ca²⁺ diffusion through the alginate network which leads to alginate reticulation. As CaCl₂ concentration increased, the number of links increased, and a contraction of the alginate network was observed. This first effect reduced the beads diameter during reticulation. The second effect occurred in excess of CaCl₂, because the supersaturation by Ca²⁺ of the alginate chains caused repulsion between chains and release of free alginate chains in the external solution due to stirring of CaCl₂ solution and final rinsing of the beads. This second phenomenon is called beads erosion. The reduced final size of the beads resulted from the cumulation of both effects.

¹ Following the results obtained during an extended study of the phenomenological model which will be presented further in chapter III, this part of the paper has been revised.

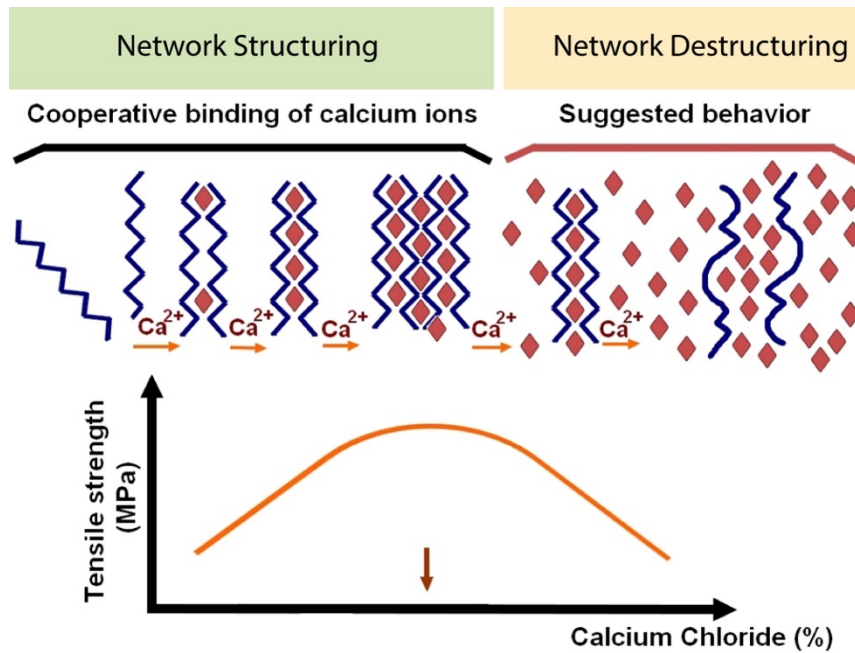


Figure 2-8. Scheme representing the mechanism of strengthening and weakening of the alginate network with the increase of calcium chloride ¹².

Based the Raleigh breakage equation, the combination of the two effects can be modelled by the following phenomenological equation:

$$\Delta V = \left(\frac{AQ}{F}\right) C + \frac{OQ}{F} \quad (2.9)$$

Where ΔV = volume variation ($V-V_0$); AQ = Alginate flow; OQ = Oil Flow; F = Frequency; C = Coefficient of size variation. If $C=0$, no size variation is observed; if $C<0$ or $C>0$, alginate retraction and/or erosion occurs.

To model these retraction effects, we used the Y1 prediction (equation 2.5) previously validated to calculate the final diameter of capsules vs alginate flow. From this calculation, we calculated easily capsules volume vs alginate flow/ F (Figure 2-9).

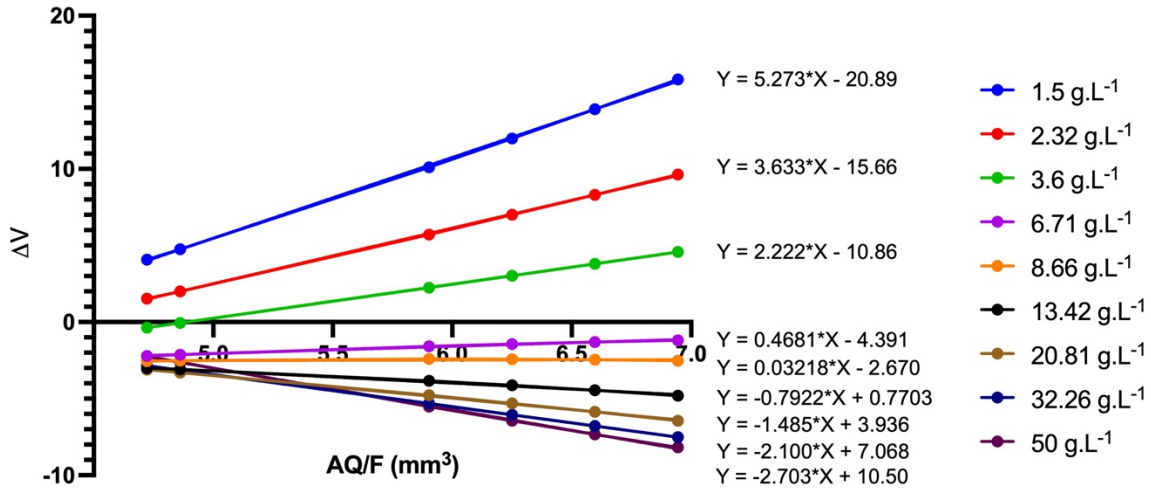


Figure 2-9. Capsules volume variation versus AQ/F for determination of C coefficients (draw slopes), using 9 CaCl₂ concentrations from 1.5 to 50 g.L⁻¹. Optimum values were applied in the Equation 2.9 to oil flow rate (14.55 mL.mn⁻¹), frequency (120 Hz), and an alginate solution age of 47 h.

In Figure 2-9, a linear evolution of the capsules volume variation was observed with the increase of Q/F. C decreased with increasing the CaCl₂ concentration, showing that the increase of the capsules size was reduced. This decrease was due to intensive retraction and erosion of the beads in Ca²⁺ excess.

The Figure 2-10 gives the modelling of C coefficient versus CaCl₂ concentration and provides the final phenomenological model to predict the capsules volume vs the alginate flow and the CaCl₂ concentration (Equation 2.10).

$$\Delta V = \left(\frac{AQ}{F}\right) \cdot (6.749 \text{ Log}[CaCl_2])^2 - 9.258 (\text{Log}[CaCl_2]) + 2.220 + \frac{OQ}{F} \quad (2.10)$$

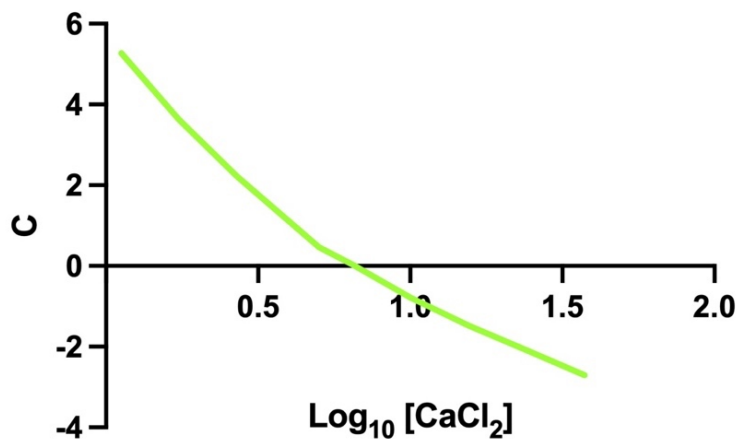


Figure 2-10. C coefficient versus CaCl₂ concentration for C coefficient modeling.

This model (Equation 2.10) can be used for direct application in the industrial process of alginate bead production. can be useful in order to estimate the effects of CaCl_2 on core-shell capsule. volume does not distinguish the effects of retraction and erosion.

2.1.4 Conclusion

In the present work, we studied the effect of alginate solution and oil flow rates, applied frequency, calcium concentration and alginate solution age, on the shape and encapsulation payload of core-shell capsules produced by annular jet coextrusion method. For that, response surface method (RSM) with Doehlert matrix produced five mathematical models that predict capsule size, sphericity index, centricity index and encapsulation payload. ANOVA statistics showed a high accuracy and significance for models obtained, so that experimental and predicted data were well correlated.

Calcium concentration presented a strong effect on capsules size and volume to that it impacted the encapsulation payload by tightening the shell hydrogel network. Also, frequency showed a great effect on capsules; an increase in vibration frequency induced the production of smaller capsules. Moreover, smaller capsules tended to provide higher centricity index as a result of reduced alginate viscoelastic resistance in smaller capsules with less alginate material.

Finally, it appeared that ageing of alginate solution does not have a significant effect on the studied responses. This suggested that an industrial application involving alginate solution preparation in great volumes and its storage for periods up to 72 hours would not significantly impact on capsules quality.

Multi-responses method with desirability function was used for process optimization. A good global value was achieved for capsules size, sphericity index and encapsulation payload. However, due to the lack of precision in the two-dimensional measurements, centricity index response does not fit perfectly in the predicted optimum model.

In this study, a mathematical model has been developed and can be utilized to predict shape and encapsulation payload of core-shell capsules, produced through annular jet breaking method. In addition, the model of interactions between alginate and oil flow rates, frequency, calcium concentration and alginate solution ageing provided a good tool for spherification and encapsulation technology in cosmetic or food industries.

Finally, a phenomenological model was successfully applied to model the effects of CaCl_2 and alginate flow rate on beads volume. This model is an essential tool to master industrial processing of core-shell alginate beads.

Key highlights

- Correlation of capsules shape and oil payload in coextrusion process.
- Obtention of quadratic models to predict capsules shape and oil payload.
- Capsules size inversely proportional to calcium concentration and frequency.
- Optimization of five experimental variables: alginate and oil flow rates, frequency, calcium concentration and alginate aging.
- Alginate ageing does not have significant effect.

2.2 Optimization of core-shell capsules properties (Olive oil/alginate) obtained by dripping coextrusion process (Published in LWT)

2.2.1 Introduction

Encapsulation technology involves entrapment of a material of interest, such as oils, bioactive compounds, and cells^{146,335,336}. Encapsulation has many objectives including enhancement of thermal, chemical, and oxidative stability^{146,337,338} and is widely used for controlled release of active agents^{339–341}. It is then used in food, cosmetics, chemical, and textile industries^{342–345}. Encapsulation recovers various techniques that produce a wide range of particle sizes from 1 μm to a few millimeters²¹⁸.

Core-shell capsules can be produced through two different methods, *i.e.* extrusion and coextrusion. In these two processes, sodium alginate is chosen for its wide use as the shell material, due to its ability to reticulate in presence of divalent ions. Extrusion consists in the injection of an internal mix containing divalent cation (Ca^{2+}) and targeted agent into an alginate gelling bath. Core-shell capsules formation is due to the Ca^{2+} ions diffusion from the core solution and alginate gelation at the surface of the drop. Ca^{2+} and residence time are the limiting factors of the gelation and thickness of the shell. This process is well-developed among encapsulation technologies used for liquid core-shell capsules production^{346,347}. Another application for extrusion allows to produce solid microcapsules^{348–350} by dripping alginate droplet into a calcium bath.

The second method to produce core-shell capsules is called coextrusion, coaxial extrusion or annular jet extrusion. It corresponds to the simultaneous injection through a coaxial nozzle of two solutions for core and shell capsule respectively, into a cationic solution (Ca^{2+}). In this coextrusion process, shell thickness results from the amount of alginate coextruded on each droplet. The control of the process also depends on solutions properties and compatibilities²⁰⁶. Compared to extrusion coextrusion presents the advantage to solve problems encountered for simple extrusion methods, such as agglomeration, shell non-uniformities, encapsulation of hydrophobic core, where Ca^{2+} is non-soluble^{78,173,351}. Coextrusion processes are applied today to encapsulate ingredients, as oils^{273,276,352}, probiotics^{246,296}, and cells^{313,353}.

The two main methods for coextrusion using alginate are vibrating jet-breaking system that has been previously studied^{271,354} and dripping system which is used in the present study to produce

larger core-shell capsules of millimetric size. This technology is simple and allows the formation of core-shell capsules by extrusion of internal (oil) and external (alginate) phases through a coaxial injector in a drop-by-drop system ³⁵⁵.

The present paper aimed to study the effects of dripping coextrusion parameters on core-shell capsules properties. From preliminary studies, the three main individual factors acting on spherification processes have been selected: calcium chloride concentration (X_1), alginate/oil total feed rate (X_2), and dripping height (X_3). The following responses of the spherification process have been selected to analyze the capsules produced by dripping coextrusion process: capsules diameter (Y_1), capsules sphericity index (Y_2), capsules rupture strength (Y_3), and encapsulation payload (Y_4). Collected responses were analyzed through statistical method of Response Surface Method (RSM) with an experimental design, to study effects of selected factors and their interactions on capsules characteristics. The purpose of this study was to promote and simplify the production of high-quality capsules by dripping coextrusion for industrial applications.

2.2.2 Materials and methods

2.2.2.1 Materials

Virgin Olive oil used for the spherification process was purchased from Puget (Marseille, France). Sodium alginate was purchased from FMC international (Cork, Ireland). Calcium chloride $\geq 99\%$ was purchased from Beauseigneur (Belfort, France). HPLC grade heptane 99% was purchased from Carlo Erba (Val-de-Reuil, France) and ethylenediaminetetraacetic acid disodium salt dihydrate (EDTA) came from Sigma-Aldrich (Saint Quentin Fallavier, France). Polysorbate 20 (pharmaceutical grade) was purchased from Lonza (Bâle, Switzerland).

2.2.2.2 Preparation of alginate/oil capsules

For the study, both alginate (2.5 % (w/w) sodium alginate and 2% (w/w) polysorbate 20 in distilled water) and oil were injected, using a gear pump, through a coaxial nozzle, where oil was injected into the internal tube and sodium alginate into the external tube (Figure 2-11). The drip flow system produced droplets which fell by gravity into the gelling bath when its weight is higher than the capillary force maintaining it attached to the nozzle ²⁰⁸. Figure 2-11 presents a photograph of the injecting nozzle with a droplet that will fall in the gelling bath. The total feed rate corresponds

to the sum of both oil and alginate rates with an oil feed rate value three times higher than alginate feed rate.

Alginate and oil rates are presented in Table 2-8. Alginate/olive oil capsules were maintained in gelation bath just for 2 minutes for complete crosslinking. Capsules were then rinsed with distilled water, weighted, and stored in distilled water at 20°C before analysis.

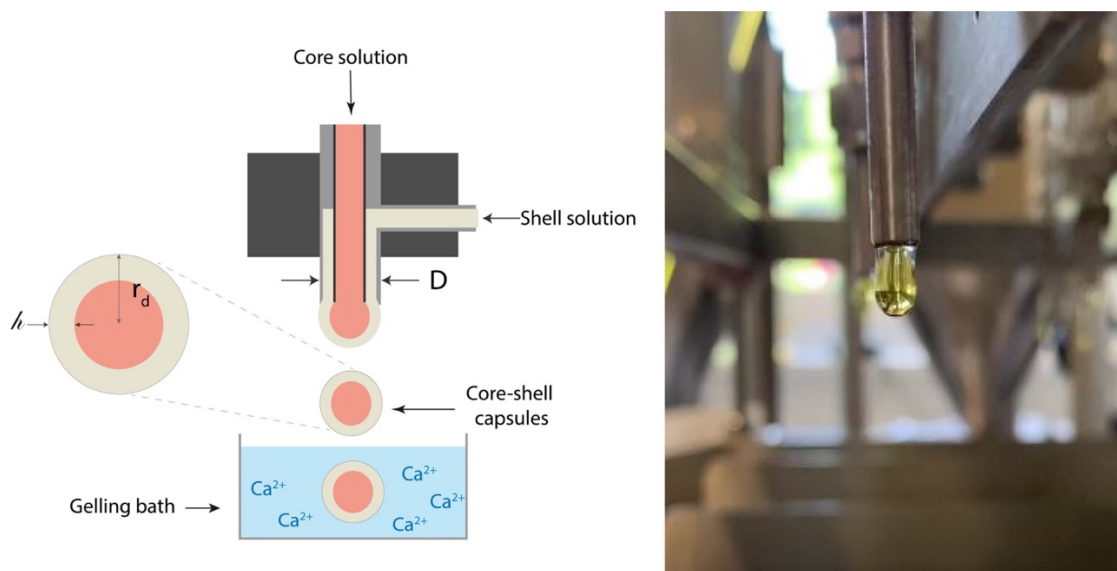


Figure 2-11. Dripping coextrusion assembly with a forming oil/alginate core-shell capsule.

Table 2-8. Alginate, olive oil feed rates and calculated total feed rate variable (g.min⁻¹).

Alginate feed rate (g.min ⁻¹)	Olive oil feed rate (g.min ⁻¹)	Total feed rate (g.min ⁻¹)
10.00	30.0	40
12.83	38.5	51
15.67	47.0	63
18.50	55.5	74
21.33	64.0	85
24.17	72.5	97
27.00	81.0	108

2.2.2.3 Capsules diameter (Y1)

Average diameter value was used to determine capsules size. To measure diameter, five capsules of each sample were observed using a 5-megapixel digital microscope Edge 5.0 (model AM7515MT8A, Dino-lite). Diameters were calculated using Dino Capture 2.0 software²⁷¹.

2.2.2.4 Sphericity index (Y2)

Sphericity index was calculated using a previously described method³³¹ where minimum diameter and maximum diameter are measured from captured images using Dino Capture 2.0 software. The following equation defines the sphericity index:

$$\text{Sphericity index} = \frac{d_{\min}}{d_{\max}} \quad (2.11)$$

Where d_{\max} is the maximum diameter and d_{\min} is the minimum diameter. Knowing that a perfectly spherical capsule corresponds to a sphericity index of 1.

2.2.2.5 Capsules rupture strength (Y3)

Capsules rupture strength was evaluated through a compressive test performed using a precision universal tensile-compressive tester (model AGS-X, Shimadzu). Capsules samples were placed between two plates (40 mm for the lower plate and 10 mm for the upper place) and compressed by the upper part descending at a speed of 2 mm.min⁻¹ and stopping when the capsule breaks under pressure. Rupture strength (N) was collected during experiments with four replicates for each experiment batch.

2.2.2.6 Encapsulation payload (Y4)

To determine oil encapsulation payload, oil phase was extracted by disintegrating 15 g of capsules in 50 mL of EDTA solution (0.2 mol. L⁻¹) and mixed with a vortex mixer until complete capsules dissolution. 20 mL of heptane was then added to extract the oil. After decantation, the supernatant was collected using a separating funnel into a pre-weighed flask. The supernatant was then evaporated with a rotavapor²⁷¹.

The following equation was used to calculate encapsulation payload:

$$\text{Encapsulation payload} = \frac{\text{Weight of the residue}}{\text{Weight of the capsules sampled}} \quad (2.12)$$

2.2.2.7 Experimental design

To evaluate the effect of three process variables on core-shell capsules properties, an experimental design was established from preliminary studies on experimental domain of the dripping coextrusion system. Encapsulation independent variables are presented in Table 2-9.

Encapsulation variables have been studied with a Doehlert experimental design, which has the advantage to provide a uniform distribution of experimental points and good flexibility³³². The

independent variables studied were calcium chloride (X_1), concentration total feed rate (X_2), and dripping height (X_3) (Table 2-9).

Table 2-9. Experimental design levels for independent variables used in the dripping coextrusion process.

Factor	Name	Unit	Low level value	High Level value	Number of levels
X_1	[CaCl ₂]	g.L ⁻¹	37.5	187.5	5
X_2	Total feed rate	g.min ⁻¹	40	108	8
X_3	Dripping height	cm	7	15	3

NEMRODW® software was used for sequence and number of experiments determination. A total number of 16 experiments, including three replicates at the center point, were calculated in Doehlert design as $N \geq K^2 + K + cp$, where K is the number of variables studied and cp is the number of replicates at center point.

As output data, four responses were considered, including capsules average diameter (Y1), capsules sphericity index (Y2), capsules rupture strength (Y3), and encapsulation payload (Y4). For output data prediction and responses modeling, experimental data were used to build an empirical model. Thus, linear, interaction, and quadratic effects involving four independent variables can be approximated as the following:

$$Y = b_0 + \sum_{i=1}^k b_i x_i + \sum_{i=1}^k b_{ii} x_i^2 + \sum_{i=1}^{k-1} \sum_{j=i+1}^k b_{ij} x_i x_j \quad (2.13)$$

Where Y is the studied dependent response, where the i and j vary from 1 to 3 (number of independent variables studied here). b_0 is a constant term and b_i is regression coefficient for linear effects; b_{ii} are regression indices for squared effects and b_{ij} are regression indices for interaction effects. x_i and x_j are coded experimental levels of the independent variables.

Considering the 3 independent variables ($x_1 = [\text{CaCl}_2]$, $x_2 = \text{total feed rate}$ and $x_3 = \text{dripping height}$), respective factors f_1 , f_2 and f_3 can be defined as follows:

$$f_1 = b_1 x_1 + b_{1-1} x_1^2 \quad (2.14)$$

$$f_2 = b_2 x_2 + b_{2-2} x_2^2 \quad (2.15)$$

$$f_3 = b_3 x_3 + b_{3-3} x_3^2 \quad (2.16)$$

With b_1 is regression coefficient for linear effect of [CaCl₂], b_2 is regression coefficient for linear effect of feed rate, b_3 is regression coefficient for linear effect of dripping height, b_{1-1} is

regression index for squared effect of $[\text{CaCl}_2]$, b_{2-2} is regression index for squared effect of feed rate and b_{3-3} is regression index for squared effect of dripping height.

From f_1 , f_2 , f_3 and the general equation 2.13 becomes:

$$Y = b_0 + f_1 + f_2 + f_3 + \sum_{i=1}^{k-1} \sum_{j=i+1}^k b_{ij} x_i x_j \quad (2.17)$$

2.2.2.8 Statistics

The ANOVA (Analysis of Variance) is essential to test the significance of the model. ANOVA, regression, and graphical study of variables were studied using NEMRODW® a design of experiment implementation software.

2.2.2.9 Optimization and model validation

To optimize processing conditions, maximization simulation was applied on dependents variables as constraints during multifactorial optimization using NEMRODW® software. Three experiments were carried out with optimized conditions to validate the model. Experimental results of capsules diameter, sphericity index, rupture strength, and encapsulation payload were compared to the predicted data to evaluate its precision and validate the model.

2.2.3 Results and discussion

2.2.3.1 Effect of experimental parameters on capsules characteristics

Capsules diameter (Y1), Sphericity index (Y2), Rupture strength (Y3), and Encapsulation payload (Y4) have been analyzed to study the impact of experimental variables (calcium chloride concentration, feed rate, and dripping height) on capsules characteristics. 16 experiments were carried out and the resulting responses are presented in Table 2-10.

2.2.3.2 Capsules shape (Diameters and sphericity index)

Doehlert experimental design and analysis of results determined validity and fitness of the experimental design responses. As described in the material and methods part, capsules diameter and sphericity index responses were chosen as capsules shape characteristics. Regression coefficient corresponding to capsules diameter ($R^2 = 0.886$) and capsules sphericity index ($R^2 = 0.788$) indicated that polynomial models fitted well with experimental values.

Table 2-10. Experimental responses obtained by the application of the experimental design.

Experience	Independent variables			Responses			
	[CaCl ₂]	Feed rate	Dripping height	Diameter	Sphericity	Rupture strength	Payload
	g.L ⁻¹	g.min ⁻¹	cm	mm	%	N	% (v/w)
1	187.5	74	11	4.916	99.60	4.943	60.92
2	37.5	74	11	4.994	95.54	1.624	63.55
3	150	108	11	5.210	97.22	4.073	62.60
4	75	40	11	4.879	99.62	5.129	63.92
5	150	40	11	4.806	98.78	2.956	59.76
6	75	108	11	5.231	96.05	2.337	61.65
7	150	85	15	5.222	98.17	2.553	61.29
8	75	63	7	4.941	98.35	3.631	72.16
9	150	63	7	4.998	98.61	2.605	58.81
10	112.5	97	7	5.120	98.11	2.148	60.34
11	75	85	15	5.109	96.90	1.348	61.65
12	112.5	51	15	5.083	98.05	2.412	62.02
13	112.5	74	11	5.209	98.27	2.206	59.83
14	112.5	74	11	5.075	95.53	1.798	60.85
15	112.5	74	11	5.229	97.25	2.645	58.81
16	112.5	74	11	5.143	97.33	2.603	61.07

Model adequacy and significance have been deduced from ANOVA performed for capsules diameter and sphericity index. Good significance was shown for diameter with $0.01 < P \text{ value} < 0.05$ while Sphericity index showed $P \text{ value} > 0.05$ which is probably due to excellent general sphericity index indicated by a mean value $< 97 \%$.

Based on experimental data, the following polynomial equation represents capsules diameter response (Y1)

$$Y1 = 5.1695 - 0.0428x_1 + 0.2163x_2 + 0.1261x_3 - 0.2145x_1^2 - 0.1125x_2^2 - 0.1199x_3^2 + 0.0300x_1x_2 + 0.1844x_1x_3 - 0.1048x_2x_3 \quad (2.18)$$

From this general equation, individual progression for each factor can be extracted in order to represent the impact of each variable, as follows:

$$f_1 = -0.0428x_1 - 0.2145x_1^2 \quad (2.19)$$

$$f_2 = 0.2163x_2 - 0.1125x_2^2 \quad (2.20)$$

$$f_3 = 0.1261x_3 - 0.1199x_3^2 \quad (2.21)$$

A graphical regression has been realized using equations 2.19, 2.20 and 2.21 to study the impact of variable individually (Figure 2-12b). Capsules diameters were mainly impacted by feed rate, as indicated by coefficient $b_2 = 0.2163$ (Figure 2-12a), especially at lower feed rates as illustrated in Figure 2-12b.

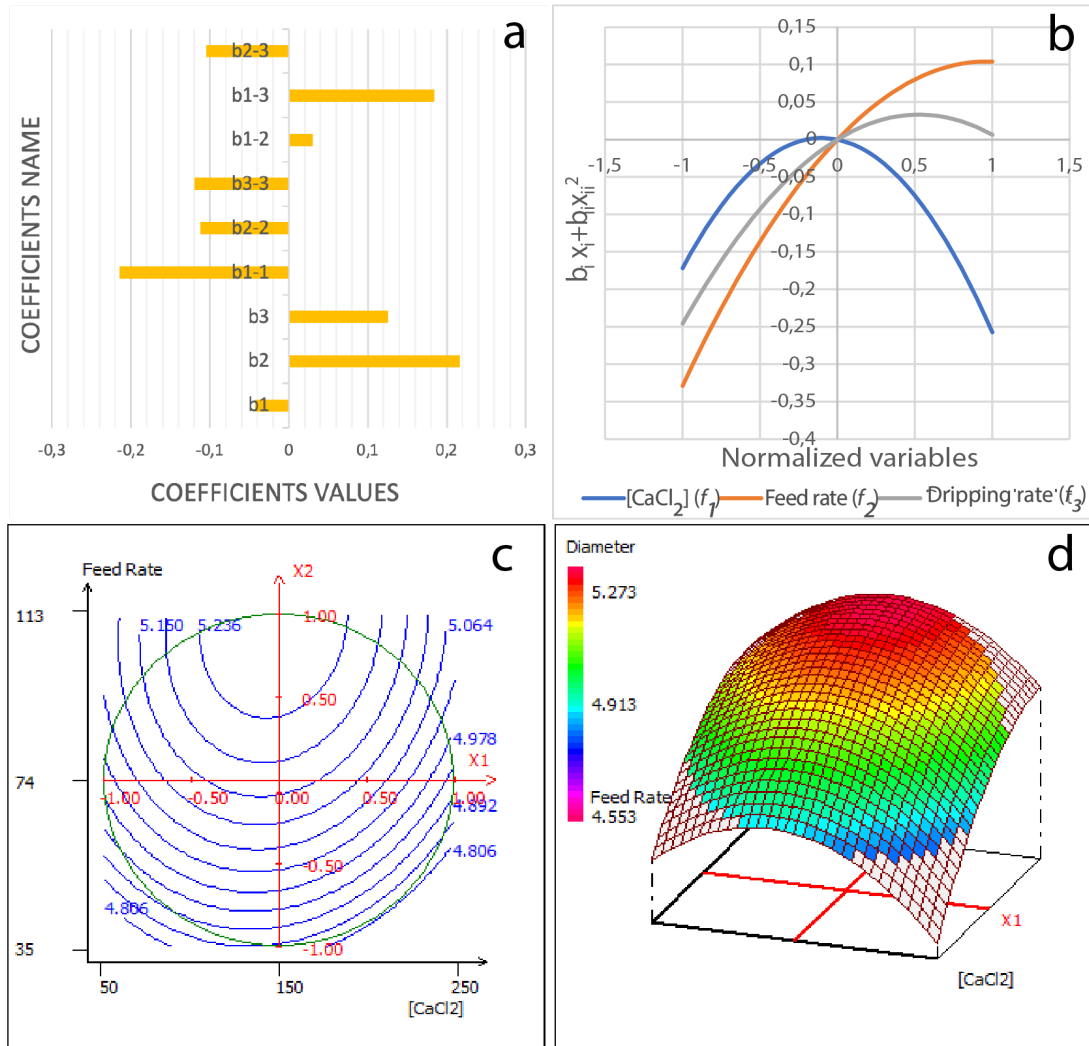


Figure 2-12. Pareto chart of main effects obtained from Doehlert experimental design for capsules size response (a), regression of $f_1, f_2,$ and f_3 as function of factors levels (b), surface (c) and contour plots (d) showing the effects of mutual interaction between feed rate and calcium chloride concentration on capsules diameters, while the other variables are kept at their center point.

The effects of the 3 factors were positive in equation 2.18 below the domain center. Above the domain center, only feed rate effect remains clearly positive while dripping height has no more effect (f_3 close to 0) and $[CaCl_2]$ has a strong negative effect ($f_1 < 0$). Thus, an increase in feed rate always increased capsules diameters, which was predictable since more material added to the capsule makes a larger diameter ^{356,357}

Both graphical representations of capsules diameter as a function of calcium chloride concentration showed a two-phase process (Figure 2-12c and Figure 2-12d). Calcium chloride influenced positively capsule size in the first phase. This corresponds to a previously described behavior where Ca^{2+} diffusion through the shell alginate network induced a cooperative binding of alginate chains and Ca^{2+} . In the second phase, the effect is adverse and higher calcium ions concentrations produced smaller capsules due to network shrinking and erosion. For large excess of CaCl_2 , alginate chain repulsion occurs, and alginate is released in the external gelling solution, capsules undergo then an erosion phenomenon ^{12,212,271,358}.

The capsules sphericity index, Y2, was modeled, from experimental data, with the following equation:

$$Y2 = 97.617 + 1.247x_1 - 1.238x_2 - 0.398x_3 - 0.047x_1^2 + 0.417x_2^2 + 0.530x_3^2 + 1.161x_1x_2 + 0.208x_1x_3 + 0.061x_2x_3 \quad (2.22)$$

Individual progressions were also isolated from the general equation as follow:

$$f_1 = 1.247x_1 + 0.047x_1^2 \quad (2.23)$$

$$f_2 = -1.238x_2 + 0.417x_2^2 \quad (2.24)$$

$$f_3 = -0.398x_3 + 0.530x_3^2 \quad (2.25)$$

From equations 2.23, 2.24 and 2.25, graphical regressions have been realized and represent the evolution of sphericity index response according factors modification and is illustrated in Figure 2-13b.

From equation 2.22, capsules sphericity index (Y2) is positively linked to calcium chloride concentration with a coefficient $b_1 = 1.247$ (Figure 2-13a). This effect is well represented by the linear progression of f_1 with the calcium chloride concentration Figure 2-13b. The negative coefficient $b_2 = -1.238$ indicates and antagonist effect of feed rate (factor X_2) (Figure 2-13a). An increase in feeding rate results in a decrease in capsules sphericity as illustrated Fig.3b. Similar results have been observed in a previous study for inner solution flow rate, where high oil feed rate resulted in capsules with low sphericity ^{271,359}.

An antagonist effect was also observed on the coefficient $b_3 = -0.398$, this indicated that sphericity decreased with the increase of dripping height. This observation could be due to the

deformation of the forming capsule when it hits the gelling bath surface: the higher dripping, the higher deformation^{210,354,360}. But for the second half of the study domain, dripping height has no more influence on the sphericity (Figure 2-13b). This can be explained by the fact that the maximum dripping speed of the capsules was achieved, and increasing dripping height has no more effect (as already observed for capsule diameter).

Interaction effect of both calcium concentration and feed rate is also represented with the interaction coefficient $b_{1-2} = 1.161$. Effect of these 2 factors is clearly illustrated in Figure 2-13c,d.

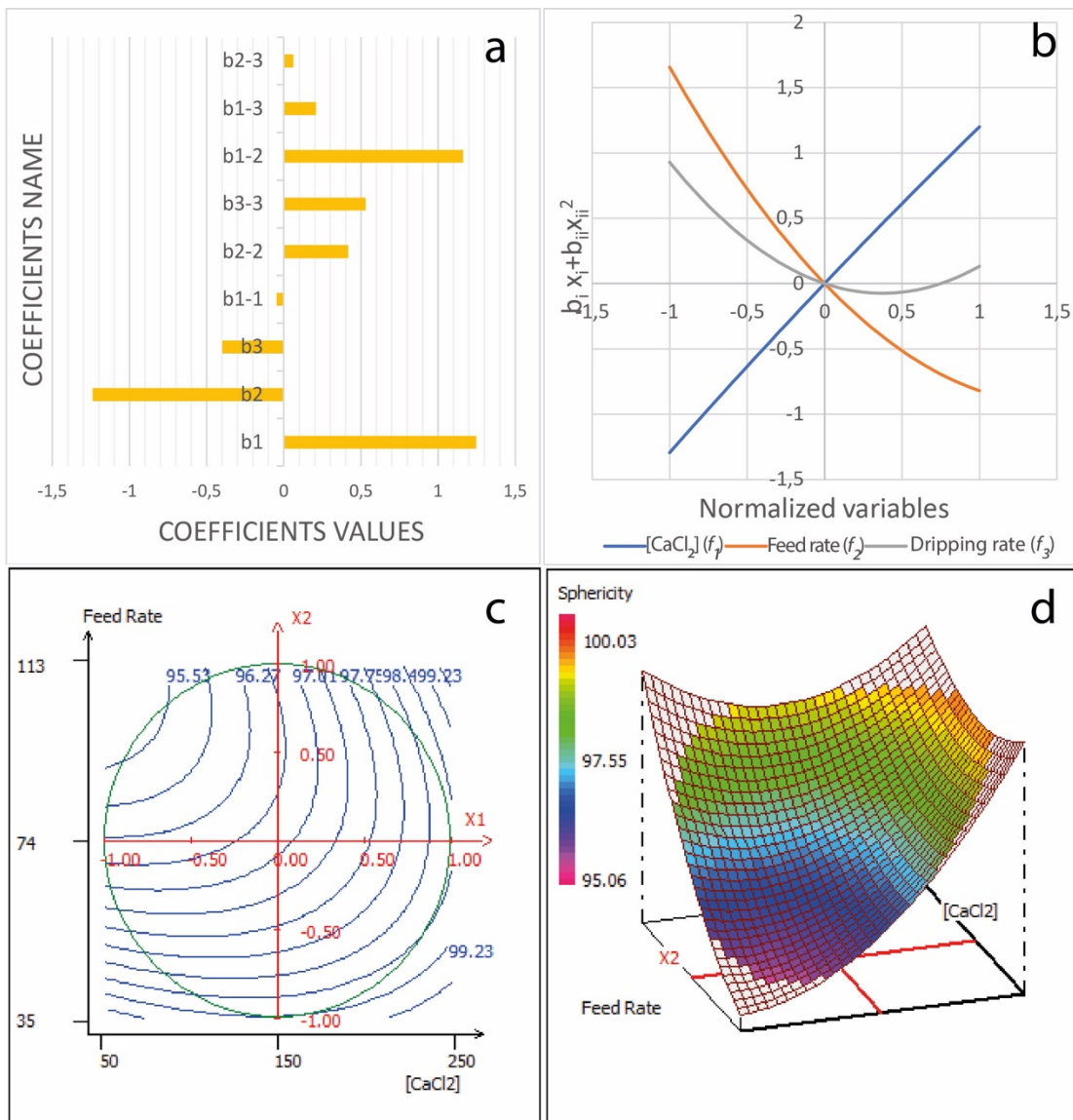


Figure 2-13. Pareto chart of main effects obtained from Doehlert experimental design for sphericity index response (a), regression of $f_1, f_2,$ and f_3 as function of factors levels (b), surface (c) and contour plots (d) showing the effects of the mutual interaction between feed rate and calcium chloride concentration on the capsules sphericity index.

2.2.3.2.1 Capsules rupture strength

The validity and fitting of the experimental data have been determined from statistical analysis of the experimental design. Rupture strength data was considered an indicator of capsules resistance. A great coefficient of determination ($R^2 = 0.954$) was obtained with a well-fitting polynomial model for experimental data. Also, ANOVA indicated model significance and adequacy with $0.001 < P \text{ value} < 0.01$.

Rupture strength response (Y3) was modelled with the following polynomial equation:

$$Y3 = 2.3130 - 0.0645x_1 - 0.5693x_2 - 0.4227x_3 - 0.7535x_1^2 + 1.9990x_2^2 - 0.1067x_3^2 + 2.2569x_1x_2 + 0.5682x_1x_3 + 1.3327x_2x_3 \quad (2.26)$$

From the general equation we isolated the following individual progressions as:

$$f_1 = -0.0645x_1 - 0.7535x_1^2 \quad (2.27)$$

$$f_2 = -0.5693x_2 + 1.9990x_2^2 \quad (2.28)$$

$$f_3 = -0.4227x_3 - 0.1067x_3^2 \quad (2.29)$$

To represent the evolution of rupture strength response according to factors modification, a graphical regression has been realized using equations 2.27, 2.28 and 2.29, and is illustrated in Figure 2-14b.

According to equation 2.26, all factors coefficients are high compared to the mean rupture strength response value, *i.e.* $b_0=2.3130$, which indicates that a slight modification in parameters levels, highly impacts the resulting rupture strength response.

From the Pareto chart corresponding to rupture strength response represented in Figure 2-14a, and according to linear, quadratic, and interactions coefficients ($b_2, b_{2-2}, b_{1-2}, b_{1-3}$), feed rate factor (X_2) appears to be the most impacting on the capsules rupture strength, as represented in Figure 2-14c,d. This result can also be observed in the regression graph related to feed rate levels illustrated in Fig 2.14b. However, coefficient b_{1-2} corresponding to the interaction between feed rate and $[CaCl_2]$, was the most impacting on rupture strength Figure 2-14a. Also, from equations 2.27, 2.28 and 2,29 It appeared that calcium chloride concentration had an antagonist effect on capsules rupture strength in all experimental domain, while feed rate variable had a protagonist impact, as illustrated in Figure 2-14b. This indicated that calcium chloride concentration generally

reduced capsules rupture strength while total feed rate enhanced rupture strength, probably due to increase of alginate available amount to cross-linking reaction.

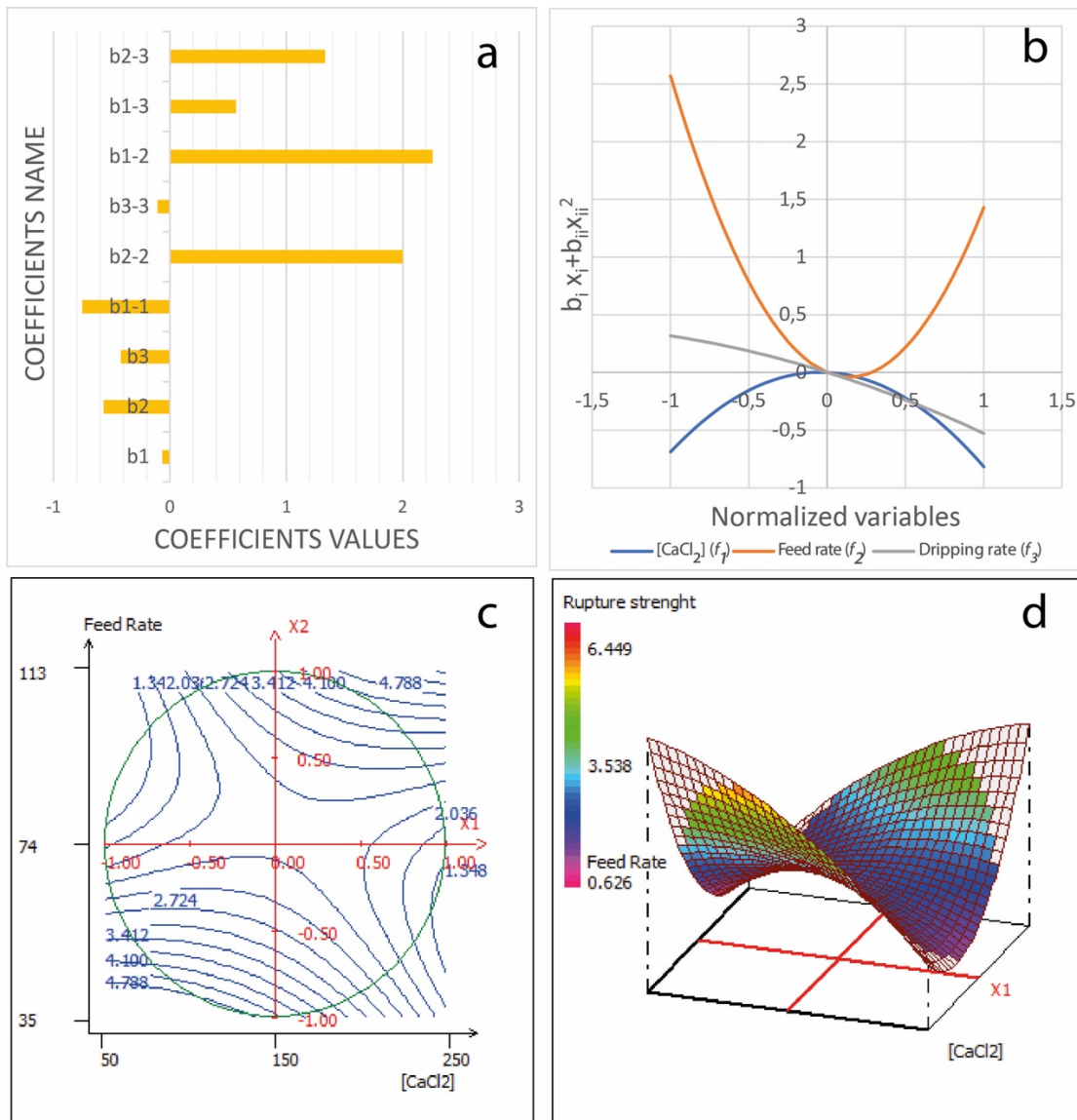


Figure 2-14. Pareto chart of main effects obtained from Doehlert experimental design for rupture strength response (a), regression of $f_1, f_2,$ and f_3 as function of factors levels (b), surface (c) and contour plots (d) showing effects of mutual interaction between feed rate and calcium chloride concentration on the capsules rupture strength.

As illustrated in Figure 2-14c,d, maximal values of rupture strength were obtained whether at low $[CaCl_2]$ /low feed rate values or at high $[CaCl_2]$ /high feed rate values, which suggested sufficient calcium ions for alginate chains reticulation. Also, lowest rupture strengths were observed where calcium ions were insufficient for high feed rate, and where calcium gelling bath was supersaturated for low feed rate (Figure 2-14c,d). This behavior corresponds to the two phases

phenomenon previously described concerning the dependence of capsules size with $[CaCl_2]$ and illustrated in Figure 2-15^{271,358}.

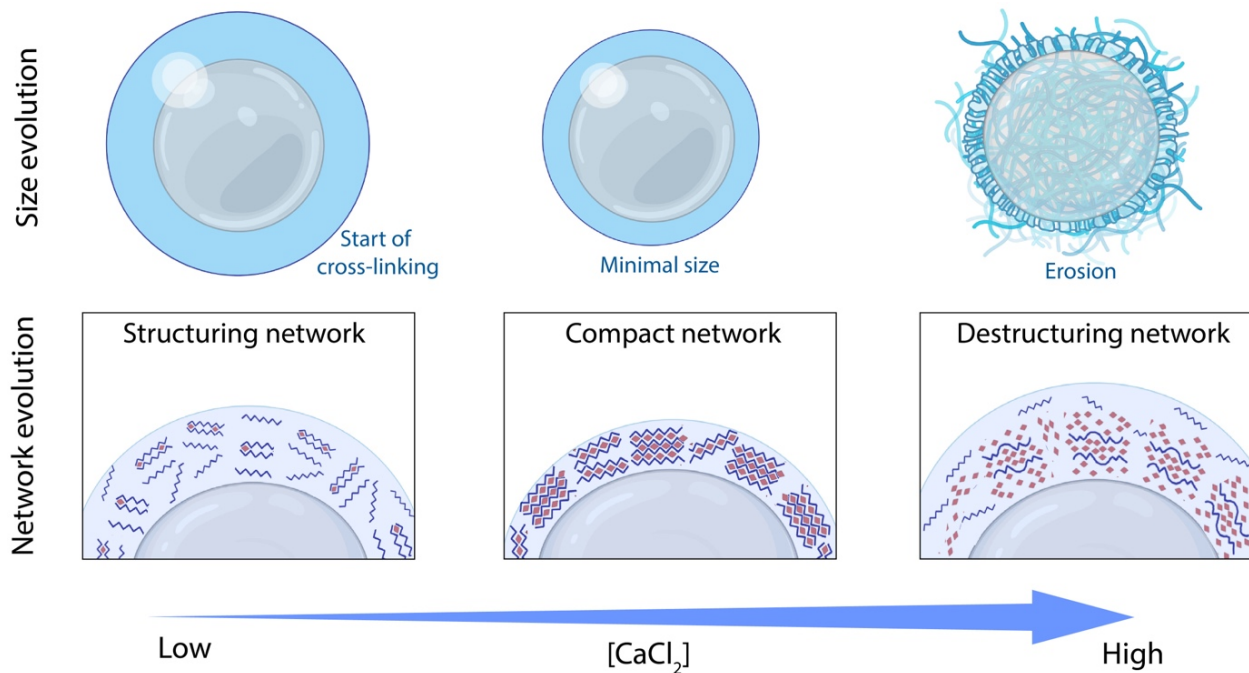


Figure 2-15. Illustration of the $[CaCl_2]$ impact on alginate network during core-shell capsule formation mechanism with constant alginate amount.

2.2.3.2.2 Encapsulation payload

Study of experimental parameters on capsules oil payload has been performed. Experimental data were fitted, and a mathematical model was obtained, with a high coefficient of regression ($R^2 = 0.896$). Furthermore, ANOVA of encapsulation payload showed a good significance at the levels comprised between 95% and 99%, for $0.01 < P \text{ value} < 0.05$.

The following quadratic equation models the encapsulation payload responses (Y4):

$$Y4 = 60.1400 - 1.3772x_1 + 0.1106x_2 + 0.9828x_3 + 2.0975x_1^2 + 1.7576x_2^2 + 0.1035x_3^2 + 2.9492x_1x_2 + 0.0739x_1x_3 - 0.8167x_2x_3 \quad (2.30)$$

From Y4, the following individual progressions were isolated as follow:

$$f_1 = -1.3772x_1 + 2.0975x_1^2 \quad (2.31)$$

$$f_2 = 0.1106x_2 + 1.7576x_2^2 \quad (2.32)$$

$$f_3 = 0.9828x_3 + 0.1035x_3^2 \quad (2.33)$$

Evolution of capsules payload response according to factors adjustment has been modelled using equations 2.31, 2.32 and 2.33, and is illustrated in Figure 2-16.

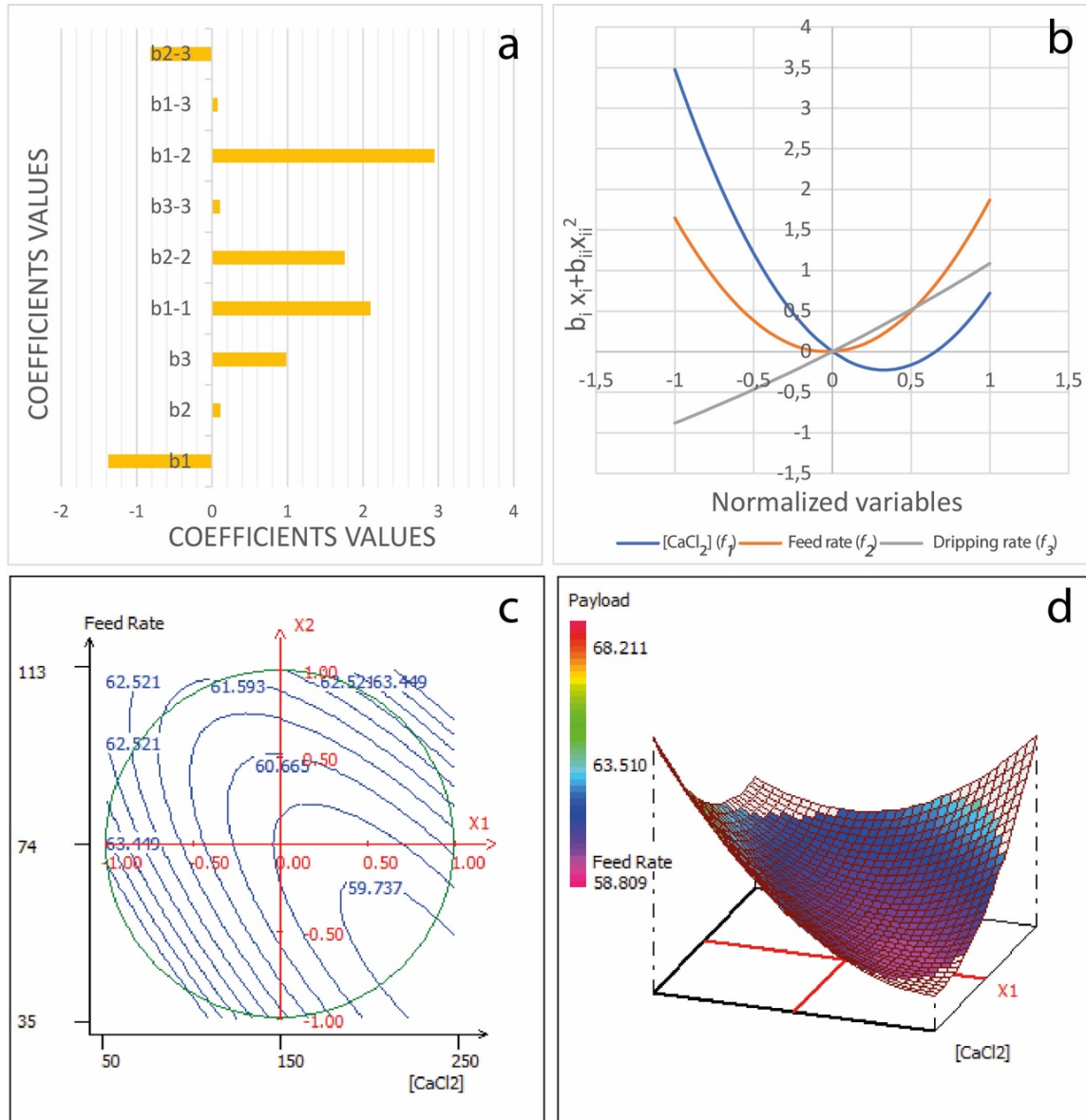


Figure 2-16. Pareto chart of main effects obtained from Doehlert experimental design for encapsulation payload (a), regression of $f_1, f_2,$ and f_3 as function of factors levels (b), surface (c) and contour plots (d) showing effects of mutual interaction between feed rate and calcium chloride concentration on the encapsulation payload.

According to equation 2.30, it appears from coefficient $b_1 = -1,3772$, that factor X_1 ($[CaCl_2]$) is the most impacting process parameters on encapsulation oil payload, which is confirmed by the regression of f_1 related to $[CaCl_2]$ effect, where encapsulation payload response generally decreases

with enhancement of calcium chloride concentration levels. During shell network formation calcium ions diffusion through alginate induced its reticulation^{59,361}. However, with the increase of calcium ions concentration and at excessively high concentrations, repulsion between alginate chains causes shell erosion leading to a higher shell porosity^{271,358,362}, which could allow oil dispersion through the shell and thus decrease the oil quantity present in the capsule.

As expected, encapsulation payload is mainly impacted by the factors related to shell and core characteristics, as suggested by coefficient $b_{1-2} = 2.9492$ related to calcium chloride concentration and total feed rate interaction.

For the first time in our study, the dripping height has a small but significant positive effect on payload on the whole domain. The dripping time increase with height and could explain a better capsule formation due to increased dripping time.

2.2.3.3 Optimization and validation of the model

According to the results obtained, capsules characteristics were mainly impacted by calcium chloride concentration and alginate/oil total feed rate, while dripping height factor had a lower impact. Calcium chloride impacted the formation of alginate shell by tightening its network, thus influencing capsules diameter and sphericity, high calcium concentration produced smaller capsules with good sphericity index, due to a shrinking effect. However, at excessively high calcium chloride concentrations, shell erosion occurred as a consequence of alginate chains supersaturated with Ca^{2+} ions. Thus, shell was weakened and allowed oil leaking from alginate capsules. Thus, encapsulation payload and rupture strength were reduced.

Total feeding rate factor was correlated to calcium chloride concentration, as expected, and reflects alginate and calcium interactions. Higher feeding rate increased capsules diameters but resulted in lower sphericity index and rupture strength.

Based on statistical study, four mathematical models for prediction and description of capsules diameter, sphericity, rupture strength, and encapsulation payload were studied by RSM using Doehlert matrix. High models significance, good accuracy, and correlation between experimental and predicted values have been demonstrated with ANOVA statistics. Thus, a desirability simulation was done to produce capsules defined with maximal encapsulation payload, and maximal sphericity.

A calcium chloride concentration of 75 g.L⁻¹, a dripping height of 7 cm, and a total feed rate of 63 g.min⁻¹ corresponding to 15,75 g.min⁻¹ for alginate feed rate and 47,25 g.min⁻¹ for oil feed rate, have been obtained from the model as optimal conditions for coextrusion process using multi-response NEMRODW® software.

To validate the predicted optimum, experiments were carried out using the optimal conditions proposed by the model. Experimental results were then compared to the predicted data. Experimental optimal conditions, corresponding experimental results, and predicted results are presented in Table 2-11.

Table 2-11. Optimum conditions, experimental and predicted value of response at optimized conditions

Sample	Diameter mm	Sphericity %	Rupture strength N	Payload % (v/w)
Predicted optimum	4,97	94,72	5,2	66
Experimental Optimum	4,96 ± 0,05	95,56 ± 0,02	4,7 ± 0,7	64 ± 3

The model predictions are in good agreement with experimental data, including diameter, sphericity index, rupture strength, and encapsulation payload. In addition, results from Table 2-11. showed a good correlation between experimental results and mathematical model.

2.2.4 Conclusion

This study permitted the development of a mathematical model predicting of diameter, sphericity, rupture strength, and encapsulation payload of core-shell olive oil capsules produced by dripping coextrusion technology. Also, specific mathematical approach of each production parameter allowed to study their individual impact on capsules characteristics. Analyses provided great description of dripping process parameters that impacted alginate hydrogel formation. As any other encapsulation techniques, coextrusion process has limitations. The main ones are the risk of nozzles obstruction due to their small size, the difficulty to encapsulate extremely viscous matrix, and the high process dependency on core and shell fluids rates. However, the core-shell structure offered by coextrusion technology provided a large payload, additional protective barrier brought by the shell and slow-release kinetics compared to other encapsulation methods ¹².

The dripping coextrusion process was optimized using multi-response method through a desirability function. The resulting models provided great tools for industrial applications of core-shell encapsulation technology, including nutraceuticals, beverages, confectionery products, and frozen foods.

Key highlights

- Olive oil/alginate capsules were prepared by dripping coextrusion technique.
- Optimization targets capsules shape, rupture strength and oil encapsulation payload.
- Shell network structure was mainly impacted by $[\text{CaCl}_2]$ and total feed rate.
- Calcium ions concentration impacts alginate network through shrinkage and erosion mechanisms.
- Quadratic models can predict capsules physical properties and oil payload.

Chapter 3. Capsules design through parameters and formulation adjustments.

Dans ce chapitre les données acquises sur la formulation et les paramètres des deux procédés de coextrusion sont mis à profit pour la conception de capsules aux propriétés contrôlées : taille, résistance mécanique et centricité du cœur. Les caractéristiques des capsules produites sont étroitement liées aux paramètres du procédé, comme démontré dans le chapitre précédent. L'étude de l'impact du chlorure de calcium et du type d'alginate sur les capsules produites est approfondie dans ce chapitre en choisissant deux alginates de ratio M/G distincts (article soumis dans *Polymers*).

Des biomolécules d'intérêt ont été sélectionnées comme exemples d'applications des capsules cœur-couronne. L'encapsulation de la microcine J25 a été réalisée par coextrusion. Cette biomolécule de nature hydrophile est la molécule modèle du Département de Technologie Alimentaire de l'Université Laval au Canada où une mobilité de six mois a été réalisée dans le cadre du dispositif DrEAM (Doctor, Explore and Achieve More). Des huiles ont également été choisies pour illustrer la capacité de protection de l'enveloppe d'alginate contre les contraintes mécaniques.

In this chapter, the data acquired on the formulation and parameters of the two coextrusion processes are used to design capsules with defined properties, i.e. size, mechanical strength, and core centricity. Capsules characteristics are highly related to process parameters as investigated in the previous chapter. Impact of calcium of calcium chloride concentration and alginate type on produced capsules have been explored in this chapter by selecting to distinct M/G alginate ratios (paper presently submitted in *Polymers*). Biomolecules of interest have been chosen as examples in core-shell capsules applications.

Microcin J25 encapsulation was achieved through coextrusion. This hydrophilic biomolecule serves as the model molecule for the Food Technology Department at Laval University in Canada, where I had the opportunity to spend a six-month internship as part of the DrEAM (Doctor, Explore and Achieve More) program. Oils were also selected to illustrate alginate-based shell ability to protect against mechanical stresses and oxidation, particularly. The impact of different formulation parameters on the properties of oil-based core-shell capsules was evaluated across various batches.

3.1 Influence of alginate properties and calcium chloride concentration on alginate beads reticulation and size

3.1.1 Introduction

Encapsulation technology has gained widespread use, particularly for stabilization and controlled delivery of compounds of interest, including active food ingredients and probiotics. Depending on encapsulation purpose and core material nature, various encapsulation methods can be employed ^{42,363,364}. Even if encapsulation technology adds cost to final product, it offers numerous benefits to the food industry. Extrusion is a conventional and cost-effective method that can be carried out under mild conditions, resulting in minimal loss of entrapped bioactive components ³⁶⁵. Extrusion technology consists in injection of a polymeric solution (*i.e.* alginate) containing active ingredients through a nozzle into an ionic gelling bath containing typically calcium ions ³⁴⁸. Several techniques are derived from dripping extrusion for beads production. They usually differ in droplet formation and separation step ². In the present paper, electro-vibrating extrusion was chosen to produce beads.

The use of a polymers matrix In encapsulation technology provides protection for active components against external factors such as oxygen, light, humidity, and heat, thus improving stability and functionality during processing and storage ³⁶⁶. In food industry, this technology also helps to mask unwanted flavors and colors that may result from addition of bioactive compounds such as polyphenols and fatty acids, without altering food sensory quality ³⁶⁷.

Among numerous natural polymers used for encapsulation, alginate is one of the most used in beads production, being non-toxic, biocompatible, biodegradable and Generally Recognized As Safe (GRAS) ³⁶⁸. Alginate is extracted from brown marine algae and some bacteria. It is composed of β -D-mannuronic acid (M units) and α -L-guluronic acid (G units) chains, forming MM-, GG- and MG-sequences ^{194,369}. The percentage of M and G units varies depending on species from which the polymer is extracted and the treatment it has undergone ³². Different M/G ratio and molecular weight result in alginates with different properties when crosslinked with calcium ions ³⁷⁰, usually represented as the “egg-box model” ⁵¹.

Alginates that are rich in G have a greater tendency for undergoing ionic gelation. As a result, G-rich alginates tend to offer more ordered and stiffer hydrogel compared to other types of

alginates. Thus, producing a hydrogel network that maintain integrity for longer periods of time, however, those gels presented larger pores³⁷¹. On the other hand, alginates with a higher M content create an elastic and softer hydrogel and less permeable gel matrices.

In this paper, two different alginates presenting different molecular weights, mannuronate and guluronate content and distribution have been used to produce alginate beads. An experimental design was used to examine the impact of process parameters on alginate gelation and beads size.

3.1.2 Materials and Methods

3.1.2.1 Materials

High viscosity sodium alginate was purchased from Louis-François (AlgLF) (Croissy-Beaubourg, France), Sodium alginate Protanal LF200 (AlgP) was purchased from FMC BioPolymers (Lyon, France), Calcium chloride $\geq 94\%$ was purchased from VWR (VWR Chemicals ®, France). NaNO₃, EDTA and Bovine Serum Albumin were purchased from Sigma-Aldrich (Saint Quentin Fallavier, France). PEO24k and Dextran standards were purchased from Viscotek PolyCal standards (Malvern Panalytical, France).

3.1.2.2 Alginate characterization

3.1.2.2.1 . Molecular weight with size-exclusion chromatography (SEC) coupled to multi-detectors

SEC experiments were performed with a HPLC pump (LC10AD, Shimadzu) coupled to an autosampler (Autosampler VE 2001, Malvern Panalytical) and a multi-detectors system recording UV, light scattering (RALS/LALS,) intrinsic viscosity and refractive index signals (Viscotek TDA305, Malvern Panalytical). One SEC column (A6000M, 10 or 13 μm , 8 mm ID x 300 mm, void volume ~ 6 mL, total volume ~ 12.5 mL, Malvern Panalytical) was equipped with a post-column nylon filter (0.22 μm). The column was equilibrated with NaNO₃ 0.15 M; NaN₃ 0.02 %; EDTA 0.01 M in ultrapure water. The flowrate was 0.7 mL.min⁻¹ and the temperature was 30°C. Data were processed with the Omnisec software (v5.12, Malvern Panalytical).

The calibration procedure was done with Bovine Serum Albumin, and cross-validations were performed with PEO24k and Dextran standards. The refractometer was used as the concentration detector and the refractive index increment value (dn/dc) used to determine the molecular weight (M_w) was 0.150 mL/g³⁷². Alginate samples were solubilized in the afore

mentioned buffer at 2 g.L^{-1} and filtered through a $0.22 \text{ }\mu\text{m}$ PES-filter just before injection (Injection volume: $100 \text{ }\mu\text{L}$).

3.1.2.2.2 . M/G Ratio with Nuclear Magnetic Resonance (NMR) spectroscopy

One of the most reliable methods for determining alginate composition and structure is the ^1H NMR spectroscopy. Functionality of this application relies on the ability of water-soluble alginate to bind cations and form a water-insoluble gel. The gelling behavior is entirely determined by the structure of the alginate homopolymer blocks. Information about uronic acid composition of alginate can be obtained by analyzing both positions and relative areas of signals in the anomeric zone. This information helps calculate mannuronic acid to guluronic acid (M/G) ratio as well as M and G units distribution in the polymer chain. The physical properties of alginates are largely determined by the proportion of the three types of blocks, with the GG sequences being particularly important. Alginates with higher contents of MM blocks result in softer gels, while those with high GG blocks lead to stiffer gels.

Prior to ^1H liquid-state NMR analysis, alginate sample were partially hydrolyzed by following a two steps mild acid hydrolysis to reduce its molecular weight. 500 mg of alginate added to 5 ml of 96% ethanol was dissolved in 50 ml of HCl, pH was adjusted to 5.0 with NaOH, the solution was then heated at 100°C for 10 min for hydrolysis. The solution was then cooled down to room temperature before adjusting pH to 3.0 by HCl addition then reheated at 100°C for 20 min. After cooling, NaOH was added to neutralize (pH 7) the solution. Alginate was then precipitated with 96% ethanol. The precipitate was collected after centrifugation and dried overnight at 70°C . D_2O was used to dissolve the hydrolyzed alginate (100 mg.mL^{-1}). This solution was filtered using $0,45\mu\text{m}$ syringe filter then introduce into an NMR tube for analysis.

NMR measurements were performed on a Bruker Avance III operating at a 400 MHz frequency and equipped with a Broadband inverse detection probe. Experiments were conducted at $360 \text{ }^\circ\text{K}$. Spectra were acquired with an inversion recovery procedure in order to remove the water peak. The inversion time was 2.3s. The M/G ratios were calculated from ^1H NMR signals area³⁷³.

3.1.2.3 . Preparation of alginate solution

AlgLF (or AlgP) solution was prepared respectively by dissolving sodium alginate powder (0.8% w/w) in distilled water and kept under stirring for 3 h until complete dissolution then stored

at room temperature from 24 to 72 h before spherification. Alginate solutions were transferred separately into 50 mL syringes for beads production.

3.1.2.4 . Preparation of alginate beads

Alginate beads were prepared using B-395 Pro Encapsulator (Buchi, Switzerland) equipped with a coaxial nozzle (750 μm and 900 μm for internal and external nozzle, respectively). Beads production protocol was adapted to the available equipment to produce solid beads by injecting same alginate solution into internal and external nozzle simultaneously. The protocol corresponds to a simple extrusion process. Accordingly, alginate beads were produced following a design of experiment.

AlgLF beads and AlgP beads batches were produced separately. Beads production protocol is illustrated in Figure 3-1. Various vibration frequencies and 2,000 V electric charge were applied to the annular jet to break it into droplets. Alginate beads were maintained in the calcium chloride solution for one hour to ensure a complete gelation. They were then rinsed with distilled water and stored in distilled water at ambient temperature for analysis.

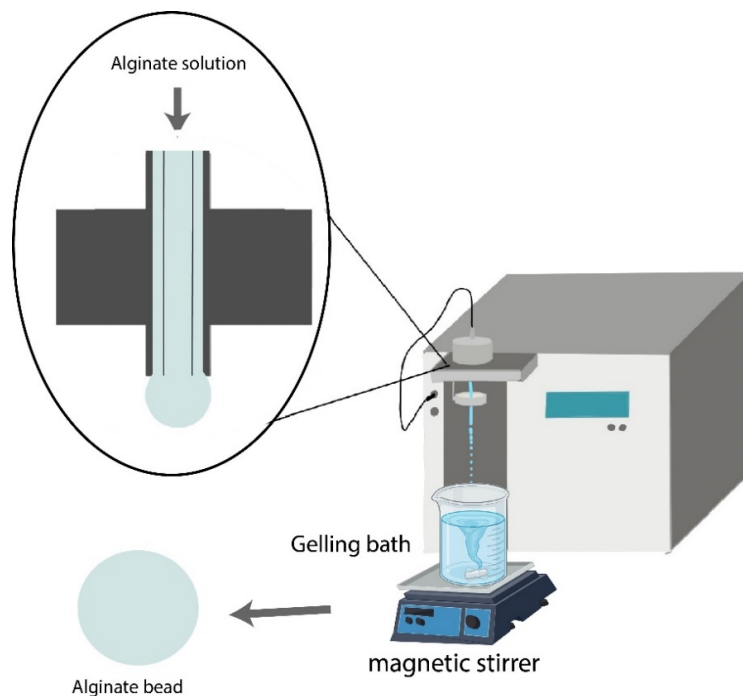


Figure 3-1. Alginate beads process used for the two types of alginate.

3.1.2.5 . Beads size measurement

To determine beads size, three beads from each sample were examined under Olympus light microscope fitted with CMOS 5 MPixels camera. To ensure accuracy, beads area (surface) was

chosen as the most appropriate measurement for the size. Toopview software® was used for image captures and size measurements.

3.1.2.6 . Experimental design

An experimental design was used to evaluate the effects of five selected variables on alginate beads size: alginate internal and external rates, frequency, Log₁₀ of calcium chloride concentration and alginate solution age. Experimental variables are detailed in Table 3-1.

Table 3-1 Levels of independent variables used in experimental design.

Factor	Name	Unit	Low level value	High Level value	Number of levels
X1	External flow rate	mL.min ⁻¹	30	50	5
X2	Internal flow rate	mL.min ⁻¹	4	18	7
X3	Frequency	Hz	80	200	7
X4	Log ₁₀ [CaCl ₂]	g.L ⁻¹	0.176	1.699	7
X5	Solution aging	Hours	24	72	3

The Doehlert matrix was chosen in the experiment design for its flexibility and the uniform distribution of experimental points. Different levels of priorities were assigned to each variable in order to emphasize collect of data on strongest effects. For this, calcium chloride effect was studied as log₁₀ [CaCl₂] to enlarge concentration studied domain and preserve focus on lowest concentration as they appeared to be crucial for alginate reticulation. Calcium concentrations corresponding to log₁₀ [CaCl₂] are displayed in Table 3-2.

Table 3-2 Calcium concentrations corresponding to Log₁₀ [CaCl₂] variable.

Log ₁₀ [CaCl ₂]	[CaCl ₂] g.L ⁻¹
0.176	1.50
0.328	2.12
0.785	6.09
0.937	8.66
1.089	12.29
1.546	35.21
1.699	50.00

NEMRODW software was used to determine the sequence and number of experiments. The total number of experiments in the Doehlert design was determined based on the formula $N \geq K^2 + K + cp$, where K represented the number of variables studied, and cp represented the number of replicates at the center point. In this study, a total of 34 experiments, including three replicates at the center point, were conducted. The output data (responses) were the capsules sizes

(Y), for which an empirical model was developed to predict the response function. The model showed linear, interaction, and quadratic effects involving the five independent variables, as defined by the following equation (3.1):

$$Y = b_0 + \sum_{i=1}^k b_i x_i + \sum_{i=1}^k b_{ii} x_i^2 + \sum_{i=1}^{k-1} \sum_{j=i+1}^k b_{ij} x_i x_j \quad (3.1)$$

Where Y was the studied dependent response, with i and j varying from 1 to 5 (number of factors studied). b_0 and b_i were respectively constant term and regression coefficient for linear effects respectively; b_{ii} were regression indices for squared effects and b_{ij} were regression indices for interaction effects. x_i and x_j were coded experimental levels of the independent variables.

3.1.2.7 . Statistics

NEMRODW software was utilized to conduct variables study as well as perform analyses of variance (ANOVA), regression, and graphical studies.

3.1.3 Results and discussion

3.1.3.1 . Alginate characterization

As observed by size-exclusion chromatography coupled to multi-detectors, AlgLF presented a higher molecular weight (Figure 3-2). The determination of Mw using light scattering gave Mw of $\sim 2.14 \times 10^5 \text{ g.mol}^{-1}$ for AlgLF and Mw of $\sim 1.22 \times 10^5 \text{ g.mol}^{-1}$ for AlgP.

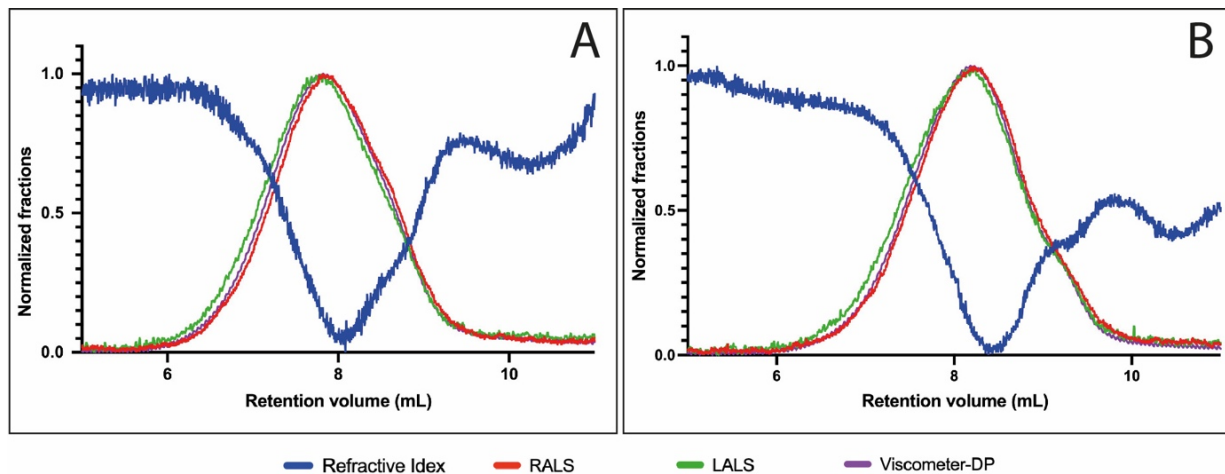


Figure 3-2. Size exclusion chromatograms for AlgLF (A) and AlgP (B) alginates.

The M/G ratio is also a key characteristic that helps determine the nature of the gel formed. A lower M/G ratio results in a brittle gel, while a higher ratio produces a more elastic gel. ^1H NMR spectra of alginates are displayed in Figure 3-3 and reveal the presence of three peaks, characteristic

of uronic acid. Peak I at 5.048 ppm and peak III at 4.446 ppm corresponded » to the C1 and C5 hydrogen of guluronic acid, respectively, and peak II at 4.655 ppm corresponded to the C1 hydrogen of mannuronic acid residues.

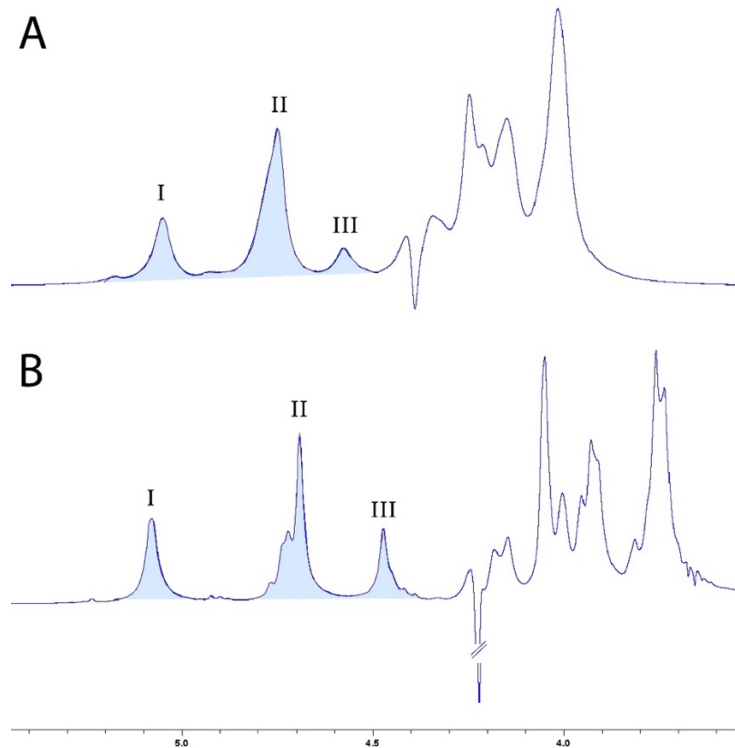


Figure 3-3. ¹H NMR spectra at 400 MHz of AlgLF (A) and AlgP (B) in D₂O solution.

The composition and structure alginate forming units were given using the methodology proposed by Grasdalen et al.³⁶⁹ using the following equations:

$$F_G = A_I / (A_{II} + A_{III}) \quad (3.2)$$

$$F_M = 1 - F_G \quad (3.3)$$

$$F_{GG} = A_{III} / (A_{II} + A_{III}) \quad (3.4)$$

$$F_{GM} = F_{MG} = F_G - F_{GG} \quad (3.5)$$

$$F_{MM} = F_{MG} - F_{GM} \quad (3.6)$$

$$M/G = (1 - F_G) / F_G \quad (3.7)$$

Where: A_I was relative area of peak I; A_{II} was relative area of peak II and A_{III} was relative area of Peak III.

Distributions and M/G ratios of alginates samples are presented in Table 3-3. AlgLF and AlgP M/G ratio were determined as 2.35 and 1.72, respectively. Thus, AlgP presented a higher G units content than AlgLF.

Table 3-3. ¹H NMR analysis of alginate sample

Sample	Composition, fraction		Doublet frequencies			M/G
	F _G	F _M	F _{GG}	F _{MM}	F _{MG}	
AlgLF	0.30	0.70	0.11	0.52	0.18	2.35
AlgP	0.37	0.63	0.29	0.56	0.07	1.72

3.1.3.2 . Influence of process variables on AlgLF beads

In order to study the impact of process parameters (*i.e.* Flow rates, frequency, [CaCl₂] and solution aging) on alginate (AlgLF) beads size, 34 experiments were carried.

Validity of experimental design response was confirmed by results analysis, verifying the experimental design responses and confirmed their validity. The coefficient of determination was used to express model consistency deduced from the Doehlert experimental design. The model presented an R² = 0.852. Significance and adequacy were confirmed by analysis of variance (ANOVA) (Table 3-4).

Table 3-4. ANOVA analysis of AlgLF beads size response from Doehlert experimental design

Response	Source of variation	Sum of squares	degree of freedom	Mean square	F-value	Significance
Beads size (Area)	Regression	47.9642	20	2.3982	3.735	0.920 **
	Residual	8.3476	13	0.6421		
	Lack-of-fit	6.2833	10	0.6283	0.913	6.04
	Pure error	2.0643	3	0.6881		
	Total	56.3118	33			

(**): significant at the levels comprised between 99% and 99.9% (for 0.001 < P value <0.01).

Based on the results, a mathematical model was developed to predict AlgLF beads size, as follow:

$$\begin{aligned}
 Y = & 2.893 + 0.523x_1 + 0.788x_2 - 0.338x_3 - 2.330x_4 - 0.098x_5 + 0.317x_1^2 - 0.046x_2^2 \\
 & + 0.128x_3^2 + 1.358x_4^2 - 0.290x_5^2 - 0.398x_1x_2 + 0.165x_1x_3 - 0.524x_2x_3 \\
 & - 1.402x_1x_4 - 1.363x_2x_4 + 0.494x_3x_4 - 0.932x_1x_5 - 0.856x_2x_5 - 0.158x_3x_5 \\
 & + 0.799x_4x_5
 \end{aligned} \tag{3.8}$$

From the general equation 3.8, to represent the impact of each factor individual evolution for each variable can be presented as follow:

$$f_1 = 0.523x_1 + 0.317x_1^2 \tag{3.9}$$

$$f_2 = 0.788x_2 - 0.046x_2^2 \quad (3.10)$$

$$f_3 = -0.338x_3 + 0.128x_3^2 \quad (3.11)$$

$$f_4 = -2.330x_4 + 1.358x_4^2 \quad (3.12)$$

$$f_5 = -0.098x_5 - 0.290x_5^2 \quad (3.13)$$

Using equations 3.9-3.13, a graphical regression has been realized and is presented in Figure 3-4. Therefore, impacts of variables have been realized individually.

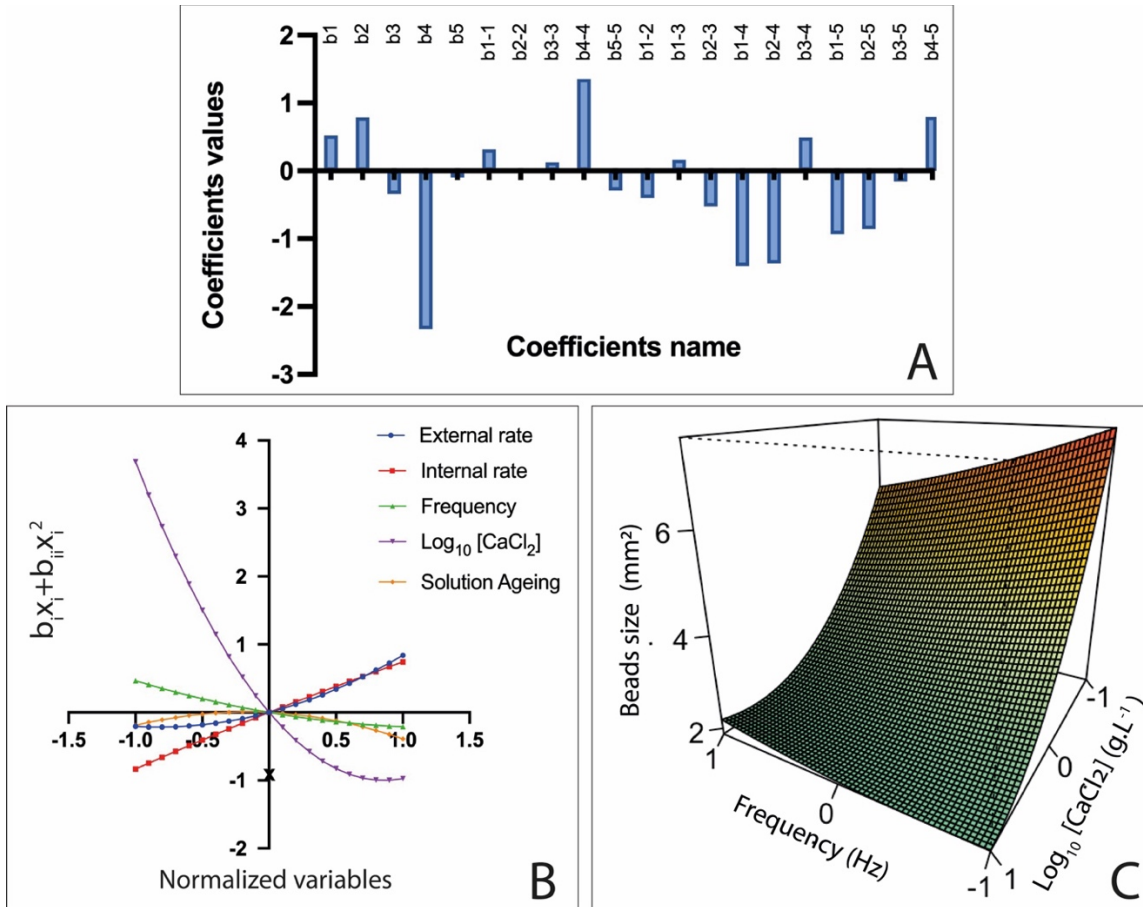


Figure 3-4. Pareto chart of main effects obtained from AlgLF Doehlert experimental design (A), regression of f1, f2, f3, f4 and f5 as function of factors levels (B), surface plots showing effects of mutual interaction between frequency and calcium chloride concentration ($\text{Log}_{10}[\text{CaCl}_2]$) on AlgLF beads size (C), while the other variables are kept at their center point.

It appeared that highest coefficient value corresponds to b_4 and b_{4-4} , which indicated that $\text{Log}_{10} [\text{CaCl}_2]$ had the greatest individual impact on beads size as illustrated in Figure 3-4A. Therefore, from individual graphical regression of equation 3.12, a decrease in alginate beads size was observed with the increase of calcium ions concentration as illustrated in Figure 3-4B.

This behavior has been previously associated to alginate network tightening,^{271,333}. Further, coefficients b_{1-4} and b_{2-4} corresponding to alginates rates and $\text{Log}_{10} [\text{CaCl}_2]$ interactions corroborated the antagonist effect between alginate and calcium ions concentration. Additionally, the X_3 factor exhibited an antagonist effect, as evidenced by coefficient b_3 (-0.338). Increasing the frequency resulted in a beads size reduction, as the fluid flow was more swiftly interrupted at each vibration break, causing solution jet to break more frequently²⁷². Solution aging seems to have a minimal and non-significative impact on beads size, more statistical data is provided in Table 3-5.

Table 3-5. Model coefficients analysis of Doehlert Design for AlgLF and AlgP beads size.

	Coefficient		Standard error		t-value		Significance	
	AlgLF	AlgP	AlgLF	AlgP	AlgLF	AlgP	AlgLF	AlgP
b0	2.893	3.133	0.401	0.227	7.22	13.81	< 0.01 ***	< 0.01 ***
b1	0.523	0.848	0.327	0.185	1.60	4.58	13.4	0.0514 ***
b2	0.788	0.758	0.327	0.185	2.41	4.10	3.16 *	0.126 **
b3	-0.338	-0.480	0.327	0.185	-1.03	-2.59	32.1	2.22 *
b4	-2.330	-1.914	0.327	0.185	-7.12	-10.34	< 0.01 ***	< 0.01 ***
b5	-0.098	0.253	0.327	0.185	-0.30	1.37	76.9	19.5
b1-1	0.317	-0.098	0.694	0.393	0.46	-0.25	65.5	80.8
b2-2	-0.046	0.306	0.694	0.393	-0.07	0.78	94.8	45.0
b3-3	0.128	-0.253	0.654	0.370	0.20	-0.68	84.8	50.6
b4-4	1.358	1.199	0.621	0.351	2.19	3.41	4.75 *	0.462 **
b5-5	-0.290	0.557	0.594	0.336	-0.49	1.66	63.3	12.2
b1-2	-0.398	0.306	0.925	0.524	-0.43	0.58	67.4	56.9
b1-3	0.165	-0.451	1.035	0.585	0.16	-0.77	87.5	45.5
b2-3	-0.524	0.638	1.034	0.585	-0.51	1.09	62.1	29.6
b1-4	-1.402	-0.855	1.075	0.608	-1.30	-1.41	21.5	18.3
b2-4	-1.363	-0.375	1.075	0.608	-1.27	-0.62	22.7	54.8
b3-4	0.494	0.747	1.075	0.608	0.46	1.23	65.3	24.1
b1-5	-0.932	0.522	1.095	0.620	-0.85	0.84	41.0	41.5
b2-5	-0.856	-1.018	1.095	0.620	-0.78	-1.64	44.8	12.4
b3-5	-0.158	-1.261	1.095	0.620	-0.14	-2.03	88.8	6.3
b4-5	0.799	-0.100	1.095	0.620	0.73	-0.16	47.8	87.5

(***): significant at the level > 99.9% (for $0.0001 < P\text{-value} < 0.001$).

(**): significant at the levels comprised between 99% and 99.9% (for $0.001 < P\text{-value} < 0.01$).

(*): significant at the levels comprised between 95% and 99% (for $0.01 < P\text{-value} < 0.05$).

3.1.3.3 Influence of variables on AlgP beads

The effects of experimental conditions on AlgP beads size have also been modeled. Experimental data were well adjusted by the generated model, as expressed by the coefficient of

determination ($R^2 = 0.935$). Further, statistical significance was determined through ANOVA, and showed a P-value < 0.01 , indicating that model significance levels were in the range between 99% and 99.9% (Table 3-6).

Table 3-6 ANOVA analysis of AlgP beads size response from Doehlert experimental design

Response	Source of variation	Sum of squares	degree of freedom	Mean square	F-value	Significance
Beads size (Area)	Regression	38.2615	20	1.9131	9.301	< 0.01 ***
	Residual	2.6738	13	0.2057		
	Lack-of-fit	2.5397	10	0.2540	5.683	9.0
	Pure error	0.1341	3	0.0447		
	Total	40.9352	33			

AlgP beads size response was modeled with following quadratic equation 3.14:

$$\begin{aligned}
 Z = & 3.133 + 0.848x_1 + 0.758x_2 - 0.480x_3 - 1.914x_4 + 0.253x_5 - 0.098x_1^2 + 0.306x_2^2 \\
 & - 0.253x_3^2 + 1.199x_4^2 + 0.557x_5^2 + 0.306x_1x_2 - 0.451x_1x_3 + 0.638x_2x_3 \\
 & - 0.855x_1x_4 - 0.375x_2x_4 + 0.747x_3x_4 + 0.522x_1x_5 - 1.018x_2x_5 - 1.261x_3x_5 \\
 & - 0.100x_4x_5 \qquad \qquad \qquad (3.14)
 \end{aligned}$$

To represent the impact of each factor individual progression, each variable has been studied through individual equations adapted from equation 3.14 as follow:

$$f_1 = 0.848x_1 - 0.098x_1^2 \qquad (3.15)$$

$$f_2 = 0.758x_2 + 0.306x_2^2 \qquad (3.16)$$

$$f_3 = -0.480x_3 - 0.253x_3^2 \qquad (3.17)$$

$$f_4 = -1.914x_4 + 1.199x_4^2 \qquad (3.18)$$

$$f_5 = 0.253x_5 + 0.557x_5^2 \qquad (3.19)$$

Using equations 3.15-3.19, a graphical regression has been realized and is presented in Figure 3-5. Therefore, impacts of variables have been realized individually.

Based on equation 3.14, describing AlgP beads size, the coefficient with the highest value is b_4 and $b_{4,4}$, signifying that here also, $\text{Log}_{10} [\text{CaCl}_2]$ had a significative negative impact on AlgP beads size. Consequently, as reported previously, an increase in calcium ion concentration leads to a decrease of alginate beads size. Furthermore, coefficients b_{1-4} and b_{2-4} , representing interactions

between AlgP solution rates and $\text{Log}_{10} [\text{CaCl}_2]$, confirmed the antagonistic effect between alginate and calcium ion concentration.

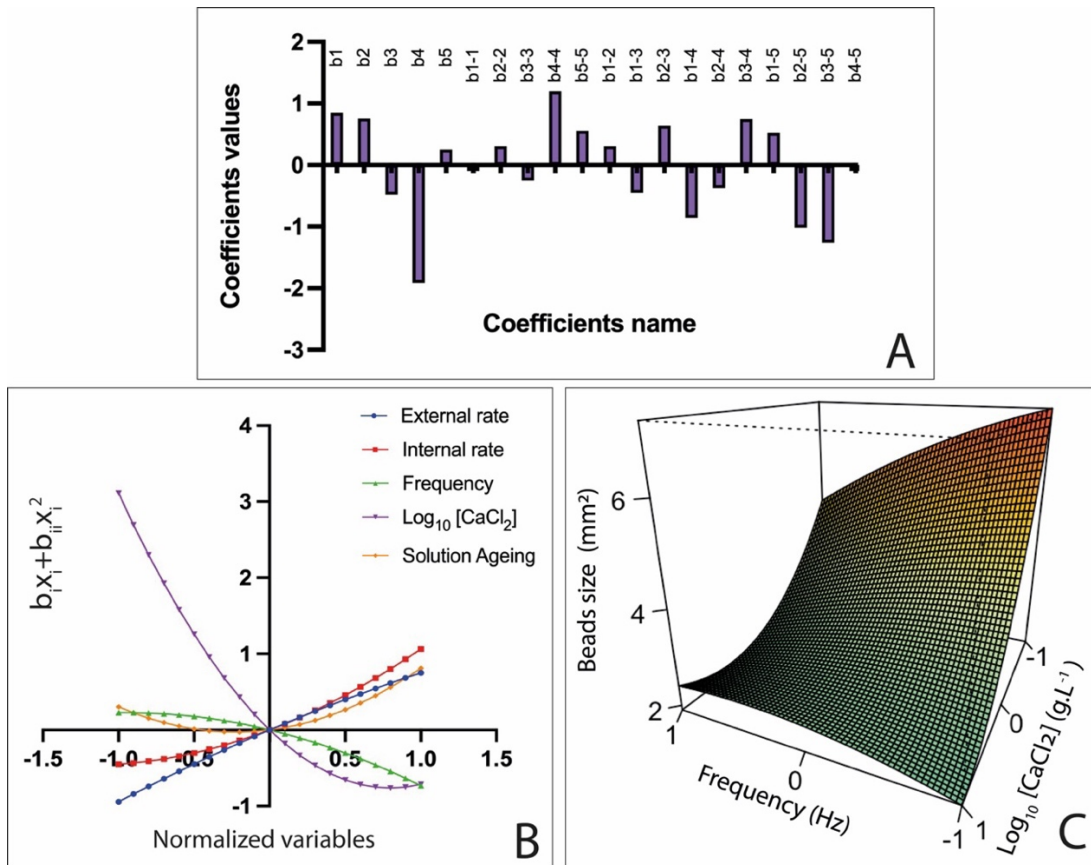


Figure 3-5. Pareto chart of main effects obtained from AlgP Doehlert experimental design (A), regression of f1, f2, f3, f4 and f5 as function of factors levels (B), surface plots showing effects of mutual interaction between frequency and calcium chloride concentration ($\text{Log}_{10}[\text{CaCl}_2]$) on AlgP beads size (C), while the other variables are kept at their center point.

Overall, as for AlgLF beads, AlgP beads size were mostly impacted by calcium ions concentration, alginate solution rates and applied frequency. Although the impact of solution ageing on bead size appeared to be minimal and statistically insignificant (Table 3-4).

3.1.3.4 Alginate characteristics impact on gelation

Considering design of experiment results concerning the influence of $\text{Log}_{10} [\text{CaCl}_2]$ on both batches, calcium chloride acted as a cross-linking agent, interacting mostly with G-blocks of alginate molecules to produce gel networks. Elevated concentrations of calcium chloride facilitated enhanced cross-linking and engendered robust gels. Also, alginate gelation was influenced by the proportion of G (guluronic acid) and M (mannuronic acid) units, which affected the rotation around the glycosidic linkage³⁷⁴.

A mathematical phenomenological model has been used to study beads reticulation and observe the two-phase gelling phenomenon previously established²⁷¹. Application of equations 3.8 and 3.14 for various values of Q/F and Log₁₀ [CaCl₂] were used to determine final volume of beads from calculated area vs alginate flow for both AlgLF and AlgP beads, respectively. Based on experimental design results and on this phenomenological model, alginate rate and calcium ions concentration impact on beads size variation can be described as follows:

$$\Delta V = \left(\frac{Q}{F}\right) C \quad (3.20)$$

Where ΔV = beads volume variation (V-V₀); Q = Total flow rate; F = frequency; C = coefficient of size variation, If C = 0, no size variation is observed; if C > 0, volume expansion is observed and C < 0, alginate retraction and/or erosion occurs.

A clear relationship was observed between the volume of beads and the flow rate of alginate, showing a linear evolution (Figure 3-6).

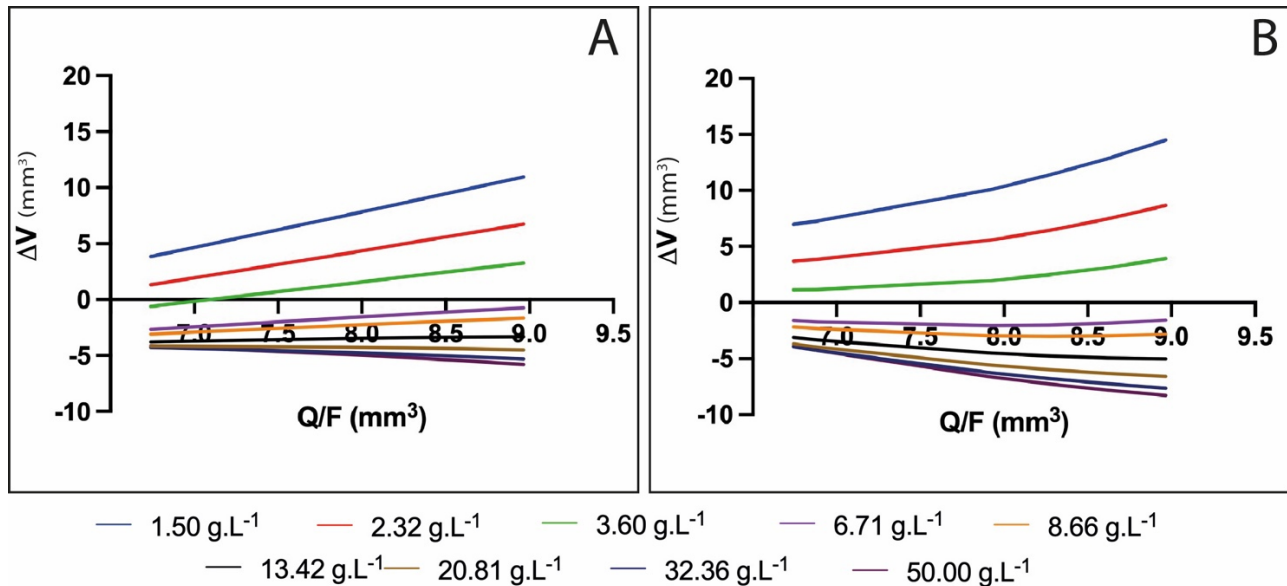


Figure 3-6. Mathematically predicted values for AlgP (A) and AlgLF (B) beads volume variations versus Q/F for determination of C coefficients (draw slopes) using nine CaCl₂ concentrations from 1.5–50 g.L⁻¹, while other variables were kept at 120 Hz for frequency and 47 h for solution aging.

In Figure 3-6, ΔV traduced the volume change between the drop volume before entering in the CaCl₂ solutions, V₀, and the final volume of the reticulated bead, V. Depending on the CaCl₂ concentration, 3 reticulation behaviors were observed.

- 1- For the lowest concentrations (below 3.6 g/L), $\Delta V \geq 0$ was measured for all flow rates. This means that no significant shrinking occurred when the drop penetrates the calcium solution. Due to low ionic gradient between internal water and calcium solution, no significant water released was observed and low and light reticulation occurred. In all cases, the slopes of the draws are positive ($C > 0$).
- 2- For CaCl_2 concentrations between 6,71 and 13.42 g/L, a significant water release and shrinking was observed leading to $\Delta V < 0$ for all Q/F values. Nevertheless, beads volume increased with (Q/F), due to lower relative shrinkage for larger beads. The slopes of the draws are still positive ($C > 0$) but, as CaCl_2 concentration rises, the slope is reduced corresponding to lower beads growing with (Q/F). It means that a denser network was formed as more Ca^{2+} ions penetrated the alginate (enhancing reticulation, contracting alginate network, reducing bead size).
- 3- For excessive CaCl_2 concentrations (above 13.42 g/L), Ca^{2+} supersaturation occurred, leading to repulsion between alginate chains, large release of water from the capsule and causing free alginate dissolution into the surrounding solution (erosion).

Moreover, a non-linear evolution of ΔV was observed for AlgLF, which could be due to the M/G ratio. Higher M content conferred more elasticity to the alginate network, and therefore a less organized network during gelation. Also, AlgLF beads size had similar evolution than core-shell oil/alginate beads produced with the same alginate in chapter 2, which indicates that the two behaviors of core-shell alginate capsules and alginate beads can be correlated. In Figure 3-6, the slope of each curve corresponded to C values (Equation 3.20). The C coefficient changes vs CaCl_2 concentration is presented in Figure 3-7, for both AlgLF and AlgP. The C values are initially positive and then became negative for both alginates. C sign change occurred at high concentration for AlgP compared to AlgLF. AlgP curve is always above the AlgLF curve.

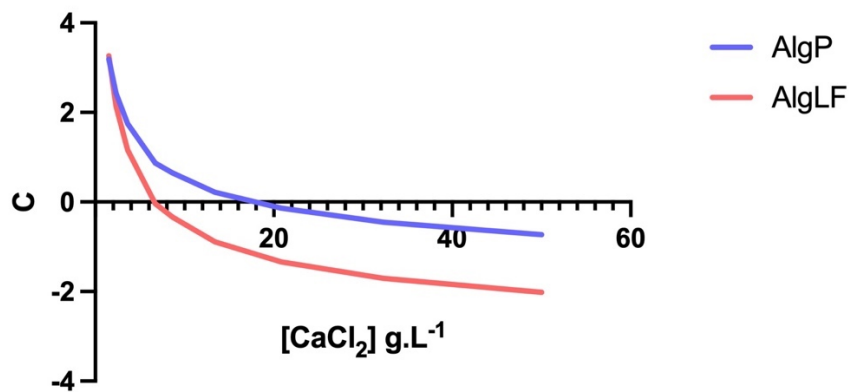


Figure 3-7. Coefficient versus CaCl_2 concentration.

Due to lower M/G ratio (1.72) and lower molecular weight, AlgP produced bigger beads than AlgLF. As AlgP contained a higher proportion of G-blocks, increasing calcium chloride concentration resulted in stronger and more extensive cross-linking. As a result, bead formation presented a reduced syneresis, leading to larger bead sizes.

The principal distinction between high and low molecular weight alginates in their binding behavior manifested primarily in the final stage of reticulation described by Fang et al (2007) in three steps via isothermal titration calorimetry. The steps were distinguished by Ca/G-block ratios as: monocomplex formation, pairing into egg-box dimers, and lateral association. In the case of high molecular weight alginates coupled with a lower G-blocks content (AlgLF), this resulted in smaller beads.

In the present research, mannuronate (M) and guluronate (G) content impacted alginate backbone. M-blocks conformation resulted in less compact alginate chains. Thus, glycosidic linkage and rotation was favored, leading to a volume effect between chains³¹. Volume variation capabilities increased during gelation, leading to a higher tightening coefficient. Alginates characteristics impact on alginate network during gelation is presented in Figure 3-8. These observations were in line with those made on alginate-based core-shell capsules.

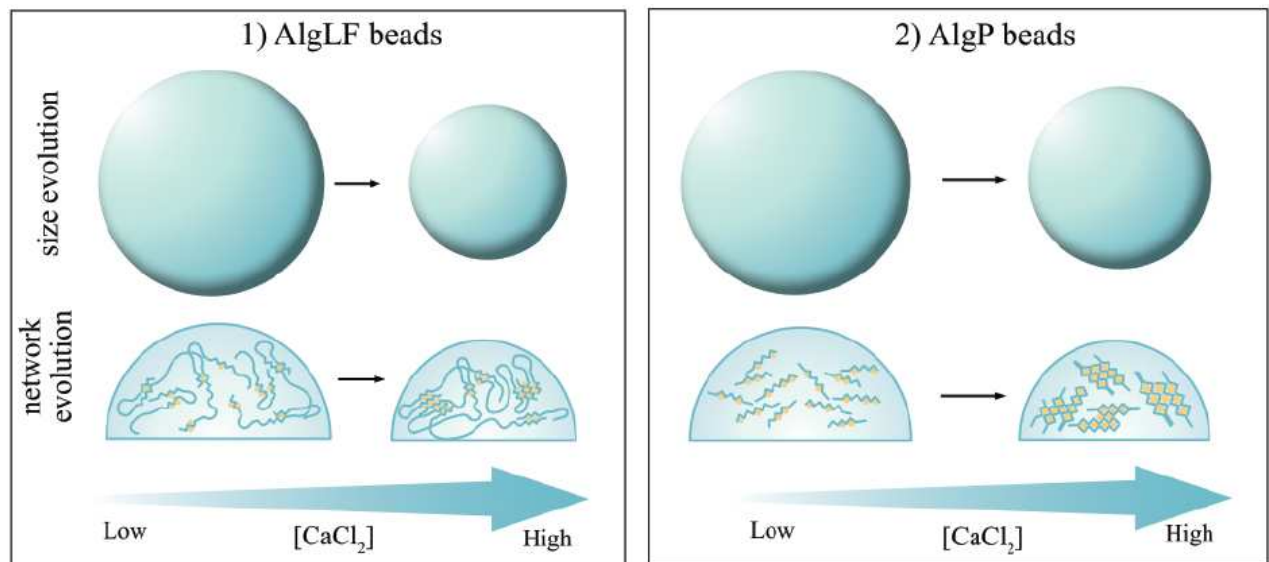


Figure 3-8. Illustration of the [CaCl₂] impact on alginates (AlgLF and AlgP presenting High Mw/Low G-blocks and Low Mw/High G-blocks, respectively) network during beads formation with given alginate amount. Adapted from²⁷¹.

3.1.4 Conclusion

This study investigated the production of beads using two types of alginates, AlgLF and AlgP, through electro-vibrating extrusion. The results demonstrated that calcium chloride concentration had the most significant impact on bead size, with higher concentrations leading to smaller beads ³⁷⁵.

The phenomenological model allowed for the examination of alginate reticulation in bead form versus core-shell capsules. It was observed that AlgP, with a lower M/G ratio and a higher proportion of G-blocks, exhibited a more prolonged gelation process, stronger cross-linking, and larger bead sizes.

The M/G ratio and the content of mannuronate and guluronate impacted alginate network, affecting the glycosidic linkage and rotation between chains during gelation. This led to a higher tightening coefficient and increased volume variation capabilities in AlgLF compared to AlgP. Furthermore, the study linked alginate beads size to previous microscopic observation (as illustrated in Figure 3-9), related to alginate binding, with the formation of monocomplexes, egg-box dimers, and lateral association of egg-box dimers ³⁷⁶. The differences in molecular size and intra-cluster association of egg-box dimers between high and low molecular weight alginates explained the variation in bead sizes for AlgLF and AlgP.

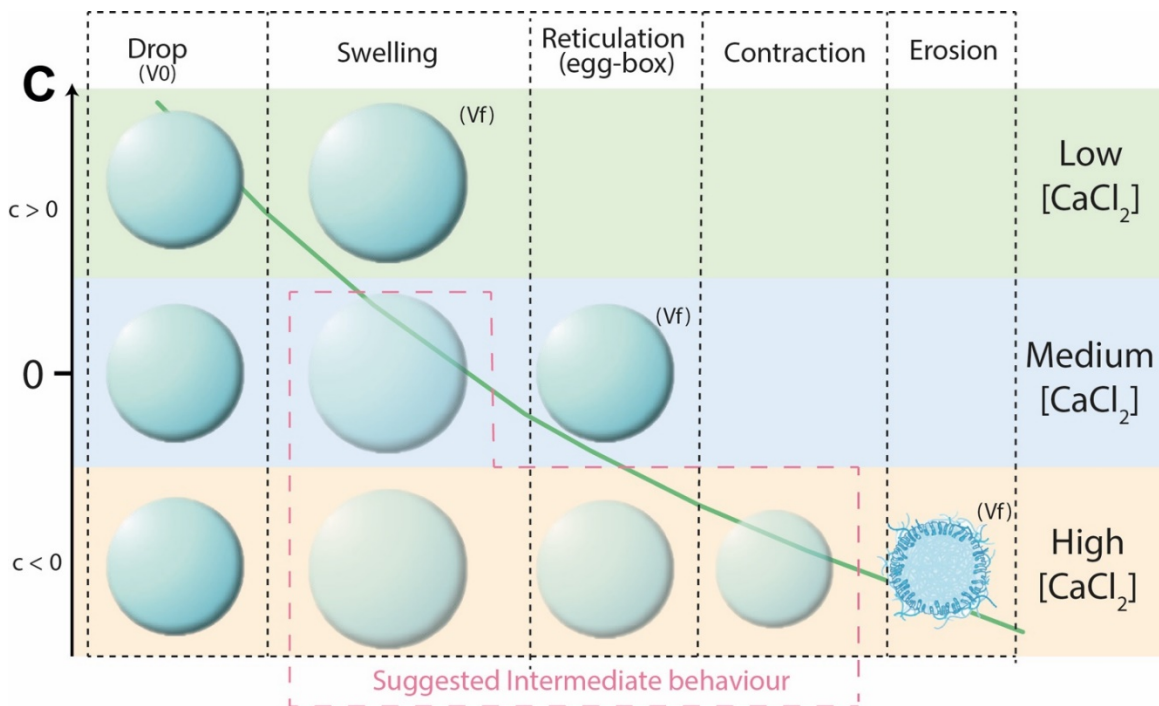


Figure 3-9. Scheme illustrating size variation and alginate network formation in low, medium and high concentration gelling baths.

In summary, the findings of this study highlighted key factors influencing bead size in alginate production, as calcium chloride concentration, alginate molecular weight and the M/G ratio. This knowledge can be valuable in optimizing the fabrication of alginate-based beads for various applications, including foods, cosmetics, and other biomedical and pharmaceutical uses.

Key highlights

- Calcium chloride concentration significantly affected bead size.
- Two mathematical models have been produced to predict beads size for AlgLF and AlgP.
- Bead sizes for AlgLF and AlgP vary due to differences in molecular size and M/G ratio.
- Differences in M/G ratio and molecular weight influence the gelation process, affecting tightening/erosion/retraction coefficient (C coefficient) and volume variation capabilities.
- Phenomenological model has been produced to define C coefficient.

3.2 Encapsulation of microcin in alginate core-shell microcapsules through coextrusion technology

Coextrusion process has been successfully adapted to produce capsules of micrometric size particularly adapted to antimicrobial peptides encapsulation for potential applications studied by the host laboratory. Preliminary studies have been realized in order to adapt our encapsulation protocol, and optimum parameters to the equipment available in the host structure of Laval University. For that, injection feed rates have been adjusted to fit an air pump, a gear pump and micronozzles. Additionally, adaptations to process variables have been studied, internal feed rate have been revised for aqueous solution injection. Further, in order to obtain required viscosities and gelling behaviour, Protanal alginate have been used instead of LF alginate used previously for annular jet breaking coextrusion protocol to produce microcapsules using an appropriate formulation. Encapsulation protocol has been adapted from previously reported results used to produce millimetric size capsules to fit the small nozzle system used in this paper.

This work was realized in the Department of Food Technology research laboratory of Laval University in Québec, Canada. Thanks to DrEAM support.

3.2.1 Introduction

Antimicrobial peptides have gained significant attention due to their potent activity against a wide range of pathogenic bacteria³⁷⁷. A well-known example, the J25 microcin has shown remarkable potential in various applications like food preservation and pharmaceutical formulations³⁷⁸. However, practical use of antimicrobial peptides is often limited by challenges such as low stability, rapid degradation, and inappropriate release kinetics^{379,380}. Encapsulation techniques can be a promising approach to address these limitations, specifically through the coextrusion method using alginate core-shell microcapsules.

The coextrusion technique involves extruding two or more solutions simultaneously, through a coaxial nozzle^{14,78}. Where one internal tube contains core solution (*i.e.* J25 suspension) and the external contains shell solution (*i.e.* alginate solution). Through this process, a core-shell structure is formed, with the encapsulated microcin within the alginate matrix. The alginate shell acts as a protective barrier that shields the encapsulated compound from external factors^{381,382}. Furthermore, the coextrusion method could allow precise control over the release kinetics, and targeted delivery of the antimicrobial peptide². Core-shell structure of alginate microcapsules could facilitate

selective release in the gastrointestinal tract ^{383,384}. However, there are also certain challenges associated with this application, selecting compatible materials, maintaining encapsulation efficiency, and ensuring stability during processing are fundamental aspects ².

Encapsulating hydrophilic molecules within core-shell microcapsules using coextrusion presents several challenges ³⁵⁵. These challenges are mainly related to the interaction of microcin with the alginate shell, which may lead to difficulties in maintaining microcapsule integrity and encapsulation efficiency, as microcin and water tend to diffuse through the shell ³⁵⁵.

The aim of this study was to encapsulate the hydrophilic bioactive in core-shell structure microcapsules with high stability.

3.2.2 Materiel and methods

3.2.2.1 Microcin J25 production and purification

Microcin J25 to be encapsulated was produced by *Escherichia coli* MC4100 carrying the plasmid PTUC 202 ³⁸⁵. For the antibacterial activity of free solutions and microcapsules *Salmonella enterica* subsp. *enterica* serovar Newport ATCC 6962 (later referred to as *Salmonella* Newport) was used as indicator strain microcin J25. *S. Newport* was cultured at 37°C overnight in Luria-Bertani (LB) (Difco Laboratories, Spark, MD, United States). Strains were maintained at -80°C as stock cultures in LB culture media supplemented with 20% glycerol and propagated twice at 24 h intervals before use. ³⁸⁶.

For J25 Production and purification, minimal medium (M63 medium) containing KH₂PO₄ (3 g.L⁻¹), K₂HPO₄ (7 g.L⁻¹), (NH₄)₂HPO₄ (2 g.L⁻¹), and casamino acid (1 g.L⁻¹) was supplemented with 1 mL.L⁻¹ of 20 % MgSO₄, 10 mL.L⁻¹ of 20 % glucose, and 1 mL.L⁻¹ of 1 g.L⁻¹ thiamine, inoculated with an overnight culture of *E. coli* MC4100 pTUC202 (2 % v/v in LB broth), followed by overnight incubation at 37°C in rotary shaking at 250 rpm. Bacterial cells were separated by centrifugation at 8,000 g for 20 min at 4°C. The supernatant was pre-purified by solid phase extraction (Sep-Pak C18) at 4°C at a flow rate of 2 mL.min⁻¹, followed by reversed-phase high-performance liquid chromatography (RP-HPLC, Beckman Coulter System Gold Preparative HPLC system, Mississauga, ON, Canada) on a preparative C18 column (Luna 10 µm, 250 mm x 21.10 mm, Phenomenex, CA, United States) at a flow rate of 10 mL.min⁻¹. Premiray Microcin J25 solution was quantified by RP-HPLC using an analytical C18 column (Aeris 3.6 µm, PEPTIDE XB-C18, 250 x 4.6 mm, Phenomenex, CA United States) ³⁸⁷, and presented high purity (Figure 3-10) to be used other studies carried out by the host laboratory ³⁸⁷.

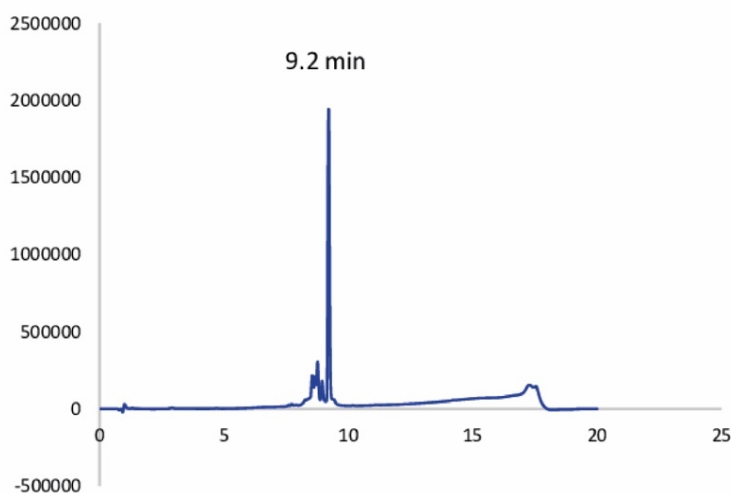


Figure 3-10. HPLC chromatograms of microcin J25 produced before encapsulation.

3.2.2.2 Solutions preparation

3.2.2.2.1 Microcin J25 solution

Microcin J25 solution previously purified was then concentrated using SpeedVac concentrator (Savant SPD131DDA, Thermo scientific) equipped with a Refrigerated Vapor Trap (Savant RVT400, Thermo scientific) at 45°C for 7h³⁸⁸. The obtained concentrated solution was filtered through a 200 µm syringe filter to be sterilized and stored at 4°C until use for encapsulation.

3.2.2.2.2 Alginate solution

Protanal alginate (Mw of $\sim 1.22 \times 10^6$ g.mol⁻¹ and M/G = 1.72) was chosen in this study. Its low viscosity and reticulation properties were adapted to the small nozzle device used for encapsulation. Alginate solution was prepared by dissolving 0.5 g of Protanal alginate powder (FMC international, Cork, Ireland) in sterile distilled water, and agitated for 3 hours, ensuring proper dispersion and homogeneity.

3.2.2.2.3 Gelling bath

Gelling bath for microencapsulation was prepared by dissolving calcium chloride (Sigma Aldrich, Canada) (8.60 g.L⁻¹) in distilled water. Solution was then sterilized using 200µm syringe filters and stored at room temperature until further use.

3.2.2.3 Microcapsules preparation

Microcin J25 microcapsules were produced through coextrusion method using Inotech Encapsulator equipped with an air pump and a peristaltic pump (MFLX78001-70, Cole-Parmer, Canada). Bacteriocin solution and the alginate shell material were simultaneously extruded through their respective nozzles, 150 μm outer nozzle for alginate and 80 μm inner nozzle for bacteriocin. Encapsulation conditions were adjusted as follows: internal rate of 1,4 mL/min, vibration frequency of 700 Hz, charge of 1600 V and an applied air pressure of 1.5 Bar.

The annular jet was fragmented as core-shell droplet due to high frequency vibration and fell into calcium chloride gelling bath. The core-shell microcapsules obtained were rinsed with distilled water to remove any residual gelation solution. Microcapsules were stored at 4°C in Eppendorf tubes (125 mg per tube) with storing solutions (250 μL per tube) for further use and analysis.

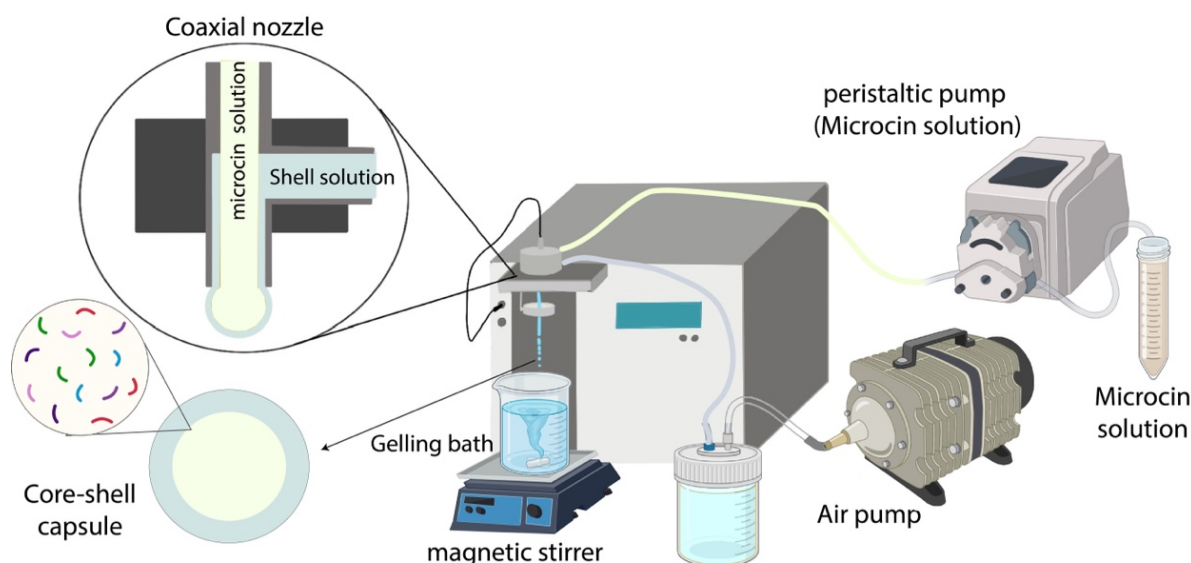


Figure 3-11. Illustration of microcapsules production Microcapsules morphology

Size and morphology of microcapsules were observed using an Olympus BX61 light microscope DP80 (x40 magnification and calibrated) equipped with an Olympus DP80 camera.

3.2.2.4 Antimicrobial activity Assays

Antimicrobial inhibitory activity of microcapsules and solutions samples were evaluated qualitatively and quantitatively through well diffusion assay and microdilution assay, methodology and sampling performed are illustrated Figure 3-12.

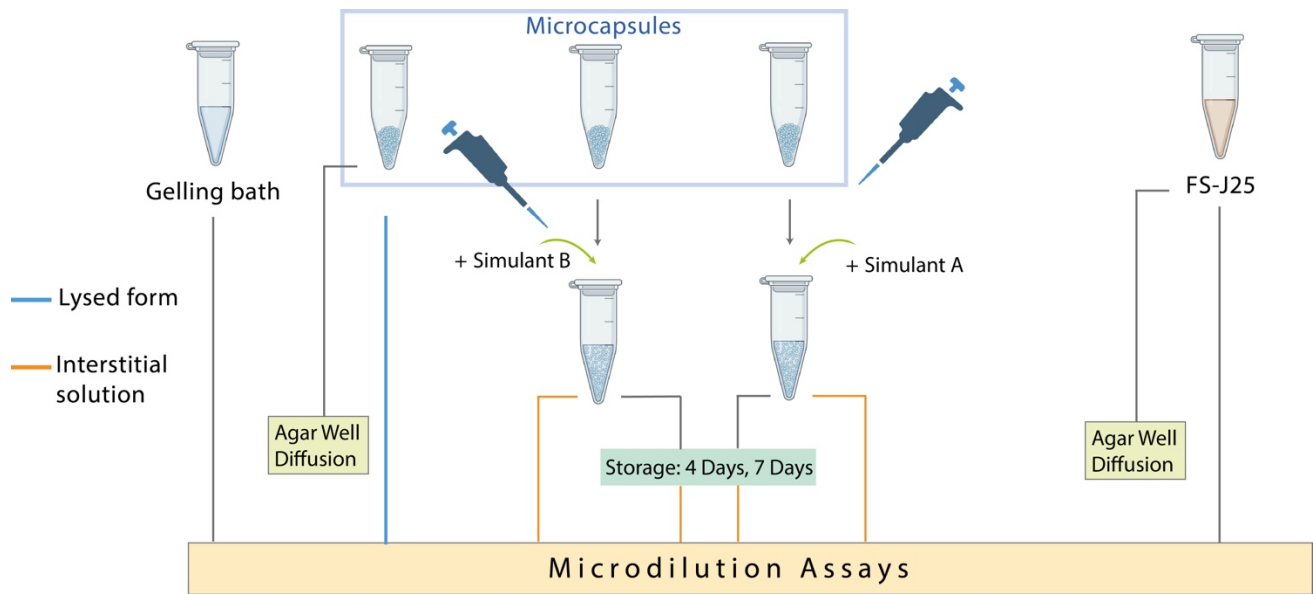


Figure 3-12. Antimicrobial activity assays performed.

3.2.2.4.1 Agar Well Diffusion Assay

The inhibitory activity was determined qualitatively on free J25 solution before its encapsulation (FS-J25) and microcapsules in their hole form, by the agar well diffusion assay. 7 mm diameter and 80 mm³ wells were punched out in a 0.75 % agar LB media (25 mL) seeded with 250 μL of overnight culture of *Salmonella* Newport. Briefly, 80 μL of FS-J25 or 80 mm³ of microcapsules were added into the wells, as illustrated in Figure 3-13. Following an 18 h incubation at 37°C inhibition zones were measured.

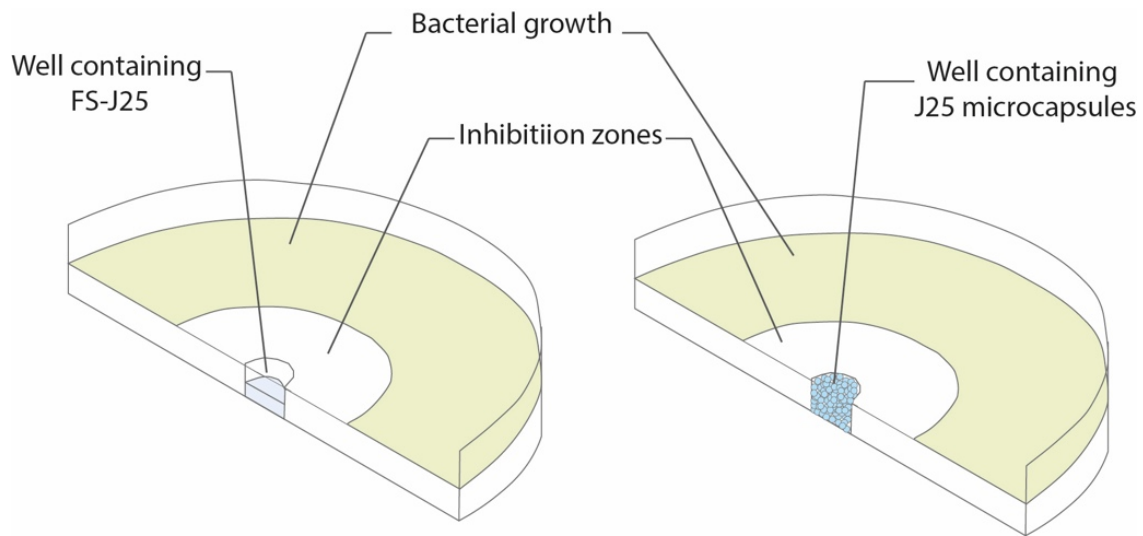


Figure 3-13. Schematic representation of agar well diffusion assay.

3.2.2.4.2 Microdilution Assay

Quantitative determination of inhibitory activity of bacteriocins was carried out using the broth microdilution method³⁸⁷, and was evaluated in FS-J25 and in lysed microcapsules (LMC). Therefore, 125 mg of J25 microcapsules were solubilized directly after encapsulation under stirring by addition of sterile 0.1 mol.L⁻¹ phosphate buffer (PB) solution at pH 8.8 (in ratio phosphate buffer : microcapsules of 3:2), dilution ratios for lysed microcapsules and storing solutions was noted to be considered for calculation. Two-fold serial dilutions of each solution (125 μL) were prepared in an appropriate medium in a clear 96-well flat-bottom microtiter plate (96 wells, Becton Dickinson Labware, Franklin Lakes, NJ, United States). Each well received 50 μL of overnight *Salmonella* Newport culture diluted 1,000-fold in fresh medium. The microtiter plates were incubated for 24 h under appropriate conditions. Control wells contained untreated culture and appropriate medium (blanks). The number of inhibition wells was noted, and the minimum inhibitory concentration (MIC) was the lowest concentration that prevented visible bacterial growth, as shown in Figure 3-14. J25 MIC was expressed as arbitrary units (AU)/mL and was calculated using the following formula.

$$MIC (AU/mL) = 2^n * \left(\frac{1000}{125}\right) = 2^{n+3} \quad (3.21)$$

Where 2 is the dilution factor, n is the number of inhibition wells, 1000 is the factor used to report results per mL and 125 is the volume of solution tested in μL.

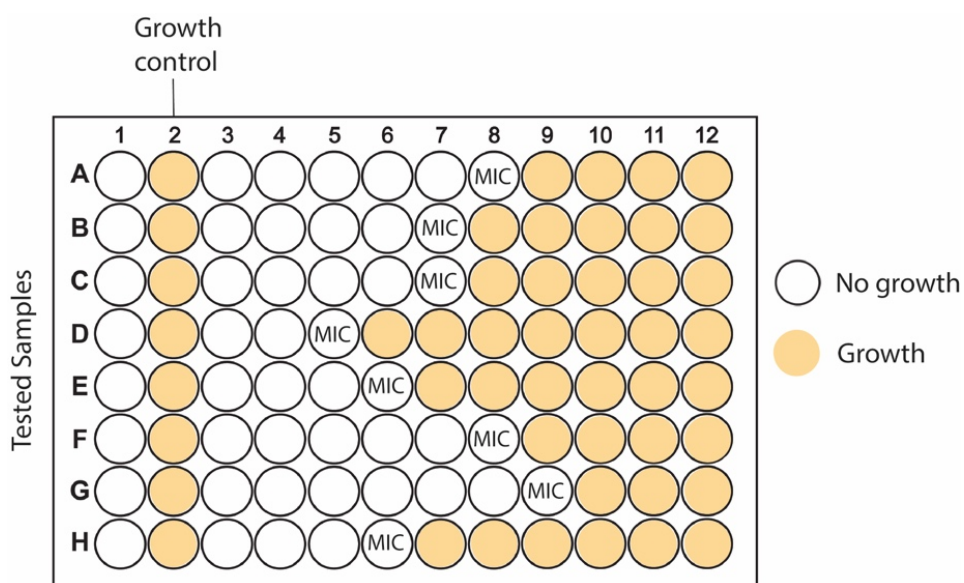


Figure 3-14. Schematic representation of microdilution assay.

3.2.2.5 Calculation of encapsulation efficiency

Encapsulation efficiency (EE) for Microcin J25 microcapsules was defined as the ratio between activity detected in lysed microcapsules (LMC) through microdilution assay and activity detected in free solution (FS-J25) previously measured and calculated with equation (3.22). Based on results obtained with microtitration, EE was calculated as follow:

$$EE (\%) = \frac{MIC \text{ detected in LMC (AU/ml)}}{MIC \text{ detected in FS_J25 (AU/ml)}} \times 100 \quad (3.22)$$

3.2.2.6 Determination of Microcin J25 release

To evaluate bacteriocin diffusion during storage in food media and residual activity in microcapsules, two food simulants were selected, simulant A (distilled water) and simulant B (distilled water + 3 % (v/v) acetic acid) to simulate neutral (*i.e* milk) and acidic beverages (*i.e* fermented milk or juice) respectively³⁸⁹. Bacteriocins microcapsules were transferred directly after production into Eppendorf tubes (125 mg/tubes) and 250 μ L of the corresponding simulant was added to each tube. Activity of the solution was then evaluated through microdilution assays as described for FS-J25 (AU/mL) at Day 0 (D0), Day 4 (D4) and Day 7 (D7) post encapsulation.

$$\text{release ratio } (\%) = \frac{MIC \text{ detected in simulant (AU/ml)}}{MIC \text{ detected in LMC (AU/ml)}} \times 100 \quad (3.23)$$

3.2.3 Results and discussion

3.2.3.1 Microcapsules morphology

Bacteriocins microcapsules were successfully produced and observed directly under light microscope. J25 microcapsules diameters were measured immediately after encapsulation as $878 \pm 64 \mu\text{m}$ (Figure 3-15).

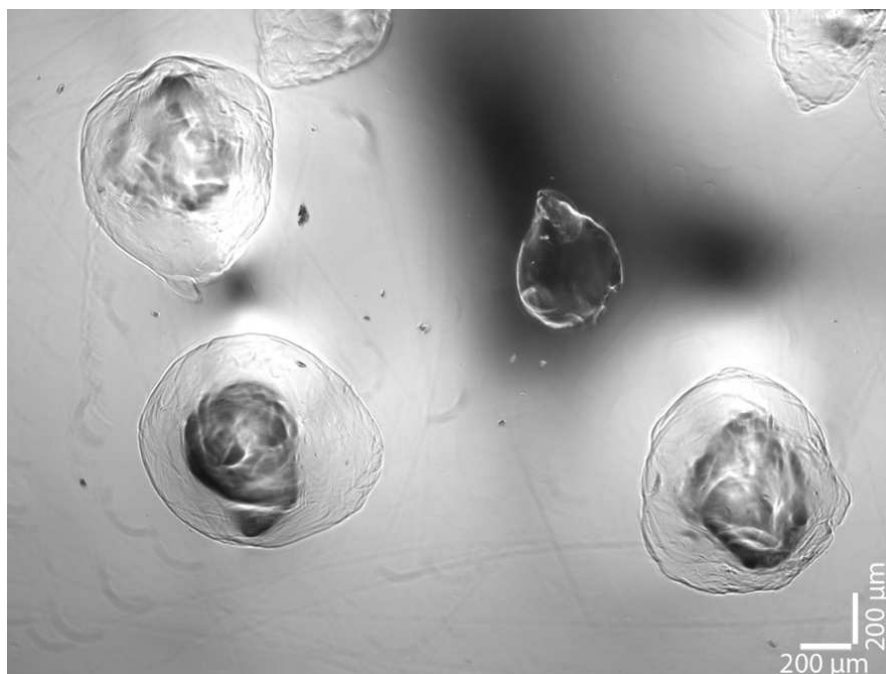


Figure 3-15. Microphotography of J25 microcapsules.

After a 7-day storage, a reduction in size was observed in simulant A, as presented in Table 3-7. This was probably due to diffusion of the content in the solution³⁵⁵. Simulant B (distilled water +3% acetic acid) had lower impact on microcapsules diameter. Probably due to a swelling behavior post J25 release with the expansion of the fragilized alginate network under pH impact.

Table 3-7. Average diameters of J25 microcapsules (n=5)

Samples and Storage time (Days)		Average diameter (μm)	Standard deviation (μm)
J25	Day 0	878	64
	Day 7 in Simulant A	721	45
	Day 7 in Simulant B	827	66

3.2.3.2 Antimicrobial Assays

3.2.3.2.1 Agar Well Diffusion Assay

Qualitatively antibacterial activity of encapsulated Microcin J25 was examined after incubation in the agar plates using *Salmonella* Newport as indicator strain. Figure 3-16. Presents inhibition zones of free solutions and bacteriocins microcapsules after 18h incubation at 37°C. J25 microcapsules showed effective antimicrobial activity. No significant difference in the halos of inhibitions (diameter $\approx 16 \pm 0.5$ mm) was observed between free and encapsulated Microcin J25.

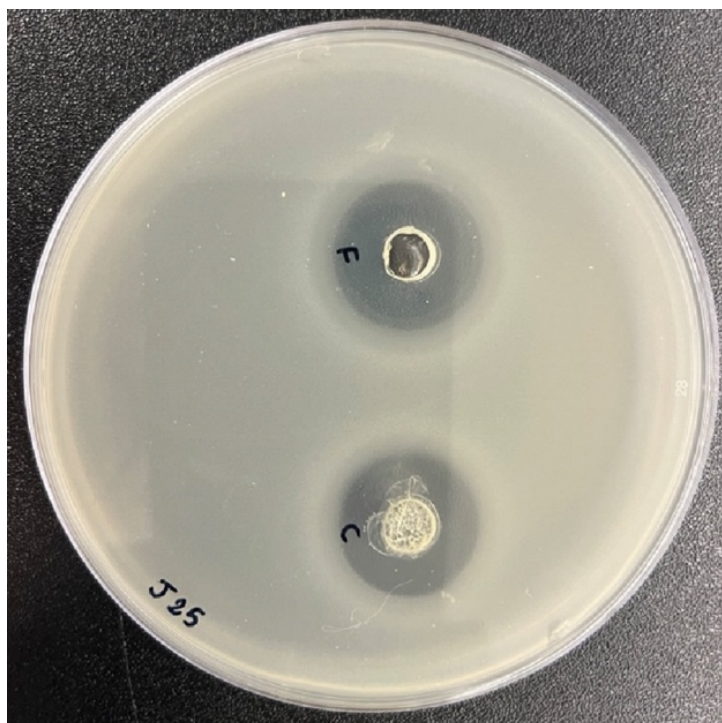


Figure 3-16. Visualization of antimicrobial activity with halo of inhibition against *S. Newport* of FS-J25 (F) and microcapsules (C) using well agar diffusion assay.

3.2.3.2.2 Microdilution assay

Quantitative determination of inhibitory activity of bacteriocins was performed on free J25 solution (FS-J25), lysed microcapsules (LMC), and on the gelling bath used during microcapsules production, to evaluate bacteriocins loss in the gelling bath during gelation process. microcapsules presented a MIC of $\sim 20,480$ AU/mL, while free solution of J25 presented a MIC of $\sim 65,536$ AU/mL. Inhibitory activities of different samples tested are displayed in Table 3-8.

Table 3-8. Inhibitory activity of microcin J25 in FS-J25, LMC, RS-J25 and in gelling bath against *Salmonella* Newport.

Samples	AU/mL
FS-J25	65,536
LMC	20,480
Gelling bath	4,096

3.2.3.3 Activity and Encapsulation efficiency (EE)

Encapsulation efficiency was calculated according to microdilution assays carried out on LMC and FS-J25 solutions directly after encapsulation using equation 3.22. where EE was

considered as the ratio between lysed microcapsules MIC and free J25 solution MIC. Therefore, J25 microcapsules were produced with an encapsulation efficiency of 31 %.

As indicated by microdilution assay on the gelling bath sample, microcin was lost in the gelling bath during encapsulation process, either directly during injection while jet breaking occurred, or through diffusion during cross-linking. Also, considering the calculated proportions, it is likely that quantities of J25 were lost during the encapsulation process, probably when the beads were rinsed.

3.2.3.4 Antimicrobial activity in food simulant

Bacteriocin release from microcapsules was investigated within two distinct food simulants: simulant A and simulant B. These simulants were selected to mimic the environmental conditions characteristic of neutral and acidic beverages. Release ratios were calculated using equation 3.23. A rapid release of bacteriocins from microcapsules immediately following encapsulation process was observed, with a 10% release ratio noted at D0 (0 day) for both simulants as presented in Table 3-9.

This early release indicated an initial burst release phenomenon, a common occurrence in drug delivery systems where a proportion of the encapsulated payload is promptly released upon exposure to the external environment ^{390,391}. The release ratio increased to 20% in both simulants after 4 days. This increase in the release ratio is likely due to Microcin J25 diffusion from the microcapsule material to external solution. The release ratio remained constant at 20% from day 4 to day 7.

Several factors may have contributed to this plateau in the release ratio, including the stability of the microcapsule material, the diffusion properties of the bacteriocins, or the equilibrium established between release and retention forces ^{392,393}. Storing temperature (4°C) could also be considered as a factor of alginate network tightness and its release kinetics properties. These observations could be useful for the development of controlled-release systems for bacteriocins in food preservation.

Table 3-9. Release ratio from J25 microcapsules to food simulant at different times (Days)

Samples and Storage (Days)	Tube content		Concentration (AU/mL)	Ratio	
	Microcapsules	Simulant			
J25 microcapsules	/		20480	/	
D0	Simulant A	125 mg	250 µL	2048	10%
	Simulant B	125 mg	250 µL	2048	10%
D4	Simulant A	125 mg	250 µL	4096	20%
	Simulant B	125 mg	250 µL	4096	20%
D7	Simulant A	125 mg	250 µL	4096	20%
	Simulant B	125 mg	250 µL	4096	20%

3.2.4 Conclusion

In this study, bacteriocin alginate microcapsules were successfully produced and exhibited an initial diameter of $880 \pm 64 \mu\text{m}$. The Microcin J25 microcapsules demonstrated an efficient antimicrobial activity against *Salmonella* Newport. Encapsulation efficiency (EE) was approximately 31%, suggesting loss of Microcin J25 during the encapsulation process.

Bacteriocin release from the microcapsules was studied in two distinct food simulants, simulant A and simulant B. A diffusion, up to 20 %, was observed 7 days after encapsulation, following an initial burst release observed directly after encapsulation ³⁹¹. These findings have significant implications for the development of controlled-release systems for bacteriocins in food industry. Studies have been focused lately on nisin encapsulation to be used as natural food preservative and presented processing results for food industry ^{394,395}, Further research is needed to optimize Microcin J25 and other bacteriocins microcapsule formulations for specific food applications.

Key highlights

- Coextrusion process has been successfully adapted to produce capsules of micrometric size.
- Coextrusion method is a promising approach for antimicrobial peptides encapsulation.
- Microcin J25 was successfully encapsulated in core-shell microcapsules, presenting an encapsulation efficiency of ~31%.

3.3 Study of formulation and process variables impact on capsule mechanical and physical properties.

In this section, the objectives were to influence the mechanical properties of the capsule membrane, the encapsulating efficiency, and the stability of encapsulated oils for COOKAL applications. Therefore, Capsule shell strength has been modulated to enhance structural stability during handling and improve the sensory experience of consuming olive oil-based capsules.

3.3.1 Impact of gelling bath ionic environment and post-encapsulation treatment on shell resistance

The aim was to adjust capsule shell strength to improve integrity and sensory experience of the consumption of olive oil-based capsule. This also ensured structural stability during handling and enhanced consumer perception. To achieve this objective, alginate/olive oil capsules were produced following the optimal conditions presented in chapter two ²⁵⁶. The ionic environment of the gelling bath was modified to impact shell resistance ³⁹⁶. Further, a post-encapsulation treatment was tested to adjust alginate network properties. Finally, the revised protocol was chosen as an industrial improvement to achieve the sensory purposes.

3.3.1.1 Material and methods

3.3.1.1.1 Materials

Virgin Olive oil used for the spherification process was purchased from Puget (Marseille, France). Sodium alginate (Protanal) was purchased from FMC international (Cork, Ireland). Calcium chloride $\geq 99\%$ was purchased from Beauseigneur (Belfort, France). Polysorbate 20 (pharmaceutical grade) was purchased from Lonza (Bâle, Switzerland). Sodium dodecyl sulfate was purchased from Sigma-Aldrich (Saint Quentin Fallavier, France).

3.3.1.1.2 Production of capsules

The studies involved the injection of both alginate (2.5% (w/v) sodium alginate and 2% (w/v) Polysorbate 20 in distilled water) and oil using a gear pump through a coaxial nozzle, with oil in the inner tube and sodium alginate in the outer tube. The dripping system produced droplets that fell into the gelling bath by gravity, when the weight of the droplets was greater than the capillary force that kept them attached to the nozzle ²⁰⁸.

Optimum parameters previously obtained through the design of experiment published in *LWT* were used for capsules production, *i.e.* 15.75 g.min⁻¹ for alginate feed rate, 47.25 g.min⁻¹ for oil feed rate, and a dripping height of 7 cm. The ionic environment of gelling bath was modified by testing 10 g.L⁻¹ and 160 g.L⁻¹ CaCl₂ concentrations. Alginate/olive oil capsules were immersed in the gelling bath 2 min for complete cross-linking. The capsules were then rinsed with distilled water, weighed, and stored in distilled water at 20°C prior to analysis.

In order to modify shell resistance, an additional treatment was added after encapsulation to study the effect of capsule immersion in acetic acid 8 % bath or NaCl bath on the alginate network.

3.3.1.1.3 Shell resistance measurements

The shell rupture strength was measured using a precision universal tensile-compressive tester (model AGS-X, Shimadzu). The capsule samples were positioned between two plates, with the lower plate set at 40 mm and the upper plate at 10 mm. The upper plate was moved down at 2 mm.min⁻¹ until the capsules fractured under pressure. Rupture strength (N) was measured in four replicates for each batch.

3.3.1.1.4 Size measurement

Average diameter value was measured using Dino capture 2.0 software on photographs captured using a 5-megapixel digital microscope Edge 5.0 (model AM7515MT8A, Dino-lite).

3.3.1.2 Results and discussion

As presented in Table 3-10, capsules produced in 10 g.L⁻¹ or 160 g.L⁻¹ gelling bath without post treatment presented the highest resistance with rupture strengths > 2N and the targeted size around 5 mm (Figure 3-17). Capsules treated in post-encapsulation stage with acetic acid or NaCl presented reduced rupture strength (from 1.155 N to 1.516 N). However, an altered taste was detected compared to standard olive oil capsules and they were discarded.

Table 3-10. Experimental conditions for gelling bath and post-encapsulation treatment of oil-alginate capsules.

Alginate	Gelling Bath [CaCl ₂] in g.L ⁻¹	Post encapsulation Treatment	Average diameter (mm)	Rupture strength (N)
2,6% + 2% PS	160	No treatment	4.903	2.372
	10	No treatment	5.048	2.236
	10 at pH 5	No treatment	5.037	1.322
	160	Acetic acid	5.092	1.366
	10	Acetic acid	4.506	1.155
	160	NaCl	4.902	1.516
2.6% + 0.2% SDS	10	NaCl	5.049	1.277
	160	No treatment	3.807	0.795

PS: Polysorbate 20; SDS: Sodium Dodecyl Sulfate.

Capsules produced in gelling bath at 10 g.L⁻¹ CaCl₂ and pH 5 had the best texture/resistance properties without having an altered taste. These conditions were then selected in the enterprise to improve capsule properties. Capsules produced with SDS as surfactant, presented an insufficient resistance to compression. Therefore, this last formulation was too fragile to be retained as an industrial improvement.

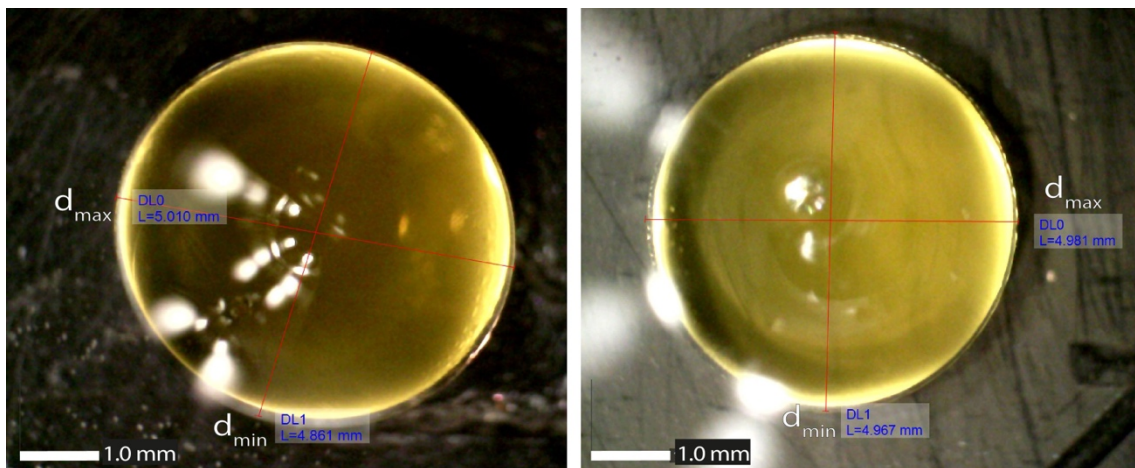


Figure 3-17. Microphotography of capsules produced with 2.6% alginate solution and 2% PS (standard formulation), at 160 g.L⁻¹ (A) and 10 g.L⁻¹ (B) CaCl₂ concentration.

3.3.2 Impact of core-oil viscosity on the core-shell centricity index of capsules

During preliminary experiments carried out prior to the study and optimization realized on capsules generated through annular jet breaking coextrusion, displayed in chapter two, variations

of core centricity index were observed. Thus, depending on oil type encapsulated, capsules presented a more or less centered core. Accordingly, this study aims to investigate the impact of core oil viscosity of core centricity index.

3.3.2.1 Materials and methods

3.3.2.1.1 Materials

High viscosity sodium alginate was purchased from Louis-François (Croissy-Beaubourg, France). Purified Calcium chloride $\geq 94\%$ was purchased from VWR (VWR Chemicals®, France). Organic virgin Sunflower oil (Bio Village, France), organic linseed oil, organic castor oil and organic rapeseed oil were purchased from leading supermarket chain based in France.

3.3.2.1.2 Oils viscosity

Oils (linseed, sunflower, rapeseed and castor oils) viscosities were measured using an HR20 Rheometer (TA Instruments Waters Corporation, New Castle, DE, USA) with a 40 mm parallel plate, the tests were carried out at a shear rate range of $0.1\text{--}100\text{ s}^{-1}$ at 20°C . Oil blends (sunflower and linseed oil blends at 1:2 and 1:1 ratios) were used to obtain additional viscosity levels. Therefore, their respective viscosity was measured.

3.3.2.1.3 Capsules production

Production of capsules was accomplished using a B-395 Pro Encapsulator (Buchi, Switzerland) employing a coaxial nozzle extrusion technique. Same protocol was used for each oil separately to produce different characteristics capsules²⁷¹. The corresponding oil and shell solution were independently loaded into separate 50 mL syringes and simultaneously injected through a coaxial nozzle featuring a $750\text{ }\mu\text{m}$ diameter internal nozzle for the core and a $900\text{ }\mu\text{m}$ diameter external nozzle for the shell.

The extruded droplets were directed into a $8.60\text{ g}\cdot\text{L}^{-1}$ calcium chloride gelation bath. During injection, an electric charge of 2000 V was applied, accompanied by vibration, to facilitate droplet separation and dispersion. Capsule formation and stabilization occurred during an hour-long residence within the gelation bath. Subsequently, each batch was rinsed with distilled water, then weighted and stored at 20°C in distilled water for subsequent analysis.

3.3.2.1.4 Centricity index

Centricity index was evaluated following same methodology used for the preliminary studies mentioned beforehand. Therefore, minimum and maximum shell thickness were used to determine the centricity index of oil core and the index was calculated using the following equation 3.23:

$$\text{Centricity index} = \frac{ST_{min}}{ST_{max}} \quad (3.23)$$

Where ST_{min} and ST_{max} are respectively minimum and maximum shell thickness. A centricity index of 1 indicates an ideally centered core. However, due to its three-dimensional nature directly visualize and measure the actual distance between the core and the shell, has been challenging, within the two-dimensional context of microscope images. Despite this limitation, the centricity index provides a valuable means of quantitatively assessing the relative positioning of the core within the capsule.

3.3.2.2 Results and discussion

3.3.2.2.1 Rheology Analysis

Absolute viscosities of oils and oil blends were measured. Linseed oil has the lowest viscosity among the oils and blends listed in the Table 3-11, with a viscosity of 0.047 Pa.s. However, Castor oil stands out with a significantly higher viscosity of 0.804 Pa.s, making it the most viscous oil. Additional data is displayed in Table 3-11.

Table 3-11. Measured absolute viscosities.

Oils	Viscosity (Pa.s)
Linseed oil	0,047
Sunflower: linseed (1:2)	0,053
Sunflower: linseed (1:1)	0,056
Sunflower oil	0,066
Rapeseed oil	0,072
Castor oil	0,804

3.3.2.2.2 Centricity index

The results demonstrate a clear correlation between oil viscosity and the centricity index of capsules. As displayed Table 3-12.

Table 3-12. Centricity indices for produced oil capsules

Oil capsules	Capsules centricity index	Standard deviation
Linseed oil	0,12	0,048
Sunflower: linseed (1:2)	0,23	0,009
Sunflower: linseed (1:1)	0,29	0,005
Sunflower oil	0,40	0,008
Rapeseed oil	0,39	0,045
Castor oil	0,47	0,022

The centricity index is notably influenced by the viscosity of the oil and its modifications. Specifically, an increase in oil viscosity leads to a corresponding rise in the core centricity index.

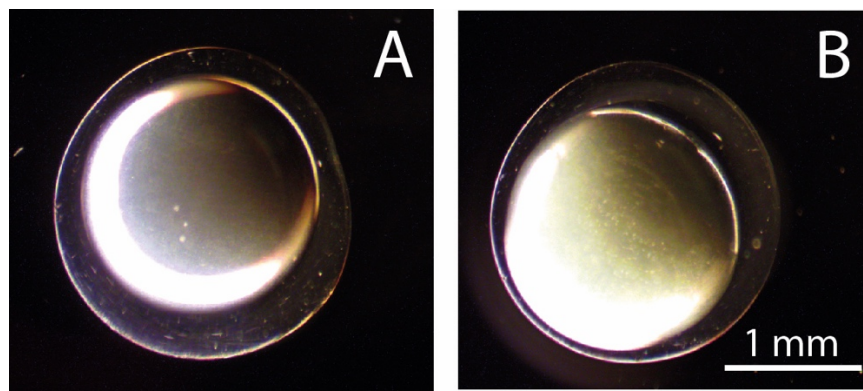


Figure 3-18. Microphotograph of core-shell capsules produced by coextrusion: (A) Rapeseed Oil, (B) linseed oil capsule.

This relationship is visually evident in Figure 3-18, where capsules produced using higher viscosity oil (Figure 3-18A) exhibit more centered cores compared to those formed with lower viscosity oil (Figure 3-18B). Nevertheless, the centricity index progression seems to level off beyond a value of 0.4, as indicated in Figure 3-19. This plateau suggests that the impact of oil viscosity on core positioning within capsules reaches a saturation point.

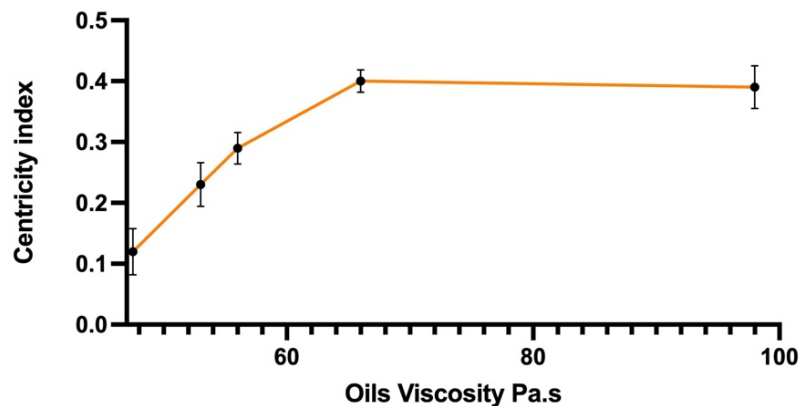


Figure 3-19. Evolution of the centricity index as a function of the theoretical viscosity of the encapsulated oil.

3.3.2.3 Conclusion

In conclusion, this study highlights the significant influence of oil viscosity on the centricity index of capsules. The observed correlation between oil viscosity and core positioning highlights the importance of careful selection and manipulation of oil properties in capsule manufacturing processes. These findings contribute to a deeper understanding of capsule formation dynamics and have implications for fields requiring precise control of core positioning within capsules, such as drug delivery and material encapsulation.

Chapter 4. General discussion

The results presented in this PhD thesis reflect a comprehensive investigation of the coextrusion encapsulation process using alginate as the protective material. Coextrusion encapsulation technique allowed to produce core-shell capsules with precise control of various parameters. Throughout this research, we examined a range of factors and their impacts on capsule properties, shedding light on the potential applications and implications of this technology. In this general discussion, we will delve the coextrusion process (jet breaking and dripping process), the process parameters and their modeling for tailoring capsules to specific applications.

The principal advantage of coextrusion lies in its ability to create capsules with distinct core and shell components, and its adaptability to various core materials, enabling a wide range of applications in fields such as pharmaceuticals, food science, and biotechnology ⁷⁸. In the food industry, coextrusion offers exciting possibilities for encapsulating oils and essential oil for their nutritional value, bioactive content, and gastronomic aspect ²¹⁰. It is essential to use appropriate coextrusion method and adjust process parameters to design targeted capsules. Therefore, designing capsules through coextrusion requires a systematic approach that involves material selection, *i.e.* viscosities, solubility, compatibilities, choosing the right nozzle size and adjusting process parameters. Figure 4-1 illustrate different coextrusion methods requirements in terms of nozzle size, feed rate and alginate viscosities. Spraying systems allow smaller capsules production through small nozzles and low feed rates use, however, adapting alginate solution to low viscosity is necessary. On the other side, dripping systems permit millimetric size capsules production requiring high alginate viscosities and low feed rate to allow drops formation. While jet breaking systems produced very homogenous millimetric capsules or microcapsules with higher feed rate, coextrusion methods have operating intervals, making it necessary to adapt process parameters and formulation for capsules development.

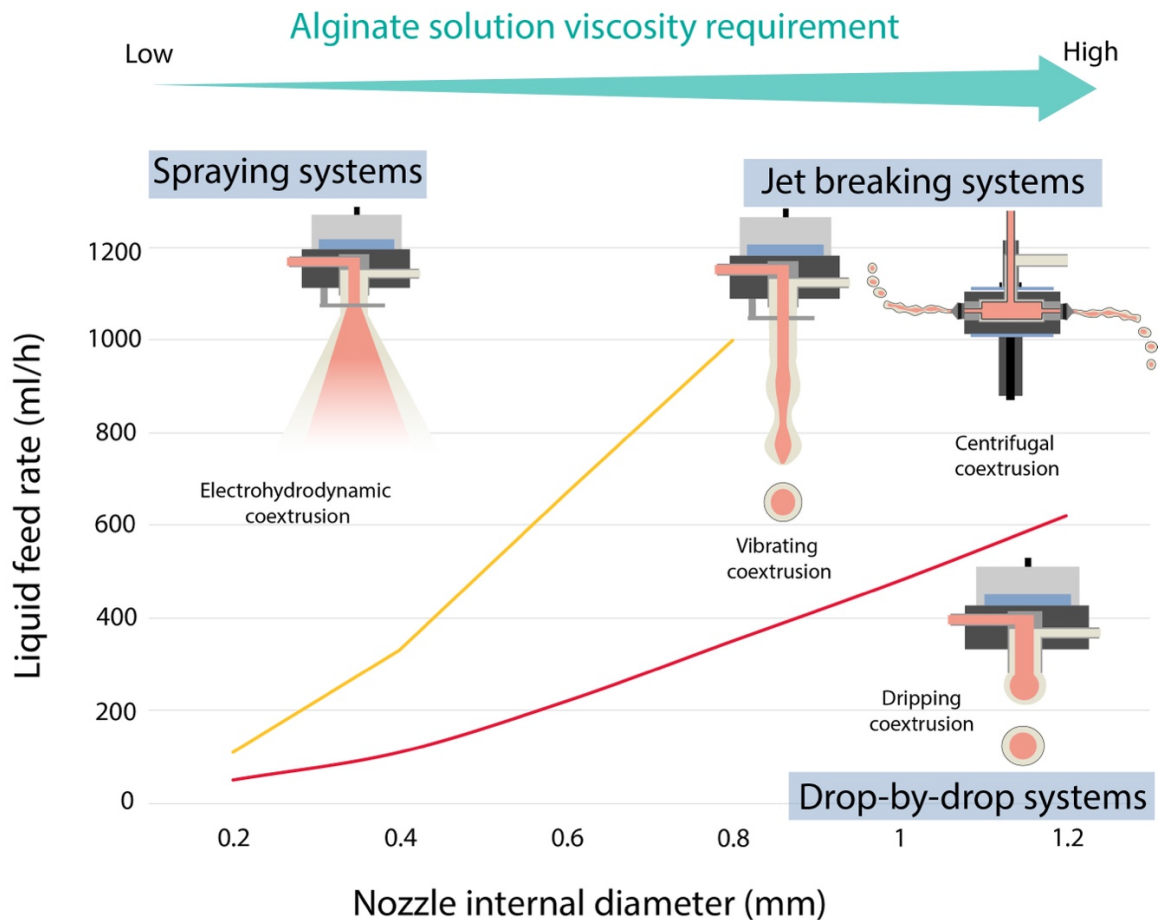


Figure 4-1. Illustration of different injection methods dependent on various feed and nozzle diameter, and shell solution viscosity as modulating tool (Adapted from Poncelet ³⁹⁷).

The main objectives of this thesis were to investigate and modulate keys process parameters that influenced capsule properties. Principally using experimental design methodology, we examined the impact of various factors jet-breaking and dripping processes (calcium chloride concentration, core and shell feed rates, dripping height, and oil viscosity) on capsule characteristics (size, sphericity, rupture strength, encapsulation payload, centricity index). Mathematical models have been developed to facilitate prediction of capsules characteristics.

The results from this research demonstrated that the choice of alginate formulation and the modulation of parameters can significantly impact capsule rupture strength and encapsulation payload, offering possibilities for enhanced flavor delivery and shelf-life extension in food products. Calcium chloride played a pivotal role in gelation process, acting as a cross-linking agent, primarily interacting with G-blocks of alginate molecules to create robust gel networks ⁴⁵. A distinct relationship between calcium chloride concentration and beads size could be observed, unfolding in two distinct phases ²⁷¹. In the first phase, as calcium ions penetrate the alginate network, provoke

water expulsion and enhanced cross-linking, resulting in network contraction and reduced bead size. Conversely, excessive calcium chloride concentrations lead to repulsion between alginate chains due to Ca^{2+} supersaturation, causing bead enlargement, this size variation is highly dependent on erosion/retraction coefficient.

A phenomenological model has been developed to predict alginate beads behavior during gelation, allowing to describe the impact of alginate rate and calcium ions concentration on bead/capsules size. Relation between alginate characteristics (Mw and M/G ratio) and its ionic gelation have been highlighted. Ultimately, studies carried out during this thesis permit to complete the state of the art presented in Table 1-2, concerning principal encapsules parameters on formed capsules characteristics, therefore, our improved key parameters are summarized in Table 4-1

Table 4-1. Effects of principal increased factors influencing capsules formation

Enhanced Parameters	Effects on capsule formation					
	Size	Strongness	Sphericity	Centricity	Rupture Strength	payload
↗ Mw	↘	↗	↗ ↘	-	↗	-
↗ M/G ratio	-	↘	-	-	↗	-
↗ [alginate]		↗	↗ ↘	-	↗	-
↗ Core viscosity				↗	↗	↘
↗ $[\text{Ca}^{2+}]$	-	-	↘	↗	↗ ↘	↘
↗ Temperature	↘	-	↗	-	↘	-
↗ Frequency	↘	-	↘ ↗ ↘ *	↗	-	-
↗ Flow rate	↗	-	↘	↘	↘	↗

*Results from interaction with flow rate.

These studies have significantly enhanced our comprehension of how process parameters intricately influence capsules properties. Moreover, they permitted to develop valuable mathematical tools for precise process modulation and formulation adjustments in accordance with desired outcomes and available equipment. This knowledge not only advanced our fundamental understanding of encapsulation processes but also offered practical tools for tailoring encapsulation matrices to meet specific objectives and applications. As an example, industrial application encapsulation of high value oil, such as Hemp oil, was done by the Cookal company. Capsules not only preserved the oil quality but also maintained its antioxidant capacity.

Another application was done for bioactive vectorization. The ability to encapsulate biomolecules, such as microcin J25, within core-shell capsules holds great promise. Our study demonstrated successful encapsulation and release of J25, showcasing coextrusion potential for antimicrobial peptide encapsulation. Moreover, coextrusion allows the encapsulation of diverse molecules, including hydrophilic biomolecules to lipophilic oils ^{383,398}. This adaptability makes it a versatile tool for encapsulating a wide array of substances, making it valuable in the pharmaceutical industry for drug delivery systems and in the food industry for flavor encapsulation and preservation. The Cookal company has now several tools for process mastering and new products development.

Chapter 5. Conclusion and perspectives

L'encapsulation est un moyen pratique de préserver les substances actives et de contrôler leur libération. Elle joue un rôle essentiel dans l'amélioration de la stabilité des produits, de la disponibilité des substances et de la précision de leur libération. Parmi les différentes techniques d'encapsulation, la coextrusion se distingue par sa capacité à créer des capsules cœur-couronne à forte charge utile. Elle offre une grande souplesse d'adaptation à des matériaux de viscosité et de caractéristiques différentes.

Cette thèse a permis l'exploration d'un polymère polyvalent et largement utilisé, l'alginate, dans diverses applications techniques, en particulier son rôle dans les processus d'encapsulation. Les propriétés gélifiantes de l'alginate, connu pour son statut « sûr » (GRAS), sa non-toxicité, sa biocompatibilité et sa biodégradabilité, ont été examinées. La gélification de l'alginate est influencée par des facteurs tels que le pH, la température, la concentration du polymère, la concentration du réticulant, le temps de séjour et la force ionique.

La technologie de coextrusion, largement abordée dans ce travail, offre des avantages tels qu'une charge en composés actifs (cœur) élevée, un processus continu et une grande flexibilité. Elle a prouvé sa valeur dans divers domaines : alimentaire, pharmaceutiques, cosmétiques, biotechnologiques et environnementales. Sa capacité à encapsuler des ingrédients complexes, des cellules et des substances actives en a fait un outil précieux pour ces industries.

Sur la base de travaux de thèse antérieurs et de l'expertise accumulée, la société COOKAL a développé avec succès une large gamme de produits encapsulés qui sont maintenant commercialisés à l'échelle internationale. Cependant, pour la préservation des composés à haute valeur ajoutée qui constituent le marché en croissance de l'entreprise, les caractéristiques des capsules doivent être contrôlées (propriétés mécaniques, chimiques, physico-chimiques). Pour cette raison, notre travail a étudié le processus de coextrusion en comprenant et en ajustant les variables du processus, telles que la concentration en calcium, les taux d'alimentation, la fréquence, les types d'alginate, la viscosité de la solution de base et le vieillissement des solutions d'alginate. Ainsi, le processus de goutte-à-goutte industriel a été optimisé pour répondre aux critères industriels concernant la forme des capsules, l'efficacité de la charge d'actifs et le rendement de production. En outre, les modèles prédictifs développés peuvent servir d'outils inestimables pour atteindre les résultats souhaités, en garantissant l'efficacité, la précision et la régularité des processus d'encapsulation.

Les alginates ont été caractérisés dans un troisième travail qui a permis d'étudier l'impact des caractéristiques des alginates (poids moléculaire et rapport M/G) sur la gélification du réseau

et la taille des billes/capsules. Un modèle phénoménologique a été développé pour décrire les propriétés de réticulation de l'alginate et sa dépendance à la concentration ionique du bain de gélification. Ces connaissances fournissent non seulement des outils précieux pour l'optimisation industrielle des capsules d'alginate.

Cette thèse souligne le potentiel de la technologie d'encapsulation, en particulier la coextrusion, dans diverses industries et met en évidence le rôle essentiel de la maîtrise et de la modélisation dans la concrétisation de ce potentiel. En outre, notre travail a contribué de manière significative au domaine de la technologie de l'encapsulation, en offrant une compréhension plus approfondie des propriétés de l'alginate, et en ouvrant des possibilités passionnantes pour des applications innovantes dans divers secteurs. De plus, les travaux de cette thèse ont été valorisés par la publication de trois revues de littérature et trois articles de recherches publiés dans les journaux internationaux (*Food Hydrocolloids*, *Drug Marines*, *Foods*, *colloids and surfaces B*, *LWT* et *polymers*).

Cependant, bien que cette thèse a fourni des informations précieuses, il existe encore plusieurs possibilités d'exploration future, afin d'améliorer les performances industrielles. D'autres études pourraient porter sur l'optimisation des techniques de coextrusion afin de surmonter les limitations liées à l'équipement (limites des pompes d'injection, multiplication des buses et perte de charge) pour une production à plus grande échelle, en maintenant des paramètres optimisés et en garantissant l'évolutivité et la rentabilité.

En outre, des études concernant la cinétique de réticulation de l'alginate pendant la formation du réseau et le comportement rhéologique pendant la liaison croisée constitueraient une étape importante vers la compréhension des particules à base d'alginate. Des études plus approfondies sur l'encapsulation des molécules hydrophiles et la stabilité à long terme des capsules produite par coextrusion dans des conditions environnementales variables seront également cruciales pour diverses applications.

Enfin, l'encapsulation à l'alginate, avec sa biocompatibilité et son adaptabilité, reste l'un des matériaux les plus prometteurs pour relever les défis complexes de l'encapsulation dans diverses industries. Le processus d'encapsulation par coextrusion a démontré sa polyvalence et son potentiel dans un large éventail d'applications. En modulant systématiquement les variables clés, les capsules peuvent être conçues pour répondre à des besoins spécifiques. Alors que la technologie continue de progresser, la coextrusion est prometteuse pour le développement de solutions d'encapsulation innovantes et personnalisables qui peuvent répondre aux défis évolutifs de diverses industries.

English Conclusion

The present report provided a comprehensive exploration of the widely used polymer, alginate, in various technical applications, particularly its role in encapsulation processes. The gelation of alginate was influenced by factors such as pH, temperature, polymer concentration, crosslinker concentration, residence time, and ionic strength. Coextrusion technology, discussed largely in this work, offers advantages such as high payload, continuous processing, and flexibility. It has proven its applicability across various fields, including food, pharmaceuticals, cosmetics, and environmental applications. The ability to encapsulate complex ingredients, cells, and active substances has made it an invaluable tool for these industries.

Based on previous thesis work and accumulated expertise, COOKAL company has successfully developed a wide range of encapsulated products that are now marketed internationally. However, for the preservation of high-value compounds, which constitute the growing market for the company, the capsules characteristics must be perfectly controlled (mechanical, chemical, physico-chemical properties). For this reason, our work allowed to study coextrusion process by comprehending and adjusting process variables, such as calcium concentration, feed rates, frequency, alginate types, core solution viscosity and alginate solutions aging. Alginates composition has also been studied to evaluate the impact of alginate characteristics (molecular weight and M/G ratio) on alginate network gelation and beads/capsules size. A phenomenological model has been developed to describe alginate cross-linking properties and its dependency to gelling bath ionic concentration. This knowledge not only provides valuable tools for alginate capsules industrial optimization, but also contributes to the field of encapsulation technology.

Thus, industrial dripping processes have been optimized to meet industrial criteria for capsules shape, payload efficiency, and production yield. In addition, mathematical models were developed as invaluable tools for predicting and achieving desired outcomes, ensuring efficiency, accuracy, and consistency in encapsulation processes. Working on two coextrusion methods permitted the adaptation of process parameters to various process requirements, *i.e.* process parameters, nozzle size. Understanding shell and core solution formulation and characteristics impact on produced hydrogel and capsules was an important step toward encapsulation modulation.

This thesis underscores the significant potential of encapsulation technology, especially coextrusion, in shaping various industries and highlighting the essential role of modulation and modeling in realizing this potential. Also, our work contributed significantly to the field of encapsulation technology, offering a deeper understanding of alginate properties, and opening-up exciting possibilities for innovative applications across diverse sectors. This thesis work allowed the publication three reviews and three research articles, publish in international peer-reviewed journals.

However, even if this thesis has provided valuable insights, there are still several possibilities for future exploration, to enhance Cookal industrial performance. Further studies can delve into the optimization of coextrusion techniques to overcome equipment-related limitations (injection pumps limits, nozzles multiplication and head loss) for scale-up, maintaining optimized parameters and ensuring scalability and cost-effectiveness.

Additionally, investigations concerning alginate reticulation kinetics during network formation and rheological behavior during cross-linking would be an important step toward alginate-based particles understanding. Also, further extended studies of hydrophilic molecules encapsulation and long-term stability of coextruded capsules under varying environmental conditions will be crucial.

Finally, alginate encapsulation, with its biocompatibility and adaptability, remains one of the most promising materials for addressing complex challenges of encapsulation in various industries. Coextrusion encapsulation process demonstrated its versatility and potential in a wide range of applications. By systematically modulating key variable, capsules can be engineered to specific needs, whether in food science, pharmaceuticals or biotechnology. As technology continues to advance, coextrusion holds promise as a key player in the development of innovative and customizable encapsulation solutions that can address the evolving challenges in various industries.

Chapter 6. References

1. Sobel, R., Versic, R. & Gaonkar, A. G. Introduction to Microencapsulation and Controlled Delivery in Foods. in *Microencapsulation in the Food Industry: A Practical Implementation Guide* 26–34 (Elsevier Inc., 2023). doi:10.1016/B978-0-12-404568-2.00001-7.
2. Bennacef, C., Desobry-banon, S. & Probst, L. Alginate Core-Shell Capsules Production through Coextrusion Methods : Principles and Technologies. *Mar Drugs* **21**, 235 (2023).
3. Almurisi, S. H., Doolaanea, A. A., Akkawi, M. E., Chatterjee, B. & Sarker, M. Z. I. Taste masking of paracetamol encapsulated in chitosan-coated alginate beads. *J Drug Deliv Sci Technol* **56**, 101520 (2020).
4. Geng, M. *et al.* Encapsulating vitamins C and E using food-grade soy protein isolate and pectin particles as carrier: Insights on the vitamin additive antioxidant effects. *Food Chem* **418**, (2023).
5. Le Priol, L. *et al.* Co-encapsulation of vegetable oils with phenolic antioxidants and evaluation of their oxidative stability under long-term storage conditions. *LWT* **142**, 111033 (2021).
6. Ghasemi, S. *et al.* Encapsulation of Orange Peel Oil in Biopolymeric Nanocomposites to Control Its Release under Different Conditions. *Foods* **12**, 831 (2023).
7. Rahiminezhad, Z. *et al.* PLGA-graphene quantum dot nanocomposites targeted against $\alpha v \beta 3$ integrin receptor for sorafenib delivery in angiogenesis. *Biomaterials Advances* **137**, 212851 (2022).
8. Ben Messaoud, G., Sánchez-González, L., Jacquot, A., Probst, L. & Desobry, S. Alginate/sodium caseinate aqueous-core capsules: A pH-responsive matrix. *J Colloid Interface Sci* **440**, 1–8 (2015).
9. Kazemi-Andalib, F., Mohammadikish, M., Sahebi, U. & Divsalar, A. pH-sensitive and targeted core-shell and yolk-shell microcarriers for in vitro drug delivery. *J Drug Deliv Sci Technol* **75**, 103633 (2022).
10. Mohammed, N. K., Tan, C. P., Manap, Y. A., Muhialdin, B. J. & Hussin, A. S. M. Spray Drying for the Encapsulation of Oils—A Review / N. K. Mohammed, C. P. Tan, Y. A. Manap. *Molecules* **25** (17), 1–16 (2020).
11. Đorđević, V. *et al.* Trends in Encapsulation Technologies for Delivery of Food Bioactive Compounds. *Food Engineering Reviews* **7**, 452–490 (2014).
12. Bennacef, C., Desobry-Banon, S., Probst, L. & Desobry, S. Advances on alginate use for spherification to encapsulate biomolecules. *Food Hydrocoll* **118**, (2021).
13. Bamidele, O. P. & Emmambux, M. N. Encapsulation of bioactive compounds by “extrusion” technologies: a review. *Crit Rev Food Sci Nutr* **0**, 1–19 (2020).
14. Bennacef, C., Desobry, S., Probst, L. & Desobry-banon, S. Alginate Based Core – Shell Capsules Production through Coextrusion Methods : Recent Applications. *Foods* **12**, 1788 (2023).
15. Selvasudha, N. *et al.* Seaweeds derived ulvan and alginate polysaccharides encapsulated microbeads—Alternate for plastic microbeads in exfoliating cosmetic products. *Carbohydrate Polymer Technologies and Applications* **6**, 100342 (2023).
16. Huang, L., Wu, K., Zhang, R. & Ji, H. Fabrication of Multicore Milli- and Microcapsules for Controlling Hydrophobic Drugs Release Using a Facile Approach. *Ind Eng Chem Res* **58**, 17017–17026 (2019).
17. Blanco-Cabra, N. *et al.* Characterization of different alginate lyases for dissolving *Pseudomonas aeruginosa* biofilms. *Sci Rep* **10**, 9390 (2020).
18. Boyd, A. & Chakrabarty, A. M. *Pseudomonas aeruginosa* biofilms: role of the alginate exopolysaccharide.
19. Günter, E. A., Popeyko, O. V., Belozarov, V. S., Martinson, E. A. & Litvinets, S. G. Physicochemical and swelling properties of composite gel microparticles based on alginate and callus cultures pectins with low and high degrees of methylesterification. *Int J Biol Macromol* **164**, 863–870 (2020).
20. Lee, K. Y. & Mooney, D. J. Alginate: Properties and biomedical applications. *Progress in Polymer Science (Oxford)* **37**, 106–126 (2012).
21. Misbah, Bhatti, I. A., Zia, K. M., Bhatti, H. N. & Shahid, M. Synthesis, biological efficiency evaluation and application of sodium alginate-based polyurethane dispersions using cycloaliphatic isocyanate, as antibacterial textile coating. *Journal of Industrial Textiles* 1528083719867445 (2019) doi:10.1177/1528083719867445.
22. Mancini, F. & Mchugh, T. H. Fruit-alginate interactions in novel restructured products. doi:10.1002/1521-3803(20000501)44:3<152::AID-FOOD152>3.0.CO;2-8.
23. Adli, S. A. *et al.* Development of Biodegradable Cosmetic Patch Using a Polylactic Acid/Phycocyanin-Alginate Composite. doi:10.3390/polym12081669.
24. Shi, S. S., Lei, S. J. & Fu, C. xia. Studies of the properties of CHG-Loaded alginate fibers for medical application. *Polym Test* **83**, (2020).
25. Su, C. *et al.* Effect of sodium alginate on the stability of natural soybean oil body emulsions. *RSC Adv* **8**, 4731–4741 (2018).
26. Parreidt, T. S., Müller, K. & Schmid, M. Alginate-Based Edible Films and Coatings for Food Packaging Applications. (2018) doi:10.3390/foods7100170.
27. Smith, A. M. & Miri, T. Alginates in Foods. in *Practical Food Rheology* 113–132 (2011). doi:https://doi.org/10.1002/9781444391060.ch6.
28. Qin, Y., Jiang, J., Zhao, L., Zhang, J. & Wang, F. Applications of Alginate as a Functional Food Ingredient. in *Biopolymers for Food Design* 409–429 (Elsevier Inc., 2018). doi:10.1016/B978-0-12-811449-0.00013-X.
29. Lee, B. B., Bhandari, B. R. & Howes, T. Air Extrusion System for Ionotropic Alginate Microgel Particle Formation: A Review. *Chemical Engineering and Technology* vol. 39 2355–2369 Preprint at https://doi.org/10.1002/ceat.201600088 (2016).
30. Martău, G. A., Mihai, M. & Vodnar, D. C. The Use of Chitosan , Alginate , and Pectin in the Biomedical and Food Sector _ Biocompatibility, Bioadhesiveness, and Biodegradability. *Polymers (Basel)* **11**, 1837 (2019).
31. Ramos, P. E. *et al.* Effect of alginate molecular weight and M/G ratio in beads properties foreseeing the protection of probiotics. *Food Hydrocoll* **77**, 8–16 (2018).
32. Rhein-Knudsen, N., Ale, M. T., Ajallouecian, F. & Meyer, A. S. Characterization of alginates from Ghanaian brown seaweeds: *Sargassum* spp. and *Padina* spp. *Food Hydrocoll* **71**, 236–244 (2017).
33. Hecht, H. & Srebnik, S. Structural Characterization of Sodium Alginate and Calcium Alginate. *Biomacromolecules* **17**, 2160–2167 (2016).
34. Haug, A., Larsen, B., Smidsrød, O., Munch-Petersen, J. & Munch-Petersen, J. The Degradation of Alginates at Different pH Values. *Acta Chem Scand* **17**, 1466–1468 (1963).
35. Yang, J. S., Xie, Y. J. & He, W. Research progress on chemical modification of alginate: A review. *Carbohydrate Polymers* vol. 84 33–39 Preprint at https://doi.org/10.1016/j.carbpol.2010.11.048 (2011).
36. Chhatbar, M., Meena, R., Prasad, K. & Siddhanta, A. K. Microwave assisted rapid method for hydrolysis of sodium alginate for M/G ratio determination. *Carbohydr Polym* **76**, 650–656 (2009).

37. Aida, T. M., Yamagata, T., Watanabe, M. & Smith, R. L. Depolymerization of sodium alginate under hydrothermal conditions. *Carbohydr Polym* **80**, 296–302 (2010).
38. Hartmann, M., Dentini, M., Ingar Draget, K. & Skjåk-Bræk, G. Enzymatic modification of alginates with the mannuronan C-5-epimerase AlgE4 enhances their solubility at low pH. *Carbohydr Polym* **63**, 257–262 (2006).
39. Kelishomi, Z. H. *et al.* Antioxidant activity of low molecular weight alginate produced by thermal treatment. *Food Chem* **196**, 897–902 (2016).
40. Vold, I. M. N., Kristiansen, K. A. & Christensen, B. E. A study of the chain stiffness and extension of alginates, in vitro epimerized alginates, and periodate-oxidized alginates using size-exclusion chromatography combined with light scattering and viscosity detectors. *Biomacromolecules* **7**, 2136–2146 (2006).
41. Feng, L., Cao, Y., Xu, D., Wang, S. & Zhang, J. Molecular weight distribution, rheological property and structural changes of sodium alginate induced by ultrasound. *Ultrason Sonochem* **34**, 609–615 (2017).
42. Taha, A. *et al.* Ultrasonic emulsification: An overview on the preparation of different emulsifiers-stabilized emulsions. *Trends Food Sci Technol* **105**, 363–377 (2020).
43. Salachna, P., Grzeszczuk, M., Meller, E. & Soból, M. Oligo-Alginate with low molecular mass improves growth and physiological activity of *eucomis autumnalis* under salinity stress. *Molecules* **23**, (2018).
44. Eu, J. S. *et al.* Effects of γ -irradiation on the anti-allergic activity of alginate. *Food Sci Biotechnol* **17**, 1003–1009 (2008).
45. Kabir, I. I. *et al.* Alginate/Polymer-Based Materials for Fire Retardancy: Synthesis, Structure, Properties, and Applications. *Polymer Reviews* vol. 61 357–414 Preprint at <https://doi.org/10.1080/15583724.2020.1801726> (2021).
46. Warsinger, D. E. M. *et al.* The Combined Effect of Air Layers and Membrane Superhydrophobicity on Biofouling in Membrane Distillation. Reynolds, A. E. & Enquist, L. W. Biological interactions between herpesviruses and cyclooxygenase enzymes. *Reviews in Medical Virology* vol. 16 393–403 Preprint at <https://doi.org/10.1002/rmv.519> (2006).
47. Stokke, B. T. *et al.* Small-angle X-ray scattering and rheological characterization of alginate gels. 1. Ca-alginate gels. *Macromolecules* **33**, 1853–1863 (2000).
48. Bajpai, M., Shukla, P. & Bajpai, S. K. Ca(II)+Ba(II) ions crosslinked alginate gels prepared by a novel diffusion through dialysis tube (DTDT) approach and preliminary BSA release study. *Polym Degrad Stab* **134**, 22–29 (2016).
49. Rezvanian, M., Ahmad, N., Mohd Amin, M. C. I. & Ng, S. F. Optimization, characterization, and in vitro assessment of alginate-pectin ionic cross-linked hydrogel film for wound dressing applications. *Int J Biol Macromol* **97**, 131–140 (2017).
50. Cao, L., Lu, W., Mata, A., Nishinari, K. & Fang, Y. Egg-box model-based gelation of alginate and pectin: A review. *Carbohydrate Polymers* vol. 242 116389 Preprint at <https://doi.org/10.1016/j.carbpol.2020.116389> (2020).
51. Hernández-González, A. C., Téllez-Jurado, L. & Rodríguez-Lorenzo, L. M. Alginate hydrogels for bone tissue engineering, from injectables to bioprinting: A review. *Carbohydr Polym* **229**, 115514 (2020).
52. Liu, X. D. *et al.* Characterization of structure and diffusion behaviour of Ca-alginate beads prepared with external or internal calcium sources. *Journal of Microencapsulation* vol. 19 775–782 Preprint at <https://doi.org/10.1080/0265204021000022743> (2002).
53. Arriola, N. D. A. *et al.* Encapsulation of stevia rebaudiana Bertoni aqueous crude extracts by ionic gelation – Effects of alginate blends and gelling solutions on the polyphenolic profile. *Food Chem* **275**, 123–134 (2019).
54. McClements, D. J. Designing biopolymer microgels to encapsulate, protect and deliver bioactive components: Physicochemical aspects. *Adv Colloid Interface Sci* **240**, 31–59 (2017).
55. Spadari, C. de C., de Bastiani, F. W. M. da S., Lopes, L. B. & Ishida, K. Alginate nanoparticles as non-toxic delivery system for miltefosine in the treatment of candidiasis and cryptococcosis. *Int J Nanomedicine* **14**, 5187–5199 (2019).
56. Sun, Q., Zhang, Z., Zhang, R., Gao, R. & McClements, D. J. Development of Functional or Medical Foods for Oral Administration of Insulin for Diabetes Treatment: Gastroprotective Edible Microgels. *J Agric Food Chem* **66**, 4820–4826 (2018).
57. Sagdicoglu Celep, A. G., Demirkaya, A. & Solak, E. K. Antioxidant and anticancer activities of gallic acid loaded sodium alginate microspheres on colon cancer. *Current Applied Physics* **40**, 30–42 (2022).
58. Puguan, J. M. C., Yu, X. & Kim, H. Characterization of structure, physico-chemical properties and diffusion behavior of Ca-Alginate gel beads prepared by different gelation methods. *J Colloid Interface Sci* **432**, 109–116 (2014).
59. Strobel, S. A. *et al.* Industrially-Scalable Microencapsulation of Plant Beneficial Bacteria in Dry Cross-Linked Alginate Matrix. *Industrial Biotechnology* **14**, 138–147 (2018).
60. Strobel, S. A. *et al.* Stability of Fish Oil in Calcium Alginate Microcapsules Cross-Linked by In Situ Internal Gelation During Spray Drying. *Food Bioproc Tech* **13**, 275–287 (2020).
61. Javvaji, V., Baradwaj, A. G., Payne, G. F. & Raghavan, S. R. Light-activated ionic gelation of common biopolymers. *Langmuir* **27**, 12591–12596 (2011).
62. Ching, S. H., Bansal, N. & Bhandari, B. Alginate gel particles—A review of production techniques and physical properties. *Crit Rev Food Sci Nutr* **57**, 1133–1152 (2017).
63. Blandino, A., Macías, M. & Cantero, D. Formation of calcium alginate gel capsules: Influence of sodium alginate and CaCl₂ concentration on gelation kinetics. *J Biosci Bioeng* **88**, 686–689 (1999).
64. Bannikova, A., Evteev, A., Pankin, K., Evdokimov, I. & Kasapis, S. Microencapsulation of fish oil with alginate: In-vitro evaluation and controlled release. *LWT* **90**, 310–315 (2018).
65. Benavides, S., Cortés, P., Parada, J. & Franco, W. Development of alginate microspheres containing thyme essential oil using ionic gelation. *Food Chem* **204**, 77–83 (2016).
66. Gholamian, S., Nourani, M. & Bakhshi, N. Formation and characterization of calcium alginate hydrogel beads filled with cumin seeds essential oil. *Food Chem* **338**, 128143 (2021).
67. Hariyadi, D. M. & Islam, N. Current status of alginate in drug delivery. *Advances in Pharmacological and Pharmaceutical Sciences* vol. 2020 Preprint at <https://doi.org/10.1155/2020/8886095> (2020).
68. Dehkordi, S. S., Alemzadeh, I., Vaziri, A. S. & Vossoughi, A. Optimization of Alginate-Whey Protein Isolate Microcapsules for Survivability and Release Behavior of Probiotic Bacteria. *Appl Biochem Biotechnol* **190**, 182–196 (2020).
69. Praepanitchai, O.-A., Noomhorm, A. & Anal, A. K. Survival and Behavior of Encapsulated Probiotics (*Lactobacillus plantarum*) in Calcium-Alginate-Soy Protein Isolate-Based Hydrogel Beads in Different Processing Conditions (pH and Temperature) and in Pasteurized Mango Juice. (2019) doi:10.1155/2019/9768152.
70. Kurayama, F., Mohammed Bahadur, N., Furusawa, T., Sato, M. & Suzuki, N. Facile preparation of aminosilane-alginate hybrid beads for enzyme immobilization: Kinetics and equilibrium studies. *Int J Biol Macromol* **150**, 1203–1212 (2020).

72. Su, Y. *et al.* Encapsulation and release of egg white protein in alginate microgels: Impact of pH and thermal treatment. *Food Research International* **120**, 305–311 (2019).
73. Pedrali, D., Barbarito, S. & Lavelli, V. Encapsulation of grape seed phenolics from winemaking byproducts in hydrogel microbeads – Impact of food matrix and processing on the inhibitory activity towards α -glucosidase. *LWT* **133**, (2020).
74. Nikoo, A. M., Kadkhodae, R., Ghorani, B., Razzaq, H. & Tucker, N. Electrospray-assisted encapsulation of caffeine in alginate microhydrogels. *Int J Biol Macromol* **116**, 208–216 (2018).
75. Paulo, B. B., Ramos, F. de M. & Prata, A. S. An investigation of operational parameters of jet cutting method on the size of Ca-alginate beads. *J Food Process Eng* **40**, (2017).
76. Yin, Y. & Cadwallader, K. R. Spray-chilling encapsulation of 2-acetyl-1-pyrroline zinc chloride complex using hydrophobic materials: Feasibility and characterization of microcapsules. *Food Chem* **265**, 173–181 (2018).
77. Strasdat, B. & Bunjes, H. Incorporation of lipid nanoparticles into calcium alginate beads and characterization of the encapsulated particles by differential scanning calorimetry. *Food Hydrocoll* **30**, 567–575 (2013).
78. Oxley, J. D. *Coextrusion for food ingredients and nutraceutical encapsulation: principles and technology. Encapsulation Technologies and Delivery Systems for Food Ingredients and Nutraceuticals* (Elsevier Masson SAS., 2012). doi:10.1533/9780857095909.2.131.
79. Lucía, C., Marcela, F. & Ainhoa, L. Encapsulation of Almond Essential Oil by Co-Extrusion/Gelling Using Chitosan as Wall Material. *Journal of Encapsulation and Adsorption Sciences* **07**, 67–74 (2017).
80. Wang, W., Waterhouse, G. I. N. & Sun-Waterhouse, D. Co-extrusion encapsulation of canola oil with alginate: Effect of quercetin addition to oil core and pectin addition to alginate shell on oil stability. *Food Research International* **54**, 837–851 (2013).
81. Silva, M. P. *et al.* Comparison of extrusion and co-extrusion encapsulation techniques to protect *Lactobacillus acidophilus* LA3 in simulated gastrointestinal fluids. *LWT - Food Science and Technology* **89**, 392–399 (2018).
82. Hu, M., Zheng, G., Zhao, D. & Yu, W. Characterization of the structure and diffusion behavior of calcium alginate gel beads. *J Appl Polym Sci* **137**, 1–9 (2020).
83. Fernández Farrés, I. & Norton, I. T. Formation kinetics and rheology of alginate fluid gels produced by in-situ calcium release. *Food Hydrocoll* **40**, 76–84 (2014).
84. Jiao, W. *et al.* molecules Effects of Molecular Weight and Guluronic Acid/Mannuronic Acid Ratio on the Rheological Behavior and Stabilizing Property of Sodium Alginate. (2019) doi:10.3390/molecules24234374.
85. Harte, F. & Venegas, R. A model for viscosity reduction in polysaccharides subjected to high-pressure homogenization. *J Texture Stud* **41**, 49–61 (2010).
86. Braccini, I., Grasso, R. P. & Pérez, S. *Conformational and configurational features of acidic polysaccharides and their interactions with calcium ions: a molecular modeling investigation.* www.elsevier.nl/locate/carres (1999).
87. Leivvåg, I. T. *Strategies for Stabilising Calcium Alginate Gel Beads: Studies of Chitosan Oligomers, Alginate Molecular Weight and Concentration.* Norwegian University of Science and Technology (2017).
88. Yang, J., Steck, J. & Suo, Z. Gelation kinetics of alginate chains through covalent bonds. *Extreme Mech Lett* **40**, 100898 (2020).
89. Li, Z. Q., Hou, L. Da, Li, Z., Zheng, W. & Li, L. Study on shape optimization of calcium-alginate beads. in *Advanced Materials Research* vol. 648 125–130 (2013).
90. Li, J., Wu, Y., He, J. & Huang, Y. A new insight to the effect of calcium concentration on gelation process and physical properties of alginate films. *J Mater Sci* **51**, 5791–5801 (2016).
91. Fang, Y. *et al.* Multiple steps and critical behaviors of the binding of calcium to alginate. *Journal of Physical Chemistry B* **111**, 2456–2462 (2007).
92. Cuadros, T. R., Skurtys, O. & Aguilera, J. M. Mechanical properties of calcium alginate fibers produced with a microfluidic device. *Carbohydr Polym* **89**, 1198–1206 (2012).
93. Evageliou, V., Richardson, R. K. & Morris, E. R. *Effect of pH, sugar type and thermal annealing on high-methoxy pectin gels.* www.elsevier.com/locate/carbpol.
94. Park, D. *et al.* PH-Triggered Silk Fibroin/Alginate Structures Fabricated in Aqueous Two-Phase System. *ACS Biomater Sci Eng* **5**, 5897–5905 (2019).
95. Sonogo, J. M., Santagapita, P. R., Perullini, M. & Jobbágy, M. Ca(II) and Ce(III) homogeneous alginate hydrogels from the parent alginic acid precursor: A structural study. *Dalton Transactions* **45**, 10050–10057 (2016).
96. Zazzali, I., Aguirre Calvo, T. R., Pizones Ruiz-Henestrosa, V. M., Santagapita, P. R. & Perullini, M. Effects of pH, extrusion tip size and storage protocol on the structural properties of Ca(II)-alginate beads. *Carbohydr Polym* **206**, 749–756 (2019).
97. Augst, A. D., Kong, H. J. & Mooney, D. J. Alginate hydrogels as biomaterials. *Macromol Biosci* **6**, 623–633 (2006).
98. Jeong, H. S. *et al.* Hydrogel Microcapsules with a Thin Oil Layer: Smart Triggered Release via Diverse Stimuli. *Adv Funct Mater* **31**, 1–11 (2021).
99. Moe, S. T., Draget, K. I., Skj-k-Br-k, G. & Smidsrod, O. *Temperature dependence of the elastic modulus of alginate gels.* *Carbohydrate Polymers* vol. 19 (1992).
100. Topuz, F., Henke, A., Richtering, W. & Groll, J. Magnesium ions and alginate do form hydrogels: A rheological study. *Soft Matter* **8**, 4877–4881 (2012).
101. Chuang, J.-J. *et al.* Effects of pH on the Shape of Alginate Particles and Its Release Behavior. (2017) doi:10.1155/2017/3902704.
102. Jeong, C., Kim, S., Lee, C., Cho, S. & Kim, S.-B. Changes in the Physical Properties of Calcium Alginate Gel Beads under a Wide Range of Gelation Temperature Conditions. *Foods* **9**, (2020).
103. Leo, W. J., Mcloughlin, A. J. & Malone, D. M. *Effects of Sterilization Treatments on Some Properties of Alginate Solutions and Gels.* *Biotechnol. Prog* vol. 6 <https://pubs.acs.org/sharingguidelines> (1990).
104. Oates, C. G. & Ledward, D. A. Studies on the effect of heat on alginates. *Top Catal* **4**, 215–220 (1990).
105. Cerciello, A. *et al.* Synergistic effect of divalent cations in improving technological properties of cross-linked alginate beads. *Int J Biol Macromol* **101**, 100–106 (2017).
106. Gu, Y. *et al.* The effects of cross-linking cations on the electrochemical behavior of silicon anodes with alginate binder. *Electrochim Acta* **269**, 405–414 (2018).
107. Sanchez-Ballester, N. M., Soulaïrol, I., Bataille, B. & Sharkawi, T. Flexible heteroionic calcium-magnesium alginate beads for controlled drug release. *Carbohydr Polym* **207**, 224–229 (2019).
108. Vu, H. C. *et al.* Magnetite graphene oxide encapsulated in alginate beads for enhanced adsorption of Cr(VI) and As(V) from aqueous solutions: Role of crosslinking metal cations in pH control. *Chemical Engineering Journal* **307**, 220–229 (2017).

109. van Leusden, P. *et al.* Permeation of probe molecules into alginate microbeads: Effect of salt and processing. *Food Hydrocoll* **73**, 255–261 (2017).
110. Poncelet, D. *et al.* *Applied AFicrobiology Bioteehnology Production of alginate beads by emulsification/internal gelation. I. Methodology. Appl Microbiol Biotechnol* vol. 38 (1992).
111. Guo, J., Giusti, M. M. & Kaletunç, G. Encapsulation of purple corn and blueberry extracts in alginate-pectin hydrogel particles: Impact of processing and storage parameters on encapsulation efficiency. *Food Research International* **107**, 414–422 (2018).
112. Zhang, B. *et al.* Modulation of calcium-induced gelation of pectin by oligoguluronate as compared to alginate. *Food Research International* **116**, 232–240 (2019).
113. de Avelar, M. H. M. & Efraim, P. Alginate/pectin cold-set gelation as a potential sustainable method for jelly candy production. *LWT* **123**, (2020).
114. Oh, G. W., Nam, S. Y., Heo, S. J., Kang, D. H. & Jung, W. K. Characterization of ionic cross-linked composite foams with different blend ratios of alginate/pectin on the synergistic effects for wound dressing application. *Int J Biol Macromol* **156**, 1565–1573 (2020).
115. Vaziri, A. S., Alemzadeh, I., Vossoughi, M. & Khorasani, A. C. Co-microencapsulation of *Lactobacillus plantarum* and DHA fatty acid in alginate-pectin-gelatin biocomposites. *Carbohydr Polym* **199**, 266–275 (2018).
116. Mousavi, S. M. R., Rafe, A. & Yeganehzad, S. Textural, mechanical, and microstructural properties of restructured pimiento alginate-guar gels. *J Texture Stud* **50**, 155–164 (2019).
117. Rastegar, S. & Atrash, S. Effect of alginate coating incorporated with Spirulina, Aloe vera and guar gum on physicochemical, respiration rate and color changes of mango fruits during cold storage. *Journal of Food Measurement and Characterization* **15**, 265–275 (2021).
118. Mousavi, S. M. R., Rafe, A. & Yeganehzad, S. Structure-rheology relationships of composite gels: Alginate and Basil seed gum/guar gum. *Carbohydr Polym* **232**, 115809 (2020).
119. Aguirre Calvo, T. R., Santagapita, P. R. & Perullini, M. Functional and structural effects of hydrocolloids on Ca(II)-alginate beads containing bioactive compounds extracted from beetroot. *LWT* **111**, 520–526 (2019).
120. Aguirre-Calvo, T. R., Molino, S., Perullini, M., Rufián-Henares, J. Á. & Santagapita, P. R. Effect of in vitro digestion-fermentation of Ca(II)-alginate beads containing sugar and biopolymers over global antioxidant response and short chain fatty acids production. *Food Chem* **333**, (2020).
121. Tsai, F. H., Kitamura, Y. & Kokawa, M. Effect of gum arabic-modified alginate on physicochemical properties, release kinetics, and storage stability of liquid-core hydrogel beads. *Carbohydr Polym* **174**, 1069–1077 (2017).
122. Sabet, S. *et al.* The interactions between the two negatively charged polysaccharides: Gum Arabic and alginate. *Food Hydrocoll* **112**, 106343 (2021).
123. Nayak, A. K., Das, B. & Maji, R. Calcium alginate/gum arabic beads containing glibenclamide: Development and in vitro characterization. *Int J Biol Macromol* **51**, 1070–1078 (2012).
124. Hamed, H., Kargozari, M., Shotorbani, P. M., Mogadam, N. B. & Fahimdanesh, M. A novel bioactive edible coating based on sodium alginate and galbanum gum incorporated with essential oil of *Ziziphora persica*: The antioxidant and antimicrobial activity, and application in food model. *Food Hydrocoll* **72**, 35–46 (2017).
125. Kulig, D., Zimoch-Korzycza, A., Jarmoluk, A. & Marycz, K. Study on Alginate-Chitosan Complex Formed with Different Polymers Ratio. doi:10.3390/polym8050167.
126. Afzal, S., Maswal, M. & Dar, A. A. Rheological behavior of pH responsive composite hydrogels of chitosan and alginate: Characterization and its use in encapsulation of citral. *Colloids Surf B Biointerfaces* **169**, 99–106 (2018).
127. Fernandes, L., Pereira, E. L., do Céu Fidalgo, M., Gomes, A. & Ramalhosa, E. Physicochemical properties and microbial control of chestnuts (*Castanea sativa*) coated with whey protein isolate, chitosan and alginate during storage. *Sci Hortic* **263**, 109105 (2020).
128. Raeisi, M. *et al.* Effects of Sodium Alginate and Chitosan Coating Combined with Three Different Essential Oils on Microbial and Chemical Attributes of Rainbow Trout Fillets. *Journal of Aquatic Food Product Technology* **29**, 253–263 (2020).
129. Taqieddin, E. & Amiji, M. Enzyme immobilization in novel alginate-chitosan core-shell microcapsules. *Biomaterials* **25**, 1937–1945 (2004).
130. Romo, I., Abugoch, L. & Tapia, C. Soluble complexes between chenopodins and alginate/chitosan: Intermolecular interactions and structural-physicochemical properties. *Carbohydr Polym* **227**, 115334 (2020).
131. De Prisco, A., Maresca, D., Ongeng, D. & Mauriello, G. Microencapsulation by vibrating technology of the probiotic strain *Lactobacillus reuteri* DSM 17938 to enhance its survival in foods and in gastrointestinal environment. *LWT - Food Science and Technology* **61**, 452–462 (2015).
132. Atencio, S., Maestro, A., Santamaría, E., Gutiérrez, J. M. & González, C. Encapsulation of ginger oil in alginate-based shell materials. *Food Biosci* **37**, (2020).
133. Hamed, S. F. *et al.* Edible alginate/chitosan-based nanocomposite microspheres as delivery vehicles of omega-3 rich oils. *Carbohydr Polym* **239**, 116201 (2020).
134. Wong, T. W., Chan, L. W., Kho, S. Bin & Sia Heng, P. W. Design of controlled-release solid dosage forms of alginate and chitosan using microwave. *Journal of Controlled Release* **84**, 99–114 (2002).
135. Necas, J. & Bartosikova, L. Carrageenan: a review. *Vet Med (Praha)* **58**, 187–205 (2013).
136. Tavassoli-Kafrani, E., Shekarchizadeh, H. & Masoudpour-Behabadi, M. Development of edible films and coatings from alginates and carrageenans. *Carbohydr Polym* **137**, 360–374 (2016).
137. Li, L. *et al.* Effects of concentration variation on the physical properties of alginate-based substrates and cell behavior in culture. *Int J Biol Macromol* **128**, 184–195 (2019).
138. Mohamadnia, Z., Zohuriaan-Mehr, M. J., Kabiri, K., Jamshidi, A. & Mobedi, H. Ionically cross-linked carrageenan-alginate hydrogel beads. *J Biomater Sci Polym Ed* **19**, 47–59 (2008).
139. Lim, H. P., Ooi, C. W., Tey, B. T. & Chan, E. S. Controlled delivery of oral insulin aspart using pH-responsive alginate/ κ -carrageenan composite hydrogel beads. *React Funct Polym* **120**, 20–29 (2017).
140. Gu, L. *et al.* Formulation of alginate/carrageenan microgels to encapsulate, protect and release immunoglobulins: Egg Yolk IgY. *Food Hydrocoll* **112**, 106349 (2021).
141. López Córdoba, A., Deladino, L. & Martino, M. Effect of starch filler on calcium-alginate hydrogels loaded with yerba mate antioxidants. *Carbohydr Polym* **95**, 315–323 (2013).
142. da Silva Fernandes, R., Tanaka, F. N., de Moura, M. R. & Aouada, F. A. Development of alginate/starch-based hydrogels crosslinked with different ions: Hydrophilic, kinetic and spectroscopic properties. *Mater Today Commun* **21**, 100636 (2019).

143. Okunlola, A. & Adewusi, S. A. Development of theophylline microbeads using pregelatinized breadfruit starch (*artocarpus altilis*) as a novel co-polymer for controlled release. *Adv Pharm Bull* **9**, 93–101 (2019).
144. Feltre, G., Almeida, F. S., Sato, A. C. K., Dacanal, G. C. & Hubinger, M. D. Alginate and corn starch mixed gels: Effect of gelatinization and amylose content on the properties and in vitro digestibility. *Food Research International* **132**, (2020).
145. Hassan, H. *et al.* Novel design for alginate/resistant starch microcapsules controlling nisin release. *Int J Biol Macromol* **153**, 1186–1192 (2020).
146. Feltre, G. *et al.* Encapsulation of wheat germ oil in alginate-gelatinized corn starch beads: Physicochemical properties and tocopherols' stability. *J Food Sci* **85**, 2124–2133 (2020).
147. Jain, S., Winuprasith, T. & Suphantharika, M. Encapsulation of lycopene in emulsions and hydrogel beads using dual modified rice starch: Characterization, stability analysis and release behaviour during in-vitro digestion. *Food Hydrocoll* **104**, (2020).
148. Guedes Silva, K. C., Feltre, G., Dupas Hubinger, M. & Kawazoe Sato, A. C. Protection and targeted delivery of β -carotene by starch-alginate-gelatin emulsion-filled hydrogels. *J Food Eng* **290**, 110205 (2021).
149. Rahmani, V. & Sheardown, H. Protein-alginate complexes as pH-/ion-sensitive carriers of proteins. *Int J Pharm* **535**, 452–461 (2018).
150. Liu, H. *et al.* Improved survival of *Lactobacillus zeae* LB1 in a spray dried alginate-protein matrix. *Food Hydrocoll* **78**, 100–108 (2018).
151. Rajam, R., Karthik, P., Parthasarathi, S., Joseph, G. S. & Anandharamakrishnan, C. Effect of whey protein - alginate wall systems on survival of microencapsulated *Lactobacillus plantarum* in simulated gastrointestinal conditions. *J Funct Foods* **4**, 891–898 (2012).
152. Chakravartula, S. S. N. *et al.* Characterization of composite edible films based on pectin/alginate/whey protein concentrate. *Materials* **12**, (2019).
153. De Matos, E. F., Scopel, B. S. & Dettmer, A. Citronella essential oil microencapsulation by complex coacervation with leather waste gelatin and sodium alginate. *J Environ Chem Eng* **6**, 1989–1994 (2018).
154. Heckert Bastos, L. P., Vicente, J., Corrêa dos Santos, C. H., Geraldo de Carvalho, M. & Garcia-Rojas, E. E. Encapsulation of black pepper (*Piper nigrum* L.) essential oil with gelatin and sodium alginate by complex coacervation. *Food Hydrocoll* **102**, (2020).
155. Li, Y. *et al.* Development of alginate hydrogel/gum Arabic/gelatin based composite capsules and their application as oral delivery carriers for antioxidant. *Int J Biol Macromol* **132**, 1090–1097 (2019).
156. Lemos, Y. P., Mariano Marfil, P. H. & Nicoletti, V. R. Particle size characteristics of buriti oil microcapsules produced by gelatin-sodium alginate complex coacervation: Effect of stirring speed. *Int J Food Prop* **20**, 1438–1447 (2017).
157. Lopes, S., Bueno, L., De Aguiar Júnior, F. & Finkler, C. L. L. Preparation and characterization of alginate and gelatin microcapsules containing *Lactobacillus Rhamnosus*. *An Acad Bras Cienc* **89**, 1601–1613 (2017).
158. Belscak-Cvitanić, A. *et al.* Improving the controlled delivery formulations of caffeine in alginate hydrogel beads combined with pectin, carrageenan, chitosan and psyllium. *Food Chem* **167**, 378–386 (2015).
159. Rajmohan, D. & Bellmer, D. Characterization of Spirulina-Alginate Beads Formed Using Ionic Gelation. *Int J Food Sci* (2019) doi:10.1155/2019/7101279.
160. Wu, Y., Weller, C. L., Hamouz, F., Cuppett, S. & Schnepf, M. *Moisture Loss and Lipid Oxidation for Precooked Ground-Beef Patties Packaged in Edible Starch-Alginate-Based Composite Films*. 486 *JOURNAL OF FOOD SCIENCE* vol. 66 (2001).
161. Oliveira Filho, J. G. de *et al.* Active food packaging: Alginate films with cottonseed protein hydrolysates. *Food Hydrocolloids* vol. 92 267–275 Preprint at <https://doi.org/10.1016/j.foodhyd.2019.01.052> (2019).
162. Fang, Z. & Bhandari, B. *Spray drying, freeze drying and related processes for food ingredient and nutraceutical encapsulation. Encapsulation Technologies and Delivery Systems for Food Ingredients and Nutraceuticals* (Elsevier Masson SAS., 2012). doi:10.1533/9780857095909.2.73.
163. Fang, Z. & Bhandari, B. Encapsulation of polyphenols - A review. *Trends Food Sci Technol* **21**, 510–523 (2010).
164. Rodríguez, J., Martín, M. J., Ruiz, M. A. & Clares, B. Current encapsulation strategies for bioactive oils: From alimentary to pharmaceutical perspectives. *Food Research International* **83**, 41–59 (2016).
165. Sun, X., Cameron, R. G. & Bai, J. Effect of spray-drying temperature on physicochemical, antioxidant and antimicrobial properties of pectin/sodium alginate microencapsulated carvacrol. *Food Hydrocoll* **100**, (2020).
166. Jeoh *et al.* How alginate properties influence in situ internal gelation in Cross-linked Alginate Microcapsules (CLAMs) formed by spray drying. *ChemRxiv. Cambridge: Cambridge Open Engage* (2020) doi:10.26434/chemrxiv.12611057.v1.
167. Oxley, J. D. *Spray-cooling and spray-chilling for food ingredient and nutraceutical encapsulation. Encapsulation Technologies and Delivery Systems for Food Ingredients and Nutraceuticals* (Elsevier Masson SAS., 2012). doi:10.1533/9780857095909.2.110.
168. Chalella Mazzocato, M., Thomazini, M. & Favaro-Trindade, C. S. Improving stability of vitamin B12 (Cyanocobalamin) using microencapsulation by spray chilling technique. *Food Research International* **126**, (2019).
169. Dong, Q. Y. *et al.* Alginate-based and protein-based materials for probiotics encapsulation: A review. *International Journal of Food Science and Technology* vol. 48 1339–1351 Preprint at <https://doi.org/10.1111/ijfs.12078> (2013).
170. Thies, C. *Microencapsulation methods based on biopolymer phase separation and gelation phenomena in aqueous media. Encapsulation Technologies and Delivery Systems for Food Ingredients and Nutraceuticals* (Elsevier Masson SAS., 2012). doi:10.1533/9780857095909.2.177.
171. Gorji, E. G. *et al.* Complex Coacervation of Milk Proteins with Sodium Alginate. *J Agric Food Chem* **66**, 3210–3220 (2018).
172. Devi, N., Hazarika, D., Deka, C. & Kakati, D. K. Study of complex coacervation of gelatin a and sodium alginate for microencapsulation of olive oil. *Journal of Macromolecular Science, Part A: Pure and Applied Chemistry* **49**, 936–945 (2012).
173. Gouin, S. Microencapsulation: Industrial appraisal of existing technologies and trends. *Trends Food Sci Technol* **15**, 330–347 (2004).
174. Liliansa, S. C. & Vladimir, V. C. Probiotic encapsulation. *Afr J Microbiol Res* **7**, 4743–4753 (2013).
175. Bouquerand, P.-E., Dardelle, G., Erni, P. & Normand, V. *An industry perspective on the advantages and disadvantages of different flavor delivery systems. Encapsulation Technologies and Delivery Systems for Food Ingredients and Nutraceuticals* (Elsevier Masson SAS., 2012). doi:10.1533/9780857095909.4.453.
176. Ozkan, G., Franco, P., De Marco, I., Xiao, J. & Capanoglu, E. A review of microencapsulation methods for food antioxidants: Principles, advantages, drawbacks and applications. *Food Chem* **272**, 494–506 (2019).
177. Saravanan, M. & Rao, K. P. Pectin-gelatin and alginate-gelatin complex coacervation for controlled drug delivery: Influence of anionic polysaccharides and drugs being encapsulated on physicochemical properties of microcapsules. *Carbohydr Polym* **80**, 808–816 (2010).
178. Bangham, A. D. & Horne, R. W. Action of saponin on biological cell membranes. *Nature International Journal of Science* **196**, 1048–1050 (1962).
179. Green, B. K. & Schleicher, L. Microcapsules Containing Oil, U.S. Patent 2800457. (1957).

180. Cairns, W. Apparatus for sugar coating confectionery, pilsn etc. (1985).
181. Bangham, A. D. & Horne, R. W. Negative staining of phospholipids and their structural modification by surface-active agents as observed in the electron microscope. *J Mol Biol* **8**, 660–668 (1964).
182. Lim, F. & Richard, D. Process for producing controlled porosity microcapsules. (1982).
183. Sonawane, S. H., Bhanvase, B. A., Sivakumar, M. & Potdar, S. B. *Current overview of encapsulation. Encapsulation of Active Molecules and Their Delivery System* (INC, 2020). doi:10.1016/b978-0-12-819363-1.00001-6.
184. Acharya, S., Jakeer, S., Shilpa, P. & Andhale, S. Review: Flavor encapsulation by spray drying technique. *Int J Chem Stud* **9**, 1836–1840 (2021).
185. Potdar, S. B., Landge, V. K., Barkade, S. S., Potoroko, I. & Sonawane, S. H. *Flavor encapsulation and release studies in food. Encapsulation of Active Molecules and Their Delivery System* (INC, 2020). doi:10.1016/b978-0-12-819363-1.00016-8.
186. Chiaoprakobkij, N., Suwanmajo, T., Sanchavanakit, N. & Phisalaphong, M. molecules Curcumin-Loaded Bacterial Cellulose/Alginate/Gelatin as A Multifunctional Biopolymer Composite Film. doi:10.3390/molecules25173800.
187. Laha, B. & Maiti, S. Design of Core-Shell Stearyl Pullulan Nanostructures for Drug Delivery. *Mater Today Proc* **11**, 620–627 (2019).
188. Feng, L., Zhou, Y., Ashaolu, T. J., Ye, F. & Zhao, G. Physicochemical and rheological characterization of pectin-rich fraction from blueberry (*Vaccinium ashei*) wine pomace. *Int J Biol Macromol* **128**, 629–637 (2019).
189. Bae, E. K. & Lee, S. J. Microencapsulation of avocado oil by spray drying using whey protein and maltodextrin. *J Microencapsul* **25**, 549–560 (2008).
190. Costa, E. M. *et al.* Textile dyes loaded chitosan nanoparticles: Characterization, biocompatibility and staining capacity. *Carbohydr Polym* **251**, 117120 (2021).
191. Matos, J. C., Pereira, L. C. J., Waerenborgh, J. C. & Gonçalves, M. C. *Encapsulation of active molecules in pharmaceutical sector: the role of ceramic nanocarriers. Encapsulation of Active Molecules and Their Delivery System* (INC, 2020). doi:10.1016/b978-0-12-819363-1.00004-1.
192. Mejías, F. J. R. *et al.* One-step encapsulation of ortho-disulfides in functionalized zinc MOF. Enabling metal–organic frameworks in agriculture. *ACS Appl Mater Interfaces* **13**, 7997–8005 (2021).
193. Martínez-Cano, B. *et al.* Review and Perspectives of the Use of Alginate as a Polymer Matrix for Microorganisms Applied in Agro-Industry. *Molecules* vol. 27 Preprint at <https://doi.org/10.3390/molecules27134248> (2022).
194. Łętocha, A., Miastkowska, M. & Sikora, E. Preparation and Characteristics of Alginate Microparticles for Food, Pharmaceutical and Cosmetic Applications. *Polymers (Basel)* **14**, (2022).
195. Rashedy, S. H., Abd El Hafez, M. S. M., Dar, M. A., Cotas, J. & Pereira, L. Evaluation and characterization of alginate extracted from brown seaweed collected in the red sea. *Applied Sciences (Switzerland)* **11**, (2021).
196. Zhang, H., Cheng, J. & Ao, Q. Preparation of alginate-based biomaterials and their applications in biomedicine. *Marine Drugs* vol. 19 Preprint at <https://doi.org/10.3390/md19050264> (2021).
197. Banks, S. R., Enck, K., Wright, M., Opara, E. C. & Welker, M. E. Chemical Modification of Alginate for Controlled Oral Drug Delivery. *J Agric Food Chem* **67**, 10481–10488 (2019).
198. Wei, Q. *et al.* Modification, 3D printing process and application of sodium alginate based hydrogels in soft tissue engineering: A review. *Int J Biol Macromol* **232**, 123450 (2023).
199. Zaeim, D. *et al.* Microencapsulation of probiotics in multi-polysaccharide microcapsules by electro-hydrodynamic atomization and incorporation into ice-cream formulation. *Food Structure* **25**, 100147 (2020).
200. Shahabivand, S., Mortazavi, S. S., Mahdavinia, G. R. & Darvishi, F. Phenol biodegradation by immobilized *Rhodococcus qingshengii* isolated from coking effluent on Na-alginate and magnetic chitosan-alginate nanocomposite. *J Environ Manage* **307**, (2022).
201. How, Y. H., Hubert, C. & Pui, L. P. Encapsulation of probiotic strain *Lactobacillus rhamnosus* GG with black bean extract in alginate-pectin microcapsules. *Malays J Microbiol* **17**, 190–199 (2021).
202. Gouin, S. Microencapsulation: Industrial appraisal of existing technologies and trends. in *Trends in Food Science and Technology* vol. 15 330–347 (2004).
203. Li, M. *et al.* Composition design and medical application of liposomes. *Eur J Med Chem* **164**, 640–653 (2019).
204. Fangmeier, M., Lehn, D. N., Maciel, M. J. & Volken de Souza, C. F. Encapsulation of Bioactive Ingredients by Extrusion with Vibrating Technology: Advantages and Challenges. *Food Bioproc Tech* **12**, 1472–1486 (2019).
205. Ching, S. H., Bansal, N. & Bhandari, B. Alginate gel particles—A review of production techniques and physical properties. *Crit Rev Food Sci Nutr* **57**, 1133–1152 (2017).
206. Doméjean, Hugo. Formation de capsules d'hydrogel à coeur aqueux par fragmentation d'un jet composé de fluides complexes. (Université Pierre et Marie Curie - Paris VI., 2014).
207. Yildirim, O. E., Xu, Q. & Basaran, O. A. Analysis of the drop weight method. *Physics of Fluids* **17**, 1–13 (2005).
208. Rolland, L. Propriétés physico-chimiques de capsules d'hydrogel à cœur liquide. (Université Pierre et Marie Curie - Paris VI, 2013).
209. Berthier, J. *The Physics of Droplets. Micro-Drops and Digital Microfluidics* (2013). doi:10.1016/b978-1-4557-2550-2.00003-1.
210. Bremond, N., Santanach-Carreras, E., Chu, L. Y. & Bibette, J. Formation of liquid-core capsules having a thin hydrogel membrane: Liquid pearls. *Soft Matter* **6**, 2484–2488 (2010).
211. Pereda, M., Poncelet, D. & Renard, D. Characterization of Core-Shell Alginate Capsules. *Food Biophys* **14**, 467–478 (2019).
212. Saqib, M. N., Ahammed, S., Liu, F. & Zhong, F. Customization of liquid-core sodium alginate beads by molecular engineering. *Carbohydr Polym* **284**, (2022).
213. Jin, Y., Zhao, D. & Huang, Y. Fabrication of double-layered alginate capsules using coaxial nozzle. *J Micro Nanomanuf* **5**, 1–9 (2017).
214. Farahmand, A., Emadzadeh, B., Ghorani, B. & Poncelet, D. Droplet-based millifluidic technique for encapsulation of cinnamon essential oil: Optimization of the process and physicochemical characterization. *Food Hydrocoll* **129**, (2022).
215. Teo, A. J. T., Malekpour-Galogahi, F., Sreejith, K. R., Takei, T. & Nguyen, N. T. Surfactant-free, UV-curable core-shell microcapsules in a hydrophilic PDMS microfluidic device. *AIP Adv* **10**, (2020).
216. Dormer, N. H., Berkland, C. J. & Singh, M. *Monodispersed Microencapsulation Technology. Microencapsulation in the Food Industry* (Elsevier Inc., 2014). doi:10.1016/b978-0-12-404568-2.00011-x.
217. Mitchell, B. R., Klewicki, J. C., Korkolis, Y. P. & Kinsey, B. L. Normal impact force of Rayleigh jets. *Phys Rev Fluids* **4**, 1–23 (2019).
218. Whelehan, M. & Marison, I. W. Microencapsulation using vibrating technology. *J Microencapsul* **28**, 669–688 (2011).
219. Heinzen, C., Berger, A., & Marison, I. Use of Vibration Technology for Jet Break-Up for Encapsulation of Cells and Liquids. *Fundamentals of cell immobilisation biotechnologisation biotechnology* 257–275 (2004).

220. Doméjean, H. *et al.* Controlled production of sub-millimeter liquid core hydrogel capsules for parallelized 3D cell culture. *Lab Chip* **17**, 110–119 (2017).
221. Clanet, C. & Lasheras, J. C. Transition from dripping to jetting. *J Fluid Mech* **383**, 307–326 (1999).
222. Hu, L., Fang, Y., She, L., Su, R. & Fu, X. Dripping–jetting transition of liquid stream from plate-type micro-orifice affected by wetting and dewetting. *Exp Therm Fluid Sci* **122**, 110302 (2021).
223. Rayleigh, Lord. On the instability of jets. *Proceedings of the London Mathematical Society* **s1-10**, 4–13 (1878).
224. Chew, S. C. & Nyam, K. L. Microencapsulation of kenaf seed oil by co-extrusion technology. *J Food Eng* **175**, 43–50 (2016).
225. Brandau, T. Preparation of monodisperse controlled release microcapsules. *Int J Pharm* **242**, 179–184 (2002).
226. Jaworek, A. A. & Sobczyk, A. T. Electro spraying route to nanotechnology : An overview. **66**, 197–219 (2008).
227. Desai, K. G. H. & Park, H. J. *Recent developments in microencapsulation of food ingredients*. *Drying Technology* vol. 23 (2005).
228. Jeyakumari, A., Zynudheen, A. & Parvathy, U. Microencapsulation of Bioactive Food Ingredients and Controlled Release - A Review. *MOJ Food Processing & Technology* **2**, (2016).
229. Ghayempour, S. & Mortazavi, S. M. Fabrication of micro-nanocapsules by a new electro spraying method using coaxial jets and examination of effective parameters on their production. *J Electrostat* **71**, 717–727 (2013).
230. Yang, Z., Peng, H., Wang, W. & Liu, T. Crystallization behavior of poly(ϵ -caprolactone)/layered double hydroxide nanocomposites. *J Appl Polym Sci* **116**, 2658–2667 (2010).
231. Jaworek, A. *Electrohydrodynamic microencapsulation technology*. *Encapsulations* (Elsevier Inc., 2016). doi:10.1016/b978-0-12-804307-3.00001-6.
232. Bocanegra, R. *et al.* Production of cocoa butter microcapsules using an electro spray process. *J Food Sci* **70**, e492–e497 (2005).
233. Jayaprakash, P., Maudhuit, A., Gaiani, C. & Desobry, S. Encapsulation of bioactive compounds using competitive emerging techniques: Electro spraying, nano spray drying, and electrostatic spray drying. *J Food Eng* **339**, (2023).
234. Nguyen, D. N., Clasen, C. & Van den Mooter, G. Pharmaceutical Applications of Electro spraying. *J Pharm Sci* **105**, 2601–2620 (2016).
235. Zhou, D., Jiang, B., Yang, R., Hou, X. & Zheng, C. One-step synthesis of monodispersed Pt nanoparticles anchored on 3D graphene foams and its application for electrocatalytic hydrogen evolution. *Chinese Chemical Letters* **31**, 1540–1544 (2020).
236. Fernandez de La Mora, J. & Loscertales, I. G. The current emitted by highly conducting Taylor cones. *J. Fluid Mech* **260**, 155–184 (1994).
237. Poncelet, D. & Tam, S. K. Microencapsulation technologies for a bioartificial endocrine pancreas. *Pancreas, The Bioartificial Therapies, Other Biohybrid* **661**, 37–50 (2009).
238. Uludag, H., Horvath, V., Black, J. P. & Sefton, M. V. Viability and Protein Secretion from Human Hepatoma (HepG2) Cells Encapsulated in 400-pm Polyacrylate Microcapsules by Submerged Nozzle-Liquid Jet Extrusion. *Biotechnol Bioeng* **44**, 119961204 (1994).
239. Ponrasu, T., Yang, R. F., Chou, T. H., Wu, J. J. & Cheng, Y. S. Core-Shell Encapsulation of Lipophilic Substance in Jelly Fig (*Ficus awkeotsang* Makino) Polysaccharides Using an Inexpensive Acrylic-Based Millifluidic Device. *Appl Biochem Biotechnol* **191**, 360–375 (2020).
240. Wu, F. *et al.* Monodisperse hybrid microcapsules with an ultrathin shell of submicron thickness for rapid enzyme reactions. *J Mater Chem B* **3**, 796–803 (2015).
241. Sun, H. *et al.* Monodisperse Alginate Microcapsules with Spatially Confined Bioactive Molecules via Microfluid-Generated W/W/O Emulsions. *ACS Appl Mater Interfaces* **11**, 37313–37321 (2019).
242. Huang, L., Wu, K., Zhang, R. & Ji, H. Fabrication of Multicore Milli- And Microcapsules for Controlling Hydrophobic Drugs Release Using a Facile Approach. *Ind Eng Chem Res* **58**, 17017–17026 (2019).
243. Zhao, C. *et al.* Dual-Core Prebiotic Microcapsule Encapsulating Probiotics for Metabolic Syndrome. *ACS Appl Mater Interfaces* **12**, 42586–42594 (2020).
244. Qu, Q. *et al.* Gas-shearing synthesis of core–shell multicompartmental microparticles as cell-like system for enzymatic cascade reaction. *Chemical Engineering Journal* **428**, 132607 (2022).
245. He, F. *et al.* Controllable Multicompartmental Capsules with Distinct Cores and Shells for Synergistic Release. *ACS Appl Mater Interfaces* **8**, 8743–8754 (2016).
246. How, Y. H., Lai, K. W., Pui, L. P. & In, L. L. A. Co-extrusion and extrusion microencapsulation: Effect on microencapsulation efficiency, survivability through gastrointestinal digestion and storage. *J Food Process Eng* **45**, 1–16 (2022).
247. Piazza, L. & Roversi, T. Preliminary study on microbeads production by co-extrusion technology. *Procedia Food Sci* **1**, 1374–1380 (2011).
248. Shinde, T., Sun-Waterhouse, D. & Brooks, J. Co-extrusion Encapsulation of Probiotic *Lactobacillus acidophilus* Alone or Together with Apple Skin Polyphenols: An Aqueous and Value-Added Delivery System Using Alginate. *Food Bioproc Tech* **7**, 1581–1596 (2014).
249. Cimino, C. *et al.* Essential oils: Pharmaceutical applications and encapsulation strategies into lipid-based delivery systems. *Pharmaceutics* **13**, 1–35 (2021).
250. Zobot, G. L. *et al.* Encapsulation of Bioactive Compounds for Food and Agricultural Applications. *Polymers (Basel)* **14**, (2022).
251. Vega-Vásquez, P., Mosier, N. S. & Irudayaraj, J. Nanoscale Drug Delivery Systems: From Medicine to Agriculture. *Frontiers in Bioengineering and Biotechnology* vol. 8 Preprint at <https://doi.org/10.3389/fbioe.2020.00079> (2020).
252. Chaudhary, Z. *et al.* Encapsulation and Controlled Release of Resveratrol Within Functionalized Mesoporous Silica Nanoparticles for Prostate Cancer Therapy. *Front Bioeng Biotechnol* **7**, (2019).
253. Ben Messaoud, G., Sánchez-González, L., Probst, L. & Desobry, S. Influence of internal composition on physicochemical properties of alginate aqueous-core capsules. *J Colloid Interface Sci* **469**, 120–128 (2016).
254. Brandau, T. Annular nozzle in laminar flow encapsulation processes. In *Microencapsulation in the Food Industry* 137–154 (2023). doi:10.1016/b978-0-12-821683-5.00020-0.
255. Ben Messaoud, G. *et al.* Physico-chemical properties of alginate/shellac aqueous-core capsules: Influence of membrane architecture on riboflavin release. *Carbohydr Polym* **144**, 428–437 (2016).
256. Bennacef, C., Desobry-Banon, S., Probst, L. & Desobry, S. Optimization of core-shell capsules properties (Olive oil/alginate) obtained by dripping coextrusion process. *LWT* **167**, 113879 (2022).
257. Martins, E., Poncelet, D., Rodrigues, R. C. & Renard, D. Oil encapsulation in core–shell alginate capsules by inverse gelation II: comparison between dripping techniques using W/O or O/W emulsions. *J Microencapsul* **34**, 522–534 (2017).
258. Wang, P. *et al.* Electro spraying Technique and Its Recent Application Advances for Biological Macromolecule Encapsulation of Food Bioactive Substances. *Food Reviews International* **38**, 566–588 (2022).
259. Cai, Y. *et al.* Encapsulated Microstructures of Beneficial Functional Lipids and Their Applications in Foods and Biomedicines. *J Agric Food Chem* **70**, 8165–8187 (2022).

260. Ma, S. *et al.* Development of encapsulation strategies towards the commercialization of perovskite solar cells. *Energy Environ Sci* **15**, 13–55 (2022).
261. Miletić, A., Pavlič, B., Ristić, I., Zeković, Z. & Pilić, B. Encapsulation of fatty oils into electrospun nanofibers for cosmetic products with antioxidant activity. *Applied Sciences (Switzerland)* **9**, (2019).
262. Belostozky, A., Bretler, S., Koltitz-Domb, M., Grinberg, I. & Margel, S. Solidification of oil liquids by encapsulation within porous hollow silica microspheres of narrow size distribution for pharmaceutical and cosmetic applications. *Materials Science and Engineering C* **97**, 760–767 (2019).
263. Lopez, M. D., Maudhuit, A., Pascual-Villalobos, M. J. & Poncet, D. Development of formulations to improve the controlled-release of linalool to be applied as an insecticide. *J Agric Food Chem* **60**, 1187–1192 (2012).
264. Jerobin, J., Sureshkumar, R. S., Anjali, C. H., Mukherjee, A. & Chandrasekaran, N. Biodegradable polymer based encapsulation of neem oil nanoemulsion for controlled release of Aza-A. *Carbohydr Polym* **90**, 1750–1756 (2012).
265. Chen, Q., Zhong, F., Wen, J., McGillivray, D. & Quek, S. Y. Properties and Stability of Spray-Dried and Freeze-Dried Microcapsules Co-Encapsulated with Fish Oil, Phytosterol Esters, and Limonene. *Drying Technology* **31**, 707–716 (2013).
266. Wang, P. *et al.* Electrospayed Soft Capsules of Millimeter Size for Specifically Delivering Fish Oil/Nutrients to the Stomach and Intestines. *ACS Appl Mater Interfaces* **12**, 6536–6545 (2020).
267. Sun-Waterhouse, D., Zhou, J., Miskelly, G. M., Wibisono, R. & Wadhwa, S. S. Stability of encapsulated olive oil in the presence of caffeic acid. *Food Chem* **126**, 1049–1056 (2011).
268. Waterhouse, G. I. N., Wang, W. & Sun-Waterhouse, D. Stability of canola oil encapsulated by co-extrusion technology: Effect of quercetin addition to alginate shell or oil core. *Food Chem* **142**, 27–38 (2014).
269. Dolça, C. *et al.* Microencapsulation of Rosemary Essential Oil by Co-Extrusion/Gelling Using Alginate as a Wall Material. *Journal of Encapsulation and Adsorption Sciences* **05**, 121–130 (2015).
270. Wu, Q., Zhang, T., Xue, Y., Xue, C. & Wang, Y. Preparation of alginate core-shell beads with different M/G ratios to improve the stability of fish oil. *LWT - Food Science and Technology* **80**, 304–310 (2017).
271. Bennacef, C. *et al.* Study and optimization of core-shell capsules produced by annular jet breaking coextrusion. *Colloids Surf A Physicochem Eng Asp* **629**, (2021).
272. Rodríguez-Dorado, R. *et al.* A novel method for the production of core-shell microparticles by inverse gelation optimized with artificial intelligent tools. *Int J Pharm* **538**, 97–104 (2018).
273. Mania, S., Tylingo, R. & Michalowska, A. The drop-in-drop encapsulation in chitosan and sodium alginate as a method of prolonging the quality of linseed oil. *Polymers (Basel)* **10**, (2018).
274. Jin, H. *et al.* Producing mixed-soy protein adsorption layers on alginate microgels to controlled-release β -carotene. *Food Research International* **164**, 112319 (2023).
275. Sun-Waterhouse, D., Penin-Peyta, L., Wadhwa, S. S. & Waterhouse, G. I. N. Storage Stability of Phenolic-Fortified Avocado Oil Encapsulated Using Different Polymer Formulations and Co-extrusion Technology. *Food Bioproc Tech* **5**, 3090–3102 (2012).
276. Goh, K. M., Low, S. S. & Nyam, K. L. The changes of chemical composition of microencapsulated roselle (*Hibiscus sabdariffa* L.) seed oil by co-extrusion during accelerated storage. *Int J Food Sci Technol* **56**, 6649–6655 (2021).
277. Chew, S. C. & Nyam, K. L. Oxidative Stability of Microencapsulated Kenaf Seed Oil Using Co-extrusion Technology. *JAOCs, Journal of the American Oil Chemists' Society* **93**, 607–615 (2016).
278. Hue, W. L. & Nyam, K. L. *Physicochemical properties of kenaf seed oil microcapsules before and after freeze drying and its storage stability. International Food Research Journal* vol. 25 (2018).
279. Sun-Waterhouse, D., Wang, W. & Waterhouse, G. I. N. Canola Oil Encapsulated by Alginate and Its Combinations with Starches of Low and High Amylose Content: Effect of Quercetin on Oil Stability. *Food Bioproc Tech* **7**, 2159–2177 (2014).
280. Chew, S. C., Tan, C. P., Long, K. & Nyam, K. L. In-vitro evaluation of kenaf seed oil in chitosan coated-high methoxyl pectin-alginate microcapsules. *Ind Crops Prod* **76**, 230–236 (2015).
281. Leong, M. H., Tan, C. P. & Nyam, K. L. Effects of Accelerated Storage on the Quality of Kenaf Seed Oil in Chitosan-Coated High Methoxyl Pectin-Alginate Microcapsules. *J Food Sci* **81**, C2367–C2372 (2016).
282. Shahidi, F. & Zhong, Y. Measurement of antioxidant activity. *J Funct Foods* **18**, 757–781 (2015).
283. Burgos-Díaz, C., Opazo-Navarrete, M., Soto-Añual, M., Leal-Calderón, F. & Bustamante, M. Food-grade Pickering emulsion as a novel astaxanthin encapsulation system for making powder-based products: Evaluation of astaxanthin stability during processing, storage, and its bioaccessibility. *Food Research International* **134**, (2020).
284. Solomando, J. C., Antequera, T. & Perez-Palacios, T. Evaluating the use of fish oil microcapsules as omega-3 vehicle in cooked and dry-cured sausages as affected by their processing, storage and cooking. *Meat Sci* **162**, (2020).
285. de Moura, S. C. S. R. *et al.* Stability of Hibiscus Extract Encapsulated by Ionic Gelation Incorporated in Yogurt. *Food Bioproc Tech* **12**, 1500–1515 (2019).
286. Ngamnikom, P. *et al.* Fabrication of core-shell structured macrocapsules by electro-coextrusion with agar-hydrocolloid mixtures for precooked food applications: textural and release characteristics. *Int J Food Sci Technol* **52**, 2538–2546 (2017).
287. Ilyas, R. A. *et al.* Nanocomposites for Various Advanced Applications. (2022).
288. Liu, R. & Mabury, S. A. Synthetic Phenolic Antioxidants: A Review of Environmental Occurrence, Fate, Human Exposure, and Toxicity. *Environ Sci Technol* **54**, 11706–11719 (2020).
289. Mukurumbira, A. R., Shellie, R. A., Keast, R., Palombo, E. A. & Jadhav, S. R. Encapsulation of essential oils and their application in antimicrobial active packaging. *Food Control* vol. 136 Preprint at <https://doi.org/10.1016/j.foodcont.2022.108883> (2022).
290. Yu, J. *et al.* Strategies for Taste Masking of Orally Dispersible Dosage Forms: Time, Concentration, and Perception. *Mol Pharm* **19**, 3007–3025 (2022).
291. Yee, W. L., Yee, C. L., Lin, N. K. & Phing, P. L. Microencapsulation of lactobacillus acidophilus NCFM incorporated with mannitol and its storage stability in mulberry tea. *Ciencia e Agrotecnologia* **43**, 64–75 (2019).
292. Śliżewska, K., Markowiak-Kopeć, P. & Śliżewska, W. The role of probiotics in cancer prevention. *Cancers (Basel)* **13**, 1–22 (2021).
293. Silva, M. P. *et al.* Microcapsules loaded with the probiotic *Lactobacillus paracasei* BGP-1 produced by co-extrusion technology using alginate/shellac as wall material: Characterization and evaluation of drying processes. *Food Research International* **89**, 582–590 (2016).
294. Champagne, C. P., Ross, R. P., Saarela, M., Hansen, K. F. & Charalampopoulos, D. Recommendations for the viability assessment of probiotics as concentrated cultures and in food matrices. *International Journal of Food Microbiology* vol. 149 185–193 Preprint at <https://doi.org/10.1016/j.ijfoodmicro.2011.07.005> (2011).

295. Sanders, M. E. How Do We Know When Something Called “ Probiotic ” Is Really a Probiotic ? A Guideline for Consumers and Health Care Professionals. *1*, 3–12 (2009).
296. Chean, S. X., Hoh, P. Y., How, Y. H., Nyam, K. L. & Pui, L. P. Microencapsulation of Lactiplantibacillus plantarum with inulin and evaluation of survival in simulated gastrointestinal conditions and roselle juice. *Brazilian Journal of Food Technology* **24**, 1–13 (2021).
297. Sarkar, S. Approaches for enhancing the viability of probiotics: a review. *British Food Journal* **112**, 329–349 (2010).
298. Reque, P. M. & Brandelli, A. Encapsulation of probiotics and nutraceuticals: Applications in functional food industry. *Trends Food Sci Technol* **114**, 1–10 (2021).
299. Lipan, L. *et al.* Spray drying and storage of probiotic-enriched almond milk: probiotic survival and physicochemical properties. *J Sci Food Agric* **100**, 3697–3708 (2020).
300. Pour, H. M., Marhamatizadeh, M. H. & Fattahi, H. Encapsulation of Different Types of Probiotic Bacteria within Conventional / Multilayer Emulsion and Its Effect on the Properties of Probiotic Yogurt. **2022**, (2022).
301. Ng, S. L., Lai, K. W., Nyam, K. L. & Pui, L. P. Microencapsulation of Lactobacillus plantarum 299v incorporated with oligofructose in chitosan coated-alginate beads and its storage stability in ambarella juice. *Malays J Microbiol* **15**, 408–418 (2019).
302. Jasińska, U. T., Skapska, S., Owczarek, L., Dekowska, A. & Lewińska, D. Immobilization of Bifidobacterium infantis Cells in Selected Hydrogels as a Method of Increasing Their Survival in Fermented Milkless Beverages. *J Food Qual* **2018**, 1–12 (2018).
303. Khangwal, I. & Shukla, P. Potential prebiotics and their transmission mechanisms: Recent approaches. *Journal of Food and Drug Analysis* vol. 27 649–656 Preprint at <https://doi.org/10.1016/j.jfda.2019.02.003> (2019).
304. Sredkova, P., Batsalova, T., Moten, D. & Dzhambazov, B. Prebiotics can change immunomodulatory properties of probiotics. *Central European Journal of Immunology* **45**, 248–255 (2021).
305. Siang, S. C., Wai, L. K., Lin, N. K. & Phing, P. L. Effect of added prebiotic (Isomalto-oligosaccharide) and coating of beads on the survival of microencapsulated lactobacillus rhamnosus gg. *Food Science and Technology (Brazil)* **39**, 601–609 (2019).
306. Kumar Yadav, M., Kumari, I., Singh, B., Kant Sharma, K. & Kumar Tiwari, S. Probiotics, prebiotics and synbiotics: Safe options for next-generation therapeutics. *Appl Microbiol Biotechnol* **106**, 505–521 (2022).
307. Shinde, T., Sun-Waterhouse, D. & Brooks, J. Co-extruded Encapsulation of Probiotic Lactobacillus acidophilus Alone or Together with Apple Skin Polyphenols: An Aqueous and Value-Added Delivery System Using Alginate. *Food Bioproc Tech* **7**, 1581–1596 (2014).
308. Kaur, R., Simnani, F. Z. & Singh, S. Enhancement of Probiotics for Functional Food. in *Recent Advances in Food Biotechnology* (eds. Kumar, A., Patruni, K. & Singh, V.) 97–137 (Springer Nature Singapore, 2022). doi:10.1007/978-981-16-8125-7_6.
309. Lai, K. W., How, Y. H. & Pui, L. P. Storage stability of microencapsulated Lactobacillus rhamnosus GG in hawthorn berry tea with flaxseed mucilage. *J Food Process Preserv* **44**, 0–3 (2020).
310. Lai, J. T., Lai, K. W., Zhu, L. Y., Nyam, K. L. & Pui, L. P. Microencapsulation of Lactobacillus plantarum 299v and its storage in kuini juice. *Malays J Microbiol* **16**, 235–244 (2020).
311. Yong, A. K. L., Lai, K. W., Ghazali, H. M., Chang, L. S. & Pui, L. P. Microencapsulation of bifidobacterium animalis subsp. Lactis BB-12 with mannitol. *Asia Pac J Mol Biol Biotechnol* **28**, 32–42 (2020).
312. Chan, L. Y. & Pui, L. P. Microencapsulation of Lactobacillus acidophilus 5 with isomalto-oligosaccharide. *Carpathian Journal of Food Science and Technology* **12**, 26–36 (2020).
313. Bouhleb, W., Kui, J., Bibette, J. & Bremond, N. Encapsulation of Cells in a Collagen Matrix Surrounded by an Alginate Hydrogel Shell for 3D Cell Culture. *ACS Biomater Sci Eng* (2021) doi:10.1021/acsbio.1c01486.
314. Gryshkov, O. *et al.* Coaxial alginate hydrogels: From self-assembled 3d cellular constructs to long-term storage. *Int J Mol Sci* **22**, 1–31 (2021).
315. He, F. *et al.* Controllable Fabrication of Composite Core-Shell Capsules at a Macroscale as Organoid Biocarriers. *ACS Appl Bio Mater* **4**, 1584–1596 (2021).
316. Cohen, P. J. R. *et al.* Engineering 3D micro-compartments for highly efficient and scale-independent expansion of human pluripotent stem cells in bioreactors. *Biomaterials* **295**, (2023).
317. Alessandri, K. *et al.* Cellular capsules as a tool for multicellular spheroid production and for investigating the mechanics of tumor progression in vitro. *Proc Natl Acad Sci U S A* **110**, 14843–14848 (2013).
318. Franssen, M. F. J. *et al.* Bioprinting of kidney in vitro models: Cells, biomaterials, and manufacturing techniques. *Essays Biochem* **65**, 587 (2021).
319. Nebel, S. *et al.* Alginate Core-Shell Capsules for 3D Cultivation of Adipose-Derived Mesenchymal Stem Cells. *Bioengineering* **9**, 1–15 (2022).
320. Windbergs, M., Zhao, Y., Heyman, J. & Weitz, D. A. Biodegradable core-shell carriers for simultaneous encapsulation of synergistic actives. *J Am Chem Soc* **135**, 7933–7937 (2013).
321. Whelehan, M., von Stockar, U. & Marison, I. W. Removal of pharmaceuticals from water: Using liquid-core microcapsules as a novel approach. *Water Res* **44**, 2314–2324 (2010).
322. Furusawa, T., Ebisawa, T., Toyoshima, A., Mori, Y. & Taniguchi, Y. Oleic acid esterification with methanol to methyl oleate under light irradiation using modified alginate capsules loaded with a solid acid catalyst. *Chemical Engineering Journal* **429**, 132524 (2022).
323. Kamali Moghaddam, M. & Mortazavi, S. M. Preparation, characterisation and thermal properties of calcium alginate/n-nonadecane microcapsules fabricated by electro-coextrusion for thermo-regulating textiles. *J Microencapsul* **32**, 737–744 (2015).
324. Mizielinska, M. & Lopusiewicz, L. Encapsulation and evaluation of probiotic bacteria survival in simulated gastrointestinal conditions. *Rom Biotechnol Lett* **23**, 13690–13696 (2018).
325. de Moura, S. C. S. R., Berling, C. L., Germer, S. P. M., Alvim, I. D. & Hubinger, M. D. Encapsulating anthocyanins from Hibiscus sabdariffa L. calyces by ionic gelation: Pigment stability during storage of microparticles. *Food Chem* **241**, 317–327 (2018).
326. Chew, S. C. *et al.* Encapsulation technologies: A tool for functional foods development. *International Journal of Innovative Technology and Exploring Engineering* **8**, 154–160 (2019).
327. Maherani, B., Arab-Tehrany, E., Mozafari, M. R., Gaiani, C. & Linder, M. *Liposomes: A Review of Manufacturing Techniques and Targeting Strategies*. *Current Nanoscience* vol. 7 (2011).
328. Phawaphuthanon, N., Behnam, S., Koo, S. Y., Pan, C. H. & Chung, D. Characterization of core-shell calcium-alginate macrocapsules fabricated by electro-coextrusion. *Int J Biol Macromol* **65**, 267–274 (2014).
329. Martins, E., Poncelet, D., Rodrigues, R. C. & Renard, D. Oil encapsulation techniques using alginate as encapsulating agent: applications and drawbacks. *J Microencapsul* **34**, 754–771 (2017).

330. Abang, S., Chan, E. S. & Poncelet, D. Effects of process variables on the encapsulation of oil in ca-alginate capsules using an inverse gelation technique. *J Microencapsul* **29**, 417–428 (2012).
331. Partovinia, A. & Vatankehah, E. Experimental investigation into size and sphericity of alginate micro-beads produced by electrospraying technique: Operational condition optimization. *Carbohydr Polym* **209**, 389–399 (2019).
332. Nde Bup, D., Abi, C. F., Tenin, D., Kapseu, C. & Tchiegang, C. Optimisation of the Cooking Process of Sheanut Kernels (*Vitellaria paradoxa* Gaertn.) Using the Doehlert Experimental Design. *Food Bioproc Tech* **5**, 108–117 (2012).
333. Niizawa, I., Espinaco, B. Y., Zorrilla, S. E. & Sihufe, G. A. Natural astaxanthin encapsulation: Use of response surface methodology for the design of alginate beads. *Int J Biol Macromol* **121**, 601–608 (2019).
334. Tsai, F. H., Kitamura, Y. & Kokawa, M. Liquid-core alginate hydrogel beads loaded with functional compounds of radish by-products by reverse spherification: Optimization by response surface methodology. *Int J Biol Macromol* **96**, 600–610 (2017).
335. Seth, D., Mishra, H. N. & Deka, S. C. Effect of microencapsulation using extrusion technique on viability of bacterial cells during spray drying of sweetened yoghurt. *Int J Biol Macromol* **103**, 802–807 (2017).
336. Strobel, S. A., Knowles, L., Nitin, N., Scher, H. B. & Jeoh, T. Comparative technoeconomic process analysis of industrial-scale microencapsulation of bioactives in cross-linked alginate. *J Food Eng* **266**, (2020).
337. Wang, W., Waterhouse, G. I. N. & Sun-Waterhouse, D. Co-extrusion encapsulation of canola oil with alginate: Effect of quercetin addition to oil core and pectin addition to alginate shell on oil stability. *Food Research International* **54**, 837–851 (2013).
338. Xu, X. Q., Shen, H., Xu, J. R., Xie, M. Q. & Li, X. J. The colloidal stability and core-shell structure of magnetite nanoparticles coated with alginate. *Appl Surf Sci* **253**, 2158–2164 (2006).
339. Ryu, S. *et al.* Biodegradable nanoparticles-loaded plga microcapsule for the enhanced encapsulation efficiency and controlled release of hydrophilic drug. *Int J Mol Sci* **22**, 1–11 (2021).
340. Baek, J. *et al.* Encapsulation and controlled release of vitamin C in modified cellulose nanocrystal/chitosan nanocapsules. *Curr Res Food Sci* **4**, 215–223 (2021).
341. Chaudhary, Z. *et al.* Encapsulation and Controlled Release of Resveratrol Within Functionalized Mesoporous Silica Nanoparticles for Prostate Cancer Therapy. *Front Bioeng Biotechnol* **7**, (2019).
342. Liu, H. *et al.* Microfluidic Assembly: An Innovative Tool for the Encapsulation, Protection, and Controlled Release of Nutraceuticals. *Journal of Agricultural and Food Chemistry* vol. 69 2936–2949 Preprint at <https://doi.org/10.1021/acs.jafc.0c05395> (2021).
343. Figueroa-Robles, A., Antunes-Ricardo, M. & Guajardo-Flores, D. Encapsulation of phenolic compounds with liposomal improvement in the cosmetic industry. *International Journal of Pharmaceutics* vol. 593 Preprint at <https://doi.org/10.1016/j.ijpharm.2020.120125> (2021).
344. Cherunova, I., Kornev, N., Lukyanova, E. & Varavka, V. Development and study of the structure and properties of a composite textile material with encapsulated heat-preserving components for heat-protective clothing. *Applied Sciences (Switzerland)* **11**, (2021).
345. Chaudhary, Z. *et al.* Encapsulation and Controlled Release of Resveratrol Within Functionalized Mesoporous Silica Nanoparticles for Prostate Cancer Therapy. *Front Bioeng Biotechnol* **7**, (2019).
346. Low, Y. L. & Pui, L. P. Optimization of mango-pineapple jelly sphere production by frozen reverse spherification using a full factorial design [pdf]. *Acta Sci Pol Technol Aliment* **19**, 207–218 (2020).
347. Bubin, S. F. A. *et al.* Characterization and stability of pitaya pearls from hydrocolloids by reverse spherification. *Int J Food Prop* **22**, 1353–1364 (2019).
348. Prabha, K. *et al.* Recent development, challenges, and prospects of extrusion technology. *Future Foods* **3**, 100019 (2021).
349. Rodriguez-Félix, F. *et al.* Preparation and Characterization of Quercetin-Loaded Zein Nanoparticles by Electrospraying and Study of In Vitro Bioavailability. *J Food Sci* **84**, 2883–2897 (2019).
350. Tapia-Hernández, J. A. *et al.* Gallic Acid-Loaded Zein Nanoparticles by Electrospraying Process. *J Food Sci* **84**, 818–831 (2019).
351. Ching, S. H., Bansal, N. & Bhandari, B. Alginate gel particles—A review of production techniques and physical properties. *Crit Rev Food Sci Nutr* **57**, 1133–1152 (2017).
352. Cai, Y. *et al.* Encapsulated Microstructures of Beneficial Functional Lipids and Their Applications in Foods and Biomedicines. *J Agric Food Chem* **70**, 8165–8187 (2022).
353. Nebel, S. *et al.* Alginate Core – Shell Capsules for 3D Cultivation of Adipose-Derived Mesenchymal Stem Cells. 1–15 (2022).
354. Truong, V., Nguyen, P. T. & Truong, V. T. The prediction model of nozzle height in liquid jet-drop method to produce Ca-alginate beads under microencapsulation process. *J Food Process Eng* **44**, (2021).
355. Rolland, L., Santanach-Carreras, E., Delmas, T., Bibette, J. & Bremond, N. Physicochemical properties of aqueous core hydrogel capsules. *Soft Matter* **10**, 9668–9674 (2014).
356. Mou, C. L. *et al.* Controllable preparation of monodisperse alginate microcapsules with oil cores. *J Colloid Interface Sci* **569**, 307–319 (2020).
357. Phawaphuthanon, N., Behnam, S., Koo, S. Y., Pan, C. H. & Chung, D. Characterization of core-shell calcium-alginate macrocapsules fabricated by electro-coextrusion. *Int J Biol Macromol* **65**, 267–274 (2014).
358. Cuadros, T. R., Skurtys, O. & Aguilera, J. M. Mechanical properties of calcium alginate fibers produced with a microfluidic device. *Carbohydr Polym* **89**, 1198–1206 (2012).
359. Anani, J., Noby, H., Zkria, A., Yoshitake, T. & Elkady, M. Monothetic Analysis and Response Surface Methodology Optimization of Calcium Alginate Microcapsules Characteristics. *Polymers (Basel)* **14**, (2022).
360. Zhao, J. *et al.* Shape tuning and size prediction of millimeter-scale calcium-alginate capsules with aqueous core. *Polymers (Basel)* **12**, 1–16 (2020).
361. Villaverde Cendon, F., Busnardo Salomão, B., Maria Matos Jorge, R. & Luiz Mathias, A. Mechanical and optical evaluation of alginate hydrospheres produced with different cross-linking salts for industrial application. *Colloid Polym Sci* **299**, 693–703 (2021).
362. Murata, Y., Nakada, K., Miyamoto, E., Kawashima, S. & Seo, S. H. Influence of erosion of calcium-induced alginate gel matrix on the release of Brilliant Blue. *Journal of Controlled Release* **23**, 21–26 (1993).
363. Wang, P. *et al.* Electrospraying Technique and Its Recent Application Advances for Biological Macromolecule Encapsulation of Food Bioactive Substances. *Food Reviews International* **38**, 566–588 (2022).
364. Timilsena, Y. P., Haque, Md. A. & Adhikari, B. Encapsulation in the Food Industry: A Brief Historical Overview to Recent Developments. *Food Nutr Sci* **11**, 481–508 (2020).
365. Yun, P., Devahastin, S. & Chiewchan, N. Microstructures of encapsulates and their relations with encapsulation efficiency and controlled release of bioactive constituents: A review. *Compr Rev Food Sci Food Saf* **20**, 1768–1799 (2021).

366. Sultana, M., Chan, E. S., Pushpamalar, J. & Choo, W. S. Advances in extrusion-dripping encapsulation of probiotics and omega-3 rich oils. *Trends Food Sci Technol* **123**, 69–86 (2022).
367. Caballero, S., Li, Y. O., McClements, D. J. & Davidov-Pardo, G. Encapsulation and delivery of bioactive citrus pomace polyphenols: a review. *Crit Rev Food Sci Nutr* **62**, 8028–8044 (2022).
368. Abka-khajouei, R. *et al.* Structures, Properties and Applications of Alginates. *Mar Drugs* **20**, (2022).
369. Grasdalen, H., Larsen, B. & Smisrod, O. ¹³C-n.m.r. studies of monomeric composition and sequence in alginate. *Carbohydr Res* **89**, 179–191 (1981).
370. Jeoh, T. *et al.* How alginate properties influence in situ internal gelation in crosslinked alginate microcapsules (CLAMs) formed by spray drying. *PLoS One* **16**, 1–14 (2021).
371. G. Gómez-Mascaraque, L., Martínez-Sanz, M., Hogan, S. A., López-Rubio, A. & Brodkorb, A. Nano- and microstructural evolution of alginate beads in simulated gastrointestinal fluids. Impact of M/G ratio, molecular weight and pH. *Carbohydr Polym* **223**, 115121 (2019).
372. Syanda, A. M. *et al.* Sulfated Alginate Reduces Pericapsular Fibrotic Overgrowth on Encapsulated cGMP-Compliant hPSC-Hepatocytes in Mice. *Front Bioeng Biotechnol* **9**, (2022).
373. Salomonsen, T., Jensen, H. M., Larsen, F. H., Steuernagel, S. & Engelsen, S. B. Direct quantification of M/G ratio from ¹³C CP-MAS NMR spectra of alginate powders by multivariate curve resolution. *Carbohydr Res* **344**, 2014–2022 (2009).
374. Solberg, A., Draget, K. I., Schatz, C. & Christensen, B. E. Alginate Blocks and Block Polysaccharides : A Review. **2200072**, 1–5 (2023).
375. Anani, J., Noby, H., Zkria, A., Yoshitake, T. & Elkady, M. Monothetic Analysis and Response Surface Methodology Optimization of Calcium Alginate Microcapsules Characteristics. *Polymers (Basel)* **14**, (2022).
376. Fang, Y. *et al.* Multiple steps and critical behaviors of the binding of calcium to alginate. *Journal of Physical Chemistry B* **111**, 2456–2462 (2007).
377. Botelho Sampaio de Oliveira, K., Lopes Leite, M., Albuquerque Cunha, V., Brito da Cunha, N. & Luiz Franco, O. Challenges and advances in antimicrobial peptide development. *Drug Discov Today* **28**, 103629 (2023).
378. Wang, M. *et al.* Recent Advances and Perspectives on Expanding the Chemical Diversity of Lasso Peptides. *Front Bioeng Biotechnol* **9**, 741364 (2021).
379. Migoñ, D., Neubauer, D. & Kamysz, W. Hydrocarbon Stapled Antimicrobial Peptides. *Protein Journal* **37**, 2–12 (2018).
380. Li, D. *et al.* N-terminal acetylation of antimicrobial peptide L163 improves its stability against protease degradation. *Journal of Peptide Science* **27**, e3337 (2021).
381. Nalini, T., Basha, S. K., Mohamed Sadiq, A. M., Kumari, V. S. & Kaviyarasu, K. Development and characterization of alginate / chitosan nanoparticulate system for hydrophobic drug encapsulation. *J Drug Deliv Sci Technol* **52**, 65–72 (2019).
382. Farahmand, A. *et al.* Millifluidic-assisted ionic gelation technique for encapsulation of probiotics in double-layered polysaccharide structure. *Food Research International* **160**, 111699 (2022).
383. Liu, L. *et al.* Fish oil-gelatin core-shell electrospun nanofibrous membranes as promising edible films for the encapsulation of hydrophobic and hydrophilic nutrients. *LWT* **146**, 111500 (2021).
384. Huang, X. *et al.* Encapsulation of resveratrol in zein/pectin core-shell nanoparticles: Stability, bioaccessibility, and antioxidant capacity after simulated gastrointestinal digestion. *Food Hydrocoll* **93**, 261–269 (2019).
385. Solbiati, J. O. *et al.* Sequence analysis of the four plasmid genes required to produce the circular peptide antibiotic microcin J25. *J Bacteriol* **181**, 2659–2662 (1999).
386. Ben Said, L. *et al.* Phenomic and genomic approaches to studying the inhibition of multiresistant Salmonella enterica by microcin J25. *Environ Microbiol* **22**, 2907–2920 (2020).
387. Soltani, S. *et al.* Gastrointestinal Stability and Cytotoxicity of Bacteriocins From Gram-Positive and Gram-Negative Bacteria: A Comparative in vitro Study. *Front Microbiol* **12**, (2022).
388. Rosengren, K. J. *et al.* Microcin J25 has a threaded sidechain-to-backbone ring structure and not a head-to-tail cyclized backbone. *J Am Chem Soc* **125**, 12464–12474 (2003).
389. Arvanitoyannis, I. S. & Bosnea, L. Migration of Substances from Food Packaging Materials to Foods. *Crit Rev Food Sci Nutr* **44**, 63–76 (2004).
390. Shi, Y., Wan, A., Shi, Y., Zhang, Y. & Chen, Y. Experimental and mathematical studies on the drug release properties of aspirin loaded chitosan nanoparticles. *Biomed Res Int* **2014**, (2014).
391. Yoo, J. & Won, Y. Y. Phenomenology of the Initial Burst Release of Drugs from PLGA Microparticles. *ACS Biomaterials Science and Engineering* vol. 6 6053–6062 Preprint at <https://doi.org/10.1021/acsbiomaterials.0c01228> (2020).
392. Bradford, S. A. & Torkezaban, S. Determining parameters and mechanisms of colloid retention and release in porous media. *Langmuir* **31**, 12096–12105 (2015).
393. Chuysinuan, P. *et al.* Enhanced Structural Stability and Controlled Drug Release of Hydrophilic Antibiotic-Loaded Alginate/Soy Protein Isolate Core-Sheath Fibers for Tissue Engineering Applications. *Fibers and Polymers* **20**, 1–10 (2019).
394. Maresca, D. *et al.* Microencapsulation of nisin in alginate beads by vibrating technology: Preliminary investigation. *Lwt* **66**, 436–443 (2016).
395. Chandrasekar, V., Coupland, J. N. & Anantheswaran, R. C. Characterization of nisin containing chitosan-alginate microparticles. *Food Hydrocoll* **69**, 301–307 (2017).
396. Kuo, C. K. & Ma, P. X. Maintaining dimensions and mechanical properties of ionically crosslinked alginate hydrogel scaffolds in vitro. *J Biomed Mater Res A* **84A**, 899–907 (2008).
397. Denis Poncelet. Microencapsulation using dripping technologies . in *Bioencapsulation research Group seminar* (2022).
398. Narsaiah, K., Jha, S. N., Wilson, R. A., Mandge, H. M. & Manikantan, M. R. Optimizing microencapsulation of nisin with sodium alginate and guar gum. *J Food Sci Technol* **51**, 4054–4059 (2014).